Relationships between Observed Hydrocarbon Column Heights, Occurrence of Background Overpressure and Seal Capacity within North West Europe

---

Mr. James K. Schofield

Department of Earth Science
Durham University

2016

This thesis was submitted to the University of Durham in full fulfilment of the requirements for the degree of Master of Science by Research


Durham
University


woodside

Abstract

When reservoir pore pressures approach the fracture pressure the risk of hydrocarbon leakage increases as a result of mechanical failure. Here, relationships between overpressure, hydrocarbon column heights and seal capacities (fracture pressure – pore/aquifer pressure) will be explored, and best practice criteria for assessing seal capacity is discussed.

The term overpressure (OP) can be applied to any formation with pore pressures higher than the hydrostatic pressure. From a 129 field database, critical shear failure pressures, fault reactivation pressures and tensile failure pressures were derived. Calculating the difference between such pressures and the aquifer pressures at structural crests within fields allows quantification of the envelope between the reservoir pressure and failure pressure - a term coined by Swarbrick et al. (2010) as "aquifer seal capacity" (ASC).

Conventional approaches suggest that fractures will form when the pore fluid pressure equals that of σ_3 plus the tensile strength of the rock (Gaarenstroom et al. 1993; Converse et al. 2000; Nordgård Bolås & Hermanrud 2003; Winefield et al. 2005). However, there remains the distinct possibility that it is aquifer pressure that governs failure (Bjørkum et al. 1998; Swarbrick et al. 2010).

This research suggests a convergence of the fracture pressure gradient and S_v at 14,500 ft within the Central North Sea. At this point the principal stresses switch. Furthermore, a general reduction in hydrocarbon column height (HCH) is observed with a) increasing aquifer OP and b) a reduction in ASC. The possibility of applying upper bound cutoff lines is explored, i.e. column heights are not expected greater than χ ft given an aquifer OP. The HPHT Shearwater field is an exception for all trends within the research. The concept of a protected trap is suggested as an explanation for this apparently anomalous trap integrity.

Understanding the nature of how, when and why pressure-related seal failure occurs can help alleviate drilling dry holes and unsuccessful exploration ventures.

Table of Contents

Table of Figures

Tables

Glossary

A

Abnormal Pressure –Pore pressure that lies either above, or below (overpressure or underpressure respectively) the hydrostatic pressure.

Absolute Pressure (psia) – A zero-referenced pressure against a vacuum. Therefore absolute pressure would be equal to formation gauge pressure plus atmospheric pressure.

Aquathermal Expansion – The expansion of water within a closed environment resulting from thermal increases.

Aquifer Pressure – The pressure (or extrapolated pressure) of the water within a rock formation.

Aquifer Seal Capacity - The fracture pressure/S_v minus that of the extrapolated aquifer pressure

Atmospheric Pressure – The pressure exerted by the weight of the overlying atmosphere. Taken at mean sea level this is 14.7 psi.

B

Bulk Density – The weight of the grains and pore contents over a unit area.

Buoyancy Pressure – The upward force of a fluid resulting from density contrasts between hydrocarbons and formation water.

C

Centroid - The depth where the sand body pore pressures are equal to that of the surrounding sealing lithology.

Closure – The area between the lowest closing contour and the structural crest of a structure.

Closure Capacity – The maximum vertical height of a closure between the lowest closing contour and the structural crest. This represents the maximum column height a trap could possess.

Connate Fluids – Liquids trapped within the pores of the rocks when deposited. Primarily composed of water.

D

Diagenesis – The physical and chemical alterations a rock undergoes with burial and conversion from sediment to sedimentary rock facies.

Discovery Well – A well drilled for hydrocarbons within a new field successfully encountering petroleum.

Disequilibrium Compaction – When burial rates and increases in load stress outpace the rate at which connate fluids can dissipate. A key overpressure generation mechanism.

Drilling Fluid – Liquids, gasses or a combination used during drilling operations. Often termed drilling mud, the correct density of drilling fluid must be used to avoid kicks and losses.

Dry Hole – A well drilled for hydrocarbons but with no yield.

E

Effective Stress - the pressure exerted at a certain depth borne purely by the rock matrix grain to grain contacts.

Excess Buoyancy Pressure – The additional buoyancy pressure resulting from fluid density contrasts between hydrocarbons and aquifer pressures.

F

Failure Envelope – Used within Mohr Circle analysis, a failure envelope delineates the stable and unstable rock stress states. When a Mohr Circle intersects with the failure envelope (often defined by the Coulomb failure criterion) a rock will theoretically fail.

Fault Reactivation – Re-searing/reactivation of pre-existing faults within a formation either through changing stress regimes, increasing overpressure or a combination of both.

Fault Reactivation Pressure – The pore pressure required to reactivate a pre-existing, optimally orientated, fault.

Fluid Retention Depth – The depth at which fluid is not lost but maintained; porosity is maintained too.

Fracture Pressure – The pressure at which a formation will crack/fracture.

G

Geopressure – The pressure within the earth.

Geothermal Gradient – The rate of temperature increase with increasing depth within the Earth's interior.

H

Hydraulic Head – A measurement of the pressure of the liquid above a datum, usually mean sea level. A minimal cause of overpressure.

Hydrocarbon Leakage – The secondary migration of hydrocarbons out of a reservoir through a caprock.

Hydrocarbon Pressure – The pore pressure of the formation, taking into account the excess buoyancy pressure resulting from the presence of a hydrocarbon accumulation.

Hydrofracturing – Fracturing of the formation resulting from aquifer/formation fluids > S_3 + the tensile strength of the rock.

Hydrophilic – The physical property of a molecule with a special affinity to water.

Hydrophobic – The physical property of a molecule which is repellent of water.

Hydrostatic Pressure - the amount of force exerted by the weight of a static column of fluid in equilibrium with the surface pressure.

K

Kerogen Transformation – The conversion of solid state kerogen to hydrocarbons, oil, gas or a combination

Kick – An influx of formation fluid into the well bore resulting from underbalanced drilling.

L

Lateral Transfer - The transference of pressures within a tilted sealed permeable system (e.g. an isolated sand body) from deeper regions with naturally occurring higher pressures (resulting due to pressures increasing with depth below the FRD).

Least Principal Stress – The lowest value of all the principal stresses.

Lithostatic Pressure –The stress of the overlying sediments and pore fluids acting upon a rock at a given depth in a vertical direction. Also known as the overburden or vertical stress.

Loss – The drilling fluids fracture the formation and exit the wellbore into the formation as a result of drilling overbalanced.

M

Maximum Principal Stress – The least tensile or most compressive principal stress. Fractures will form parallel to the maximum principal stress.

Membrane Failure – The migration of hydrocarbons through the pore space of a seal having overcome the capillary entry pressure.

Minimum Effective stress – Minimum principal stress minus the pore pressure. In a rock with zero tensile strength the minimum effective stress is equal to the formation seal capacity.

Minimum Principal Stress – The most tensile or least compressive principal stress. In a rock with zero tensile strength the minimum principal stress will equal the fracture pressure. Fractures will form perpendicular to the orientation of the minimum stress.

Minimum Stress Convergence – The point at which S_v and P_{frac} are equal.

Mode 1 Failure – Tensile failure, fractures opening normal to the fracture plane.

Mohr Circle – A 2-dimensional graphical representation of rock differential stresses and failure pressures under shear and tensile regimes.

O

Osmosis – The movement of water molecules from an area of high water concentration to low.

Overburden – The stress of the overlying sediments and pore fluids acting upon a rock at a given depth in a vertical direction. Also known as lithostatic pressure or vertical stress.

Overcompaction - Uplift of normally pressured rocks that maintain pressures obtained at greater depths will lead to overpressure, assuming pressures cannot dissipate during uplift.

Overpressure - pore pressure that lies either above, or below (overpressure or underpressure respectively) the hydrostatic pressure.

P

Petroleum Play – A series of petroleum traps/fields in the same region controlled under similar connected geological circumstances.

Pore Pressure - The pressure of the fluids within the pores of a rock matrix

P_p/S_h Coupling – A coupling ratio exisiting between pore pressure and horizontal stress.

Pressure - Pressure is the measurement of the amount of force exerted on a unit area.

Pressure Cell - A compartment where subsurface overpressured fluids are in internal communication.

Primary Migration – The migration of hydrocarbons along a play fairway to a closure or trap.

Protected Trap - A structurally deeper closure which is in hydraulic connectivity with a shallower, neighbouring trap(s).

R

Retention Capacity –The fracture pressure minus the formation pressure

S

Seal Capacity – The pressure difference between the fracture pressure/minimum principal stress and the aquifer/formation pressure.

Seal Integrity – How effective a hydrocarbon seal is at maintaining a hydrocarbon column.

Secondary Migration – The migration of hydrocarbons out of a trap or closure

Spill Point – The deepest point within a reservoir. If a trap if filled to its spill point (full-to-spill) any further influx of hydrocarbons will leak from the closure.

Stress Regime – The current (or palaeo) orientations and magnitudes of stresses in a defined area.

T

Tensile Failure – Mode 1 failure, opening normal to the fracture plane.

Tensile Strength – The resistance strength a material or rock has to breaking or failing under tension (being stretched).

Threshold Capillary Pressure – The buoyancy pressure necessary to overcome the capillary entry pressure allowing hydrocarbons to migrate into a water wet seal.

Top Seal – Formation directly overlying a hydrocarbon accumulation with low/no permeability with a capillary entry pressure low enough to trap hydrocarbons beneath.

Trap – A geometric arrangement of a formation comprising a reservoir and a low permeability seal that will allow the accumulation of hydrocarbons.

Trap Integrity – How effective a trap structure is in maintaining an accumulation of hydrocarbons.

U

Undercompaction – The pore space of a rock has not been compacted under 'normal' conditions, perhaps resulting from inadequate de-watering of intergranular pore fluids.

V

Vertical Stress – The stress of the overlying sediments and pore fluids acting upon a rock at a given depth in a vertical direction. Also known as lithostatic pressure or overburden.

Virgin Pressure – Formation/reservoir pressures not affected by depletion.

Nomenclature

ASC ..... Aquifer Seal Capacity

BCU ..... Base Cretaceous Unconformity

CD ..... Crest Depth

CNS ..... Central North Sea

CQG ..... Combined Quartz Gauge

DST ..... Drill Stem Test

FG ..... Fracture Gradient

FIT ..... Formation Integrity Tool

FRD ..... Fluid Retention Depth

FRP ..... Fault Reactivation Pressure

FT ..... Formation Tests

GWC ..... Gas Water Contact

HCH ..... Hydrocarbon Column Height

HES ..... Horizontal Effective Stress

HPHT ..... High Pressure High Temperature

HWC ..... Hydrocarbon Water Contact

ISIP ..... Instantaneous Shutin Pressure

LOP ..... Leak-Off Pressure

LOT ..... Leak-Off Test

MDT ..... Modular Formation Dynamics Tester

MPa ..... Megapascal

Nm^{-2} ..... Newton per Square Meter

NNS ..... Northern North Sea

NPD ..... Norwegian Petroleum Directorate

OP ..... Overpressure

OWC ..... Oil Water Contact

P-D ..... Pressure-Depth

P_{frac} ..... Fracture Pressure

$psi\ ft^{-1}$ ..... Pounds per Square Inch Per Foot

psi ..... Pounds per Square Inch

psia ..... Absolute Pressure

RC ..... Retention Capacity

RFT ..... Repeat Formation Test

S_h ..... Horizontal Stress

SNS ..... Southern North Sea

S_v ..... Vertical Stress

T ..... Tensile Strength of the Rock

TOC ..... Total Organic Carbon

TVDml ..... Total Vertical Depth Mud Line

TVDss ..... Total Vertical Depth Sub Surface

UKCS ..... United Kingdom Continental Shelf

VES ..... Vertical Effective Stress

WFT ..... Wireline Formation Tools

XLOT ..... Extended Leak-Off Test

Declaration

The author of this report declares that the content of this thesis has not been submitted previously for a degree in this (Durham University) or any other institution. Furthermore, all content is original and not based on joint research. Where relevant, other individual's research is acknowledged by the author and referenced appropriately.

Mr. James K. Schofield

Durham University

July 2016

Copyright

Acknowledgements

I would like to extend my full gratitude to the many people, on both sides of the world, who have help shaped this thesis, and generously contributed to the final outcome.

First and foremost, I would like to extend my thanks to my academic supervisors, Professors Andy Aplin and Richard Swarbrick. In such a tough economic time for the oil industry I am truly appreciative of the opportunity, helping put me in good stead for what (I hope) will be a long and thrilling career. Furthermore, their academic assistance with, and constructive comments on this thesis are fittingly acknowledged. Their advice helped this report become the finished piece of work it is. I hope our paths will cross again.

Jurgen Streit is owed a great deal of gratitude; not only for his help with the initiation of the project but also his support and advice throughout as an industry supervisor. I'm sure we shall finally meet in person in the not so distant future! Additionally, Alwyn Vear and the rest of the London office I owe thanks for enabling me to present my research and for their assistance with following conference presentations. It goes without saying that, without Woodside Energy's input and funding this project would not have gotten off the ground, so thanks to all involved.

Special mention goes to Genni Wetherell for her continued support and contribution in proof reading and assistance in the documents early stages. Furthermore, thanks to my girlfriend Rellie, for providing a welcome distraction during challenging times, and Laura Haswell for putting up with the endless admin questions! Finally, thanks to the rest of my friends and colleagues, both in and out of the department for their contributions, academically and personally.

To close, thanks goes to my parents for their unconditional support (financial and otherwise…). Without them I would not be where I am today. I therefore, dedicate this thesis to them both as a small token of my appreciation.

Chapter 1

Introduction

Chapter 1 – Introduction

1.1 Project Rationale

It has long been understood that when reservoir pore pressures increase towards the fracture pressure the risk associated with loosing seal capacity, and as such hydrocarbon leakage, increases (Gaarenstroom et al. 1993; Holm 1998; Converse et al. 2000; Nordgård Bolås & Hermanrud 2003; Swarbrick et al. 2010; Hermanrud et al. 2014). Hydrofracturing the top seal thus permits hydrocarbon leakage from what otherwise would be a successful petroleum play. Understanding the nature of how and, importantly, when hydrofracturing (or pressure related seal failure) occurs can help alleviate against future dry holes and unsuccessful exploration ventures.

Relationships and patterns observable between overpressure, hydrocarbon column heights and seal capacities (fracture pressure – aquifer/pore pressure) will be explored and reported within the document.

1.2 Project Aim

Our key aim is to establish possible relationships between observed hydrocarbon column heights, occurrence of overpressure (aquifer pressure higher than the hydrostatic pressure) and seal capacity. The findings from this study will help reduce the risk of drilling expensive, high pressure wells for targets that have previously leaked hydrocarbons, so are subsequently dry or uneconomical to produce. Further benefit can be gained from identifying the potential and/or maximum column height that may be retained under certain overpressure conditions.

Questions to be answered include:

1. What do we already know from previous research regarding the impact of formation overpressure on hydrocarbon column heights, seal capacities and dry hole vs. discovery analysis?

2. What are controls on hydrocarbon retention and hydrocarbon column height within the study region?
3. Does seal capacity/overpressure control hydrocarbon column height within this dataset?

1.3 Project Hypothesis

1.3.1 Context

Hydrocarbon column heights may be controlled by:

1. **Caprock membrane failure** – Hydrocarbon buoyancy pressure exceeding that of the caprock capillary entry pressure thereby facilitating hydrocarbon leakage.
2. **Hydraulic fracturing of the caprock** – Formation pore pressure exceeds the minimum principal stress and tensile strength of the rock.
3. **Juxtaposing caprock fault failure –** Hydrocarbon leakage aided by juxtaposition in the caprock caused by:
    a. Reactivation of previously formed faults caused by high formation pore pressure.
    b. Earthquake nucleation at greater depths with upward propagation of fault ruptures leading to fault reactivations and breach of the trap.

1.3.2 Project Hypothesis

In regions with overpressures generated by shale undercompaction and little preserved overpressures, the caprock above a trap is expected to have a limited sealing and thus trapping integrity (no/thin seal, heavily faulted seal, no substantial closures). This scenario would display small hydrocarbon column heights.

Areas with moderate overpressures could be expected to display potentially substantial column heights. This is due to the assumption that, if

moderate overpressures are maintained, the rock possesses adequate sealing properties. In this scenario the hydrocarbon column height is limited to trap type (importantly closure), the strength of the seal defined by 1, 2, 3a and 3b (in section 1.3.1 the aforementioned failure criteria) and the pore pressure (including the buoyancy of the hydrocarbon). The exception to this would present itself in the form of earthquake-related failure.

Finally, areas with high overpressure may retain only short columns due to the likelihood of seal failure. If the aquifer pressures is only slightly less than that of the fracture pressure then only a short column can be retained – a result of excess buoyancy pressure intersecting with the fracture pressure or least principal stress, σ_3. Similarly, if the aquifer pressures equal that of the fracture pressure (i.e. the effective stress equals 0), a column cannot accumulate as top seal failure would occur and the hydrocarbons would be expelled from the trap.

1.4 Study Region

Hydrocarbon fields from the North Sea have been a main focus; however, data from the following has also been included within the study:

- Irish Sea
- West of Shetland
- Gulf of Mexico
- Porong Region - Indonesia

Overpressure is a worldwide occurrence arising in all geological environments and strata of all ages (Mouchet & Mitchell 1989; Swarbrick & Osborne 1998). The focus primarily upon the North Sea pressure systems (due to availability of data) will establish patterns that can then be compared to other prolific global petroleum basins such as the Gulf of Mexico or Australian North West Shelf.

Chapter 2

Pressure in the Subsurface

Chapter 2 - Pressure in the Subsurface

The following chapter highlights theoretical principals associated with subsurface pressures. Pore pressures, aquifer pressures, hydrostatic and lithostatic pressures are explored in further detail and their influences upon one another are expanded upon.

2.1 Terminology

In the hydrocarbon industry, standard units for measuring pressure are pounds per square inch (psi) as opposed to the SI units of newton per square meter (Nm^{-2}). Furthermore, feet and inches are still used as a measurement of distance. As a consequence, the following report will refer to pressure in psi and corresponding pressure gradients in psi ft^{-1}.

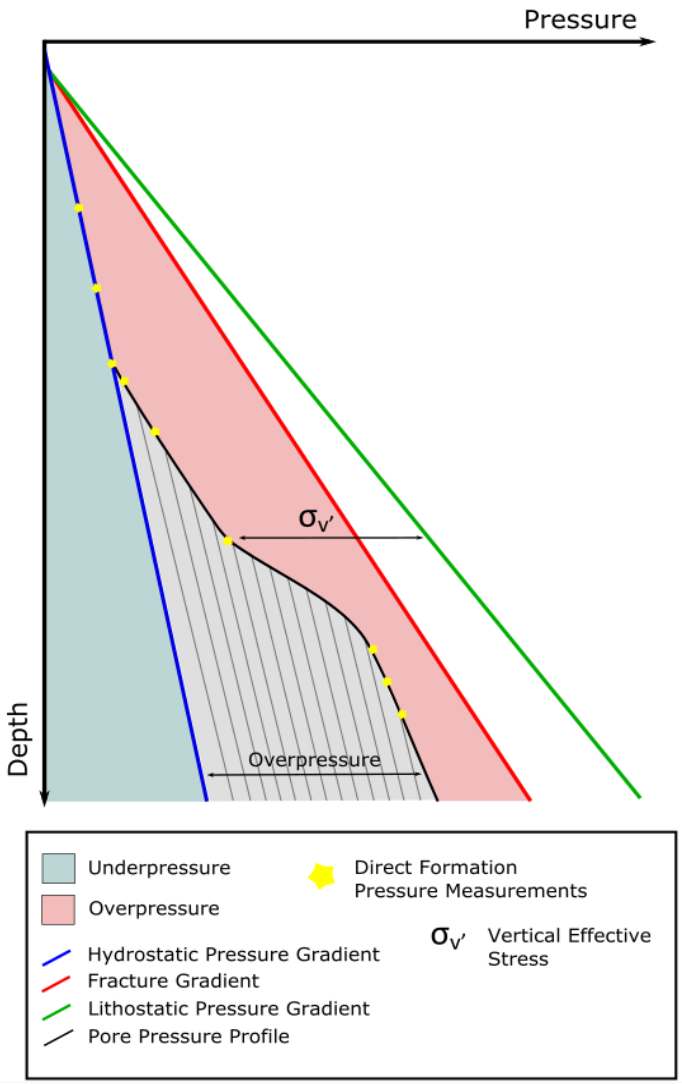

Figure 2.1 Schematic pressure-depth plot indicating different overpressure phases, gradients and stresses. The blue line represents a 'normal' hydrostatic gradient (the cumulative weight of the overlying water column). The black gradient shows an interpolated pore pressure gradient through direct pore pressure measurements (yellow stars). The red gradient shows a fracture pressure and green a lithostatic gradient.

Pressure is the measurement of the amount of force exerted on a unit area. As such, various pressure attributes are used in conjunction with geopressure. These include lithostatic pressure (the force of the overlying rock and pore fluid at a given depth within a zero

flow case), hydrostatic pressure (the pressure exerted by a fluid at a certain point within the fluid) and pore pressure (the pressure of the fluid present within the pore spaces of a rock matrix). These are all expanded upon in the following sections.

2.1.1 Hydrostatic Pressure

Hydrostatic pressure is defined as the amount of force exerted by the weight of a static column of fluid in equilibrium with the surface pressure. The weight of the overlying column is a function of the density of the water and, as such, defines the gradient on a pressure depth plot. Hydrostatic pressure is expressed by the following equation:

$$P_{hyd} = \int_{o}^{z} \rho_w . g . z \qquad \text{Eq. 2.1}$$

where P_{hyd} is hydrostatic pressure, ρ_w is the water density, g is acceleration due to gravity at the Earth's surface (32.174 ft s^{-2}) and z is vertical depth.

Equation 2.1 shows how the hydrostatic pressure will increase as a function of depth as the downward exerted force increases with the height of the overlying water column. Atmospheric pressure (14.7 psi) should be added to any pressure value calculated from mean sea level to produce an absolute pressure (psia). This takes into account the excess atmospheric pressure that is exerted onto the surface of the sea.

The hydrostatic gradient (depicted as the blue line on Figure 2.1) is defined by the density of the fluid. Pure water gives a gradient of 0.433 psi ft^{-1}. In reality the hydrostatic pressure line in Figure 2.1 would not be linear as shown, it would vary with depth. However, there is seldom data available on water salinity variations throughout the subsurface and, as such a regional linear line is generally applied. It is common for subsurface waters to be of brine composition. For example, in the Southern North Sea sub-salt aquifers, fluid gradients upwards of 0.55 psi ft^{-1} are

known. Within the Central and Northern North Sea regional densities of 0.45 psi ft^{-1} are generally applied by authors (e.g. Gaarenstroom et al., 1993; Holm, 1998; O'Connor & Swarbrick, 2008). Temperature and pressure are also noted to have an effect on the density of fluids. However, in comparison to the effects of salinity these are thought to be minimal (Mouchet & Mitchell 1989). Importantly, the hydrostatic pressure acts as a reference point determining 'normal' pressure conditions at a certain depth. Following this, abnormal pressures can then be identified, measured and compared using this datum point.

2.1.2 Lithostatic Pressure

The lithostatic pressure refers to the stress of the overlying sediments and pore fluids acting upon a rock at a given depth in a vertical direction. The lithostatic pressure (also referred to as the overburden or vertical stress) is represented by the green line on Figure 2.1. Lithostatic pressure at a given depth can be defined by the following equation:

$$S_v = \int_o^z \rho_b . g . z \qquad \text{Eq. 2.2}$$

where S_v is lithostatic pressure and ρ_b is the bulk density of the sediment (a function of both the matrix and pore pressures within the matrix pores). ρ_b may be calculated using the following equation:

$$\rho_b = \rho_m(1 - \phi) + \rho_f(\phi) \qquad \text{Eq. 2.3}$$

where ρ_m is rock matrix density, ρ_f is fluid density and ϕ is porosity. Values for ρ_b may also be obtained from the downhole measurements of the rock bulk density conducted during petrophysical logging of petroleum wellbores.

As with hydrostatic pressures, in reality the gradient of the lithostatic pressure is not a constant as depicted on Figure 2.1. Therefore, a true representation would indicate a non-linear lithostatic gradient with depth. Compaction, rock composition and fluid density all vary vertically, regionally, and locally in many basins. These are all important factors to note when undertaking detailed pore pressure analysis. A general default of 1.0 psi ft^{-1} is used based upon Mouchet & Mitchell (1989) average sediment densities. Although this is utilised by many authors it is important to note that other means of calculating lithostatic pressures can be used and are arguably more effective at computing accurate lithostatic values. This includes calculations undertaken on density logs as used by Swarbrick et al. (2010). Further discussions on lithostatic gradient calculations are in Section 4.5.3.

2.1.3 Pore Pressure

The pressure of the fluids within the pores of a rock matrix is known as the pore pressure. Abnormal pore pressure is defined as pore pressure that lies either above, or below (overpressure or underpressure respectively) the hydrostatic pressure. Pore pressure measurements can be acquired using either indirect or direct methods. The stars on Figure 2.1 represent hypothetical direct pore pressure measurements. Using these points an interpolation of a pore pressure regime can be determined and drawn (black line on Figure 2.1). If formation pressures are greater than the hydrostatic pressure the rock formation is overpressured. Underpressured rocks would express pore pressure measurements to the left of the hydrostatic gradient, within the green zone, in Figure 2.1 with the location being a function of depth and pore fluid pressure. That is, any formation pressure measurement with values less than that of the calculated hydrostatic gradient. Figure 2.2 displays a schematic of the varying locations that may represent hypothetical overpressures. Figure 2.2(A) shows a rock with moderately low overpressures. Within this example the formation pressure gradient lies close to the 'normally' pressured hydrostatic gradient. As formation pressures increase, the formation pressure gradient departs further from the hydrostatic line thereby increasing the overpressure. This is shown as B on figure 2.2. Throughout this

report underpressure is not discussed at length as the main topic is the relationship of overpressure and hydrocarbon column height.

In most geological settings pore fluid pressures are less than that of the lithostatic gradient (Kerrich 1986; Streit & Cox 2001). Within this scenario pressures are limited by the sum of the minimum principal stress and the tensile strength of the rock. Failure will cause the formation pore pressures to equilibrate or drop below the minimum stress and subsequently a hydraulic fracture will close (see Price & Cosgrove 1990 pp. 29). Shear fractures may remain permeable. Conversely, fluid pressures are known to exceed the lithostatic pressures under certain conditions (Boullier & Robert 1992; Cox 1995; Streit & Cox 2001).

2.1.4 Effective Stress

The effective stress law is, in essence, a means to convert two variables - external stress (σ) and formation pore pressure - into a singular equivalent variable - effective stress (σ').The effective stress calculation is useful for many pore pressure aspects, largely in assisting with pore pressure (Pp) prediction, but critically in defining drilling windows within drilling practices.

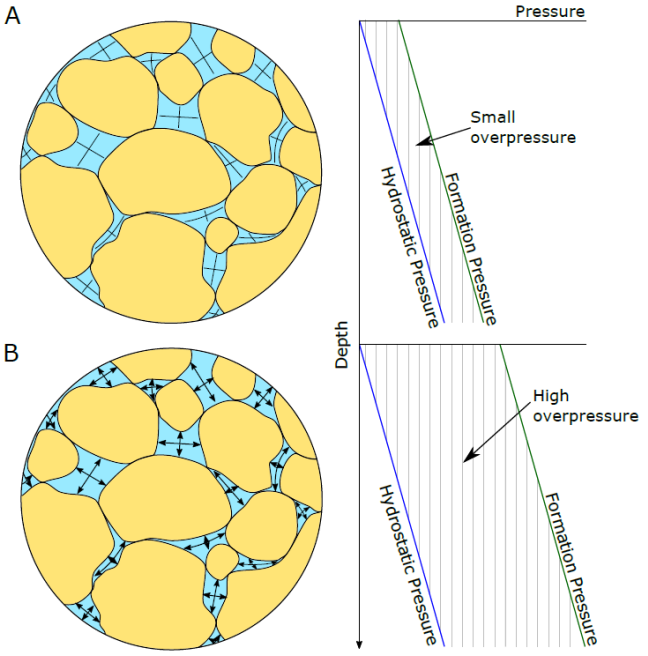

Figure 2.2 Schematic of differing phase 1 fluid pressures. Arrow thickness represents the amount of stress the inter-granular pore fluid is exerting on the rock matrix. The blue line represents the hydrostatic pressure on a generic 0.45 psi ft^{-1} gradient. The green line represents the actual formation pressures. A - Small amount of stress, therefore a small amount of overpressure. B - High formation pressures leading to larger overpressures.

One such expression for effective stress can be simply be written as:

$$\sigma' = \sigma - Pp \qquad \text{Eq. 2.4}$$

The stress variable, be it vertical (as defined by Terzaghi, 1943) or horizontal is substituted into this equation, see Price & Cosgrove (1990), pp. 25-26. The effective stress equation removes the pore pressure variable (accounted for within the S_v/S_h) and can thus be described as the pressure exerted at a certain depth borne purely by the rock matrix grain to grain contacts.

The minimum effective stress (σ'_{min}) is useful in defining how far a rock is from failing under a tensile (mode 1 fracture) regime. Depending upon the local stress regime the minimum stress orientation may be vertical (in general within extensional basins) or horizontal (as in compressional systems). Once this is established a corresponding effective stress can be determined providing a quantitative value of the additional pressure required for tensile fracturing to develop. In deep reservoir intervals the maximum principal stresses are, in general, compressive. Intergranular pore fluids, on the other hand act upon the rock matrix indiscriminately in all orientations, and thus opposing unilateral compressive stress. Therefore, when combining total stress and pore fluid pressures a lower effective stress is fashioned (Streit et al. 2005).

2.2 Overpressure Generation Mechanisms

The term overpressure can be applied to any formation with pore pressures higher than that of the hydrostatic pressure. A worldwide phenomenon, overpressures can be present in formations of all ages and in almost every geological environment (Bradley 1975; Mouchet & Mitchell 1989; Swarbrick & Osborne 1998).

Caused by the inability for fluids within a rock matrix to escape, overpressure generation mechanisms can broadly be divided into categories;

1) stress related 2) fluid expansion related 3) load transfer mechanisms 4) chemical compaction 5) other mechanisms (Swarbrick et al. 2002). Overpressure does not have to be the product of just one generation mechanism, but more possibly a combination of two or more (Gaarenstroom et al. 1993), all contributing different magnitudes. The older and deeper the formation the more likely overpressure is caused by a combination of mechanisms. A summary table of the main contribution mechanisms is presented below.

1) Stress Related Mechanisms	Disequilibrium Compaction (Vertical Loading) Tectonic Stress (Lateral Compressive Stress)
2) Fluid Volume Increases Mechanisms	Temperature Increase/Aquathermal Mineral Transformation Hydrocarbon Generation & Cracking
3) Load Transfer Mechanisms	Clay Mineral Transformations Kerogen to Oil Conversion
4) Chemical Compaction	
5) Other Generation Mechanisms	Osmosis Hydraulic Head Excess Density Contrast Buoyancy

Table 2.1- Summary table of key overpressure generation mechanisms

2.2.1 Overpressure Generation Mechanisms - Stress Related

As stress increases with burial or tectonic events, compaction can occur. When rock volume reduction or compression outpaces expulsion of intergranular connate fluids overpressure is generated. Effective stress is the driving mechanism for compaction. Clearly, the overriding control is porosity. Low porosity rocks will impede fluid expulsion rates, aiding in the generation of overpressure. As compaction continues, porosity is reduced. Often termed "loading mechanisms", stress-related mechanisms can be either vertical (as observed in extensional basins such as the North

Sea for example) or horizontal (seen in laterally compressive regions such as convergent margins).

2.2.1.1 Disequilibrium compaction (undercompaction)

A principal mechanism considered by many to be a major contributor to overpressure, disequilibrium compaction occurs when burial rates and increases in load stress outpace the rate at which connate fluids can dissipate (Dickinson 1953; King Hubbert & Rubey 1959; Secor 1965; Dickey 1976; Chapman 1980; Swarbrick & Osborne 1998). As vertical stresses increase through burial, compaction takes place with the expulsion of water from the granular space within the rock. This in turn increases the vertical effective stress condensing the pore space within the rock, reducing porosity and permeability. In a hydrostatically pressured system a balance is met between additional load stress and compaction and/or loss of fluid. Disequilibrium compaction, by definition, applies an imbalance of the equilibrium state. When the permeability is reduced to a degree where water cannot be sufficiently expelled or dewatered, the connate fluid assumes some of the load normally burdened by the grain contacts. This excess weight on the pore fluid increases the pressure to a level above that of hydrostatic, thus producing an overpressured formation. The depth at which overpressure commences is denoted in Swarbrick et al. (2002) as the "Fluid Retention Depth" (FRD).

Overpressure generation from disequilibrium compaction is a function of loading rate, compaction coefficient, temperature and permeability (Luo & Vasseur 1992; Swarbrick & Osborne 1998).

2.2.1.2 Lateral/Tectonic Stress

Using similar principals to disequilibrium compaction, the generation of overpressure due to lateral compressive stresses is noted in many basins around the world such as accretionary prisms, as documented by Fisher et al. (1996) from Brazil,

convergent margin of New Zealand's East Coast Basin in Darby & Funnell (2001) and the Andes and Papa New Guinea (Henning et al. 2002).

2.2.2 Overpressure Generation Mechanisms - Fluid Volume Increases

Increases and alterations in connate fluids can equally result in overpressure generation (Tingay et al. 2009). These alterations can be diagenetically based like that of molecular alterations or burial based, for example temperature variations associated with geothermal gradients.

2.2.2.1 Aquathermal processes

The phrase 'aquathermal expansion', first coined by Barker (1972), describes how water expands with rising temperatures. Although still disputed, recent work by (Swarbrick et al. 2002) shows that overpressures of 100 psi are associated with aquathermal expansion. Although these results support work from Chapman (1980), Daines (1982), Hunt (1990) and Lou & Vasseur (1992) (see Figure 2.3), all suggest that even small temperature increases can cause high overpressures (Figure 2.3). This is based upon basins with zero, or close to zero, permeability seals providing a completely isolated system where larger pressures could result. Osborne & Swarbrick (1997) did calculate pressure increases of 8000 psi coupled with a temperature increase from 54.4 °C to 93.3 °C (Figure 2.4) in fresh water in a sealed basin, however, this environment is considered

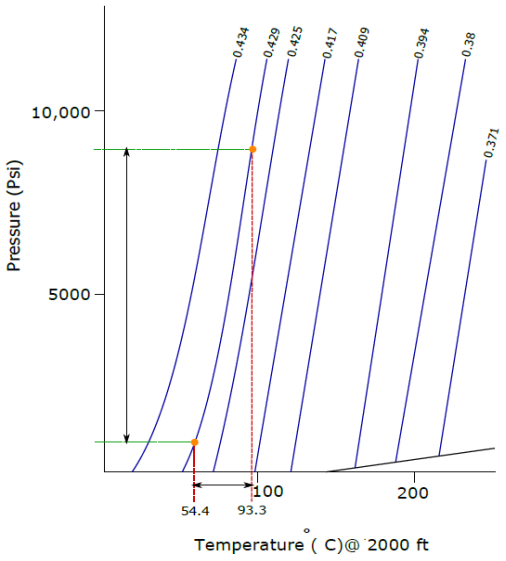

Figure 2.3 - A pressure temperature diagram illustrating how a relatively small temperature increase can result in a large pressure increase. The diagram shows 2 orange circles along a 0.429 psi/ft fluid density gradient. A 38.9 °C increase in temperature can result in upwards of 8000 psi pressure increase. (Diagram adapted from Barker (1972))

unlikely to exist in reality. Although some top seals may possess adequate permeability, lateral seals are unlikely to. The common presence of a transition zone in overpressured areas also suggests permeability in a seal, therefore reducing the effectiveness of aquathermal expansion. Aquathermal processes are a function of porosity and permeability and are, as such, hard to determine in muds and shales.

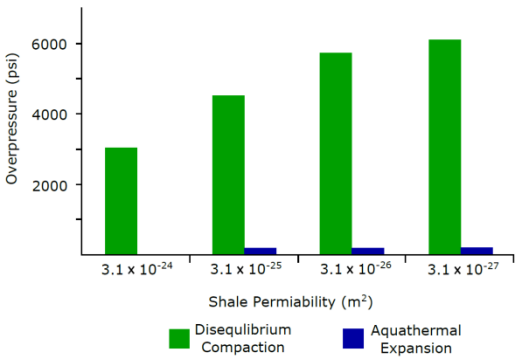

Figure 2.4 - Histogram redrawn from Osborne & Swarbrick (1997) with data from Lou and Vasseur (1992) illustrating results indicating aquathermal pressuring and disequilibrium compaction over 5 km subsidence in shale. The results suggest that, compared with disequilibrium compaction, aquathermal pressuring is negligible regarding overpressure generation.

In summary, the effects of aquathermal expansion are thought to be minimal unless the compartment is completely sealed, an unlikely scenario.

2.2.2.2 Mineral Transformation/ Diagenesis

Various processes associated with diagenetic influences are thought to contribute to overpressure generation. All are based on the principal that reactant products occupy a larger volume than the original reactants. As with kerogen transformation and cracking, overpressure can be generated through fluid expansion of connate fluids or load transfer (Lahann & Swarbrick 2011).

Smectite to illite transformation is thought to contribute to overpressure primarily from load transfer (Lahann & Swarbrick 2011) through a reduction in permeability leading to lower Darcy Flow values, therefore, insufficient dewatering with compaction. An overpressure value of up to 3000 psi was calculated from smectite rich, Neogene sediments from the Gulf of Mexico (Lahann & Swarbrick 2011). In regards to volume change Osborne & Swarbrick (1999) calculated a decrease in volume of 8.4 % to a maximum increase of 4.2% depending on varying reaction pathways. This change is thought to be relatively insignificant in terms of contribution as an overpressure generation mechanism (Swarbrick et al. 2002). Kaolinite to illite

transformation reaction, similar to smectite-illite, releases water during diagenesis. This reaction occurs at higher temperatures of 130 °C (Bjørlykke 2006) compared with that of smectite-illite at approximately 80 °C (Boles & Franks 1979) thus requiring greater burial and/or a regime with a higher geothermal gradient.

Silica phase transitions can lead to increases in pore pressures. Marine diatoms, composing porcelanite and chert undergo diagenetic alteration from opal-A (amorphous opal) to opal-CT (cristobalite and tridymite) to quartz. This transition causes reduction in porosity coupled with rapid pore fluid expulsion overpressure build up. The Faero-Shetland Basin is an example of how this overpressure generation has caused hydrofracturing (see Davies et al., 2006)

Salt diagenesis (gypsum-anhydrite dehydration) can occur at temperatures as low as 40 °C (Swarbrick & Osborne 1998). Due to the lower activation temperatures, reaction water can be produced at shallow depths. However, large overpressures may not be produced in shallower burial and this can lead the overpressure to impinge on the lithostatic stresses (Jowett et al. 1993), influencing the rocks propensity towards tensile failure.

2.2.2.3 Hydrocarbon generation

The generation of overpressure from kerogen maturation, by definition, can only occur in source rocks. The maturation of kerogen, generating liquid and gaseous hydrocarbons is thought to be dependent on time and temperature. There are 2 main mechanisms aiding in the production of fluid volume increases.

1) Kerogen maturation – This process involves the transformation of kerogen into oil and gas or both. Tissot et al. (1987) indicates the conditions for this to be met occur between 2-4 km depths and 70-120 °C.
2) Oil cracking – Oil is converted into gas between 3-5.5 km depths and between 90-150 °C temperatures (Barker 1990).

It is argued by Osborne & Swarbrick (1998) that volume changes associated with oil generation are widely unknown but it would appear to be negligible (England et al. 1987). It is however, accepted that high pressures are required to drive primary migration of hydrocarbons from their source rocks. If this pressure does not stem from volume increases it is questioned how overpressures are generated. Load transfer is one explanation for this (see section 2.2.3).

The maturation of a gas-prone source rock on the contrary is thought to produce significant volume increase percentages. Calculated by Ungerer et al. (1983), values between 50-100 % initial volume increases have been published. Despite this, the magnitude of pore fluid pressure generation is commonly disputed within the literature with early work seemingly underestimating volume increases. Latest estimates published by Hansom & Lee (2005) suggest from numerical modelling that oil generation can cause excess pore pressures 40 % larger than those generated by compaction processes alone. Gas generation can yield pressures upward of 110 % of that from solely disequilibrium compaction, while CH4 production from oil and kerogen cracking yields up to 150 % attributing to 4776 psi overpressure. Swarbrick et al. (2002) present similar results showing volume increases may be as high as 140 % in later stage oil to gas maturation attributing to upwards of 6000 psi overpressure. These values are taken within a closed system with no hydraulic connection to lower pressures. In contrast, Ungerer et al. (1983) show small decreases in volume (3-6 %) in type II kerogen to oil maturation, but up to 57 % volume increases with gas generation. Oil cracking solely encompasses overpressure generation from volume expansion (Spencer 1987; Barker 1990; Caillet 1993).

Clearly the generation of hydrocarbons has a strong impact on overpressure magnitudes in many basins world-wide (Momper 1978; Stainforth 1984; Law & Dickinson 1985); although accurate degrees of magnitude are still unclear. Within the North Sea many authors (Gaarenstroom et al. 1993; Holm 1998; Buhrig 1989;) all support the conclusion that hydrocarbon generation is a principal or even main cause of overpressures in pre-Cretaceous rocks.

2.2.3 Overpressure Generation Mechanisms – Load Transfer Mechanisms

Load transfer is a new concept and term used to describe the onset of overpressure through bulk rock compressibility. The total amount of overpressure generated by load transfer is described by the relationships between effective stress and porosity. It covers a whole range of conditions where load bearing molecules, be they kerogen or clay minerals, are altered to a state where they no longer contribute to supporting the load of the overburden, i.e. not linked to effective stress. The stress that was once supported by said molecules is now born by the pore fluids, providing the presence of a closed pore system.

As discussed previously, the transformation of kerogen to petroleum is thought to contribute to an increase in volume, and thus pressure, assuming a closed or restricted pore network system hindering fluid expulsion and pressure equilibration. Overpressure results from processes relating to load transference of the overburden from the solid kerogen compounds to the pore fluids (see Figure 2.5).

A similar principal is also observed within smectite to illite transformation (Lahann 2002) and dissolution of grain contacts (Mallon & Swarbrick 2002).

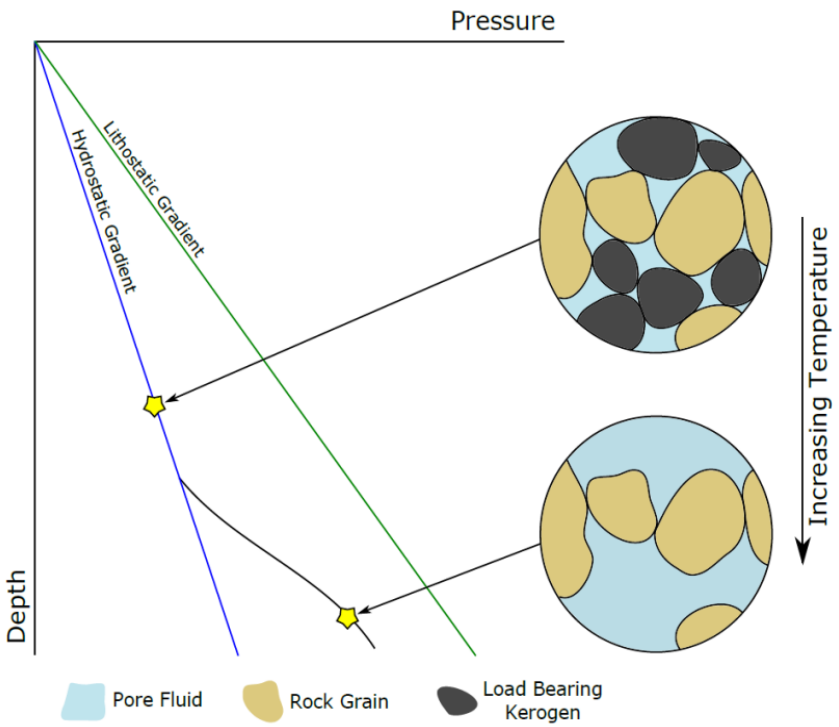

Figure 2.5 - Schematic diagram displaying the transformation of load bearing kerogen into liquid pore fluid thereby transferring the load from a solid kerogen rock matrix component to the pore fluid. This increases the pore pressure and is shown by black formation pressure gradient line. The migration of oil has removed it from this section of the rock. (Diagram adapted from Osborne & Swarbrick (1998)).

2.2.4 Overpressure Generation Mechanisms – Chemical Compaction Mechanisms

The cementation and dissolution of minerals during diagenesis will clearly have an effect on the rock permeability and porosity, thus influencing overpressure generation. In the case where permeability is sufficiently low to inhibit effective fluid expulsion, quartz cementation is considered to contribute to overpressure generation. Quartz generation is a non-direct mechanism for overpressure generation. Based upon the principal that quartz is precipitated into pore spaces (controlled by change in temperature, pressure and surface area), stylolitisation and cementation follows and porosity is reduced. This will increase the pore pressure should the permeability loss reduce the effective fluid loss during compaction. Within carbonates a similar process can be observed involving stylolites.

It is, however, considered by Osborne & Swarbrick (1998) that quartz cementation is linked with pore pressure. It is suggested that with increasing pore pressures the quartz cementation rate is reduced. Despite this, the effects of temperature and surface area of the exposed solid are also key factors in to consider. Quartz reaction rates are considered relatively slow at temperatures of approximately 200 °C and below. Therefore, although dissolution of quartz will occur at a slower rate in higher pore fluid pressures, in reality the effect is of minor relevance < 200 °C as precipitation rate in itself is low. At greater depths, and temperatures of > 200 °C precipitation of quartz can be an important mechanism, particularly regarding the lithification of faults (Streit 1997). In reality, quartz precipitation rates are defined by a gradient reaction incorporating changes in pressure, temperature and/or area of exposed surface.

2.2.5 Overpressure Generation Mechanisms – Other Mechanisms

The following comprise important factors regarding the transference of overpressure and, to an extent, the generation as well.

2.2.5.1 Buoyancy Related Overpressure

Oils and gases are generally less dense than water, and as such, display a steeper pressure gradient compared to that of the hydrostatic gradient.

As Figure 2.6 shows, the excess buoyancy overpressure pressure is a function of both fluid type (allowing for a varying density) and hydrocarbon column length. Buoyancy pressure can be calculated using the following expression:

$$P_{buoy} = (\rho_w - \rho_{hc}).g.h \qquad \text{Eq. 2.5}$$

where P_{buoy} is buoyancy pressure, h is hydrocarbon column height, g is gravity, ρ_w is water density and ρ_{hc} is the density of the hydrocarbon.

In a multi-phase system the P_{buoy} of the oil phase will have to be calculated as an addition to that of the gas phase.

2.2.5.2 Potentiometric (Hydraulic Head) Related Overpressure

Overpressure can result from an elevated water table in areas associated with highland regions. Often observed in artesian wells (Swarbrick & Osborne 1998), overpressure generated under such conditions are also observed in foreland basin interiors in North America (e.g. Alberta Basin; Bachu & Underschultz 1995).

Assuming a sealed reservoir, with no pressure drop, overpressure purely by a potentiometric head can be calculated with the expression:

$$OP = \rho_w.g.E \qquad \text{Eq. 2.6}$$

where E is the elevation above datum point (often taken as mean sea level; Mouchet & Mitchell 1989).

In general, the effects of a potentiometric head will be minimal in regards to other OP generation mechanisms. Pressures of 10,000 psi (encountered in North Sea Mesozoic reservoirs) would require a 23,000 ft water table elevation. Pre-Cambrian basement rocks reach a maximum elevation of 8,200 ft in Norway, far less than the required height to be solely responsible for observed overpressures (Swarbrick & Osborne, 1998).

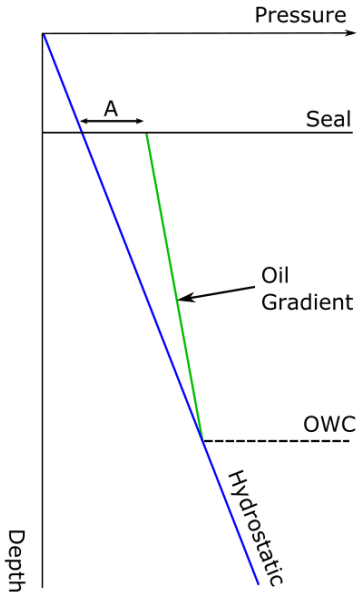

Figure 2.6 - Schematic displaying how the addition of a hydrocarbon column can increase the overpressure. A normally pressured field aquifer (blue line) can possess an overpressure (A) due to hydrocarbon buoyancy caused by lower fluid density in the hydrocarbon phase.

2.2.5.3 Osmosis

Contrasts in formation fluid brine concentrations can induce the transfer of fluids across a semi-permeable membrane. Overpressure magnitudes generated from osmotic effects are controversial due to a limited understanding of membrane properties in geological mediums (Neuzil 2000).

Swarbrick & Osborne (1998) calculated 435 psi maximum osmotic related pressures from North Sea rocks, suggesting minimal contribution to highly overpressured formations. Contrasting these North Sea results, Neuzil (2000) published calculations from Cretaceous Pierre Shales in South Dakota producing 2900 psi osmotic pressure anomalies. This suggests that the potential for osmosis related overpressure is significant, although may be overlooked in many hydrocarbon basins. It is noted, however, that brines in overpressured zones tend to be of lower salinity

than adjacent lower salinity formation waters. This will have a negative effect on maintaining overpressure.

2.2.5.4 Overcompaction

Although technically not an overpressure generation mechanism, overcompaction processes can result in overpressured formations. Uplift of normally pressured rocks that maintain pressures obtained at greater depths will lead to overpressure, assuming pressures cannot dissipate during uplift. This is a key mechanism for highly overpressured rocks at shallow depths. This is of particular interest within the Baram province, Brunei (Tingay et al. 2009). Important for this report, however, is the effects uplift and exhumation has had upon North West Europe formations. The Irish Sea basin system is thought to be subject to some of the most severe uplift. Uplift estimates range upwards of 2.2 km from geophysical log data taken from the Sellafield Borehole area (Chadwick et al. 1994).

2.2.6 Lateral Transfer and Drainage

Lateral transfer, not a generation but distribution mechanism, encompasses the transference of pressures within a tilted sealed permeable system (e.g. an isolated sand body) from deeper regions with naturally occurring higher pressures (resulting due to pressures increasing with depth below the FRD). These pressures equilibrate within the sand body producing abnormally high pressures at the structural crest and lower than expected pressures down-dip. The equilibrium point is termed the centroid and located centrally within the sand body. The centroid represents the depth where the sand body pore pressures are equal to that of the surrounding sealing lithology. This is illustrated in Figure 2.7. An isolated tilted sand body is depicted with its corresponding pressure depth plot illustrating the effects of lateral drainage. The shown sand body is enclosed within an envelope of overpressured shales, all deeper than the FRD. The black pressure gradient shows the pressure profile through the

shale. Due to the fact that overpressure increases as a function of depth below the FRD, the base of the sand body possesses higher pressures than that of the top of the sand body. The up-dip pressures are being influenced by the higher pressures down-dip and as such possess higher overpressures than expected, depicted by 'a' on Figure 2.7 - a potential drilling kick hazard. Conversely, due to the same principal, the down-dip pressures are less than expected (shown by 'b') – thus presenting a potential drilling fluid loss problem. The actual pressure profile within the sand body is indicated by the green gradient on Figure 2.7. Lateral transfer is thought to be a key contributor to overpressure encountered within Palaeocene sandstones within the North Sea.

In the case where the sand body is hydraulically connected to the surface, or a high permeability formation allowing drainage, the pressure profile would display a near hydrostatic gradient as the formation fluids, given adequate permeability, can equilibrate. In the event the surrounding formations are overpressured, the transition into the normally pressured formation could induce a loss of drilling fluid.

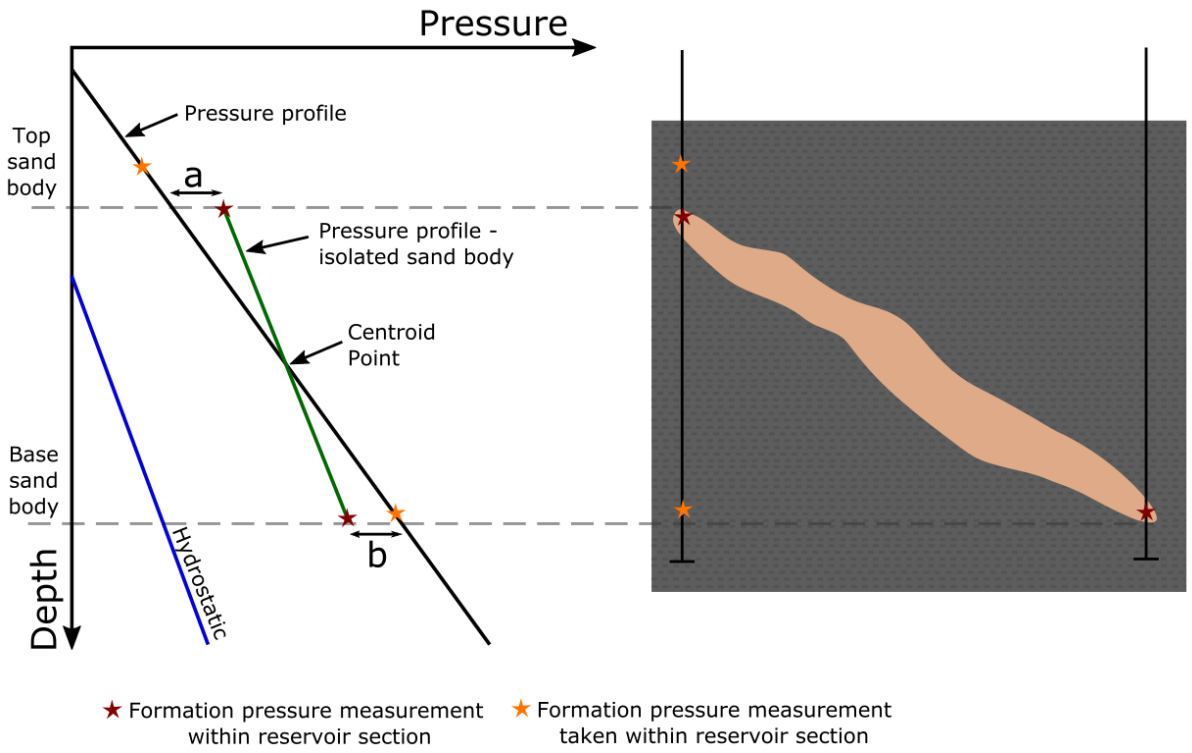

Figure 2.7 - Schematic illustrating the effects of lateral transfer. The pore pressures at the top of the sand body display higher than 'expected' pore pressures due to effects of lateral transfer from higher overpressured down-dip formations. The centroid displays the point where the sand body pore pressures equal that of the surrounding sealing lithology.

2.3 Pressure Cells

When discussing the distribution of overpressures, no matter where the location, it is important to define and understand the concept of a pressure cell. Although Bradley (1975) originally discussed low permeability pressure barriers, the paradigm of a pressure cell was first introduced by Powley (1990) and can be defined as a compartment where subsurface overpressured fluids are in internal communication. Furthermore, aquifer pressure gradients are parallel to the local hydrostatic pressure gradient (Darby et al. 1996). Pressure compartments are observed in basins worldwide (Bradley 1975; Hunt 1990; Powley 1990; Bradley & Powley 1994; Neuzil 1995; Darby et al. 1996) and are characterised by the presence of low (or zero) permeability barriers or pressure seal restricting flow (Darby et al. 1996). Pressure cells are considered to fall into 2 main categories:

1. **Static pressure cell** – The idea of a static pressure cell is based upon the concept that there is no communication between the overpressured fluids within the cell parameters and those from outside them. A zero permeability seal to pressure encloses the cell. This implies the presence of a diagenetically-cemented seal (Hunt 1990; Powley 1990; Ortoleva 1994 etc.) or capillary-pressure restricted flow (Iverson et al. 1994; Deming et al. 2002 etc.).
2. **Dynamic pressure cell** – Flow is restricted, but not prevented, by low permeability rocks (Neuzil 1995; Darby et al. 1996). This is primarily based upon the assumption that pressure cells generally occupy sedimentary rocks and, as such, must possess a degree of permeability at least.

If the concept of a dynamic pressure cell is correct then Muggeridge et al. (2005) states that the rate of overpressure generation must be sufficient to counteract the rate of pressure dispersion from the margins or the overall rate of pressure dispersal is so minimal there is little effect over geological time scales. The general rate of overpressure dissipation is debateable and perhaps not comparable on a regional level.

Having said that, there are studies that show that once the pressure generation stops, the remaining overpressure should dissipate within a period of 1 million years (Deming 1994; Luo & Vasseur 1997; Lee & Deming 2002). Conversely, it is suggested that on a reservoir scale overpressure will disperse within 10,000 years and on basin scales overpressure can be maintained for tens of millions of years (Muggeridge et al. 2005). The overriding control is permeability. The pressure distribution is slowed by barriers possessing low permeability and the storability of compartments. Pressure cell compartments are, in general, grouped together in basins deeper than 8,200 ft and above and below normally pressured compartments (Bradley 1975; Hunt 1990; Powley 1990; Bradley & Powley 1994).

Chapter 3

Failure Mechanics and Seal Breach

Chapter 3 - Failure Mechanics and Seal Breach

The following chapter elaborates upon the processes associated with hydrofracturing of reservoir caprocks resulting from high fluid pressure regimes. Furthermore, the effects and limiting nature this process has on column height are discussed. Basic concepts are explained and related previous studies within literature are reviewed.

3.1 Controls on Hydrocarbon Column Heights

Hydrocarbon column height can be affected by a long list of factors. Despite this, the main influences are summarised below. Broadly speaking these can be split into 3 categories; structurally restricted, volumetrically restricted, and geomechanical/seal failure restricted.

1) **Structurally restricted** control is independent of the hydrocarbon charge. The main influence within the structurally restricted category is closure height. This is the difference between the structural crest of the reservoir and the lowest closing contour, defined by the spill point. This is shown on Figure 3.1. 3.1(A) and 3.1(B) both represent a trap with ample supply of hydrocarbons. Trap A has a closure area (spill point – crest depth) less than that of trap B. Both traps are full-to-spill with the column height at the maximum they can structurally be. Trap B has a higher closure capacity and thus holds the larger column. The HWC (hydrocarbon-water contact) is equal to the spill-point depth. Trap C is under-filled with the spill point being deeper than the HWC. This trap is not structurally limited. The smaller column is likely due to categories 2 or 3 below.

2) **Volumetrically restricted/rate of leakage -** Column heights are independent of the traps closure capacity. This factor involves a lack of initial hydrocarbon charge entering the trap. This could be due to a source rock that is not producing a sufficient charge to fill the trap.

On the other hand, the source rock may produce a suitable hydrocarbon charge to fill the trap (as the Kimmeridge Clay within the North Sea is thought to), but the migration pathway fails to facilitate the movement towards the closure, i.e. permeable faults or lithology variations. While this could lead to a loss of hydrocarbons, it could potentially assist in the movement to stratigraphically shallower traps (e.g. the Ekofisk field – see van den Bark & Thomas, 1981).

The Jurassic organic rich facies (including that of the Kimmeridge Clay) known to supply the majority of the North Sea oil fields, commonly contains between 2 – 15 weight percent TOC[1] (Cornford 1998). The Swanworth Quarry 1 borehole displays TOC values of between 30 – 40 % (Morgans-Bell et al. 2001). High TOC rates and substantial periods of time within maturity conditions imply that source supply volume is not limiting within the North Sea. The migration pathways within the North Sea vary from between 2 -17 km (Cornford 1998) with a generally high efficiency of migration.

3) **Geomechanical/seal failure restrictions** involve the deformation of the caprock facilitating in the vertical tertiary migration of hydrocarbons. The two major influences of relevance to hydrocarbon column height preservation and, as such, to this study are:
    - *Control of capillary leakage through matrix*
    - *Control by mechanical failure (fracturing)* - This is the main discussion topic of this report and is discussed further in the section below.

[1] Total organic carbon – the concentration of organic material in a rock. Percentage is equal to the weight percent of total carbon.

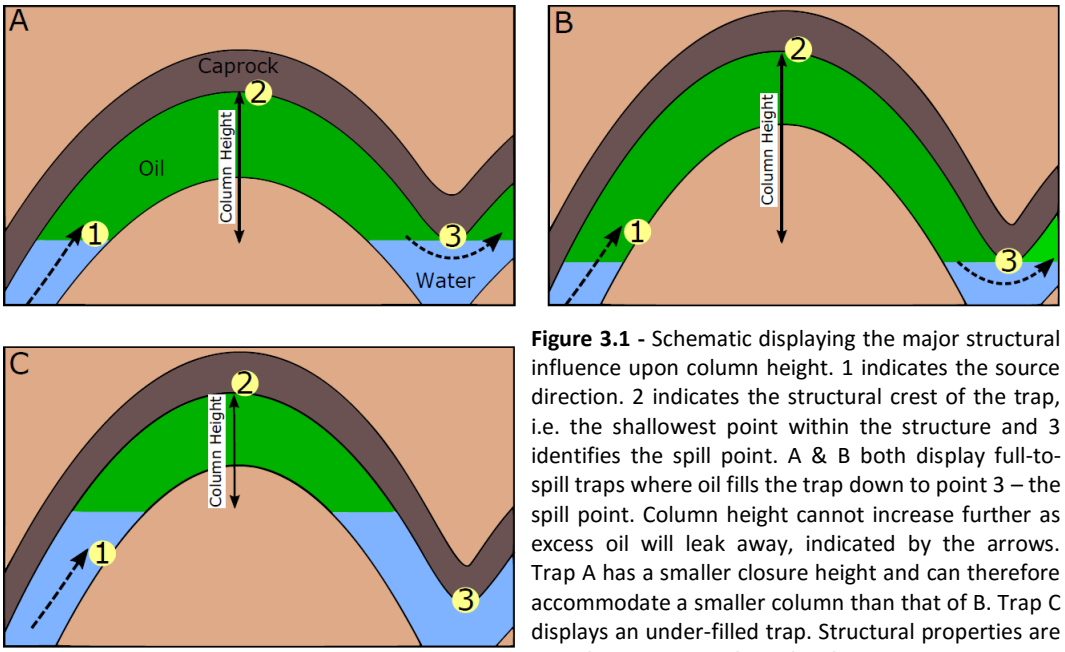

Figure 3.1 - Schematic displaying the major structural influence upon column height. 1 indicates the source direction. 2 indicates the structural crest of the trap, i.e. the shallowest point within the structure and 3 identifies the spill point. A & B both display full-to-spill traps where oil fills the trap down to point 3 – the spill point. Column height cannot increase further as excess oil will leak away, indicated by the arrows. Trap A has a smaller closure height and can therefore accommodate a smaller column than that of B. Trap C displays an under-filled trap. Structural properties are not a limitation to column height.

3.2 Capillary Seal Failure

When hydrocarbons escape through the caprock of a trap it is deemed leaking/leaked; the leakage of a seal can occur by a singular mechanism or by a combination should the correct conditions be met. These mechanisms are discussed below.

3.2.1 Caprock Membrane Failure

For petroleum to migrate into a water-wet sealing rock the caprock capillary resistance needs to be overcome (England et al. 1987). The buoyancy pressure required for this to occur is termed the threshold capillary pressure (Jennings 1987). For continual hydrocarbon migration through the caprock, critical petroleum saturation must be met. The critical saturation is the point at which oil forms a continuous film around grains allowing an uninterrupted pathway from the reservoir to closure. Schowalter (1979) estimates minimum values, based upon laboratory experiments, of oil saturation between 4.5 – 17 %, with an overall average of 10 %. Once buoyancy pressures exceed the capillary entry pressures, multi-phase movement of a non-wetting medium through the rock can occur (Ingram et al. 1997; Aplin & Larter 2005). Capillary sealing transpires at the boundary between the non-wetting reservoir and

wetting caprock. The height of a static hydrocarbon column that can theoretically be sealed by capillary sources can be calculated from Eq. 3.1 (Berg 1975; Schowalter 1979; Watts 1987):

$$P_e = \frac{2\gamma \cos\theta}{r_s} \qquad \text{Eq. 3.1}$$

Using SI units, P_e is the capillary entry pressures (Pa), γ is the surface tension (N/m), θ is the wetting angle (degrees) and r_s is the pore throat radii of the seal (m) (Ingram et al. 1997). It can therefore be said that capillary failure can occur when:

$$(\rho_w - \rho_p).g.h \geq \frac{2\gamma \cos\theta}{r_s} \qquad \text{Eq. 3.2}$$

When ρ_w and ρ_p are the subsurface densities of water and hydrocarbon respectively, g is the gravitational acceleration and h is the hydrocarbon column height. The first half the equation in essence is the buoyant driving force as a function of subsurface contrasts in density between petroleum and water and the height of the hydrocarbon column. When considering the effects to overpressure an extra component must be considered. The maximum column height which a seal can retain can be expressed as:

$$h = \frac{2\gamma \cos\theta}{r_s(\rho_w - \rho_p)g} - \frac{\Delta U}{(\rho_w - \rho_p)g} \qquad \text{Eq. 3.3}$$

where ΔU is the difference between the overpressure in the reservoir relative to the seal (Clayton & Hay 1994).

Capillary seals are independent of seal thickness (Ingram et al. 1997). Although seals with greater thicknesses may be less prone to being breached by juxtaposing hydrofractures, seals cannot in theory retain higher pressures than those of thinner seals through capillary resistance.

3.2.2 Influences on Capillary Failure

Capillary entry pressure in mudstones is primarily influenced by grain size at a given porosity (Aplin & Larter 2005). Clay rich muds, in general, can be effective capillary seals from shallow depths. However, as the silt content of mudstones increases greater burial, diagenesis, mechanical and sometimes chemical compaction is necessary (Aplin & Macquaker 2011).

On micro scales it is apparent that mudrocks contain heterogeneities caused by various aspects including waves, gravity driven processes and currents. This causes packages with varying porosity and permeability, in turn altering capillary entry pressures (Aplin & Macquaker 2011). In addition to lithological controls, trap shape can affect capillary leakage rates. Large area, low relief traps are more likely to retain greater hydrocarbon column heights in comparison to narrower, high relief traps (Ingram et al. 1997).

Aplin & Larter (2005) argue that once a water-wet caprock is breached the leak path through the seal could diverge from being primarily water-wet to more oil-wet. This process, caused by sorption of reservoir hydrophilic and, importantly, hydrophobic compounds onto mineral surfaces, can lead to a wetting state reversal. Oil-wet caprocks therefore, act as a flow hindrance slowing migration and not, in fact, a seal halting it. Once the caprock becomes oil-wet capillary forces can, theoretically maintain a continuous flow of hydrocarbons through the caprock, draining the reservoir.

Mercury injection measurements of offshore Norway caprocks display very small pore throat sizes and low permeability (k<40 nD) (Schlömer & Krooss 1997). The caprocks also hold significant hydrocarbon columns suggesting that pore network leakage, especially in the Haltenbanken region within the Norwegian Sea, is unlikely. Despite this, Snorre (Northern North Sea, Norwegian Sector) has 1000 ft economic hydrocarbon column and is thought to be subject to capillary leakage. A matter of leakage rate is now a question. Within the North Sea generally, column heights and, therefore, buoyancy pressures, are low (see Chapter 5). Although there are some fields that are thought to be subject to membrane seal failure (Snorre, for example) these

fields are rare and often discussed within the literature. Unless otherwise stated it is considered that capillary leakage will not have drastic effects on the underlying hydrocarbon column height within the North Sea. Those fields that could oppose this suggestion will likely be noted within the literature and duly considered as to their relevance to this study.

3.3 Rate of Leakage

Already mentioned, the rate at which a seal leaks is an important consideration. A seal can, by all extents, be 'leaking'[2] yet still possess an accumulation. There are 2 main reasons that this may be the case. 1) The rate of hydrocarbon leakage is less than that of hydrocarbon supply and 2) hydrocarbons are leaking but at a geologically slow time scale and as such an accumulation is still present at this period. Given time though, the closure will empty of hydrocarbons. Evidence is published (for example Caillet, 1993; Leith & Fallick, 1997 & Aplin & Larter, 2005), indicating the Snorre field, within the Norwegian sector of the Northern North Sea, has leaked with hydrocarbons found 2000 ft (Leith & Fallick 1997) into the caprock. Contrasting views on the leakage mechanisms are published. Bond, K (2001) suggests that the 1000 ft hydrocarbon column is great enough to cause membrane failure, whereas, Caillet (1993) suggests the presence of hydrocarbons within the seal is the result of hydrofracturing.

When discussing membrane seal failure, i.e. hydrocarbons are migrating through the caprock membrane, Ingram et al. (1997) states that the "leakiness" of a seal can be defined by dividing the relative permeability of a caprock (k) times a unit area (A) by the length of time in which a pressure drop is occurring (Δl) - $\frac{kA}{\Delta l}$. A low $\frac{kA}{\Delta l}$ relative to a higher $\frac{kA}{\Delta l}$ is indicative of a lower rate of seal leakage, and vice versa. Trap shape affects leakage rates. Large, low relief traps are more likely to retain large HC volumes in relation to smaller, high relief traps over a given $\frac{kA}{\Delta l}$.

[2] Facilitating the migration of hydrocarbons from the reservoir through the caprock.

3.4 Caprock Integrity and Mechanical Failure Limiting Hydrocarbon Column Heights

High or increasing pore pressures can lead to seal breach and caprock failure. The categories for mechanical failure influencing leakage can be split into 3 groups (Mathias et al. 2009):

1) Tensile Failure
2) Shear Failure
3) Re-shearing/reactivation of existing fractures

3.4.1 Mechanical Failure

It has long been recognised that overpressured fluids, be it excess buoyancy from hydrocarbons or abnormally high aquifer pore pressures, can cause natural fractures and fissures within rocks facilitating the loss of hydrocarbons (Chen et al. 1990; Capuano 1993; Bowers 1995; Roberts & Nunn 1995; Ingram & Urai 1999; Cartwright et al. 2007).

3.4.1.1 Tensile Failure

The criteria for tensile hydrofracturing can, in its simplest form, be expressed by equation 3.4 (see Jaeger et al. 2007, pg. 99):

$$P_p \geq \sigma_3 + T \qquad \text{Eq. 3.4}$$

Where P_p is pore fluid pressure, σ_3 is the minimum principal stress and T is the tensile strength of the caprock. Such fractures will form perpendicular to the minimum effective stress (σ_3). In general, passive and extensional basins have a horizontally orientated σ_3 and, as such, fractures will form in a vertical orientation facilitating top seal leakage of potential underlying hydrocarbon accumulations.

Therefore, when reservoir pore pressures (including excess hydrocarbon buoyancy) exceed the least principal stress and tensile strength of the rock, hydrocarbons can then escape via fracture networks. Fracturing leads to decreased capillary entry pressure and higher permeability, thus greater risk.

Pressure related (Mode 1) hydraulic fractures have a direct effect on the volume and as such, the column height of the reservoir's hydrocarbon accumulation. Figure 3.2 shows a simplistic schematic of just this. It is important to note that as the pore pressure equals fracture pressure (shown as a gradient on figure 3.2); fractures will open within the caprock, facilitating leakage of the reservoir fluids.

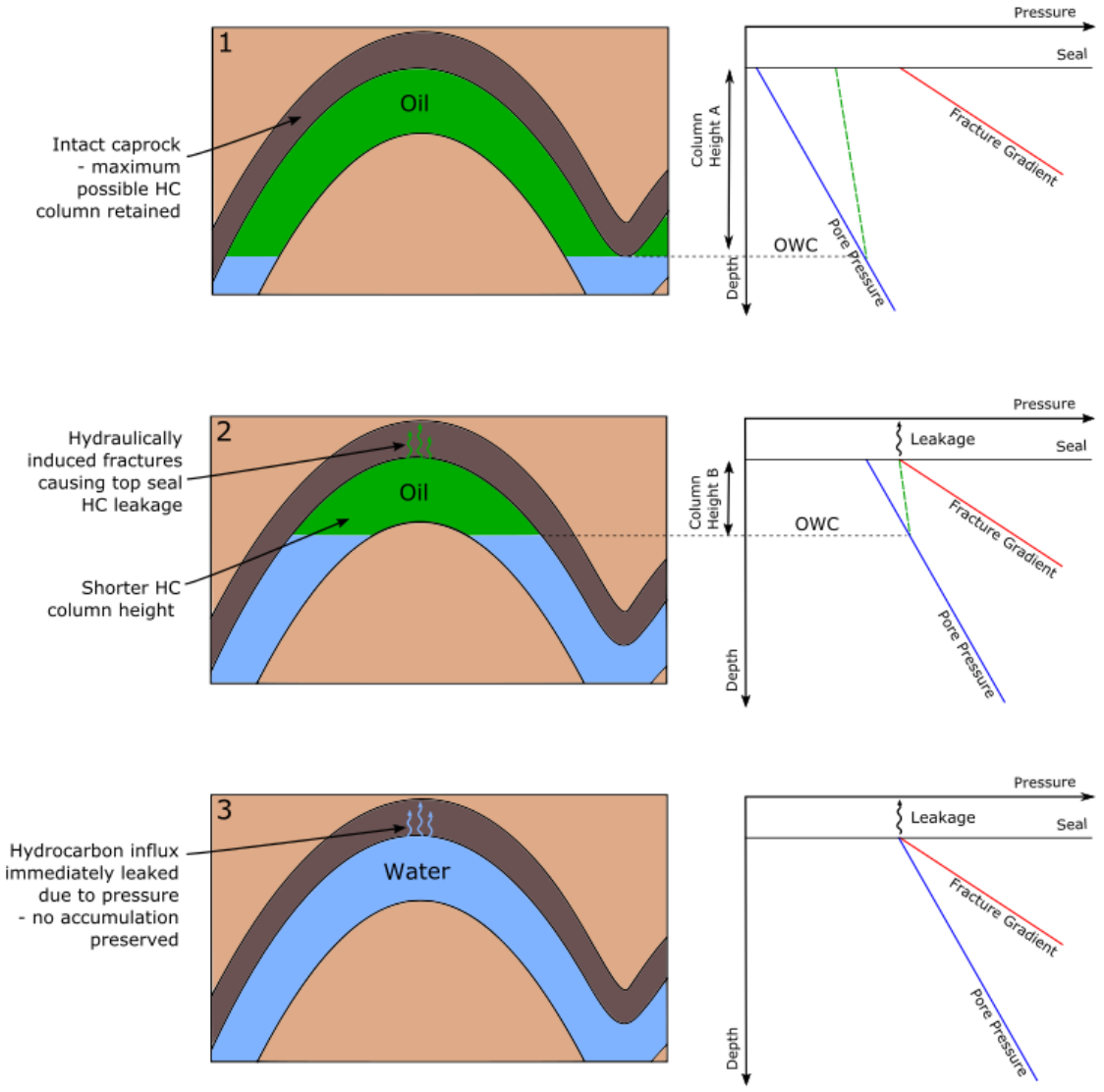

Figure 3.2 - Schematic displaying the 3 main pressure categories of traps. Closure Type 1 indicates a trap with an aquifer pressure significantly less than the fracture pressure. As a result of this, a hydrocarbon column can accumulate without impinging on the fracture pressure. The caprock remains intact. Closure Type 2 represents a pressure regime where the pore pressure at the crest of the reservoir is equal to that that of the fracture pressure, however the aquifer pressure at the structural crest is less than the fracture pressure. Any additional hydrocarbon influx will not affect the OWC or column height as mode 1 fractures will open and the excess hydrocarbons will be lost through caprock failure. Both The OWC and column height are constant. Closure Type 3 is indicative of a trap where aquifer pressure is equal to the fracture pressure. No column is retainable as any increase in pressure will hydrofracture the caprock and the hydrocarbon will leak.

This will tend to occur at the structural crest (or shallowest point on the field structure) as this is where the seal capacities will be smallest.

Figure 3.2 (1) displays a closure possessing maximum pore pressures significantly less than that of the corresponding fracture pressure – this will be termed "Closure Type 1". Figure 3.2 (2) displays a closure with pore pressures equalling close to the fracture pressure while still maintaining a hydrocarbon column, this is termed "Closure Type 2". Finally, Figure 3.2 (3) displays a closure where the aquifer pressure is equal to that of the fracture pressure. No hydrocarbon column is present. This is termed "Closure Type 3".

Closure Type 1

Closure Type 1 displays a pressure regime with reservoir pore fluid pressures less than that of the fracture pressure. This permits a hydrocarbon column to accumulate without increasing the risk of hydrofracturing the caprock. The only limit to the column height confined within the Closure Trap 1 is hydrocarbon flux into the trap or closure capacity (see section 3.1).

Closure Type 2

Closure Type 2 displays a pressure regime where the pore pressure at the crest of the reservoir is equal to that of the fracture pressure. The closure contains the maximum column height feasible with an aquifer pressure less than that of the fracture pressure. Any additional flux of hydrocarbons into the trap will further hydrofracture the caprock causing tertiary migration, leakage. The only alteration with column height would be the result of changes in hydrocarbon density/phase resulting from in influx of gas or oil. The presence of a hydrocarbon accumulation distinguishes this closure type to Closure Type 3. This is based on the commonly accepted assumption that failure occurs when pore pressures equal that of the fracture pressure. Discussed further on, there is an argument by Bjørkum et al. (1998) & Swarbrick et al. (2010) that this may not be the case in water wet seals.

The hypothesis effectively states that aquifer pressures have overriding control on the caprocks failure regime.

Closure Type 3

Closure Type 3 cannot enclose a hydrocarbon column of any phase. The aquifer pressure at the top of the reservoir is equal to that of the fracture pressure. Therefore, any petroleum influx into the trap will naturally raise the pore pressure, hydrofracture the caprock and subsequently be leaked from the structure. A hydrocarbon column could only accumulate within this structure if for example the fracture pressure is increased or the aquifer pressure itself is reduced.

Through these basic principles alone the Closure Types 2 and 3 are of particular interest when examining the effects overpressure can have on controlling the column height.

Maximum overpressure gradients (i.e.$\frac{formation\ overpressure}{TVDss}$) have been documented for a variety of regions. Timko & Fertl (1971), Leach (1993a, b, c) and Dow (1984) all propose a limit of 0.85 psi ft^{-1} for the Gulf of Mexico. Nashaat (1998) proposed similar figures for Egypt's Nile Delta and Sinai basin. Heppard et al. (1998) suggested 0.73 psi ft^{-1} as an upper limit in Trinidad and Belonin & Slavin (1998) proposed a gradient of 0.81 psi ft^{-1} in the former Soviet Union.

Vertical fractures are solely highlighted within Figure 3.2. This is due to the focus of this report being biased towards the North Sea, an extensional setting. As such σ_3 will primarily be the horizontal stress (S_h) thus promoting fracture propagation in a dominantly vertical orientation. This is not always the case however. For example in reverse fault stress regimes, hydraulic fractures planes are horizontal. For example, Robert & Brown (1986) & Sibson (1994) consider that a LOP above S_v does not automatically mean $S_{hmin} > S_v$ because of the tensile strength of the rock. There are many LOPs above S_v in carbonates within normal faulting setting due to the high tensile strength of carbonates/limestones.

3.4.1.2 Shear Failure

Shear is an important aspect when considering the geomechanical failure of a reservoir caprock. When considering shear, it is useful to utilise and understand Mohr Circles and Coulomb's failure criterion. An example Mohr Circle is shown in Figure 3.3 The black circle is intersecting with the failure envelope within the shear region. Calculated by the differential effective stress (σ'_1- σ'_3), the angle at which the circle intersects the failure envelope displays the optimum orientation for a fault to slip (2θ). As the differential effective stress increases, so does the diameter of the Mohr Circle. This brings the rock closer to the failure envelope until they intersect and shear failure occurs.

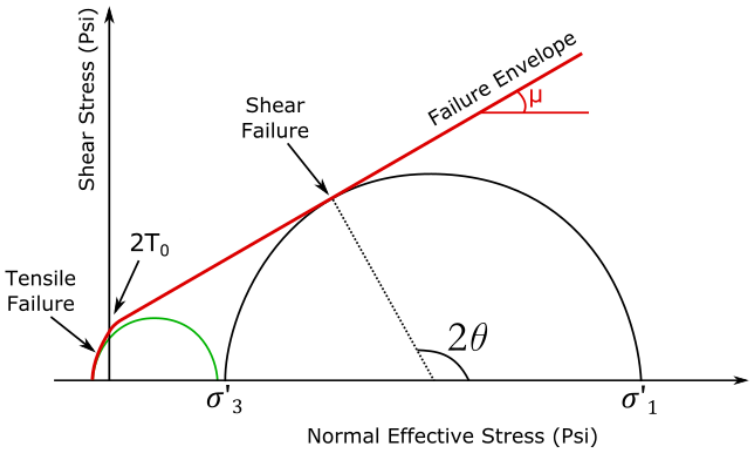

Figure 3.3 – Example of Mohr Circle. The black circle displays a formation with high differential stress. The diameter is therefore greater and intersects the failure envelope under shear regime. A low actual stress and small differential stress green circle intersects the tensile failure envelope.

Increasing the pore fluid pressure sees a leftward shift of the Mohr Circle (see Figure 3.3). Due to the nature of the failure envelope, this too brings the rock closer to failure and shows how increasing pore fluid pressure can lead a rock to fail with mode 2 fractures or mode 1 (as shown by the leftward progression of the green circles on Figure 3.4.

Delineating a failure envelope allows shear failure pressures to be estimated. The following equation from (Gudmundsson, 2011) recognised as the Coulomb failure criterion defines such an envelope.

$$\tau = \tau_0 + \mu\sigma_n \qquad \text{Eq. 3.5}$$

where τ is the slip plane shear stress, τ_0 is the cohesive strength, μ is the coefficient of internal friction and σ_n is the normal stress.

However, the Coulomb equation is based upon a 'Coulomb material', a dry rock. In-situ reservoir rocks contain formation fluids which must be considered. As such, the following equation is a better representation of the Coulomb-Griffith equation (Eq. 3.6) and can be T written as follows:

$$\tau = 2T_0 + (\sigma_n - P_p)\mu \qquad \text{Eq. 3.6}$$

where P_p is the pore fluid pressure. In equation 3.6 cohesion (τ_0), as noted in Eq. 3.5, is substituted with twice the tensile strength, so that τ_0 is replaced by $2T_0$. The modification relates to Griffith theory where $\tau_0 = 2T_0$ (Gudmundsson 2011).

3.4.1.3 Reactivation of Previous Fractures

Assessing the Coulomb failure criterion, the simple conclusion can be reached indicating that re-shearing or reactivating pre-existing fractures occur in many cases instead of formation of new fractures. This is important to consider as this suggests that a rock's actual shear failure pressure will be the reactivation of previous fractures unless they are severely mis-orientated for failure.

The reactivation pressure of pre-existing fault can be expressed as follows (Jaeger et al. 2007; Zoback 2010):

$$\frac{\sigma_3 - P_{critical}}{\sigma_1 - P_{critical}} = [(\mu^2 + 1)^{\frac{1}{2}} + \mu]^{-2} \qquad \text{Eq. 3.7}$$

Where $P_{critical}$ is the critical pore pressure of critically aligned faults with zero cohesion, μ is tan φ and φ is the angle of internal friction of the rock in degrees.

Rearranged this can provide a pore pressure at which reactivation of shear faults can occur providing φ is known. This equation can be expressed as such:

$$P_{critical} = \frac{\sigma_3[(\mu^2 + 1)^{\frac{1}{2}} + \mu]^2 - \sigma_1}{[(\mu^2 + 1)^{\frac{1}{2}} + \mu]^2 - 1} \qquad \text{Eq. 3.8}$$

It is noted by many authors (Streit & Hillis 2004; Streit et al. 2005; Morris et al. 2012) that a fault reactivation envelope intersects with the y-axis at a lower shear stress than an envelope derived for formation of new fractures. A Mohr circle will intersect with the reactivation envelope prior to the envelope distinguishing initiation of new faults. This is only true however if the fault has a lower frictional strength than that of an intact rock. Despite being true in many cases, there are some exceptions. For example, Dewhurst & Jones (2002) have tested well lithified clastic lithology fault rocks from the Otway Basin, Australia, that is stronger than the intact host rock.

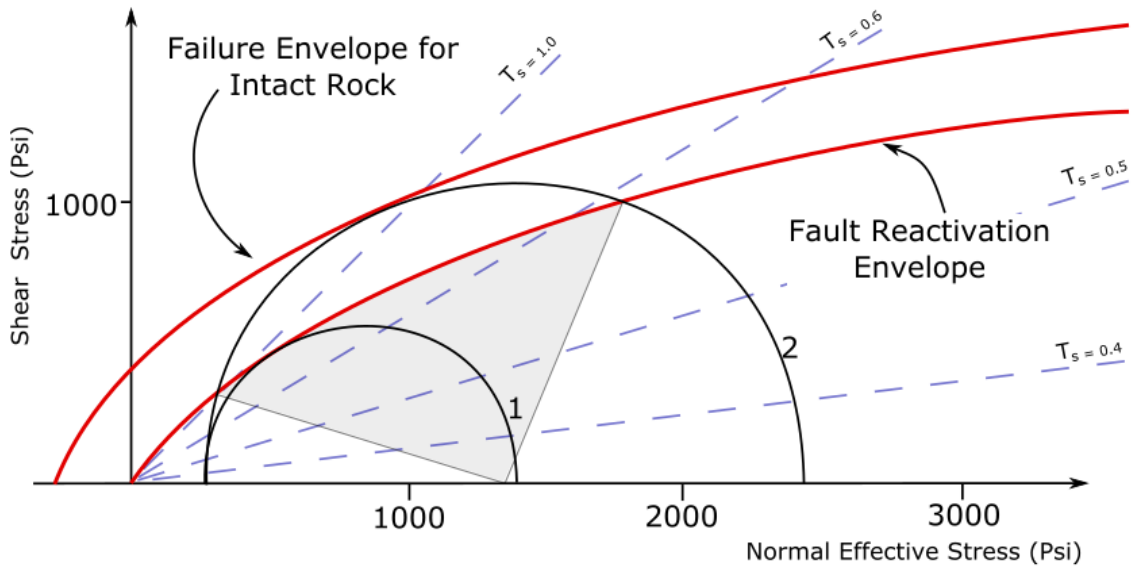

Figure 3.4 - Mohr circle indicating failure envelopes for shear of an intact rock and reactivation for a (cohesionless) fault. Important to note is the lower envelope for failure involving fault reactivation. This being true implies that a Mohr circle cannot intersect with the intact rock failure envelope as it will transect the fault reactivation envelope first. The shaded area represents all the possible angles with Mohr Circle 2 that can reactivate a (cohesionless) fault. Adapted from (Morris et al. 2012).

3.4.2 Pore Pressure Stress Coupling

A base concept that minimum horizontal stress increases as a general function of vertical stress, $\frac{\sigma_1}{\sigma_3}$ remains constant, can be applied to normally pressured formations. In reality, however, when dealing with overpressured formations, the principal that a coupling ratio exists between pore pressure and S_h must be deliberated. As pore

pressures increase, S_h can be seen to amend to higher than 'normal' values[3]. This coupling habit is observed within many pressure depth plots throughout the literature (see Gaarenstroom et. al, 1993 for North Sea, Figure 3.5) and within this report. A combination of data from the Canadian Scotian Shelf, the North Sea and the North West Shelf (Australia) all exhibit P_p/σ_h coupling values with minimum horizontal stress increasing at 60 - 80 % of the rate of pore pressure (Hillis 2003).

This is important to consider as this report focuses heavily upon the HPHT fields within the North Sea. A larger pore fluid pressure increase can be sustained prior to brittle failure and, therefore, hydrocarbon leakage than that of a standard equation applying an uncoupled approach. Simply put, a linear fracture pressure gradient derived using an equation not linked to P_p/S_h coupling, cannot be applied to deep, highly overpressured formations as this will present an underestimation of the failure pressure. Also important to note is the connotations to differential stress (σ_{diff}). Vertical stress is not coupled with pore fluid pressure. The leftward shift, combined with the reduction in σ_{diff} (and, therefore, Mohr circle diameter) thus proceeds to express the tendency for tensile failure to occur over shear failure unless a high P_p/S_h coupling ratio exists. This is shown on Figure 3.6. In a scenario where P_p/S_h coupling is not considered, increasing pore pressure will simply cause a leftward shift of the Mohr circle. This will likely, unless the

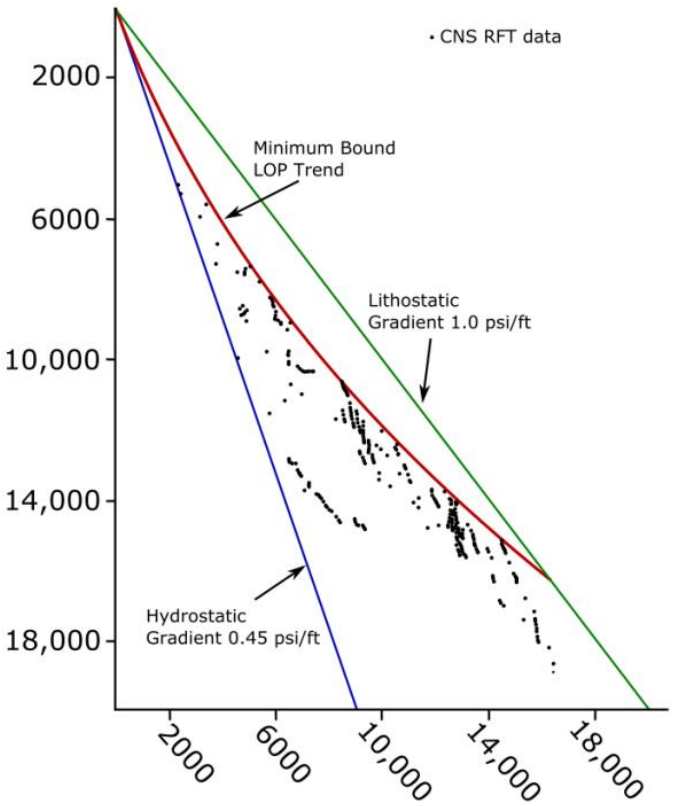

Figure 3.5 - Figure adapted from Gaarenstroom et al. (1993). Overpressured formation measurements increase in overpressure with depth. The red line (Gaarenstroom et al. (1993) minimum bound LOT line indicates Sh from LOT. This is shown to increase with increasing overpressure displaying the effects of Pp/$\mathbf{S_h}$ coupling.

[3] Normal values take into account P_p/σ_h coupling, associated with increasing overpressure, meaning σ_h does not increase on a constant gradient with depth.

differential stress is relatively small (green circles on figure 3.6), invoke shear failure. However, applying the P_p/S_h coupling theory, a reduction in differential stress causes the reduction in circle diameter (figure 3.6 (B) blue circle) permitting tensile failure. A high P_p/S_h coupling ratio could lead to the exception to this rule.

Within this report the theory of P_p/S_h coupling is applied, and within deep, highly overpressured formations differential stress is minimal. These conditions favour mode 1 failure, i.e. tensile failure. Due to complexities involving little knowledge of the permeability changes, both instantaneously and over time, post-failure fault reactivation still needs to be considered.

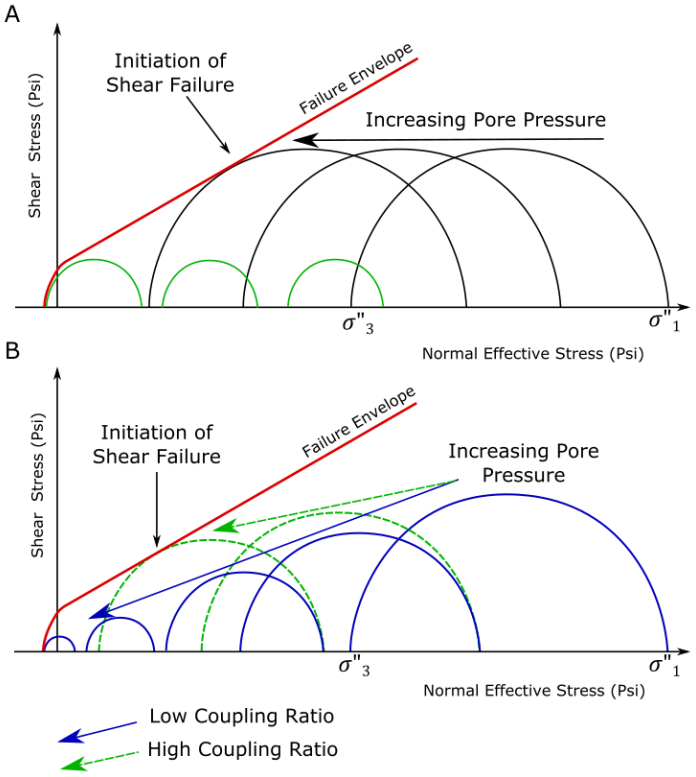

Figure 3.6 - The influence of pore pressure on Mohr Circles. A displays the uncoupled approach and an increasing pore pressure shown by a leftward shift. B shows the effect of Pp/$\mathbf{S_h}$ coupling. As a function of the coupling ratio, the leftward shift and decrease in circle diameter indicate increasing pore pressure. This suggests that Pp/$\mathbf{S_h}$ coupling favours tensile failure. Figure redrawn from (Tingay et al. 2009).

3.5 Pore Pressure Related Mechanical Failure and Associated Secondary Hydrocarbon Migration: A Review

Since the publication of Gaarenstroom et al. (1993) many authors have scrutinized, adapted and built upon work attempting to establish and quantitatively assess the relationships between overpressures, fracture gradients and the presence of economical hydrocarbon columns. Various different approaches have been used to create a regional fracture gradient, whereas other authors use local well-by-well calculations/LOTs to establish drilling windows. Despite a wealth of literature (Gaarenstroom et al. 1993; Ward et al. 1994; Holm 1998; Converse et al. 2000; Nordgård Bolås et al. 2005; Winefield et al. 2005; Swarbrick et al. 2010; Casabianca & Cosgrove 2012) no accepted views or conclusions have been reached with respect to seal failure criteria affecting hydrocarbon column heights and dry hole vs discovery.

The following section compares and reviews previous literature regarding the risk of hydrocarbon leakage and its association with high pore pressures. The following review summarises what is already understood and the high level of uncertainty associated with pressure related, mechanical seal failure.

A number of criteria need to be defined before an assessment on pressure-linked leakage is undertaken, including differing methods used to define fracture pressure, fracture/fluid pressure data and retention capacities. Furthermore, an evaluation of the validity and uncertainties of these criteria is important. What are the conflicting criteria associated with estimations of the fracture pressure (assessing stress regimes, differential stresses, the effects of Mohr Circle criteria etc.) and what are the opposing views on the relevance of buoyancy pressure[4]? For example, there remains the distinct possibility it is aquifer pressures that govern mechanical failure (Swarbrick et al. 2010) not the conventional approach of formation pressures. Finally, the idea behind the "ultimate seal" (Casabianca & Cosgrove 2012), and whether the seal capacities should be calculated at the crest (base seal) or higher in the stratigraphy (Swarbrick et al. 2010; Casabianca & Cosgrove 2012).

[4] The buoyancy pressure is defined as the excess pressure, above that of the extrapolated aquifer pressure, associated with the addition of an accumulation of hydrocarbons.

3.5.1 Estimations of Fracture Pressures

Clearly, one of the most important criteria to define is the pressure at which a caprock fails, thus permitting the leakage of hydrocarbons. There are varying methods used to calculate fracture pressures, but all can be generalised into either an algorithm method or one that utilises direct leak-off test data and whether this is taken on a well-by-well, regional or local basis. Gaarenstroom et al. (1993)'s defining paper utilises a minimum bound line defined by leak-off tests. This is stated as an estimation of the minimum horizontal stress as a function of depth. Figure 3.7, adapted from Gaarenstroom et al. (1993) indicates this minimum bound technique. LOP measurements greater than the minimum trend probably relate to the varying – and hard to accurately measure - tensile strengths of the rock, although it is not discussed. Similar to Gaarenstroom et al. (1993), Holm (1998), Converse et al. (2000) and Hermanrud & Nordgård Bolås (2002) also utilise LOT data as a proxy for minimum compressive stress/minimum horizontal stress. Again, this will all be based on the assumption that the rock or pre-exisiting fractures have no tensile strength. Despite the above assumption, within these authors analysis fracture pressure is the important parameter, and whether the tensile strength of the rock is considerable or not, the LOPs incorporate this parameter, indicating a

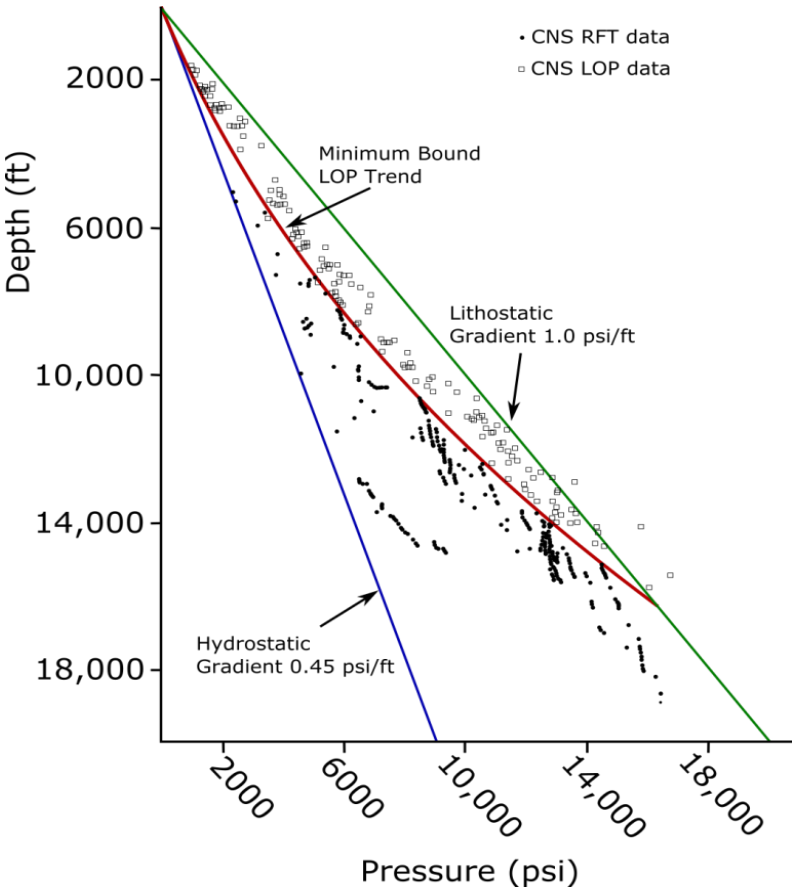

Figure 3.7 - Pore pressures and LOP as a function of depth. Pore pressures and LOP increase with depth. Black line indicates a lower bound LOT trend. (adapted from Gaarenstroom et al., 1993)

value considered a reasonable proxy to σ_3 (see Section 3.5.2.1).

Holm (1998) proceeds to use LOTs to estimate the minimum horizontal stress. LOTs are used to generate a fracture gradient but as the method for generating the line is unpublished, it is therefore unclear if the gradient is a minimum bound like that used by Gaarenstroom et al. (1993) or a different technique. Both Holm (1998) and Converse et al. (2000) discuss the impacts of effective stress and as such take the fracture pressure as equal to that of S_h.

Hermanrud & Nordgård Bolås (2002) also used leak off tests as a proxy for minimum horizontal stress. Following this, a single average overburden curve for the Haltenbanken was utilised as it was believed this was associated with a lower margin of error than density derived overburdens as discussed further in Hermanrud & Nordgård Bolås (2002) and Svare (1995).

After comparisons with a lower bound LOT curve from Gaarenstroom et al. (1993) a "Blown leaky seal line" was constructed by Winefield et al. (2005). This is defined via a best fit trend through RFT pore pressure measurements extrapolated to structual crests of leaky or blown structures (See Figure 3.8). A linear line was drawn through these crestal pressure points, indicating a minimum stress line or fracture gradient within a pressure compartment. Winefield et al. (2005) show that taking the minimum bound LOT line (adopted by Gaarenstroom et al. 1993) often underestimates true formation strength[5] and responds by extrapolating formation pressures to crestal depths of leaky and blown traps. A best-fit trend (blown/leaky seal line[6]) through these values is taken (Figure 3.8); the horizontal lines with each formation indicate top structure. Many breached traps[7] or structures are located at the crest or shallowest point within the pressure cell. Therefore, the importance of pressure communication and lateral transfer between high pressures deep within the cell and at the crest are noted. Winefield et al.'s (2005) fracture gradient applied within individual pressure cells linking blown/leaky trap pressures combines both methods to produce a sound application derived from an empirical, data driven approach.

[5] An accurate representation of the pressure at which a rock fails geomechanically.
[6] A line σ_3 defining the formation strength of the seal. Pressures at top structure of leaking/blown traps are connected using a linear trend line defined by Winefield et al. (2005).
[7] Traps/structures showing evidence of vertical hydrocarbon migration through a caprock.

Swarbrick et al. (2010) utilises a different technique to many other authors by using empirically derived fracture pressures incorporating pore-pressure stress-coupling relationships. Calculated using various pressure variables noted below, lithostatic stress values and regionally calculated coefcients (see section 4.4), the algorithum allows fracture pressure calculations to be undertaken irrespective of LOT. The following (as yet unpublished) formula is used to calculate fracture pressure.

$$P_{frac} = (a.S_v) + (b.OP) + (WD \times 0.445) + 14.7 \qquad \text{Eq. 3.9}$$

Where P_{frac} is fracture pressure (psi), OP is overpressure (psi), WD is water depth (ft) and a and b are coefficients based upon regional LOPs.

Additionally, this type of analysis allows individual well-by-well analysis. It is also imperative to note that the findings from Swarbrick et al. (2010) are based around the principal that the addition of hydrocarbons (and as such excess buoyancy pressures) within a reservoir does not bring the rock closer to fracture. Aquifer

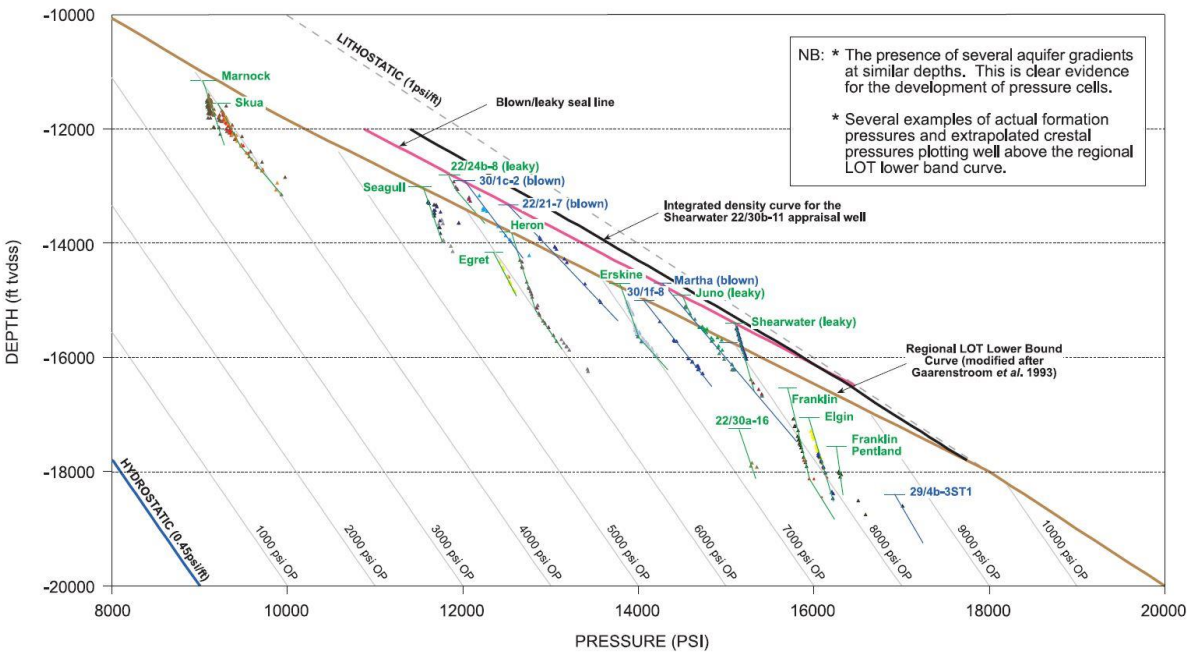

Figure 3.8 - Regional P-D plot of the Shearwater HPHT area. LOT and fracture gradients are illustrated. The red line indicates a best fit gradient linking the crest of all blown structures (blue writing), this is comparable to the Gaarenstroom et al. (1993) minimum bound LOT line and an integrated density curve (Sv) from the Shearwater appraisal well. Taken from Winefield et al., 2005).

pressures are the controlling parameter for seal breach. Aquifer pressures are extrapolated to the top reservoir depth from a known aquifer gradient below a hydrocarbon-water contact, giving an aquifer seal capacity. This is discussed in further detail below.

It is important to note P_p/S_h coupling when defining a fracture gradient (Hillis 2001). Normally pressured formations cannot lie along the same fracture gradient as overpressured formations (Nordgård Bolås et al. 2005). Comparisons between fracture pressures in overpressured and normally pressured formations should be treated separately and not linked via a linear trend line taken through all the data. All authors who utilised a general fracture pressure gradient used a curvilinear line. Although some of the earlier publications (Gaarenstroom et al. 1993) do not attribute the curved nature to P_p/S_h coupling (noted by Hillis, 2001), the effects are accounted for. The main debate stems from how to take a best fit line. The Gaarenstroom et al. (1993) lower bound method will clearly be an underestimation of many actual fracture pressures, as demonstrated by Converse et al. (2000). Converse et al. (2000)'s mean trend line method will be an overestimation of some fracture pressures and underestimation of others, with a range defined by the standard deviation of the data. By this assessment, individual well-by-well analysis will remove a great deal of uncertainty. However, the application of this method cannot be utilised as easily within a pre-drill (or wildcat well) scenario. Of course, those authors who use a well-by-well approach (Nordgård Bolås et al. 2005; Swarbrick et al. 2010) need not have to attempt a best fit line through multiple well data.

Due to the effects of P_p/S_h coupling, the fracture pressure gradient trend (however calculated) will increase with depth. The S_v on the other hand, although in reality also not a linear gradient, does not increase to the same degree, thus the S_v and fracture pressure stress lines converge. The depth at which this ensues is noted in Table 3.1.

3.5.2.1 Complications with fracture pressure calculations

It is debatable as to the relevance of LOPs displaying true fracture pressure. Lack of continuity and error associated with well practices means that it is common to not state whether a LOT is taken to completion, whether it has been extended (XLOT) or if it is simply a limit test and not taken to fracture at all. All these factors can skew the results, displaying a lower fracture pressure than in reality. XLOTs allow the user to estimate tensile strength and the minimum compressive stress of the formation (that is S_h in extensional settings) with more accuracy than the more commonly used LOT. Gaarenstroom et al. (1993) states that LOTs will generally be higher or equal to the minimum in situ stress. Converse et al. (2000) and White et al. (2002) both report that the differences between LOP and ISIP (initial shut in pressure) derived S_h magnitudes are minimal (< 5 %), well within error margins. When considering this value in terms of seal capacity 5 % is not a significant uncertainty in relation to accurately determining fracture pressures. For example, taking Swarbrick et al. (2010)'s < 1000 psi approach a 5 % difference only amounts to 50 psi.

LOTs are additionally suggested by Converse et al. (2000) as the common indicator for minimum stress and the XLOT is noted as showing a more realistic minimum horizontal stress as these are extended to register a fracture closure pressure and instantaneous shutin pressure (ISIP). Variations in depth and lithology are both cited as being factors affecting the LOP values. A sharp increase in LOP is observed below ca. 3200 m within the Central North Sea with increasing pore pressure. Converse et al. (2000) approaches the construction of a failure trend line using an empirically derived mean value between LOP and depth. The standard deviation around the fit of the trend is used to evaluate uncertainty.

Mentioned previously is the uncertainty associated with defining the tensile stregth of the rock. When authors use the fracture pressure (broadly speaking defined as σ_3 + tensile strength) as S_h they assume the rock has zero tensile strength. Holm (1998), Converse et al., (2000), Hermanrud & Nordgård Bolås (2002), and Nordgård Bolås et al. (2005) all make this assumption. This method allows comparisons of differential stresses and thus the consideration of shear failure if S_h is taken as FP. Hermanrud & Nordgård Bolås (2002), Nordgard Bolas et al. (2003) and Nordgård Bolås

et al. (2005) emphasise the importance of shear failure and show, using data from Haltenbanken, that (given high enough stress anisotropies) Mohr Circle diameters can be sufficient to meet the failure envelope. This then allows shear-related failure and hydrocarbon leakage. The Haltenbanken data is taken from the furthest extent of a palaeo-glacier having significant effects in altering the palaeo-stress regime resulting from glacial flexuring increasing the horizontal stress (Nordgård Bolås et al. 2005). It is proven not to have as great an impact in the North Sea to where the glacial edge did not extend. Nordgård Bolås et al. (2005) indicate that variations in palaeo-stress regimes in the Northern North Sea do not breach the shear failure envelope as occurs in the Haltenbanken. Furthermore, emphasis on re-shearing of pre-existing faults is also noted as a preferred failure mechanism (see Figure 3.9).

3.5.2 Fluid Pressure Data

RFTs are the preferred measurements for pore pressure by all authors; however, some use DSTs also (Hermanrud & Nordgård Bolås 2002). Many authors (Gaarenstroom et al. 1993; Holm 1998; Converse et al. 2000; Hermanrud & Nordgård Bolås 2002; Nordgård Bolås & Hermanrud 2003; Nordgård Bolås et al. 2005; Erratt et al. 2005; Swarbrick et al. 2010) additionally note the importance of taking pressures and depths from the shallowest point within the reservoir or pressure compartment where additional buoyancy pressure is highest and fracture pressures are lower due to depth.

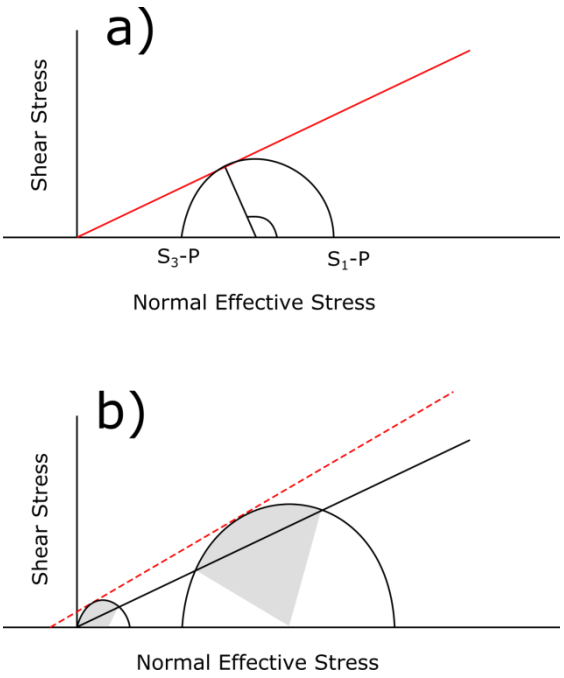

Figure 3.9 - (a) Mohr Circle with failure envelope describing a stress state indicative of failure slip normal to the fault plane. This indicates mechanical shear failure within an intact caprock. (b) Overlays a failure envelope for the reactivation/reopening of pre-existing fractures (solid line) and formation of new fractures (dotted line). This is based upon the assumption that reactivation of pre-existing fractures requires less stress than the formation of new ones. From Hermanrud & Nordgård Bolås (2002).

Although discussed as an important factor to consider, within the scope of seal capacities it is not always possible to achieve this. Poor seismic imaging and accessibility to data makes this near impossible to establish with a high degree of accuracy. Furthermore, wells, and therefore direct pore pressure measurements, are seldom drilled at field crests, especially in HPHT regions due to safety concerns. Gaarenstroom et al. (1993), Hermanrud & Nordgård Bolås (2002) and Winefield et al. (2005) report that data is taken from structural crests, whereas Nordgård Bolås & Hermanrud (2003) and Nordgård Bolås et al. (2005) indicate pressure measurements are taken within 10-15 m of the crest and Swarbrick et al. (2010) report depth variations of up to 45 m. In reality, the errors associated with taking pore pressure measurements and extracting accurate crest depth values from seismics are larger than the discrepancy caused by utilising RFT points from wells a few hundred feet away from the crest of the structure. Despite this, it is an important principal to adapt as the seal or retention capacity is at its lowest pressure at the shallowest point within the field. Authors extrapolate aquifer or formation pressures up to the noted structural crest. Assuming that there is hydraulic connectivity between the structural crest and the point where the direct pore measurement was taken, this is a legitimate technique to use and can give the closest estimation of pore pressures at the shallowest closure point.

In general, all authors within this review use the criteria that when the pore pressure of the formation (aquifer pressure + excess hydrocarbon buoyancy) reaches that of the fracture pressure, however defined, fractures will form and leakage of hydrocarbons will occur. Once the pressure equilibrates to a value less than that of the fracture pressure the fractures will close and leakage will cease. This is then repeated on an episodic pattern (Holm 1998).

Swarbrick et al. (2010) utilises a different criteria for pressure-related mechanical failure. Based on a similar principal published in Bjørkum et al. (1998), it is proposed that the additional overpressure resulting from buoyancy pressures associated with a column does not influence top seal fracturing in a water-wet seal. Simply put, there is no contact between the hydrocarbon accumulation and the

encompassing grain matrix. It is, therefore, the aquifer pressure which has the overriding control on the state of caprock failure. Evidence for this is discussed in Section 3.5.5. Fracture criteria aside, a major benefit to utilising aquifer pressures over that of the pore pressures is the ability to compare differing wells and remove the pressure differential associated with differing fluid densities and column heights.

Often overlooked, an additional parameter to consider is the conditions under which the hydrostatic and lithostatic stress variables are set. The importance of this is emphasised by authors who use lithostatic pressure values within their calculations for fracture pressures (Swarbrick et al, 2010). Swarbrick et al. (2010) uses density-derived overburden values on a well-by-well basis and a regionally derived hydrostatic value of 0.445 psi ft^{-1}. Hermanrud & Nordgård Bolås (2002), Nordgard Bolas et al. (2003) and Nordgård Bolås et al. (2005), however, use an overburden curve from Svare (1995) for both the North Sea and Norwegian Sector. These authors feel individually derived curves from density logs can have too many associated errors (see Svare 1995).

When considering that overpressure is a function of the hydrostatic pressure, clearly having an accurate hydrostatic value is of equal importance. In general standard values of 1.0 psi ft^{-1} are used as an overburden gradient and 0.45 psi ft^{-1} used as the hydrostatic gradient (Gaarenstroom et al. 1993; Nordgård Bolås et al. 2005; Erratt et al. 2005). Ward et al. (1994), Converse et al. (2000), Nordgård Bolås et al. (2005) and Hermanrud et al. (2014) do not mention values; this is due to these values not being relevant to the study or within calculations. Swarbrick et al. (2010) do not use the standard 0.45 psi ft^{-1} value but instead one derived from North Sea regional data from a large selection of well measurements.

3.5.3 Calculation of Retention Capacities

Gaarenstroom et al. (1993) coined the term "retention capacity". Retention capacitiy is defined as the difference between the reservoir pore pressures, taken from depths near the top reservoir, and the lower bound minimum horizontal stress. In discovery wells the hydrocarbon pressure was used, and in dry wells aquifer

pressures. Retention capacities were evaluated from a 29 well study. The results from the publication suggest that once the seal capacity decreases below 1000 psi the chance of seal breach is greatly increased. Six out of the 12 wells with a retention capacity with < 1000 psi had a leaking seal or were dry (1 dry hole was reported resulting from a lack of trap and another through lack of reservoir). Above 1000 psi all wells contained hydrocarbons, bar one (Figure 3.10). This dry well is attributed to a lack of trap rather than a pressure/leakage related problem. Previously discussed is the convergence of S_v and fracture pressure gradient trends. All authors (bar Swarbrick et al. 2010) do not discuss data, or in most cases, possess data below this transition. However, within the Central North Sea HPHT areas reservoirs are sub-transition, and Swarbrick et al. (2010) use the lesser value of fracture pressure and S_v.

Hermanrud & Nordgård Bolås (2002), Nordgard Bolas et al. (2003) and Nordgård Bolås et al. (2005) papers all focus on dry hole vs discovery analysis using similar methods to Gaarenstroom et al. (1993). Focusing on the previously defined "retention capacity", dry hole vs hydrocarbon discovery wells are compared between the North Viking Graben and Halten Terrace regions. Within the Nordgård Bolås & Hermanrud (2003) and Nordgård Bolås et al. (2005) studies, unlike Gaarenstroom et al. (1993) and Hermanrud & Nordgård Bolås (2002), LOPs were taken on a well by well basis rather than a regional pressure trend. The rationale behind this lay with a 5-15 MPa discrepancy range with LOP between the Halten Terrace and North Viking Graben. The Halten Terrace analysis showed 7 out of 13 wells had leakage evidence with the retention capacities of these wells being in the order of 1015-2755 psi. The North Viking Graben showed 4 out of 16 structures emptied of hydrocarbons, all with

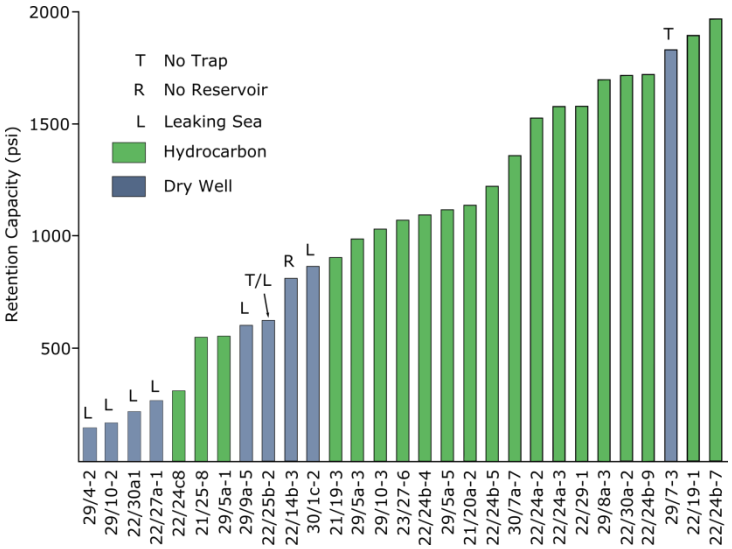

Figure 3.10 - Retention capacities of North Sea dry and discovery wells. Note that above 1000 psi there is 100% hydrocarbon presence with the exception of 29/7-3 – resulting from a lack of trap. (Adapted from Gaarenstroom et al., 1993).

retention capacities between 435-2030 psi. The Halten Terrace region, despite possessing generally higher retention capacities, displayed a greater proportion of leaked traps from overpressured systems compared with that from the North Viking Graben. It is also noted that retention capacities between 1450 – 2900 psi within the Halten Terrace are associated with a greater proportion of leaked structures than lower retention capacities. This contradicts results published by Gaarenstroom et al. (1993) and the common idea that lower retention capacities increase the risk of failure. These differences are subsequently attributed to changes in the paleo-stress regime during times of glaciation (Nordgård Bolås et al. 2005), favouring leakage through changes in the differential stress, thus increasing the stress anisotropy. Through Mohr Circle predictions this larger anisotropy increases the diameter of the circle allowing it to intersect the pre-defined failure envelope. Figure 3.11 shows how utilising Mohr Circles within the Haltenbanken indicates an explanation of leakage despite positive seal capacity values.

The final major publication exploiting the use of minimum effective stresses as the fracture pressure is Swarbrick et al. (2010). The term retention capacity has been described from previous authors, however Swarbrick et al. (2010) assuming the importance of aquifer pressures over that of the formation pressures, uses "aquifer seal capacity". This is defined as the fracture pressure minus that of the extrapolated aquifer pressure. It is the application the aquifer seal capacity and redefinition of the "ultimate seal" that Swarbrick et al. (2010) base their findings on (see Section 3.5.5).

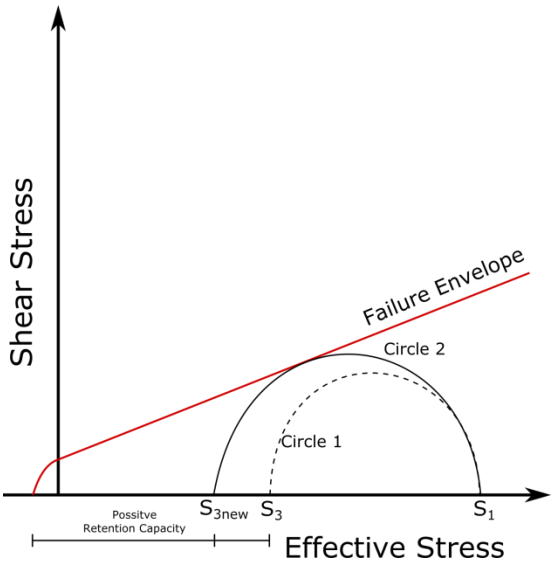

Figure 3.11 - Mohr diagram displaying states with positive retention capacities intersecting the failure envelope. Circle 1 shows a rock in an anisotropic stress state, the rock is not critically-stressed regarding failure. Circle 2 displays a rock with a larger stress anisotropy. This is now critically stressed, intersecting the failure envelope. Leakage can thus occur despite a positive retention capacity. Adapted from Nordgard Bolas et al. (2003).

3.5.4 The Ultimate Seal & Protected Traps

Winefield et al. (2005) and Swarbrick et al. (2010) suggest a re-evaluation of the stratigraphic level at which hydrocarbon 'leakage' occurs. It is suggested that the pressure seal of the Central North Sea Jurassic reservoir pressure cell (the BCU/base chalk) is the main control on the presence of a hydrocarbon accumulation and not the caprock. This is elaborated further upon below. Other authors (Gaarenstroom et al. 1993; Ward et al. 1994; Holm 1998; Converse et al. 2000; Teige et al. 2002; Nordgård Bolås & Hermanrud 2003; Nordgård Bolås et al. 2005; Winefield et al. 2005) accept that the caprock is the top seal and predominant control on the preservation of a hydrocarbon accumulation.

Winefield et al. (2005) denote the 'ultimate top seal[8]' to the Greater Shearwater area pressure cell to be the Cretaceous Chalk, and to a lesser extent Cromer Knoll Group. Casabianca & Cosgrove (2012) provide further evidence for this involving what is termed a "caprock waste zone" with fractures propagating to the "ultimate seal" described to be between the BCU and the base of the Chalk Group. Due to the so called "fluid waste zone" and the presence of fractures charged with formation fluids at a shallower depth than the low permeability horizon at the top hydrocarbon column marker, the seal capacity is reduced. The shorter the waste zone the greater the chance of finding a hydrocarbon column.

Within the Swarbrick et al. (2010) study the aquifer pressure gradient is extrapolated from Jurassic/Triassic reservoir aquifers to the base chalk or BCU[9] interval. They assume hydraulic connectivity to the base chalk, based on direct pressure measurement from the BCU and the top reservoir in selected wells. Empirical evidence suggests that the commonly accepted top seal of the Cromer Knoll, Heather or Kimmeridge Clay formations may not play a pivotal role in the preservation of hydrocarbons, whereas the base chalk may be the 'ultimate seal'. Discovery versus dry hole well analysis (65 wells in total) showed that at the base chalk horizon, 100% of dry holes are observed with a negative aquifer seal capacity value when compared with that from top reservoir (Figure 3.13). Furthermore, seal capacities taken from the base

[8] Defined as the shallowest point within the pressure cell and the stratigraphic interval that has overriding control on 'sealing' the bellow accumulation.
[9] Base Cretaceous Unconformity

chalk in comparison to top reservoir show a lower threshold of 750 psi compared with that of 1400 psi at the top reservoir (similar to Gaarenstroom et al. 1993). Above this threshold at the base chalk, 88% of wells were discoveries and only 36% below the threshold as shown in figure 3.12. Figure 3.14 highlights how retention capacities can differ drastically between different horizons. Despite this, there are are dry holes with possitve aquifer seal capacities. Swarbrick et al. (2010) explains these by error in defining the true fracture pressure (± 500 psi).

Discussing the stratigraphic level at which a retention/seal capacity is taken relates somewhat to the 'protection' of structually deeper traps within the same hydraulically connected system. Structures deeper within the pressure cell can be protected by the "pressure valve" at the compartment crest and, as such, can therefore retain a column (Figure 3.15). This is demonstrated by further analysis within the Shearwater pressure cell. A single aquifer gradient along the Shearwater, Juno and Martha structures is indicative of hydraulic connectivity. Extrapolation of pressures within the Martha well allows a Winefield et al. (2005) "local top seal line" to be constructed i.e. a linear line adjoining all structural crest pressures that are leaking and thus thought to possess pore pressures equal to that of the fracture pressure. The Juno and Shearwater structures are deeper than Martha but share the same aquifer gradient. Therefore, the strength of the seal is significant enough to withhold a hydrocarbon accumulation at Juno and Shearwater. Winefield et al. (2005) states the column heights within Juno and Shearwater are constrained by top seal strength as both spill points are deeper than their respective columns. The Martha well is dry (although both oil and condensate inclusions in quartz imply the palaeo-presence of hydrocarbons), Juno shows staining within the seal, indicating a breach, and Shearwater still contains an economic accumulation (Gilham & Hercus 2005). The aquifer overpressure within the cells is equal to the strength of the seal within the Martha structure. There simply is not a hydraulic envelope present to allow an accumulation of hydrocarbons. Any further increase in aquifer pressure would fracture the seal at Martha, however the water contact and column length would remain a constant in Juno and Shearwater. The length is only a function of the hydrocarbon density changes. Both columns are, as such, 'protected' by the pressure valve in the shallowest structure.

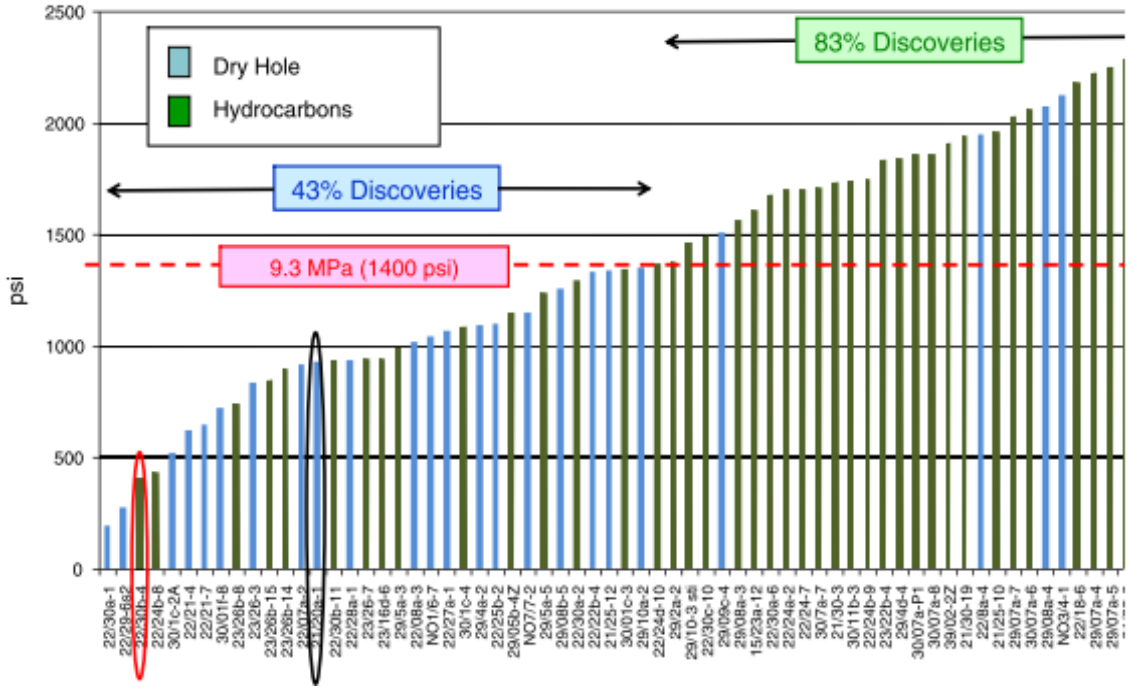

Figure 3.12 - Top reservoir histogram of aquifer seal capacities vs. dry holes and discovery wells. Some wells statuses are not explained (21/20a-1, 22/30b-4). Well 21/20a-1 (black circle) is a dry hole with hydrocarbon shows in vertical fractures through the chalk and well 22/30b-4 (red circle) possesses hydrocarbons (a long gas column) at low seal capacity. (Figure from Swarbrick et al. 2010)

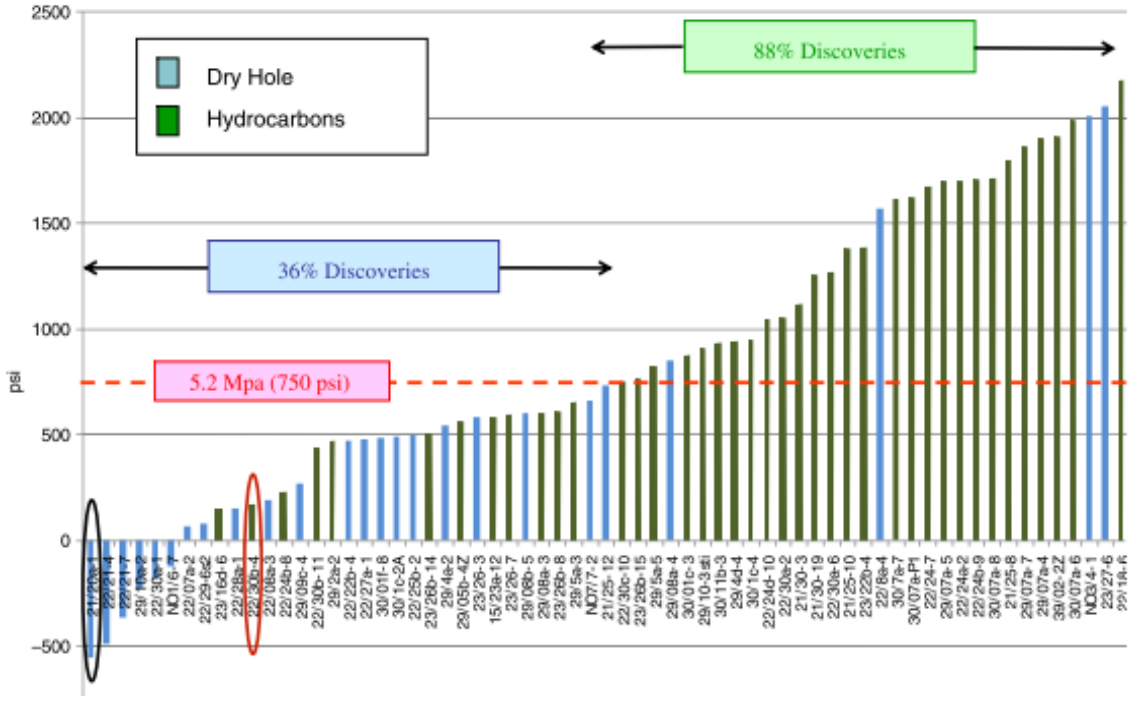

Figure 3.13 - Base chalk histogram of aquifer seal capacities vs. dry hole and discovery wells. All dry wells, predicted as breached, display a negative seal capacity. Well 22/30b-4 (possessing hydrocarbons at top reservoir, despite a low seal capacity) now still indicates a positive aquifer seal capacity at the Base Chalk. Whereas, well 21/20a-1 (dry, yet still having a positive aquifer seal capacity at top hydrocarbon) register a negative aquifer seal capacity at the Base Chalk. (Figure from Swarbrick et al. 2010)

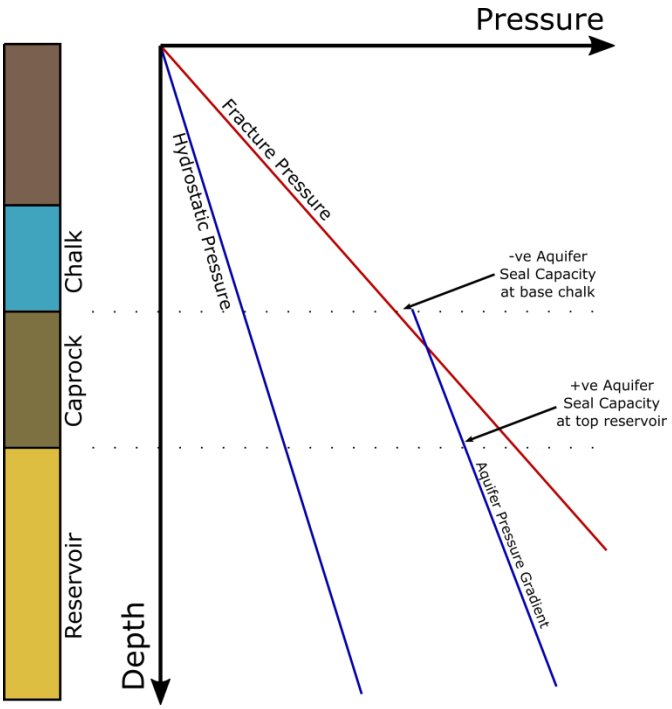

Figure 3.14 - Schematic illustration indicating how a positive aquifer seal capacity may be present at top reservoir but negative seal capacity at base chalk. Thus providing an explanation for a dry hole.

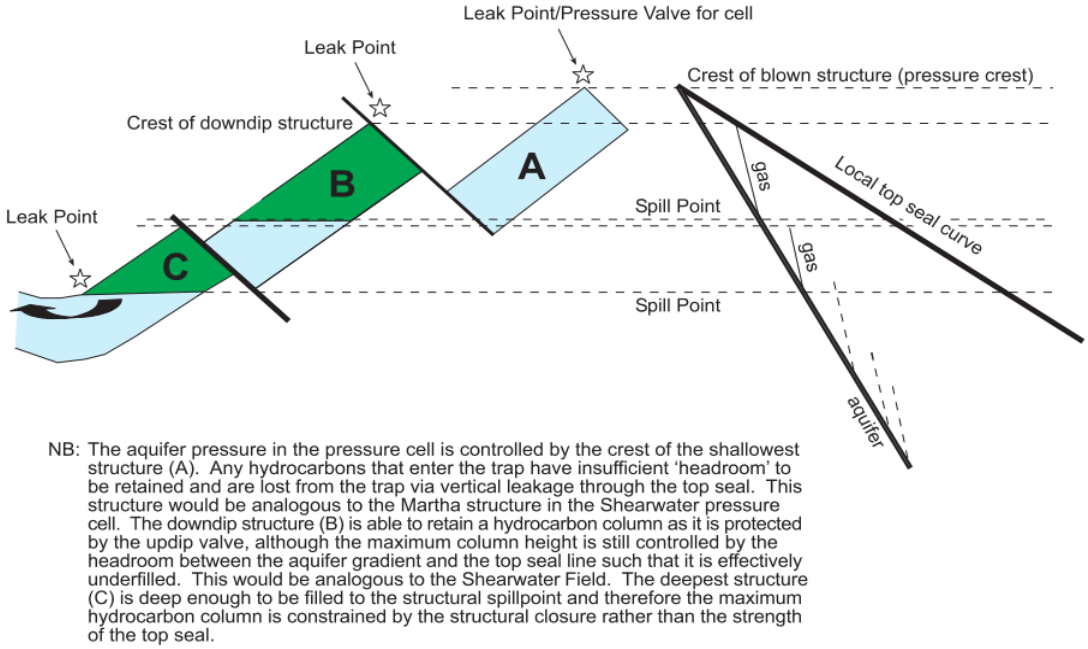

NB: The aquifer pressure in the pressure cell is controlled by the crest of the shallowest structure (A). Any hydrocarbons that enter the trap have insufficient 'headroom' to be retained and are lost from the trap via vertical leakage through the top seal. This structure would be analogous to the Martha structure in the Shearwater pressure cell. The downdip structure (B) is able to retain a hydrocarbon column as it is protected by the updip valve, although the maximum column height is still controlled by the headroom between the aquifer gradient and the top seal line such that it is effectively underfilled. This would be analogous to the Shearwater Field. The deepest structure (C) is deep enough to be filled to the structural spillpoint and therefore the maximum hydrocarbon column is constrained by the structural closure rather than the strength of the top seal.

Figure 3.15 - Schematic diagram of a dynamic trap system adapted by Winefield et al. (2005) from Sales (1997) and Converse et al. (2000). All structures (A-C) are in hydraulic connectivity. This is shown on the P-D plot as all fields share a common aquifer gradient.

3.5.5 Discussion

The major dissimilarities between all authors are the criteria used to define a fracture pressure/gradient – taken by most as the minimum horizontal stress. The major split between the authors is the idea between setting a regional or local fracture pressure. Authors who tend towards analysis on a regional level look for utilising a fracture gradient usually based upon collective LOT data (Gaarenstroom et al. 1993; Holm 1998; Converse et al. 2000). Winefield et al. (2005) also use a regional gradient, termed "blown/leaky seal line" specific to the Shearwater pressure cell, and suggests that pressure cells should be treated individually. All other authors exploit a local, well-by-well, analysis. Despite the different approaches taken all authors' data supports their individual analysis with any exceptions justified. Although useful to have a quantitative figure of 1000 psi as a cut-off regarding risks of dry hole (Gaarenstroom et al. 1993), the result that exploration risk simply increases is not overly useful as successful ventures are plausible according to Gaarenstroom et al. (1993) data with seal capacities less than 1000 psi. The Swarbrick et al; (2010) approach does quantify this however.

Nordgård Bolås et al. (2005) do note that traps can fail through leakage with a positive retention capacity through differential stress and anisotropy (Figure 3.16). This argument takes into account the caprocks propensity to fail under a shear regime should the differential stress be high enough. This is observed within the Haltenbanken, albeit under higher anisotropies than observed within the North Sea. Furthermore, reactivation of old faults displays a shallower failure envelope gradient. The shallower failure envelope for reactivation of old fractures is shown in Figure 3.9 from Hermanrud & Nordgård Bolås (2002). The shaded area also indicated on the Figure 3.9 indicates a larger range of critical angles permitting slip under the displayed conditions.

The pressure envelope between pressures in the reservoir and the fracture pressures was a key component when undertaking dry hole vs. hydrocarbon discovery analysis. Gaarenstroom et al. (1993)'s term "retention capacity" was initially used and subsequently adopted by Ward et al. (1994), Nordgård Bolås & Hermanrud (2003) and Nordgård Bolås et al. (2005). Winefield et al. (2005), although based upon the same

calculation criteria, used "sealing capacity" for defining this envelope. Recently, Swarbrick et al. (2010) proposed a slight variation to retention/sealing capacity using the term "aquifer seal capacity".

The thoughts behind top seal failure not being a function of excess hydrocarbon buoyancy are novel in academia. The evidence portrayed within Swarbrick et al. (2010) regarding all dry holes possessing < 0 psi aquifer seal capacity at the base chalk interval does imply some form of connectivity with the top of the pressure cell however. Conclusions concerning "caprock waste zones" and "ultimate seal" findings by Casabianca & Cosgrove (2012) does add a further degree of confidence to Swarbrick et al.'s (2010) ideas.

Casabianca & Cosgrove (2012) suggest a fluid waste zone consisting of fractures through the caprock to an interval between the BCU and base chalk. The "ultimate seal" is, therefore, not the top reservoir but some depth shallower than this low permeability horizon. This echoes the importance of understanding the point at which to take as the ultimate seal depth - the shallower the crest of the seal the lower the retention/seal capacities. The hypothesis that hydrocarbon buoyancy has no impact on rock failure effectively proposes the idea that no matter what aquifer overpressures are present (assuming the values are positive), a hydrocarbon column is only going to be limited by membrane failure or structural characteristics of the trap. No further literature highlighting whether excess buoyancy pressures narrowing the envelope for fracturing has been published. Additionally, it is not documented anywhere within the researched literature any scenario where pore pressures are higher than fracture pressures resulting from buoyancy. For example, the pore pressure at the crest is always ≤ P_{frac} or σ_3. This new concept clearly needs further research to be conclusive, but the pioneering ramifications of an effectively limitless hydrocarbon column (given the right closure and source conditions) are very attractive from an exploration point of view.

It is hard to assess the error margins associated with the differing author's approaches. This is primarily due to the different datasets and regions used. Furthermore, error margins are not discussed in a quantitative manner in any of the literature with the exception of Swarbrick et al. (2010) where a ± 500 psi aquifer seal

capacity error margin is calculated. This is derived from the presence of dry wells with positive seal capacities at the base chalk interval. What is understood is the importance of assessing seal capacities on a local level as highlighted by Winefield et al. (2005) when exploring the Shearwater pressure cell. Taking regional fracture pressure gradients (e.g. Gaarenstroom et al. 1993) will often underestimate the actual fracture pressure of the rock. Therefore, a well-by-well approach (Swarbrick et al. 2010) strikes as the method with the least error. The uncertainties with each method on the whole are also poorly documented. This likely mirrors the uncertainties within the subject matter. One of the biggest uncertainties lies within assessing the tensile strength and, therefore, an additional amount of resistance to overcome to fail the caprock. The use of the term fracture pressure (Swarbrick et al. 2010 for example), though ambiguous, is derived from LOTs and therefore includes tensile strength. Those who use S_{min} derived from LOPs are assuming zero tensile strength (as suggested in Zoback 2010).

In conclusion it would seem that new concepts and hypotheses surrounding failure criteria and the preservation of an economic hydrocarbon column are still developing. This, by definition, suggests that a great deal more work has to be undertaken to come to a final accurate conclusion. What can be concluded is that with higher overpressures, smaller retention/seal capacities poses greater risks of seal failure. Despite this, significant accumulations have, and still are, being discovered. This in itself suggests explorationists should remain optimistic for future discoveries in deep, highly overpressured targets.

3.5.6 Summary of Seal Breach Literature

The following table contains a summary of the important aspects taken from the literature allowing clear and quick comparison.

	Gaarenstroom 1993	Ward 1994	Holm (1998)	Converse et al. (2000)	Hermanrud and Nordgard Bolas (2002)	Nordgard Bolas & Hermanrud (2003)	Nordgard Bolas et al. (2005)	Winefield et al. (2005)	Swarbrick et al. (2010)	Hermanrud et al. (2014)
Topic	Conclusions in CNS OP generation mechanisms & OP-frac dry/discovery analysis	Use of ESL model to predict pore and fracture pressures in HPHT wells	Overpressure distribution	Controls of overpressure and failure of top seals	Similar OP observed between NS and Northern North Sea. NS shows more dry holes, Northern North Sea show HC.	Seal capacity leakage between Halten terrace and North Viking Graben	Correlations between stress history and prediction of hydrocarbon occurrence.	Pressure cells and fracture caused leakage	Seal capacity and	Column heights controlled by faulted top seal.
Data set	Central North Sea Graben – Jurassic Traps	Central Graben HPHT wells	Over 100 wells from the central graben	North Sea	Overpressured wells (13 total) in the Haltenbanken. 16 wells from North Sea – pre-production data	16 OP wells in NVG and 13 in OP wells from Halten Terrace – Jurassic Reservoirs	NVG and Haltenbanken	Central North Sea -Shearwater Pressure Cell	Sub-chalk high pressure wells from Central North Sea	2 3D pre stack seismic surveys with 16 drilled Jurassic reservoir traps. 14 used as 2 omitted.
Pressure Measurement Criteria	Hydrocarbon pressure taken if presence of hydrocarbon column. Aquifer if not.	FT – measurement types not mentioned. Log data resistivity or density for PP	RFT measurements used where available	RFT measurements used	RFT measurements used	RFT and DST measurements – level of uncertainty is an order of magnitude less than uncertainty around Sigma 3 so assumed to be negligible.	Data used from Nordgard Bolas & Hermanrud (2003)	Data taken from wireline RFT/MDT measurements	RFT measurements used	Pressure not a component within paper. Fault permeability primary control.
Lithostatic and Hydrostatic gradient values	Default 0.45 and 1.0 psi/ft.	Not mentioned – not necessary to model	0.45 psi ft. hydrostatic pressure used for maps. 1.0 psi ft. lithostatic 0.43 psi/ft. hydrostat used in graphs	Not applicable to study – not stated	Overburden curve taken from Svare (1995) – in order to eliminate problems with individually derived curves from density logs	Approximate lithostatic 1.0 psi/ft. and 0.45 psi/ft.	Not discussed – not necessary in calculations	Lithostatic 1 psi/ft., Hydrostatic 0.45 psi/ft.	Overburden derived from density logs	Not relevant to study
Definition of minimum stress	Minimum bound line defined by leak off tests (horizontal stress)	ESL model provides fracture pressure (from Holbruck et al. 1987, 1989, 1993). σ_h is noted as being min	LOT and is assumed fracture gradient	LOT pressures are assumed as min horizontal stress. In accuracies are noted however.	LOP taken as least compressive stress	Worked out on a well by well basis. LOT taken from close to the seal – only representative of σ_h. Unclear if reversal point is noted.	Data used from Nordgard Bolas & Hermanrud (2003)	Local top seal line for Shearwater pressure cell.	Minimum stress used. I.e. both horizontal/vertical depending upon the lesser value	Not relevant to study
Retention capacity/seal capacity term used	Retention Capacity – Minimum bound LOT trend (minimum effective stress) – pore pressure.	Retention Capacity	Retention/Seal capacity are not relevant within paper	Not applicable to study – not stated	Not applicable to study – not stated	Retention Capacity – RC= σ_3 -PP	Retention Capacity – RC= σ_3 –PP Inaccuracy's discussed with comparison to FAST Mildren et al. 2005	Sealing Capacity (buoyancy and aquifer exceed the sealing capacity of the top/fault seal)	Aquifer Seal Capacity – Aquifer pressure – σ_3	Not relevant to study
Fracture Gradient	Minimum bound leakoff test representing minimum effective stress	ESL model provides fracture pressure (from Holbruck et al. 1987, 1989, 1993)	Fracture Gradient defined in graph as minimum horizontal stress	Mean value derived from empirical relationship between leak off pressure and depth.	Not noted – LOT gradient taken as a best fit possibly. Not min or max bound.	Taken on a well by well basis – extrapolations of S3 estimates to LOP depth to correct for depth difference.	Fracture gradients not used – fracture pressure enough for individual well analysis	Derived from blown/leaky cell analysis	Fracture gradients not used – fracture pressure enough for individual well analysis	Not relevant to study

LOT and Lithostatic Gradient Convergence depth	16’000 ft.	Not discussed	13,100 ft.	Not discussed	Not discussed or shown – both lines are linear	16’400 ft.	Not shown	~16,500 ft.	14,000 ft.	Not relevant to study
PP/Stress coupling considered	No	N/A	Yes	Not Noted	Not Noted	Not Noted	Not Noted	N/A	Yes	N/A
Fracture criteria	True formation pressures cause fracture	True formation pressures cause fracture	True formation pressures cause fracture	No mention of extrapolated aquifer pressures therefore likely true reservoir pressures.	No mention of extrapolated aquifer pressures therefore likely true reservoir pressures.	True formation pressures cause fracture	True formation pressures cause fracture	True formation pressures cause fracture	Aquifer pressure causes failure – Bjorkum et al. 1998	Not relevant to study
Point at which leakage occurs i.e. hydraulic fracturing can occur	Retention capacities > 1000 psi increase chance of dry hole considerably.	When pp intersects with fracture pressure. When the tensile strength of the rock is overcome leak off will occur.	When pp intersects with fracture gradient or effective stress reaches 0.	When pp intersects with mean LOT fracture gradient	Notes the importance of pre-existing fractures and reactivation at a lower pressure	Failure envelopes are breached which can and usually is higher than 0 retention capacities.	Leakage occurs due to differential stress and a Mohr circle principal. I.e. when Mohr circle intersects with failure envelope.	When pore pressures intersect with the defined “leaky seal” gradient	Extrapolation of aquifer gradient from Jurassic or Triassic reservoirs to BCU/base chalk. At this point aquifer gradients intersect with minimum effective Stress.	Leakage occurs at fault intersection with reservoir. This limits column height.
Noted as wells taken at or close to crest	Yes	Not applicable. It is noted that the top of the pressure cell is the weekest.	Crestal depth is important but not mentioned if data is taken from there	Leakage is noted as being riskier at the crest but not indicated if data is taken from there.	Yes	Yes – Within 10-30 m of presumed top.	Yes – Within 10-30 m of presumed top. Data used from Nordgard Bolas & Hermanrud (2003)	Yes	Within 492 ft. of crest	Not relevant to study
Top Seal	Kimmeridge Clay, Cromer Knoll & Zechstein Group	Pressure seal described as the chalk. Top seal noted as being the weakest	Cromer Knoll & Upper Cretaceous Chalk	Seal taken as top hydrocarbon	Top seal is top hydrocarbon.	Top seal is top hydrocarbon.	Top seal is top hydrocarbon.	Top Reservoir	HC seal is top reservoir but seal to aquifer pressures is BCU or chalk as hydraulic connectivity is thought to occur to this point.	Top reservoir is noted as top hydrocarbon
Key Results	<1000 psi retention capacity = primarily dry holes. The importance of using pressure cells.	ESL model provides accurate prediction as demonstrated by FT and LOT.	Importance of gas generation as an overpressure generation mechanism. When a rock approaches fracture pressure a dynamic interplay between pp and fracture pressure conditions episodic leakage in a dynamic system.	The importance of stress unloading mechanisms is highlighted. Faults are also noted as pressure boundaries. The ultimate control on overpressure in rapidly subsiding basins is rock failure, which relates to leakage. In OP basins hydraulic failure can limit column height and important for migration.	The stress state within the Halten terrace favoured leakage through fracturing. Maximum compressive stress can be estimated and shown to be significantly higher than overburden. Glacial crustal flexuring within the Haltenbanken is proposed as the force increasing horizontal stress. Therefore, caprock leakage is suggested to be significantly higher in areas close to the shelf edge. –furthest extent of ice.	Frequencies of HC presence and retention capacities between NVG and Halten Terrace. Halten Terrace HC is thought to have leaked from shear at crest through crestal anisotropies. Stress isotropy and pore water leakage through wetting film preserved columns in NVG. Results thought to be applicable elsewhere and therefore an important ingredient in seal risk evaluations.	Retention capacity is not satisfactory. Stress anisotropy needs to be taken into account as demonstrated between Halten Terrace and North Sea.	Aquifer pressure, seal strength and HC migration key controls on HC presence in HPHT areas. Shallowest point within pressure cell. Protected traps (not term used) i.e. shearwater	Chalk is an effective pressure seal. Most robust relationship between dry holes and discoveries is the Base Chalk from extended fulmar reservoir aquifer gradient extrapolations. Buoyancy pressure no effect on fracture. More research is necessary to explain why/if the base chalk is the controlling unit regarding hydrocarbon entrapment.	Observations suggest that fault intersections have an overriding control on the position of HC-water contacts. The exception being faults at an angle of ~90 degrees. Conclusions suggest that within the Barents Sea it can be suggested that faults can indicate contacts

3.6 The Role of Buoyancy Pressures on Hydrofracking

Throughout the literature there are 2 contrasting views of the effect of buoyancy pressures on contributing to the formation of hydrofractures.

Bjørkum et al. (1998) describes that in a water-wet reservoir the risk of hydrofracking should not be increased as a function of hydrocarbon column height or fluid type. This is based on the two major principals: 1) buoyancy pressures are balanced by downward-elastic forces between the hydrocarbon and water phases, and 2) Newton's Third Law is applicable to the hydrocarbon-water interface. Further evidence for this is presented in Swarbrick et al. (2010) where aquifer pressures of dry holes all reach fracture pressure at the base chalk interval of the Central North Sea.

Watts (1987) clearly states that fractures will form when the pore fluid pressure (aquifer pressure, extrapolated to reservoir-seal interface, plus hydrocarbon buoyancy pressure) equals that of the σ_3 plus the tensile strength of the rock. This is the commonly applied rule that is utilised by the majority of the literature (Gaarenstroom et al. 1993; Holm 1998; Converse et al. 2000; Nordgård Bolås & Hermanrud 2003; Winefield et al. 2005).

Compelling evidence is presented by Swarbrick et al. (2010) suggesting the effect of hydrocarbon buoyancy is irrelevant to hydrofracturing. This is the most recent paper presented on the matter; however, it is the author of this reports consensus that further work needs to be undertaken to completely validate the hypothesis. As such, both aquifer seal capacity ($SC_{Aquifer}$) and formation pressure seal capacity (SC_{form}) will be considered within this document.

3.7 Seal Capacity

Previous literature indicates that both the term seal capacity (Swarbrick et al. 2010) and retention capacity (Gaarenstroom et al. 1993; Nordgard Bolas et al. 2003 etc) are used. Both are based on a similar principal where seal/retention capacities are equal

to the fracture pressure minus the pore/aquifer pressure. Throughout this report the term seal capacity is used and can be expressed as so:

$$SC_{form} = P_{frac} - P_p \qquad \text{Eq. 3.10}$$

Where SC_{form} is seal capacity, P_{frac} is the fracture pressure and P_p is the pore pressure.

The use of aquifer pressure ($P_{Aquifer}$) as a substitution for the formation pressure (P_p) within seal capacity calculations (see in Swarbrick et. al, 2010) is also considered through the report. In this case the second variable within Eq. 3.10 is exchanged with $P_{Aquifer}$ giving an aquifer seal capacity ($SC_{Aquifer}$). Therefore, substituting these replacements into Eq. 3.11 gives:

$$SC_{Aquifer} = P_{frac} - P_{Aquifer} \qquad \text{Eq. 3.11}$$

What is apparent from the literature is that a definitive conclusion as to the effects of the hydrocarbon phase upon fracture initiation is not reached. Both Eq. 3.10 & Eq. 3.11 will be considered throughout this report. Fig 4.16 provides a pressure-depth visualisation for Eq. 3.10 & Eq. 3.11. Seal capacity is a function of overpressure and fracture pressure. A formation pressure of normal or low overpressure (see Figure 4.18, A) will as such yield a larger seal capacity than a highly overpressured formation at the equivalent depth (see Figure 4.16, B).

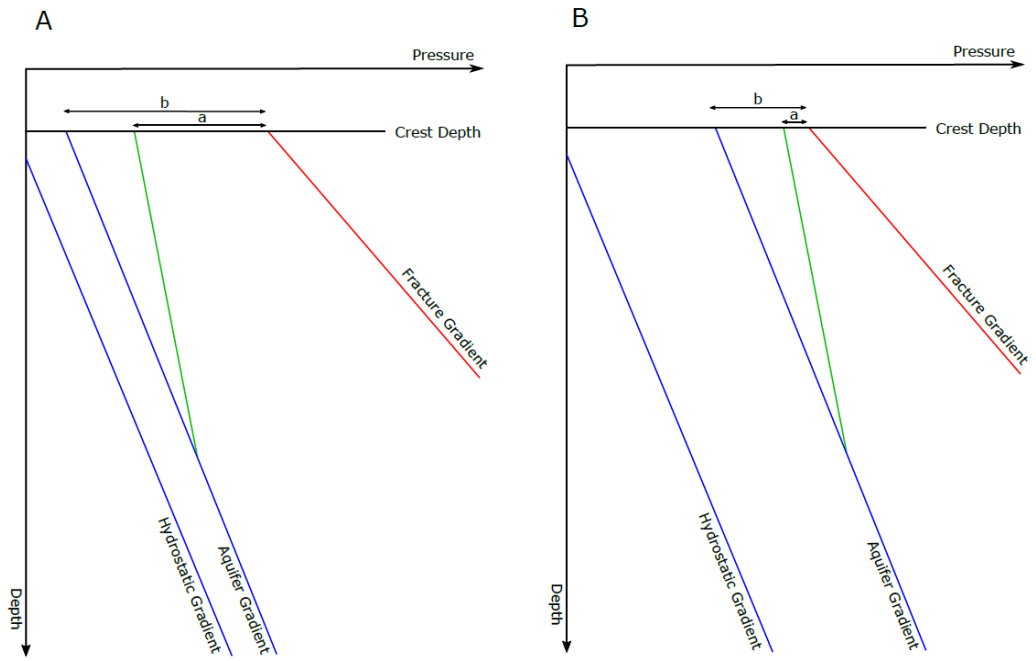

Figure 3.16 - Schematic depicting seal capacity. A shows an oil bearing formation with low overpressure values, whereas B shows an equivalent depth formation with higher overpressure values. Formation and aquifer seal capacities are indicated by arrows labelled a & b respectively. Note how as overpressure increases seal capacity decreases.

Seal capacity calculations for the dataset associated with this report and the methodology used to calculate them are elaborated further upon in Chapter 4 - Methodology. Seal capacity values will always be at their smallest, with the exception of a compartmentalised reservoir, at the crest or shallowest point within the structure. This is the product of converging aquifer and fracture gradients.

Chapter 4

Research Methodology

Chapter 4 - Research Methodology

The foremost aim of this project was to investigate the relationship between hydrocarbon column height and seal capacity. This was undertaken by utilising pressure data from various hydrocarbon fields to calculate maximum hydrocarbon field overpressure values from the structural crests and establish the pressures required to mechanically fail the caprock and permit hydrocarbon leakage. The two main mechanical failure pressures explored include fracture pressures (the pore pressure at which a rock will undergo mechanical failure) & fault reactivation pressures (the pore pressure that would allow pre-existing faults within the caprock to re-shear)[10]. Data from 129 fields (including different hydrocarbon reservoir intervals within single fields) were analysed. Fields are located in the Central North Sea, Northern North Sea, Southern North Sea, Irish Sea and West of Shetland. A regional breakdown of field locations is shown in Figure 4.1. The majority of fields are located within the Central North Sea. By contrast West of Shetland only represents 1 % of the fields used within the study (i.e. only 1 field). Further field data were collected,

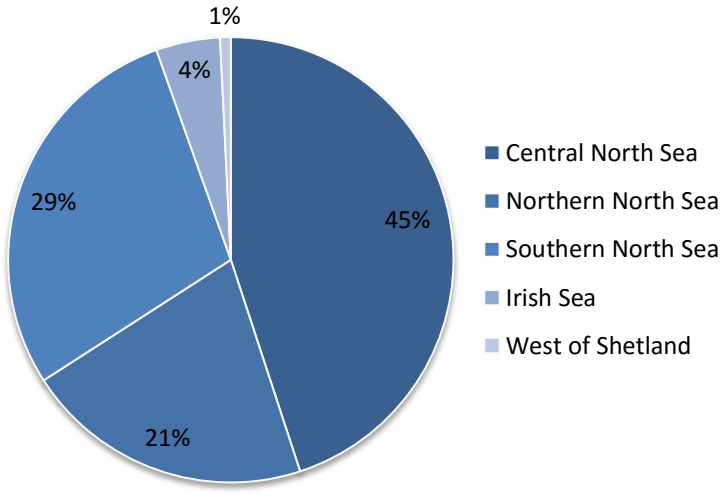

Figure 4.1 - Breakdown of study locations and percentage of fields located within these regions. The majority (45 % of fields) analysed within the study sit within the Central North Sea. Only 1 field is located within the West of Shetland basin and only represents 1 % of the total data set.

[10]Algorithm used is based on cohesionless, optimally orientated faults.

however, which was subsequently disregarded either due to not including the relevant pressure information to create a pressure profile, or the quality of the data was thought to be poor or incorrect. A full detail of criteria for rejection is explained in section 4.6

Pressure-depth (P-D) plots for each field were created using Ikon Science's RokDoc software. This package allowed a vertical visualisation of a field's pressure profile from the crest/top hydrocarbon depth downwards.

Regions, water depth, hydrocarbon type, crest depth, hydrocarbon column height and aquifer/pore pressure parameters were collected. These were then used to calculate aquifer and hydrocarbon overpressure, hydrostatic pressure, lithostatic pressure, minimum horizontal stress, fault reactivation pressure and seal capacities. Furthermore, the fill state of the closure (i.e. under filled or full–to-spill) can be calculated if a lowest closing contour (or leak point depth) is known. All these can then be analysed using the established field pressure regime.

4.1 Sources of data

Collection of data and data sources primarily fell into 2 categories; primary, or direct, and secondary, or indirect. Primary pressure measurements, for the purpose of this document, were data directly taken from well reports or composite logs. Secondary pressure data were sourced from the literature. Primary and secondary source data were processed using slightly varying methods, although the principle is the same. Both utilise P-D crossplots to derive overpressure values (see section 4.2).

4.1.1 Primary Source Pressure Data

The Norwegian Petroleum Directorate (NPD), based in Stavanger, is a Norwegian government agency that regulates hydrocarbon resources located on the Norwegian continental shelf. The website contains a public access database of all released well documentation. If the operators took pressure measurements they are often noted in the final well report or composite log. Furthermore, details of fluid contacts, formation depths and the presence of overpressure are often discussed within

summaries. This agency only regulates well data from the Norwegian Sector. For fields or wells within the UKCS, and where open source data were not available, data was purchased from IHS – an upstream data acquisition and analytics company.

4.1.2 Secondary Source Pressure Data

Although data from secondary sources originate from a range of publications, the United Kingdom Oil and Gas Fields publication (Gluyas & Hichens 2003) was a particularly useful source. Within the literature singular field pressure value points or gradients were common. This, for example, could be a reservoir pressure, a hydrocarbon gradient or HWC. The challenge lay with producing a pore pressure profile from the information present. Field summary tables within the United Kingdom Oil and Gas Fields publication (Gluyas & Hichens 2003) were particularly informative as data, in general, included fluid contacts, structural information (crest depth, lowest closing contour etc.), virgin reservoir pressures, pay zone formation and hydrocarbon column heights.

4.2 Calculating Overpressure Values from P-D Cross-Plots

Pressure data were calculated differently depending on source, however all pressure data were loaded into a single field/well P-D plot. Pressure data are measured data from (or extrapolated from) the literature, whereas overpressure is derived from pressure and an assumed hydrostat. A constant hydrostatic pressure gradient of 0.445 psi ft^{-1} was assumed for all depths. This gradient acted as a base from which overpressure values were derived. A 0.445 psi ft^{-1} (±0.1 psi ft^{-1}) gradient agrees with the literature for hydrostatic pressures from within the North Sea. For each field an aquifer overpressure and formation pressure (including buoyancy effects of the hydrocarbon) at the top hydrocarbon/structural crest will be taken as these are assumed to represent, or be close to representing, the maximum overpressures within a field.

The general methodology used is as follows:

1. Set regional standards within the RokDoc software including hydrostatic pressure (0.445 psi ft^{-1}).
2. Generate hydrocarbon gradient and extrapolate down to the HWC and up to the structural crest/top hydrocarbon column. Note value as pore pressure at the structural crest/top hydrocarbon.
3. Extrapolate a water/aquifer gradient through the pressure at the HWC to the crest of the structure/top hydrocarbon column. Note value as aquifer pressure at the structural crest/top hydrocarbon.
4. Evaluate the overpressure by subtracting the regional hydrostatic gradient of 0.445 psi ft^{-1} from the pressure, i.e. $OP = P\text{-}P_{hydr}$

A further, more detailed breakdown, is described in the following sections. Variations depend on quality of data as well as the data source.

4.2.1 Calculating Overpressure from the Direct Pressure Measurements & Composite Logs

Primary source data, from IHS, NPD or hard copy operator reports, were identified within completion reports or the final composite logs. Within well reports, or at the base of composite logs, a table of the well pressure data with direct pressure measurements can be found. The composite logs, or formation top notation within the reports, provide values for top hydrocarbon depth and often HWC.

Wireline formation tests (WFT) provide direct pore pressure measurements (RFT, MDT and FIT tools) and are common within end of well reports. Wireline formation tests are the most common and reliable way to acquire accurate pressure data. Although the exact process to acquire the data varies depending on the tool, the principle is the same. An inflow of a formation fluid enters a chamber on the tool and a gauge measures the pressure build-up until the pressure stabilises (the point where the pressure in the tool chambers equals that of the formation). Depending on the permeability of the formation this process can last anywhere from 1 – 15 minutes.

However, this process can only be taken in permeable units and, as such, shales are not tested.

4.2.1.1 Operational Restrictions to Wireline Data

Common issues found within direct pressure measurements in well reports include:

- **Tight** – When the pressure build up time is long, the operator may decide to abandon the test to avoid the tool becoming 'stuck' to the formation. This could lead to the tool or even well bore being abandoned and side tracked. These measurements should be disregarded from analysis.
- **Supercharged** – Often identified in low permeability sections. Supercharging occurs when the formation retains borehole pressures present when drilling resulted in values higher than static mud pressures and that of the formation. These measurements should be disregarded from analysis as being invalid.
- **Seal failure** – This problem arises when the seal surrounding the formation penetrating probe fails. This leads to a quick build-up of pressure due to the influx of drilling mud. Pressures then equal hydrostatic mud pressure, not that of the formation. These measurements should be disregarded from analysis as being invalid.

4.2.1.2 Deriving Overpressure Values from P-D Crossplots

WFT measurements are taken at intervals throughout the reservoir. A best-fit gradient can be fitted through the direct pore pressure measurements. The resulting gradients reveal the hydrocarbon phase present within the reservoir. Theoretical gradient ranges (based from the North Sea) for the different pore fluids are as follows; water – 0.43 psi ft^{-1} to 0.59 psi ft^{-1}, oil – 0.29 psi ft^{-1} to 0.42 psi ft^{-1}, gas - 0.01 psi ft^{-1} to 0.30 psi ft^{-1}. These are however, only guides. For example, oil can be found with gradients of 0.25 psi ft^{-1} at great depths and high pressures. The important aspect to note is that the fluid type for every field analysed is known, either through the literature, or within operator reports. Although developing a fluid gradient can be undertaken with just 2

values, the more RFT measurements used will add accuracy to the gradient value (assuming accurate measurement values initially). A best fit gradient has been applied to the P-D plot (Figure 4.2); the Free Water Level (often a proxy for the oil water contact) is taken as the intersection of the oil gradient and aquifer gradient when extrapolated beyond the data. Cross checking with operator defined fluid contacts which will include petrophysical log analysis, where available, adds further confidence to the interpretation.

Once a water gradient within the reservoir is established, that gradient can then be extrapolated to the top hydrocarbon/crest depth (a value taken from the composite log or formation tops). If no pressure points are available within the water leg a standard 0.445 psi ft^{-1} can be taken and extrapolated from the hydrocarbon-water contact. Extrapolating these gradients provides pore pressure and aquifer pressure values at any depth within the closure, vitally the crest depth. It is important to note that primary data derive purely from well data. Unless the field data are published either within well reports or the literature, the actual structural crest of the field is

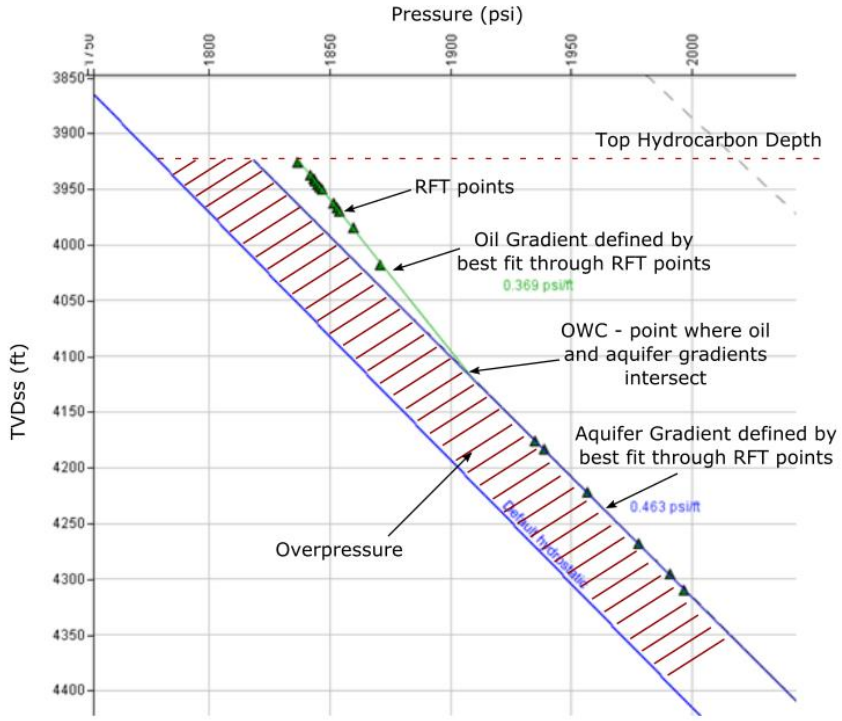

Figure 4.2 - Example Central North Sea P-D plot displaying best fit gradients through an oil phase and water phase interval. The gradients are determined by the RFT points (triangles). The lack of spread of RFT points around the gradient reduces the error.

unlikely to intersect with the well penetration. Often a reasonable estimation of the well closest to the structural crest can be attained; however, this is not always the case. Unlike the structural crest, the fluid contact depths should be constant throughout the structure (with the exception of hydrodynamically affected formations). If a contact is known and a maximum hydrocarbon column height within a field is known from a published source, a simple calculation can be made to estimate the structural crest:

$$CD = HWC - Column\ Height_{max} \quad \text{Eq. 4.1}$$

Where CD is crest depth (ft), HWC is hydrocarbon water contact depth (ft) and $Column\ Height_{max}$ is the maximum column height within that field (ft)[11].

For example, if a composite log or well report notes an OWC at 4000 ft TVDss and a 200 ft maximum hydrocarbon column is described within the literature, the structural crest, or shallowest point within the structure, can be determined by:

Structural crest = 4000 – 200

Structural crest = **3800 ft TVDss**

Likewise, a similar principle can be used to determine fluid contact depth or column height by rearranging equation 4.1. This is useful for gradient extrapolations.

4.2.2 Deriving Overpressure Values from Secondary Source Data - a Single Pressure Value

Within much of the secondary source data, pressure values are often stated as a reservoir value attached to a datum. In the event a reservoir pressure was recorded within the literature, but without a depth measurement, a mid-hydrocarbon column depth was used (i.e. a depth determined to be within the middle of the hydrocarbon reservoir – termed the mid-reservoir method). Using RokDoc pressure software, the

[11] Either collected from the literature or derived from the well report if described.

data was input onto a P-D plot. The green triangle on Figure 4.3 represents the reservoir pressure value input mid-point between crest and HWC.

A gradient can be taken through this point. Within a single phase system a standard density, if actual hydrocarbon density is unknown, allowed a gradient to be extrapolated intersecting the data point to the HWC and the top hydrocarbon/crest depths – red line on Figure 4.3. The gradients used for standardised hydrocarbon gradients are shown in Table 4.2. In the event of a multi-phase system either the hydrocarbon column heights of the different phases needs to be known or the GOC and OWC. The process of gradient extrapolation to the HWC is the same as previously described.

The generated pressure profile provided a top hydrocarbon/crestal formation pressure and formation pressure at the base of the hydrocarbon column. The base hydrocarbon pressure, by definition also represents the aquifer pressure at the HWC. Following the same principle, water gradients (either standard or actual if available) can be extrapolated to the structural crest and/or deeper within the trap. This allows identification of the aquifer pressure throughout the closure, but importantly at the structural crest – the crestal aquifer pressure.

For this form of data processing, apart from a pressure and depth datum, values for two of the following variables are necessary; the structural crest, HWC and/or hydrocarbon column height. The third value, if not provided, can be calculated from the other two. The flowchart (Figure 4.4) displays the process followed to calculate overpressure values from secondary source data.

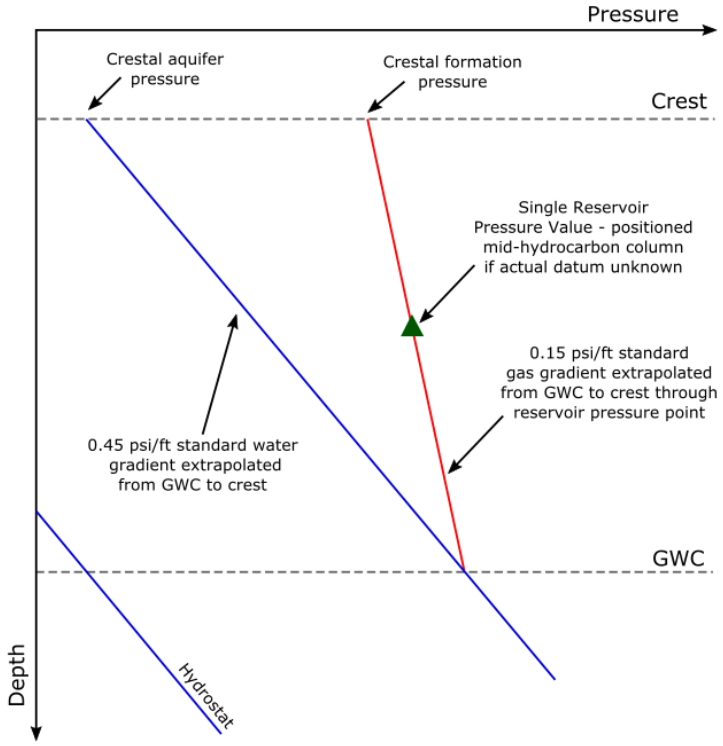

Figure 4.3 - Schematic P-D plot displaying the central reservoir datum method. A hydrocarbon gradient is extrapolated through the pressure point placed in the central reservoir depth to the crest and HWC. A water/aquifer gradient is then extrapolated the structural crest allowing a crestal aquifer pressure to be derived.

Fluid Phase	Standard density gradients (psi ft^{-1})
Water	0.445
Oil	0.35
Gas	0.15

Table 4.1 – Table indicating the chosen standardised fluid gradients when gradients cannot be derived from direct pore pressure measurements or are not noted within the literature.

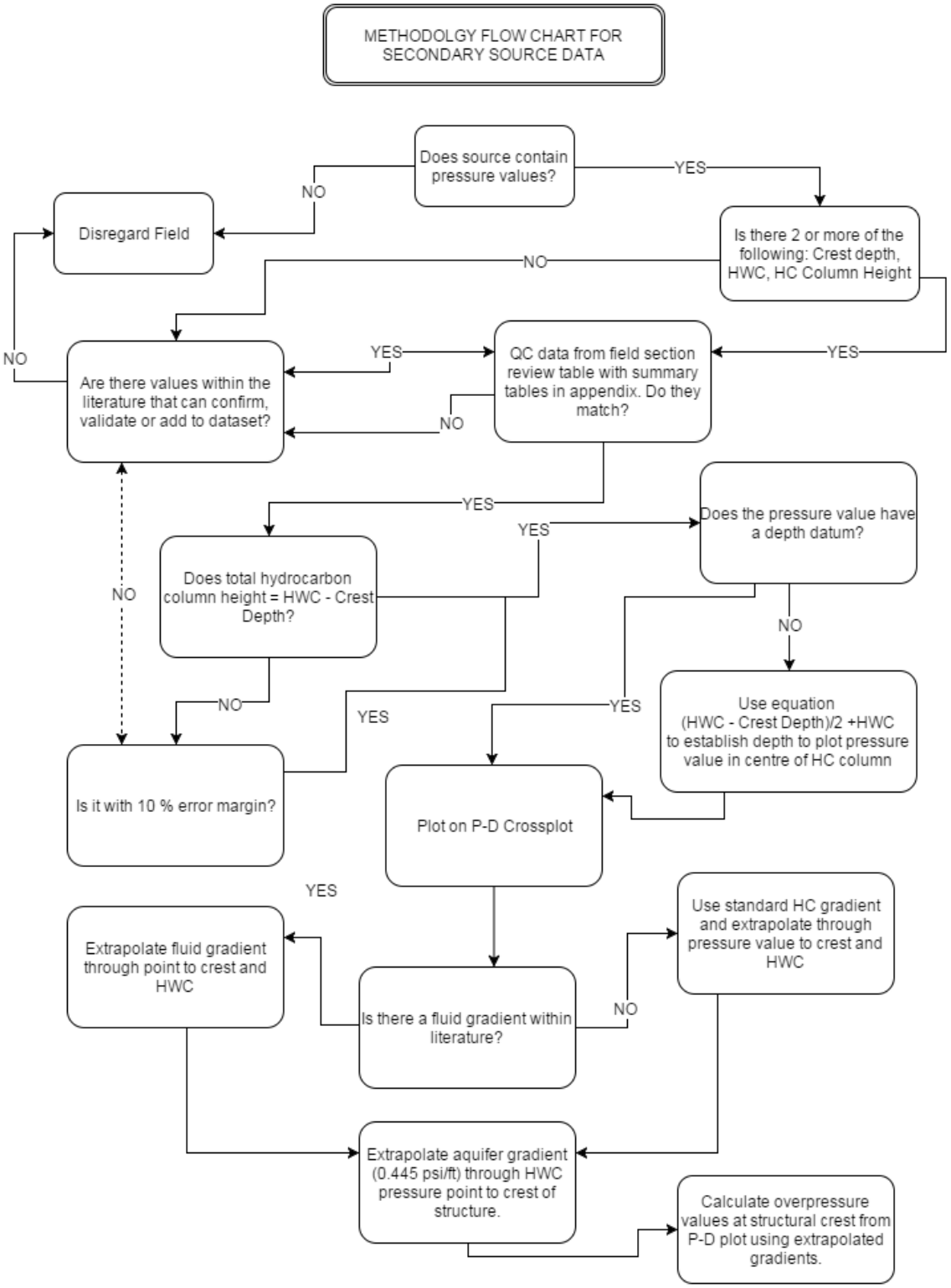

Figure 4.4 - Flow chart displaying the method used to process secondary data to establish crestal overpressure values.

4.3 Calculating Overburden Values

Calculation of overburden pressure is vital within North Sea principal stress studies. From Chapter 3 it is noted that despite the overburden representing the maximum principal stress (as would be normal in an extensional basin) a minimum stress conversion is observed within deep, highly overpressured formations (see Swarbrick et al. 2010). The nature of this study requires analysis regarding such overpressured formations; therefore, discerning the principal stresses will allow the derivation of seal capacity values.

Chapter 3 highlighted 3 different approaches to calculate the overburden; 1) using a standard 1.0 psi ft^{-1} (Gaarenstroom et al. 1993; Holm 1998), 2) individual well density derived values (Swarbrick et al. 2010), 3) regional overburden values (Hermanrud & Nordgård Bolås 2002; Nordgård Bolås et al. 2005; Nordgård Bolås & Hermanrud 2003).

Svare (1995) described how using density-derived overburden values posed too many inaccuracies on individual wells. However, Swarbrick et al. (2010) utilises the well-by-well approach. It is the opinion of the author of this report that, in order to eliminate as much inaccuracy as possible, but still account for the limitation of access to density log data, a combination of both approaches should be undertaken. This approach, therefore, takes into account local & regional variability of overburden values derived from density data and additionally the error is reduced by taking averages.

Using data from Swarbrick et al. (2010), depth intervals every 1000 ft TVDml were taken between 8000 ft and 18,000 ft and each well's overburden gradient was calculated. Following this, the overall average overburden gradient was calculated for each interval, $(\frac{\Sigma \text{ all } S_v \text{ in interval}}{No.of \text{ wells in interval}})$. The results of this calculation are displayed in Figure 4.5.

Figure 4.5 shows a positive correlation between overburden gradient and depth. This suggests that a generic linear S_v (for example 1.0 psi ft^{-1}) cannot be used as

standard. Therefore, the following equation was used on this reports dataset to determine vertical stress (S_v):

$$S_v = [(Z - WD).Avg_{Litho}] + (WD * 0.445) + P_{atmosphere} \quad \text{Eq. 4.2}$$

Where Z is the depth (TVDss), Avg_{Litho}, is the average lithostatic pressure derived from Swarbrick et al. (2010) for the corresponding interval, WD is water depth and $P_{atmosphere}$ is atmospheric pressure (14.7 psi). Although this is the method chosen for this study there are errors associated with it, primarily Swarbrick et al's (2010) dataset is based on the Central North Sea. It therefore may have a degree of uncertainty within other regions however this is mostly < 100 psi, within project error margins associated with calculating seal capacity.

This equation importantly incorporates the weight of the overlying water column between TVDml and TVDss (i.e. the water depth). Within the North Sea this has a limited effect due to the generally shallow water depths. However, when considering deep and ultra-deep water fields, within the Gulf of Mexico for example, this is imperative.

Depth Interval TVDml (ft)	Lithostatic Gradient (psi/ft)
< 8000	0.988
8001 – 9000	0.9707
9001 – 10,000	0.9614
10,001 – 11,000	0.9692
11,001 – 12,000	0.9672
12,001 – 13,000	0.9845
13,001 – 14,000	0.9863
14,001 – 15,000	0.99
15,001 – 16,000	0.991
16,001 – 17,000	0.9989
> 17,001	1.0068

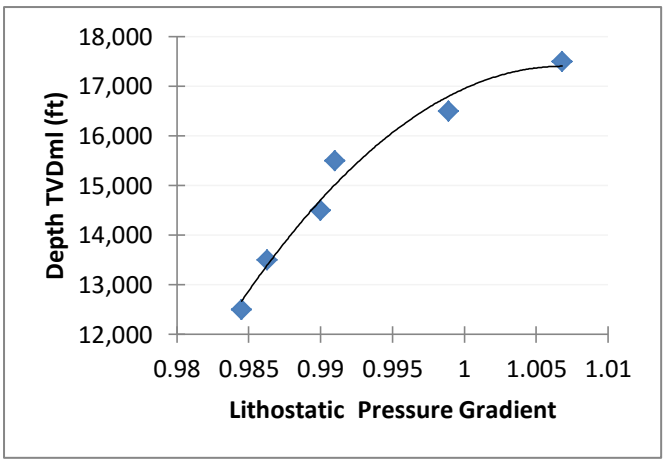

Figure 4.5 - Table showing changes in overburden gradients at differing depth intervals from derived from averaged density data from Swarbrick et al. 2010.

4.4 Calculating Fracture Pressure

There are several commonly used algorithms to determine fracture pressure profiles. The main ones being published by:

- Matthews & Kelly (1967)
- Eaton (1969)
- Daines (1982)
- Breckels & van Eekelen (1982)

The equation used within this report incorporates components of all the above authors' methods. Accurate calculations of fracture pressures need to account for pore pressure – stress coupling effects relating to horizontal stress magnitude through poro-elastic fluid-stress interactions. The fracture pressure algorithm below (used by Swarbrick et al. 2010) does take this into account.

$$P_{frac} = (a.S_v) + (b.OP) + (WD.\delta P_w) + P_{atmosphere} \qquad \text{Eq. 4.3}$$

Where: P_{frac} is fracture pressure, δP_w gradient of the sea water, P_{atmos} is atmospheric pressure and a & b are regional coefficients. P_{atmos} is taken as 14.7 psi and δP_w is 0.445 psi ft^{-1}.

Values for a & b were provided – 0.87 and 0.35 respectively. Comparing the values of LOT and S_v when the pressures are 'normal', i.e. the LOT/S_v ratio at the same depth denotes how a is derived. Coefficient b is derived from ΔFP/Overpressure ratio.

Coefficients a & b do vary from region to region, however such variations are noted to be minimal, despite incongruently differing geological settings. Global records suggest that that "a" varies from around 0.8 to .094 but most commonly between 0.85 and 0.9. "b" varies from about 0.25 to 0.4 but most commonly between 0.27 and 0.35 (Swarbrick & Lahann, unpublished). Using the same coefficient value throughout the North West Europe data set initiates no problems and error margins are of negligible values.

4.5 Calculating Fault Reactivation Pressure

When structures have faults associated with the traps that either displace the seal or work in a network juxtaposing permeable horizons allowing the displacement of fluids to leak through the sealing strata, reactivation needs to be considered. Equation 4.4 allows the calculation of the pore pressure value sufficient to reactivate a pre-existing fault should the fault be optimally orientated and be cohesionless.

$$\frac{\sigma_1 - Pp}{\sigma_3 - Pp} = \left[(\mu^2 + 1)^{1/2} + \mu\right]^2 \qquad \text{Eq. 4.4}$$

μ can be taken to = 0.6 (see Streit & Hillis, 2004) for the purpose of this study and therefore, to find the pore pressure required to allow slip:

$$Pp = \frac{[\sigma_1 - (3.119\sigma_3)]}{1 - 3.119} \qquad \text{Eq. 4.5}$$

Should fault reactivation and re-shearing occur, dilation along the re-activated fault/shear could lead to hydrocarbon leakage, especially in an area such as the extensional North Sea.

4.6 Quality Control

Within the dataset the wide range of sources and differing techniques used to analyse data predetermined the need for quality control. The quality control checks and error margin associations within primary and secondary source data are assessed and expanded upon below.

4.6.1 Primary Source Data

Quality control was undertaken extensively throughout the process of primary data analysis. The following flow chart (Figure 4.6) indicates the work flow to assure continuity and repeatability of the results, whilst removing any spurious data. This

approach was followed for all primary source data analysis. Furthermore, 2 categories are determined indicating data quality.

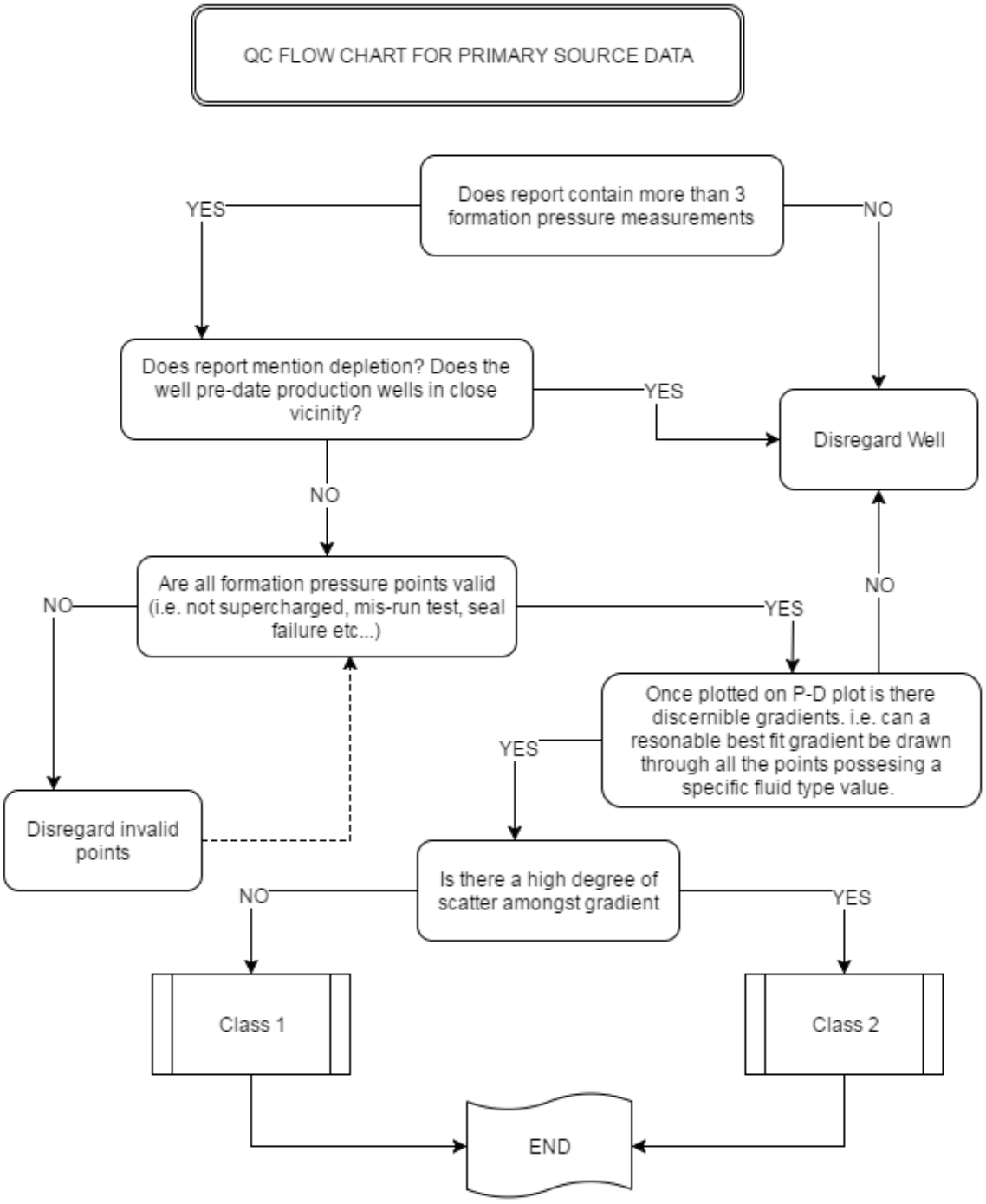

Figure 4.6 – Quality control flow chart for primary source data. Data can be categorised into 2 classes; class 1 represents data with higher levels of confidence, whereas class 2 will possess larger levels of uncertainty.

- **Class 1** – Data with more than 5 pressure values contributing to a single phase gradient. Furthermore, the values all have little variation from the best fit gradient – scatter is minimal.
- **Class 2** - Data that contains less than 5 pressure values within one gradient interval. Pressure values that present a high degree of scatter around the gradient also fall under class 2. This data could still be accurate; however, the reliability is questionable. It can still be considered but should be noted as having greater uncertainty than Class 1.

Depletion (i.e. pressures lower than in the original geological state due to production) is a further issue when considering primary data. As with the previous comment, little in the way can be done to certify and put quantitative error margin on this. Unless the well report states depletion from neighbouring production wells or the results are anomalously low it is hard to determine. Virgin pressures (those not subject to depletion) were assured to the highest confidence possible by selecting wells that pre-date any production wells within close vicinity.

The significant advantage of utilising primary data or well reports is the ability to accurately analyse fluid gradients and compare to results interpreted by operators, thus providing an extra level of cross checking and reliability. For example, if an interpreted gradient derived from primary data is equal, or very close, to that of the operators more confidence can be had regarding interpretation. However, in many wells (date drilled being a major factor) the WFT results sometimes produce erratic data, hard to distinguish an accurate representative gradient. Correlating data from neighbouring wells and operator interpretations helps add confidence to the final analysis.

As stated previously due to the nature of this study, pore pressure data ideally needs to be taken from the structural crest. Field structure maps are often not released; however, there are some examples where structure maps are available in the literature (e.g. Gullfaks field). Using composite logs the top reservoir depths were noted from exploration wells. By comparing depths of the top reservoir interval between logs the

well with the shallowest value was chosen. It was generally found that the discovery or wildcat wells were drilled close to or on the structural crest. If the well drilled on crest did not contain, or contained poor, pressure data, neighbouring well data was combined on the assumption the wells are within the same pressure compartment. Due to the small nature of the structural height of North Sea fields traps, not being fully on crest is thought to be minimal in terms of final pressure differences. For example, a crest depth with an uncertainty value of ±100 ft will likely only have a pore pressure uncertainty of < 100 psi. Discovery or wildcat wells being the primary source of data also helped remove the effects of depletion due to measurements being taken prior to production wells being drilled so virgin pressures can be assured.

4.6.1.1 Pressure Tool/Gauge Limitations

Using direct pressure measurements means that the tool and associated gauge influences the accuracy and error margins associated with the recording. Since the development of the downhole test valve in the 1930s, advances have allowed more precise and accurate measurements, from clock-driven mechanical gauges to electronic quartz gauges (Vella et al. 1992). The following table from Vella et al. (1992) summarises the differences between them.

	Mechanical Gauge	Convectional Strain Gauge	Standardised Quartz Gauge	Combined Quartz Gauge
Advantages	• Reliable • Rugged • Simple	• Better resolution • Fast Response • Rugged and Small	• High Resolution • Lower Power	• Best dynamics • Best Stability • Higher pressures than standard quartz gauge

Disadvantages	• Poor resolution, accuracy and stability	• Mediocre stability, resolution and accuracy	• Sensitive to temperature change • Limited pressure range	• More electronics
Max Range	20,000 psi 200 °C	20, 000 psi 175 °C	11,000 psi 175 °C	15,000 psi 175 °C
Accuracy	40 psi	15 psi	± [0.025 % of reading + 0.5 psi]	± [0.01 % of reading + 1 psi]
Cost	Low ⟶			High

Table 4.2 - Table summarises tool gauge advantages, disadvantages, ranges, accuracies and costs. With higher operational costs quartz gauges provide the highest levels of accuracy. However, these gauges are also more sensitive to temperature changes than mechanical and strain gauge. The accuracy level of all tool gauges are within acceptable error margins and will not drastically skew the data. Table is adapted from Vella et al. 1992.

As can be seen from the table, various tool gauges have advantages and disadvantages. In general, increased accuracy and resolution come coupled with higher sensitivity to temperature changes and greater operational costs. What is also important to note is the maximum pressure limits within the standardised quartz and combined quartz gauge (CQG) of 11,000 psi and 15,000 psi respectively. This is below the threshold for some deep HPHT Central North Sea wells. These however, are operator's considerations. What should be noted in regards to this report are the accuracies. Quartz gauges represent the higher accuracies and resolutions with ± [0.025 % of reading + 0.5 psi] & ± [0.01 % of reading + 1 psi], minimal inaccuracies within the scope of this project. Mechanical and strain gauges used for higher pressure formations display higher inaccuracies of ±40 psi & ±15 psi respectively. These error margins are still considered minimal and are absorbed into other variable margins. Where multiple formation pressure runs were taken comprising both strain, mechanical and/or quartz gauge measurements quartz gauge is preferred.

Within well reports there is often a choice between quartz gauge and strain gauge. More often than not, standardised quartz gauges are used by operators and these are always chosen over strain gauges for analysis if both are recorded.

4.6.1.2 Primary Source Data Limitation Summary Table

The following table highlights the main limitations, the solutions and associated error margins with primary data sources.

Primary Source Data	
Limitation	**Solution**
Often from well logs – not always at field crestal depths	Structural maps are studied, if present, to establish closest well to crest. Failing this, the first well drilled within the field vicinity i.e. xx/xxx-1 is thought most likely to be drilled on crest. This assumption can be verified by comparing top reservoir depths with neighbouring wells.
Inaccurate pressure measurements	Classes are attached to qualitatively assess the validity of the measurements. Class 1 shows data with little scatter around the gradient and Class 2 the opposite. Pressure measurements that are noted as not representative of the formation pressure (supercharged etc.) are invalid and disregarded.
No lowest closing contour	Within well reports it is never noted whether the field is full-to-spill or where the spill point depth is. Literature is used to try and find a value. Not crucial to analysis, but useful.
Data from the Norwegian sector is free, UK from CDA is a costly service	NPD is utilised. Data from the UK sector will be purchased from IHS if/when it is deemed necessary. Data access within the UK is limited and wells cannot be assessed prior to purchasing.
More time consuming than using secondary source data	Scouring well reports for pressure data, assuring measurements are accurate and data input takes time, especially with older wells where reports are scanned/hand written, not well organised or not compiled into one document.
Well release period	Although applicable to both primary and secondary data sources, operators are not obliged to release data for 15 years to the public. This means that well data is seldom up to date/current.

Inaccuracies of tool	Accuracy of pressure gauges vary from 40 psi (mechanical gauge) to 0.5 psi (quartz gauges). Where possible quartz gauge measurements are used. Despite this, all values are within other error margins and negligible in relation to skewing results.

Table 4.3 - Summary table emphasising key inaccuracies and limitations with primary source data and the solutions that have been implemented to reduce error.

4.6.2 Secondary Source Data

Despite several benefits of secondary source data, there are problems regarding consistency. Under some circumstances, parameters, for example crest depths, differed depending on where the data are sourced, which paper or book. Another issue arose regarding consistency with column heights within The United Kingdom Oil and Gas Fields publication. The publication noted column heights, which theoretically should equal the fluid contact depth minus the crest depth. There were discrepancies in some fields where these figures are considerably different.

Due to limited open access data, especially regarding accurate field pressure values, the values used within this report relies heavily on the accuracy of the data analysed by previous authors. The ability to compare values from differing secondary sources was limited.

Difficulties also arose regarding pressure data. In 38 fields, although a pressure value was recorded, no datum was noted with it. Therefore, a reservoir pressure was known but it is unclear as to whether that value is the pressure at the hydrocarbon-water contact, the field crest or at any interval in-between. In the event that a datum is

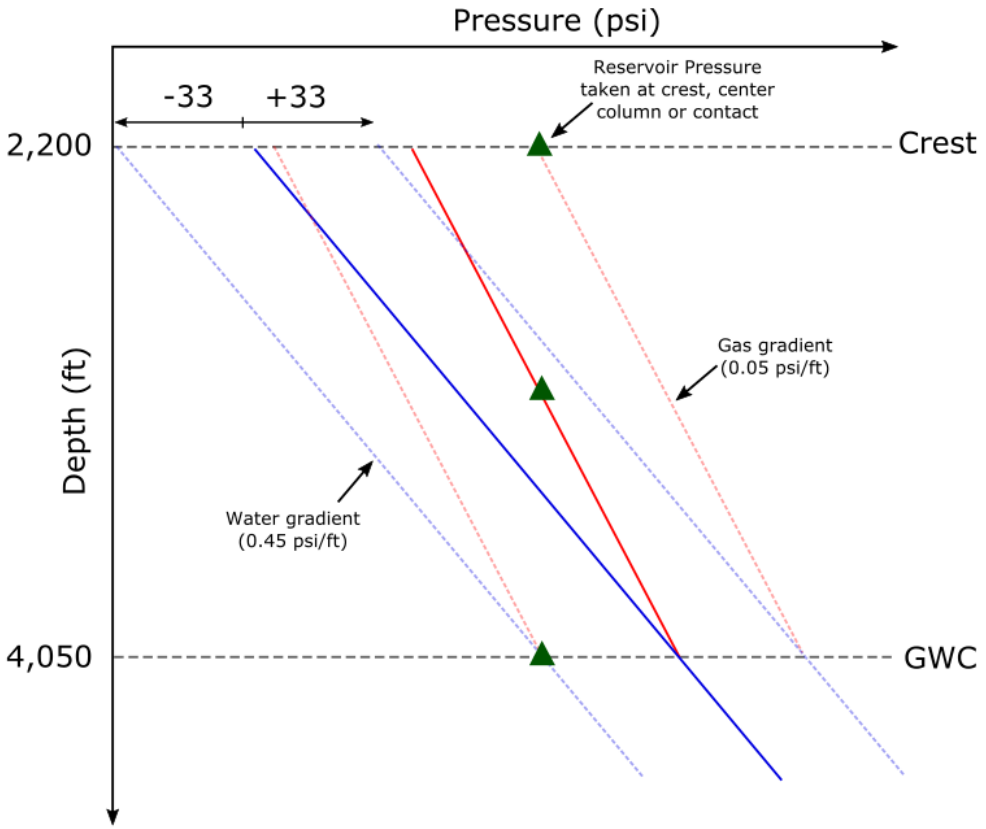

Figure 4.7 - Schematic P-D diagram emphasising the value of error associated with the central reservoir datum method used for data without a noted depth. The example is from the Corvette Field and a discrepancy of ±33 psi is observed depending on where the depth datum is set.

unknown the pressure value was plotted in the middle of the hydrocarbon column. The median value for the closure height within the North West Europe data set used within this report is 525 ft – a relatively small closure height. When considering the error values associated with an unknown data depth the values are minimal. Within the data set, 39 fields out of 129 had no depth datum. The range of error associated with the mid-reservoir technique was ±6 psi to ±177 psi, with a median of ±33 psi. A schematic of the Corvette Field P-D plot is illustrated as Figure 4.7. This indicates the effect of the maximum variance on psi determined by differing pressure point

locations. The solid gradients indicate the central reservoir method used and dotted gradients the variation should the pressure value be taken shallower or deeper that the centre of the hydrocarbon column. Pressure data with a known depth datum was categorised as "Class 1" as was pressure data with an error margin of < 100 psi. Data without a depth datum or error margins associated with the mid-reservoir technique of < than 100 psi are classed as "Class 2".

4.6.2.1 Secondary Source Data Limitation Summary Table

Table 4.1 summarises the key limitations, error margins and solutions to secondary data sources.

Secondary Source Data

Limitation	Solution
No depth datum with reservoir pressure	Mid-hydrocarbon column technique used – error is 3 psi to 177 psi (median 33 psi).
Column height discrepancies	HWC-crest depth should = column height. This is not always the case. If > 10 % discrepancy confirmation of column height was sought from literature.
Reliance on other secondary interpretations	The data come from a secondary source and so rely upon the accuracy and analyses from the primary author's interpretations. Although a degree of QC is possible the reliability and methods of the initial authors and reviewers is required.
Standardised fluid phase gradients	The hydrocarbon gradient is often omitted from literature. To undertake analysis of data gradient extrapolations are pivotal. Standardised gradients are used. Depending on fluid type the following error margins are calculated for the mean column height throughout the dataset: Water ±38.4 psi, Oil ±34.7 psi & Gas ±69.6 psi from the standard constants used. In reality these are dependent upon column height and the difference between actual and assumed density. Due to the extrapolation method of aquifer pressures, the oil/gas error margin must be added to the water gradient error.

Lowest closing contour & crest depth values	Field crest depths and lowest closing contours are often noted. These are determined from seismic data, although these cannot be 100 % accurate. The quality (age) of seismic, time-depth transformation all effect uncertainty. There is no solution or determinable error margin to this but should be considered within analysis.
Pressure data & compartmentalisation	One pressure value is taken per field reservoir interval. However, it should be noted that some fields encompass various compartments with varying pressure regimes. Therefore, the pressure provided may not represent the most overpressured compartment.

Table 4.4 - Summary table emphasising key inaccuracies and limitations with secondary source data and the solutions that have been implemented to reduce error.

4.6.3 Use of Constant Hydrostatic Gradient (0.445 psi ft-1)

Using a linear constant 0.445 psi ft^{-1} gradient as hydrostatic implies that there is no variation in aquifer salinities either with depth or regionally. This is of course not the case. The constant gradient of 0.445 psi ft^{-1} was chosen due to the majority of fields within the study being located within the Central and Northern North Sea, this is utilised by authors and is considered a reasonable regional aquifer. The Southern North Sea is noted to having more saline aquifer compositions. Pore pressure gradients taken within the Leman Sandstone formation underlying the Zechstein salt - the formation containing most SNS fields within this study, registers 1.3 g cm^{-3} (0.49 psi ft^{-1}). This is typical of formations within the Rotliegend Group (Yielding et al. 2011). With the Leman Sandstones field being 5000 ft – 8000 ft depths the hydrostatic discrepancies amounts to between 225 psi to 360 psi error margins. Although these pressures are substantial the error in hydrostatic pressure does not impact the actual pore pressure at the crest.

4.7 Calculating Seal Integrity

Seal integrity (in this study, which is ignoring membrane leakage) can be defined as the formation's ability to retain fluids within a closure without breaching the top seal, thus facilitating leakage of hydrocarbons. As pore pressure increases, the

formation's seal capacity is reduced, as is the caprock's ability to maintain a hydrocarbon column. A quantitative value defining the envelope between the pore pressure and minimum effective stress/fault reactivation pressure can be assessed by seal capacities. The seal capacity value is dependent upon what pressure is used to define failure (i.e. fracture pressure, fault reactivation pressure etc.) and what pressure influences the latter (i.e. aquifer pressure or actual formation pressure – see chapter 3). The different seal capacity notations, descriptions and equations are referred to in the table below.

Title	Description	Equation
Frac SC_{aq}	The seal capacity defined by the difference between top reservoir aquifer pressure and fracture pressure[12].	Frac SC_{aq} = FP – AQ PP
Frac SC_{form}	The seal capacity defined by the difference between top reservoir formation pressure and fracture pressure.	Frac SC_{form} = FP - PP
FR SC_{aq}	The seal capacity defined by the difference between top reservoir aquifer pressure and fault reactivation pressure[13].	FR SC_{aq} = FRP – AQ PP
FR SC_{form}	The seal capacity defined by the difference between top reservoir formation pressure and fault reactivation pressure.	FR SC_{form} = FRP – AQ PP

Table 4.5 - The definition of seal capacity varies amongst the literature and so differing attributes thought to have an effect on top seal failure are considered. There notations, descriptions and linked equations are summarised within the table.

[12]The minimum principle stress or σ_3

[13] The pore pressure required to reactivate a pre-existing fault causing it to re-shear (based on a cohesionless fault, optimally orientated for slip).

4.8 Summary

To summarise, the following data were collected:

- Aquifer pressure and overpressure at the field crest/top hydrocarbon structural crest.
- Fault reactivation overpressure and pressure at field crest/top hydrocarbon.
- Fracture overpressure and pressure at field crest/top hydrocarbon.
- The overburden/Sv is also noted at the field crest/top hydrocarbon depth.
- In-place hydrocarbon column height.
- Hydrocarbon fluid phase.
- Furthermore, the lowest closing contour within the field is useful. This can be used to calculate maximum closure capacity regarding HC column height which in turn can provide a quantitative value for reservoir percentage fill within the closure or if the field is full-to-spill.

All these variables are compared to establish patterns and correlations that exist between them in the following chapters.

Chapter 5

Seal Capacity & Hydrocarbon Column Height of North West Europe

Chapter 5 - Seal Capacity and Hydrocarbon Column Height of North West Europe

The purpose of the following chapter is to provide the reader with sufficient background information on the study region to provide context for the data analysis and discussions that follows.

5.1 Geography & Geology of North West Europe

The main region of study within North West Europe is the North Sea. Although primarily located between Great Britain and Scandinavia, coastlines are also held by Belgium, Germany and France all hold a coastline (see Figure 5.1). Situated on the European continental shelf, the North Sea is an epicontinental sea of the Atlantic Ocean bound to the South by the English Channel and the North by the Norwegian Sea. Water depths are shallow, generally less than 200 m (Evans 2003) with the exception of some recent glacial erosion within the Norwegian Sector.

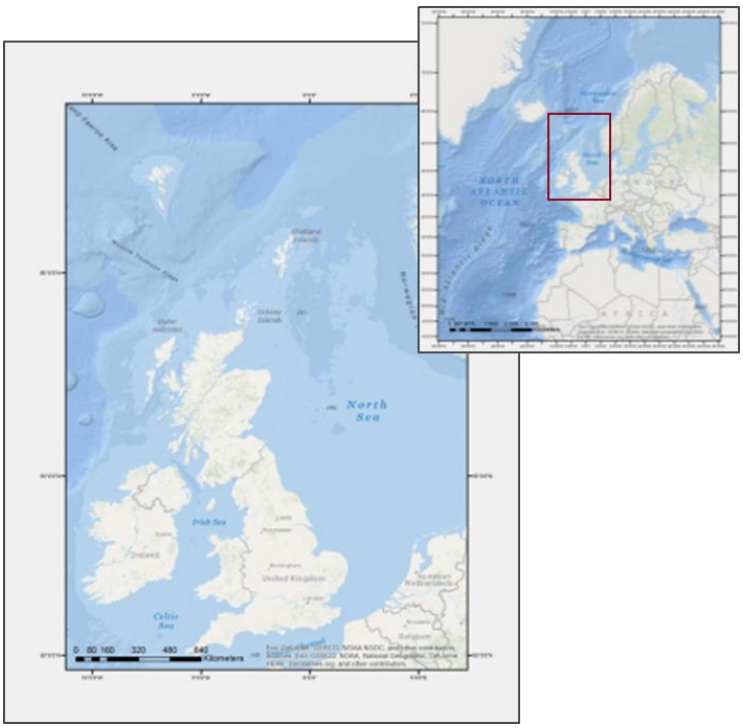

Figure 5.1 - Geographical map of the North Sea showing coastlines with the UK, Norway, Netherlands, Belgium, Germany and France.

5.1.1 Geological History of the Northern and Central North Sea

The geological history, and petroleum significance, of the North Sea primarily dates from the Carboniferous through to the Cenozoic. The Central and Northern North Sea are dominated by a three-pronged failed rift system. The basement rocks, comprising crystalline and metamorphic lithologies, formed during the Caledonian Orogeny and underlie the prolific North Sea hydrocarbon bearing sedimentary basins. The subsequent closures of the Iapetus Ocean and Tornquist Sea, forming the Iapetus Suture and Trans-European Fault respectively, created lines of weakness. Many of these newly formed weaknesses are reactivated. The key tectonic events, including their timings and basin locations are summarised in Figure 5.2. A more detailed geological history is provided below.

Figure 5.2 - Table summarising major regional and North Sea tectonic events, adapted from (Evans 2003)

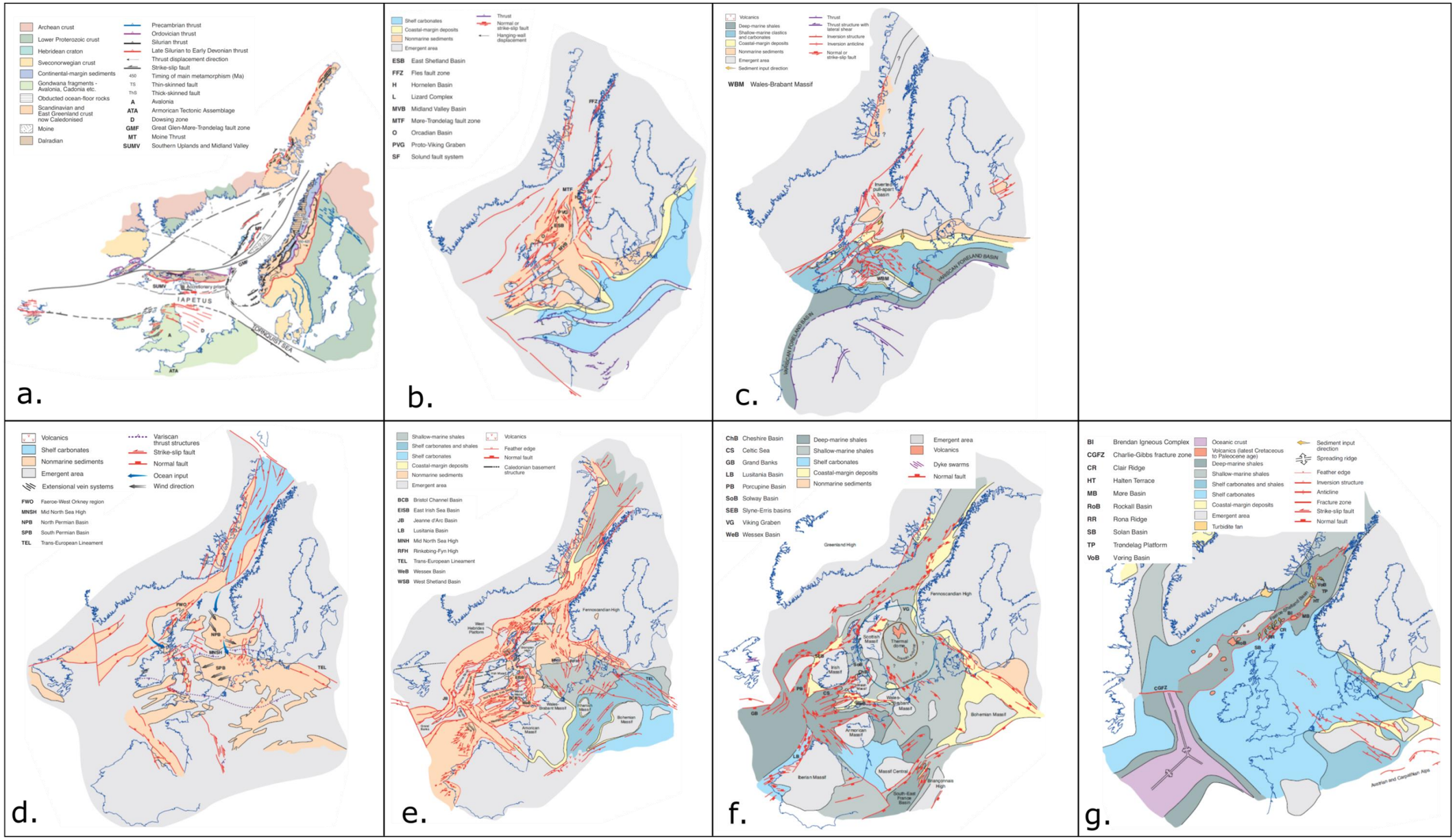

Figure 5.3 - Palinspastic maps from Evans (2003) throughout geological time showing the sediment facies and distribution of active structures. A – Precambrian, B – Devonian, C – Early Carboniferous, D – Permian, E – Triassic, F – Early-Mid Jurassic, G – Late Cretaceous.

Pre-Cambrian – The geologic events prior to the Caledonian are still known only on a basic level (Glennie 1998). The exact ages of Precambrian rocks are still debated but confidence levels in ages are increasing (Harris et al. 1994).

Towards the late Precambrian, suggested ages of 780 Ma (Soper & Anderton 1984) or 800-750 Ma (Drinkwater et al. 1996), Laurentia and Baltica subcontinents separated, initiating the preliminary foundation of the Iapetus Ocean (see Figure 5.3a). Northern Britain lay on the eastern edge of Laurentia whilst southern Britain lay within the southern regions of the Iapetus Ocean.

Cambrian – Cambrian times were dominated by periods of continental collisions and orogenies including the Finnmarkian, Atholian and Caledonian. The Cambrian transgression resulted from wide-spread increases in world mid-ocean ridge activity. The Alum oil-shale sequence was deposited during this time within Baltica; however, quickly became post-mature for Denmark region where the rock is prevalent (Thomsen et al. 1983).

Devonian – The formation of Laurussia, resulting from the closure of the Iapetus Ocean (Figure 5.3b), was a time of uplift (creation of the Appalachian ranges) and granitic intrusion emplacement – all likely aiding in the destruction of local source rocks, such as the Lake District Seathwaite Formation (Parnell 1982). Erosional material, sourced from the recently formed Caledonian mountain range fashioned red-bed molasses and lacustrine sediments for the Central and Northern North Sea basins. Devonian fish beds were deposited within Orcadian Basin lacustrine sediments. These are considered a potential source rock for the Inner Moray Firth fields including the Beatrice Field (Peters et al. 1989). To the south of the Central North Sea, marine limestones developed in a narrow (< 150 km width) NNW trending mid-Devonian sea branching from the Proto Tethys. Forming along a likely line of weakness these marine limestones extended as far North as the Auk Field.

Carboniferous – Drifting northward, the continent of Laurussia (Figure 5.3c) transitioned from arid sedimentation to equatorial deposition, facilitating the development of Carboniferous Coal Measures (Habicht 1979). The Millstone Grit sequences (a common carboniferous reservoir and source rock formation) was deposited as Late Visean fluviodeltaic sedimentation. Though not yet mature, the Carboniferous saw the deposition of the Southern North Sea source and reservoir rocks (Westphalian Groups) and Dutch-German-Polish gas belts. Within the United Kingdom Continental Shelf (UKCS) the Westphalian Carboniferous sequences reach 1200 m in thickness within the Sole Pit, with the German and Polish sectors known to reach twice that (Ziegler & Den Haag 1977).

The late Carboniferous Variscan Orogeny (a collision between Gondwana and Laurussia) caused the recently deposited rocks to subsequently be faulted, folded, uplifted and eroded. Deformation within the foreland of the collision zone is thought to have shaped the trapping structures within the Southern North Sea and east Midlands.

Permian – Since the early Permian the North Sea has been located in an intraplate setting. Transpressive, right-lateral movements (Figure 5.3d), resulted in local Carboniferous basin inversion, including that of the Sole Pit. Transtensional movements led to widespread volcanism, preceded by aeolian, shallow marine and alluvial sedimentation. The important Rotliegend sequences, significant sequences for UKCS petroleum reservoirs, comprising volcanics and clastic sediments, were formed. The Rotliegend reservoirs provide the Auk formation, for example (the reservoir to the Central Graben Auk Field).

The regionally extensive Zechstein evaporite group (see Figure 5.4 for salt basin extents) was deposited resulting from marine transgressions and cyclic evaporate successions. The evaporitic halites and anhydrites form effective seals within the Southern North Sea.

The combination of organic-rich Carboniferous coal, Rotliegend reservoir and seal rocks and the regionally extensive Zechstein seal has had strong influence in

trapping the Southern North Sea gas fields. The thickness of the Zechstein evaporites has an impact on the differing vertical stresses of the Southern and Central/Northern North Sea as a result of salt density differences.

Triassic –Palaeo half graben systems, including the East Irish Sea Basins are subject to extension followed by subsidence. Sand and mudstone red-bed successions were deposited regionally across the Central and Northern North Sea until the Toarcian (Glennie 1998) where the North Sea was subject to a phase of uplift, fabricating the Mid-Cimmerian Unconformity. Thermal doming and erosion has warranted little Permian sediments remain (Erratt et al. 1999). See Figure 5.3e for Triassic palaespastic reconstruction.

By the end of the Triassic, the Southern North Sea lay in a marine setting. Differential subsidence patterns on the Sole Pit basin's western extremity, accentuated by faulting, explain the different sediment characteristics and thicknesses in lower-mid Jurassic deposits between the Sole Pit and East Midlands Shelf.

Jurassic - Permo-Triassic rifting, following a stage of thermal subsidence, led to a relatively uniform spread of Jurassic marine sediments across much of the North Sea. A subaerial thermal dome formed in the middle-Jurassic, located at a triple junction between the Viking and Central Graben and Moray Firth, thought to be a result of a mantle-plume, (Underhill & Partington 1993) created a

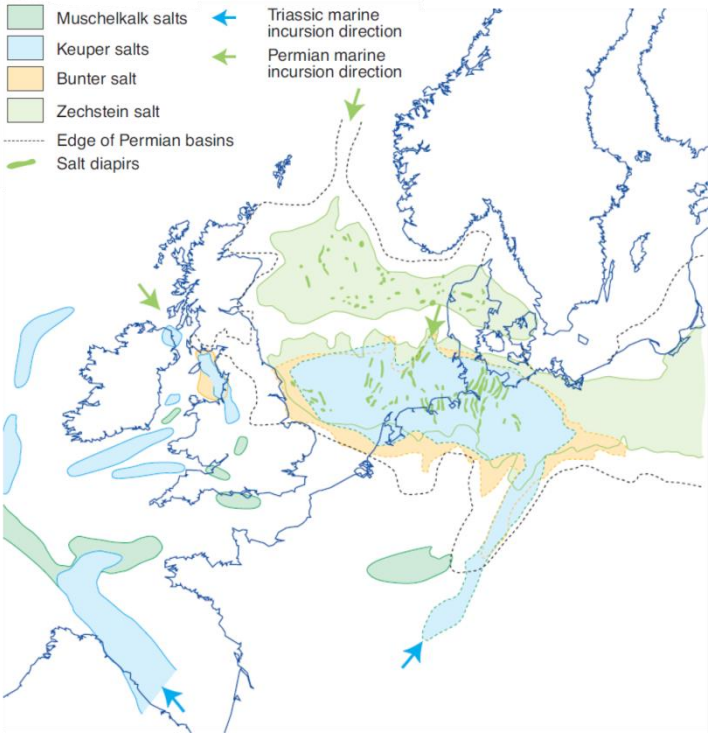

Figure 5.4 - Map displaying the distribution of the Permian-Triassic salt basins indicating the extent of the Zechstein salt formation. (Evans 2003)

marine regression giving way to shore-face, paralic sediments (see Figure 5.3f). These sediments form the reservoirs of the Brent group present in the North Viking Graben, and within the Central North Sea, the Fladen Group.

Although extensional rifting is thought to have initiated in the Triassic and several extensional phases occurred culminating in the early Cretaceous, the late Jurassic displayed the major extensional faulting regime, noted as the major trap forming event (Erratt et al. 2010) for the Northern and Central North Sea. Figure 5.5 displays a map indicating tectonic stresses during the Jurassic rifting event emphasising the failed graben system the North Sea. Seismic reflection data does suggest initial intensities were located within the basin margins, but with time propagated inwards toward the uplifted dome (Rattey & Hayward 1993) prior to continuing on a westward migration path, analogous to the North Atlantic Margin evolution (Erratt et al. 2010). Jurassic age, syn-rift, source rocks of the highly productive Kimmeridge Clay were deposited, in general displaying an increase in organic content towards the boundary with the lower Cretaceous. Structurally this extensional phase formed major faults, which in time will form the prominent half graben petroleum plays the North Sea is renowned for. The late Jurassic saw the deposition of the Fulmar reservoir rocks (Curlew, Fulmar fields) and the Brae formations, supporting those of the Brae, Kingfisher, Thelma fields.

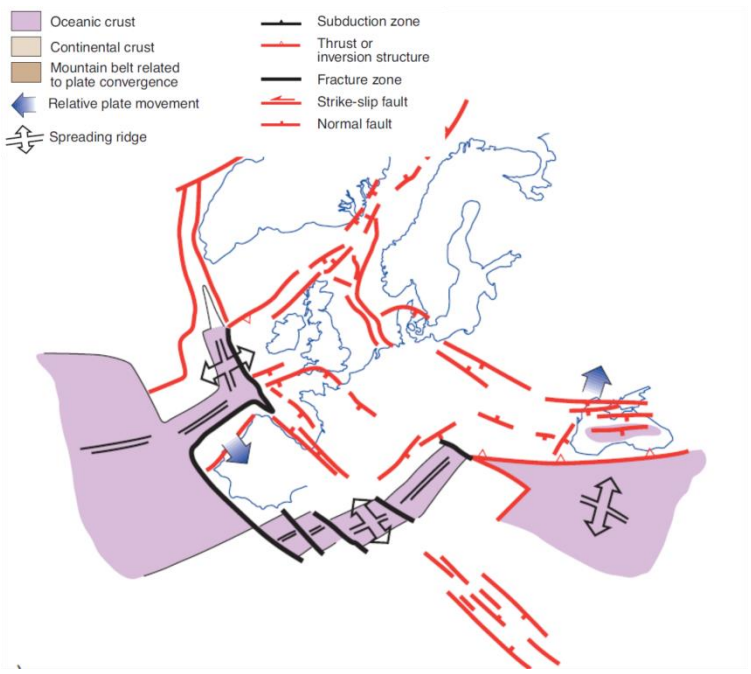

Figure 5.5 - Jurassic tectonics and structures of North West Europe. Important to note is the failed 3-pronged rift system of the North Sea. (Evans 2003)

Although the Northern and Central North Sea are in close vicinity geographically, the resulting rift styles differ drastically. Many factors are thought to play a contributing role in these

differences, however two principal dynamics are assumed. Firstly, the basement rocks are compositionally different between the Central and Northern North Sea. The Central North Sea displays more complex rift structures, segmented along a NE trend associated with Caledonian Fault Zones and a NW along the Trans European fault zone (Erratt et al. 1999; Jones et al. 1999). The second major variation lies with the presence of Upper Permian Zechstein salts, or specifically the lack of, within the Northern North Sea. The presence of Permian salt provides a detachment surface separating the basement rocks from the carapace (Hodgson et al. 1992; Smith et al. 1993; Helgeson 1999). This structural difference is represented by smaller sized pre/syn-rift oil and gas fields within the Central North Sea region. Within the Southern North Sea, deep burial of the depocenters, including the Sole Pit basin, occurred throughout the Late Jurassic. This ultimately led to the maturation of the Southern North Sea Carboniferous source rocks.

North Sea extension values are still disputed although β factors of 1.2 at the Jurassic basin margins to 1.3 in the basin centre are observed (Roberts et al. 1993). The characteristic three pronged graben system was the result of this stage of rifting.

Cretaceous - The epicentre of extensional forces swap from the North Sea to the proto-Atlantic. A time of tectonic quiescence prevailed, the Cretaceous exhibited mainly periods of deposition in accommodation space created from Triassic and Jurassic multi-phase extension. The Cretaceous was, however, an important time for North Sea play systems providing most of the seals to Jurassic Reservoirs. These were both in the form of effective Early Cretaceous mudrock seals and wide-spread Late Cretaceous chalk deposits (see Figure 5.3g).

Cenozoic – Thermal subsidence dominated the majority of the Cenozoic resulting from the Mesozoic rifting of the Triassic/Jurassic this is shown in Figure 5.6. The exception to this is Northern Scotland and the Orkney-Shetland Platform. These regions saw thermal uplifting resulting from the development of the Iceland plume (White 1988; White & Lovell 1997). This uplift caused increased erosion of these areas with the detritus being deposited in large debris flows and turbidites within the UKCS,

primarily during the Paleocene. Structural inversion played a role in uplifting Southern Britain Carboniferous source rocks out of their kitchen temperatures, effectively halting hydrocarbon generation. Further transpressional deformation resulted in the formation of major trap developments within the Southern North Sea (Alberts et al. 1991). The sedimentation rate during the Cenozoic was low in the Central North Sea, less than 100 m/Ma, with the exception of the last 2 Ma of glacial-influenced sedimentation when burial rates are recorded at >500 m/Ma (Swarbrick et al., 2000). These rapid burial rates are thought to lead to disequilibrium compaction, the main overpressure generation mechanism for the Central North Sea Palaeogene strata. However, although disequilibrium compaction is considered the primary mechanism for overpressured Palaeogene reservoirs the magnitude of overpressure generation mechanisms is disputed for the deeper sub-chalk HPHT formations. Modelling by Swarbrick et al. (2000) and Swarbrick et al. (2005) states that disequilibrium compaction alone accounts for only 70 % of the Jurassic reservoir formation pressures. The excess pressure is considered a result of gas generation of the high TOC Kimmeridge clay (Holm 1998; Swarbrick et al. 2005). Again, the maturation history of the Kimmeridge clay has meant that gas generation is currently present at depths greater than 12,700 ft (Cornford 1994), thus from Figure 5.4 can be dated back to the past 20-30 Mya (Eocene to present) (Goff 1983; Pegrum & Spencer 1990). The Cenozoic era, as such plays, an important role in the generation of both overpressure within the shallower Paleogene strata and the deep Mesozoic formations.

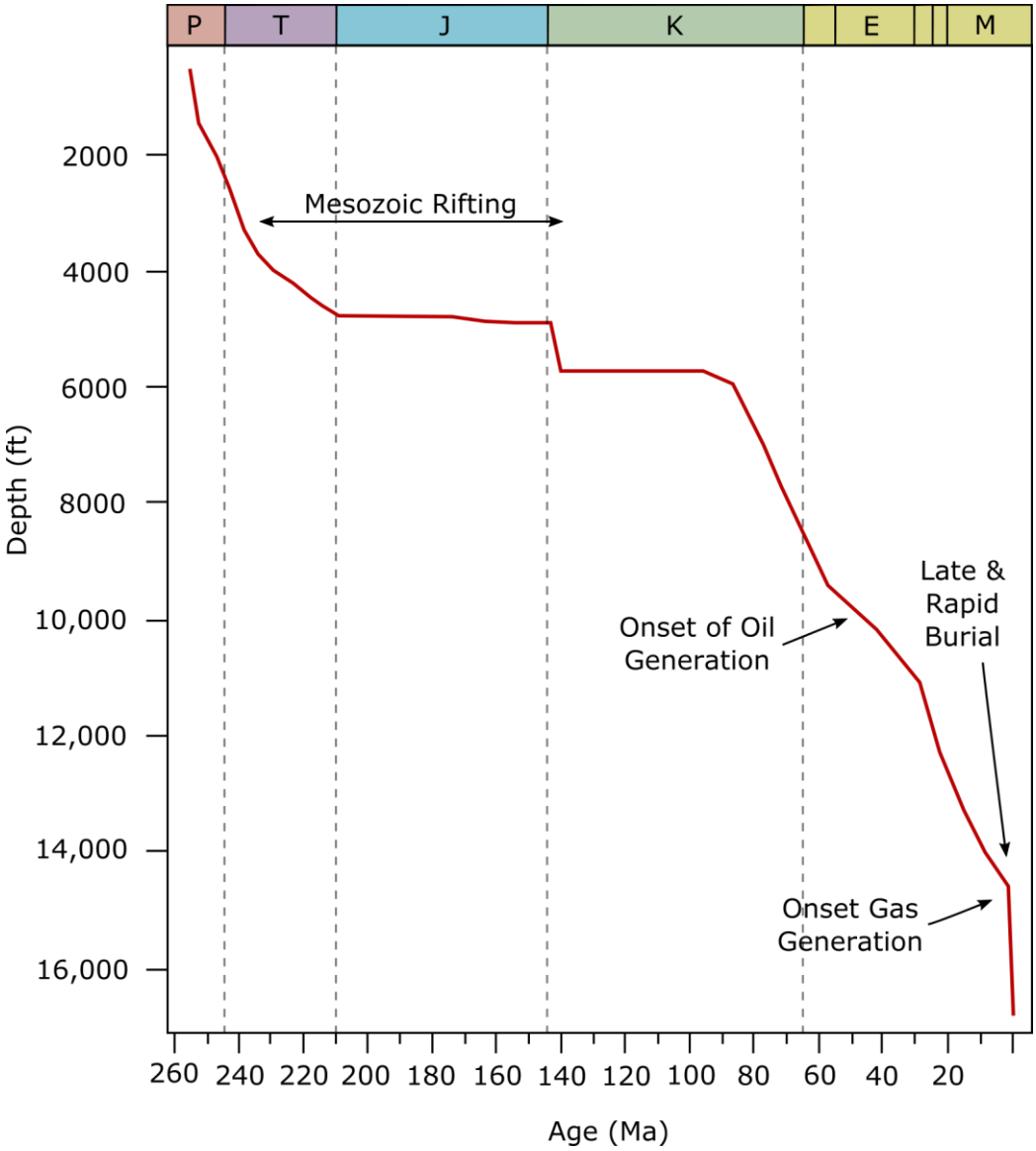

Figure 5.6 - Burial history curve modified from Swarbrick et. al (2005) constructed via basin modelling using stratigraphic and depth data from UK well 30/7a-4, thought to be a reasonable proxy for the Central North Sea

5.1.2 Petroleum Distribution and Significance of the North Sea

The North Sea is considered a mature petroleum exploration province. A stratigraphical chart from the Central, Northern and Southern North Sea is shown in Figure 5.7 (the major reservoir formations are indicated by filled and clear circles). Note the abundance of reservoir formations within the Jurassic and Triassic. With an exploration history dating back to 1959 with the discovery of the Groningen Permian, onshore gas field, further surveying in the Southern North Sea followed in an attempt

to prove that offshore prospects existed. This being the case companies sought to acquire exclusive exploration and investment rights. This saw the beginning of North Sea petroleum.

In 1996, at its peak, the North Sea produced 9% of the world's oil, providing it with the accolade of the fourth largest producing region in the world at the time (Evans et al. 2003). This not only brought a great deal of economic wealth to those oil-

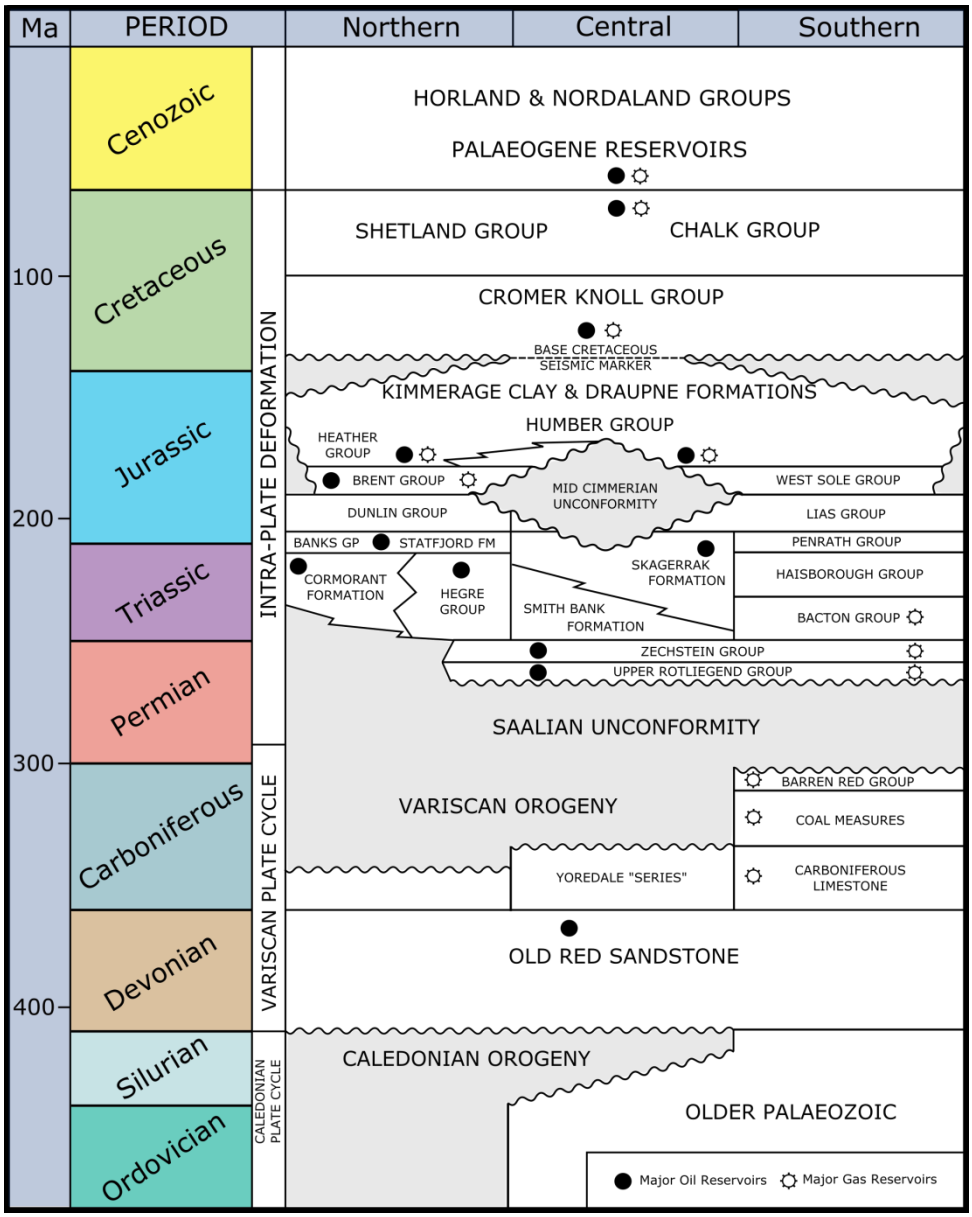

Figure 5.7 - Simplified Northern, Central and Southern North Sea stratigraphy correlated against geological time periods. The filled circles indicate formations that are important reservoir rocks for oil. White filled circles indicate important reservoir rocks for major gas fields. Adapted from Evans (2003)

producing countries, but also an abundance of knowledge to the industry and the Earth Science discipline.

Encompassing approximately 570'000 $km^{2,}$ the North Sea can be split, in the broadest sense, into two main hydrocarbon provinces; the Southern North Sea and the Northern North Sea (Central & Northern North Sea). The main distinction between the two being source rock age and hydrocarbon fluid type. The Northern and Central North Sea petroleum is sourced, almost in its entirety, from Jurassic aged, regionally extensive, Kimmeridge Clay. Oil is the dominant hydrocarbon phase within this region. Despite this, gas and gas condensate in more recent times are becoming increasingly important. The Southern North Sea fields are almost exclusively gas-bearing reservoirs sourced from Carboniferous Westphallian, coal measures. The Kimmeridge Clay maturity results from almost continuous burial dating from Cretaceous times (Pegrum & Spencer 1990). Oil Generation started from the Kimmeridge Clay by Eocene times, whereas gas generation is only achieved later, within the Neogene to recent (Goff 1983; Pegrum & Spencer 1990). This late onset of gas generation is considered an important overpressure generation mechanism in addition to disequilibrium compaction within the pre-Cretaceous reservoirs.

Further divisions of the northern North Sea can be defined by the Northern North Sea, containing the North Viking Graben, the Central North Sea, including the Central Graben and Moray Firth. The distributions of hydrocarbons are concentrated along this three-armed graben system. Although the Central and North Sea trapping structures are varied, in general, most have direct connotations to half graben fault blocks of the failed rift system.

5.1.3 Geology of the Irish Sea Basin

The dataset of this study, although primarily North Sea data, does include some Irish Sea basin fields and a brief geological history is important to consider. The Irish Sea basin comprises sub-basins and is one of many that span a line from south London to the Irish Sea, all separated from one another by basement highs.

The basins are the product of an early Permian rifting event, creating a set of normal faults all trending in a NNW orientation. Marls, sandstones evaporites are all deposited throughout the Permian in shallow marine, fluvial and terrestrial environments. Triassic sediments are influenced by a major drainage system forming both aeolian and fluvial lithologies. Upper Triassic evaporites and mudstones (named the Mercia Group) were deposited in a period of marine incursion and a restricted marine age.

Many early hydrocarbon traps were breached in the Jurassic as a consequence of a period of uplift resulting in erosion and reactivation of the Permian normal faults. The basin was subsequently buried as a result of its footprint lying in the foreland basin of the Alpine Orogeny. This burial transported many of the source rocks into the gas kitchen generating a hydrocarbon charge. Further, uplift and erosion resulted in much of the Tertiary being eroded and removed. Finally, glaciation has caused much of the basin to be concealed beneath a thick till section.

5.2 North West Europe Results

The following section discusses the results and interpretations of a North West Europe pressure data set. Over the following sections stress transitions[14], fracture pressures, fault reactivation and seal capacity pressures are discussed in relation to overpressures and seal capacities. Anomalous results are also identified. Chapter 6 discusses the results in the context of relationships between aquifer/formation pressures, overpressure, hydrocarbon column heights and seal capacities.

5.2.1 Pressure-Depth Plots of North West Europe Hydrocarbon Fields

Pressure-depth plots are useful for providing a regional or local overview of the pressure regime. Available formation pressures from selected fields are shown on Figure 5.8 displaying data from all study regions. A linear 0.445 psi ft^{-1} hydrostatic gradient is utilised as a regional standard. A best fit 3rd order polynomial trend line[15] has been applied to P_{frac} and σ_v data, derived using the fracture pressure algorithm and lithostatic algorithm respectively - discussed in Chapter 4. The field data points, coloured by region, represent formation pressures[16] at the structural crest/top hydrocarbon column.

A clear increase in overpressure with depth is observable, especially within the Northern and Central North Sea. The total number of fields reduces with increasing pore pressure and depth also. Figure 5.9 plots field formation pressures in a P-D cross plot, divided by region.

[14] Stress transition of fracture gradient from less than S_v to greater than S_v.
[15] Trend line application based purely on a line of best fit incorporating all data. This is elaborated further upon in section 2.2.2.
[16] Formation pressures include the excess buoyancy pressure caused by a hydrocarbon accumulation.

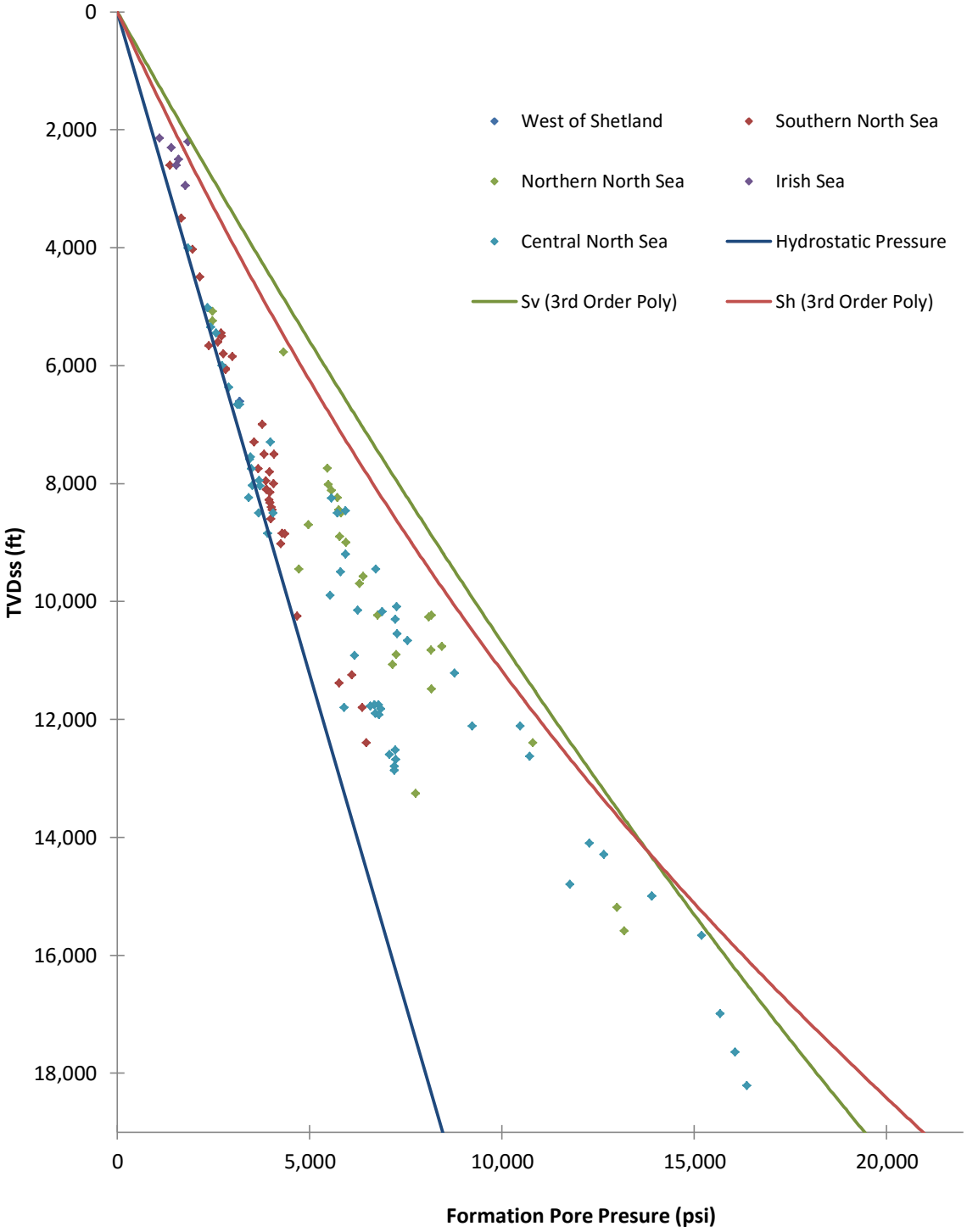

Figure 5.8 - Pressure depth plot with all field formation pressures plotted by region. A linear hydrostatic gradient of 0.445 psi ft^{-1} is shown in blue. 3rd order polynomial trend lines are applied to P_{frac} and S_v derived from calculated fracture pressures and overburden pressures. These trend lines are discussed further in Section 5.2.2 and at this point should simply be accepted as general examples of the P_{frac} and S_v. The Central and Northern North Sea are the only 2 regions to indicate high overpressure values. In comparison the Southern North Sea, Irish Sea and West of Shetland all show little to no overpressure. Formation overpressure is seen to increase with depth in NNS and CNS.

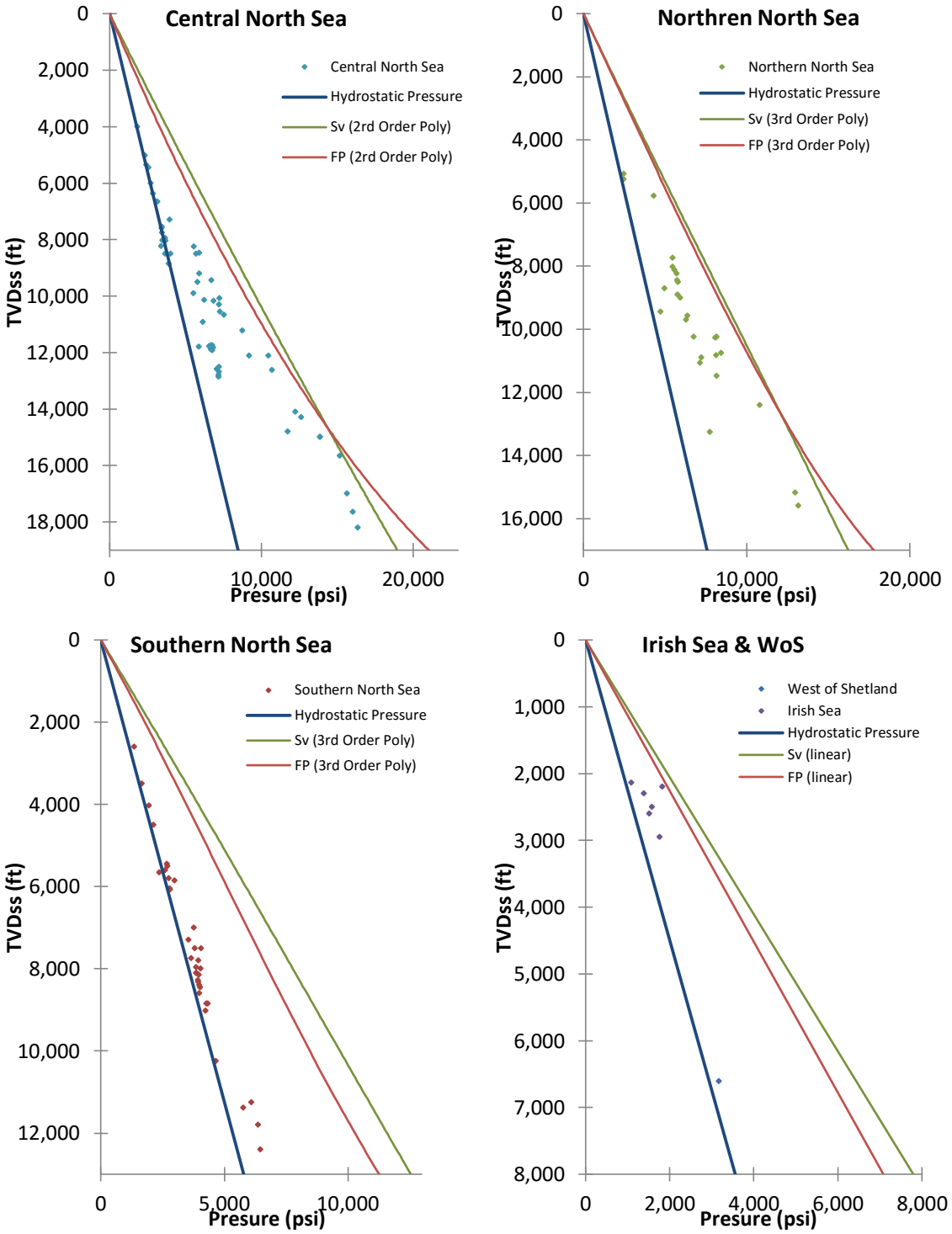

Figure 5.9 - Breakdown of Figure 5.8 into region specific pressure-depth cross plots. The plot titled "other P-D plot" displays fields from the Irish Sea and the West of Shetland. All use a linear 0.445 psi ft^{-1} hydrostatic gradient, except the Southern North Sea, where more saline aquifers are present and a 0.48 psi ft^{-1} hydrostat fits more accurately with the data. These plots emphasise the larger ranges of overpressures within the Central and Northern North Sea, minimal overpressures in the Southern North Sea and small overpressures within the Irish basin. The depth range of fields is also notable. Greatest within the Central North Sea, with the Northern North Sea indicating depths not far off the Central. Irish Sea Fields show the shallowest field crest depths. The σ_v and P_{frac} trend lines differ also. These are discussed further in Section 2.2.2.

The Central North Sea data exhibits the largest range regarding both field depths and pressures. Fields span from 4,900 ft to 18,209 ft in depth, with aquifer pressures between 1,818 psi and 16,220 psi. The Central North Sea also displays the greatest range of aquifer overpressures. The Cyrus field registers the lowest abnormal pressure with an underpressure value of -333 psi, whereas Glenelg, the deepest structure within this Central North Sea dataset, records the highest overpressures of 8013 psi. The shallowest (notable) overpressured field, Fife, lies at 8,250 ft TVDss and indicates 1,753 psi overpressure. With increasing depths down to Fife, all fields (with the exception of Auk) lie along a normally pressured hydrostatic gradient.

The Northern North Sea denotes the second largest data range for field depths and pressures. The shallowest reservoir lies at 5,000 ft, whereas the deepest is 15,587 ft TVDss. The majority of Northern North Sea fields have some degree of overpressure with just 2 field reservoirs, Harding (Central) and Harding (South), with normal hydrostatic pressures. The shallowest reservoir (5,767 ft), Gullfaks field, displays notable overpressures of 1,625 psi. The Statford (Brent reservoir), is overpressured by 1837 psi at depths of 7743 ft and is the shallowest overpressured Northern North Sea reservoir within the data (with the exception of Gullfaks).

Comparatively, the Southern North Sea and West of Shetland all indicate formations at, or close to, hydrostatic values. A 0.48 psi ft^{-1} hydrostatic gradient is used for the Southern North Sea P-D plot, differing slightly from the regional 0.45 psi ft^{-1} hydrostat applied on Figure 5.8. This accounts for the added salinity associated with the Southern North Sea Zechstein Salts. Some of the deeper Southern North Sea fields, Murdoch, Schooner, Windermere and Bolton, indicate a degree of overpressure, however, only by a few hundred psi (Boulton being the most overpressured at 357 psi). Fields from the Irish Sea basin are the shallowest, with depth values in-between 2000 to 3000 ft.

5.2.1.1 Interpretation

All regions within the study show both fields with little or no overpressure to varying degrees of overpressure. Below 10,500 ft TVDss no fields lie on the hydrostatic

gradient. This is not to say that normally pressured reservoirs do not exist below 10,500 ft. The data selection process focused upon overpressured fields, so the resulting pattern may be as much a data selection bias rather than an actual proxy for the North Sea and North West Europe. Top overpressure (defined by the fluid retention depth) is noted to occur at depths around 3280 ft (1 km) TVDss within the Central North Sea (Leonard 1993; O'Connor & Swarbrick 2008). Large magnitudes of overpressure within this data set are observed from 7,000 ft depth and not as shallow as the 3280 ft as suggested within the literature. This variation is the result of this report's data utilising purely reservoir data, and as such does not include shale pressure interpretations. Furthermore, reservoir intervals are not stratigraphically sorted in a fashion where an accurate pressure trend can be established determining a top overpressure depth (FWD). This report can only conclude that overpressures are observable deeper than 7000 ft depths. The Northern North Sea field Gullfaks, indicated earlier, possess a larger overpressure value at shallow depths. The reason for this is attributed to be the result of lateral transfer from overpressured reservoirs in hydraulic communication at greater depths, for example, the Snorre field.

The Irish Sea fields all appear to have higher formation pressures than that of the hydrostatic pressure, and are all at very shallow depths, eliminating many overpressure generation mechanisms. The Irish Sea basin, as discussed in Section 2.4.4, has had major uplift events. Assuming these fields are within an unbreached pressure cell, basin uplift has decreased the depths of the fields whilst the sealed pressure cell has maintained their palaeo-pressures prior to uplift. It is debatable as to whether these fields can be compared in the same category as the Central and Northern North Sea where disequilibrium compaction and gas generation are widely considered to be the generation mechanisms (Swarbrick et al. 2005).

It is important to note that the fields within this data set are limited by the availability of data obtainable through the public domain, as well as project time constraints. There are, therefore, fields that have not been included that may differ from the trends outlined above. Although the data are, in general, regionally representative, anomalous fields are likely present outside of the collection.

5.2.2 Overburden, Horizontal Stress Estimates & Fault Reactivation Effects

An important component in deriving the seal capacity is determining the minimum and maximum principal stress values. As stated previously, both the overburden stress and fracture pressures were calculated using LOT independent algorithms, a different approach to the one used in previous work (e.g. Gaarenstroom et al. 1993). Actual analysis involving seal capacity was undertaken on a well-by-well basis (such a method used by Swarbrick et al. 2010), not using a regionally defined trend line (Gaarenstroom et al. 1993; Converse et al. 2000 etc.). However, establishing a regional depth value at which a stress transition of the minimum stress from P_{frac} to S_v (in the North Sea) is useful. This stress transition occurs when the fracture pressure becomes greater than the vertical stress as a result of P_p/S_h coupling.

Figure 5.10 shows this stress transition in the deeper fields with overpressured fields P_{frac} plotting higher than that of S_v. It is not good practice to compare regions of differing overpressure settings however, such that a breakdown and analysis by region are shown in Figure 5.11.

5.2.2.1 Regional Stress Transitions

When comparing P_{frac} and S_v with depth it becomes clear that despite shallower values of P_{frac} being less than that of the corresponding S_v, deeper than ~14,500 ft P_{frac} displays larger values than S_v (Figure 5.10). To assess this situation more confidently and compare to previous literature regarding either a stress transition or simple convergence[17] (Holm 1998; Nordgård Bolås & Hermanrud 2003; Winefield et al. 2005) a breakdown of stress regimes on a regional scale (i.e. Northern North Sea, Central North Sea etc.) is necessary.

[17] Point at which P_{fract} is equal to S_v.

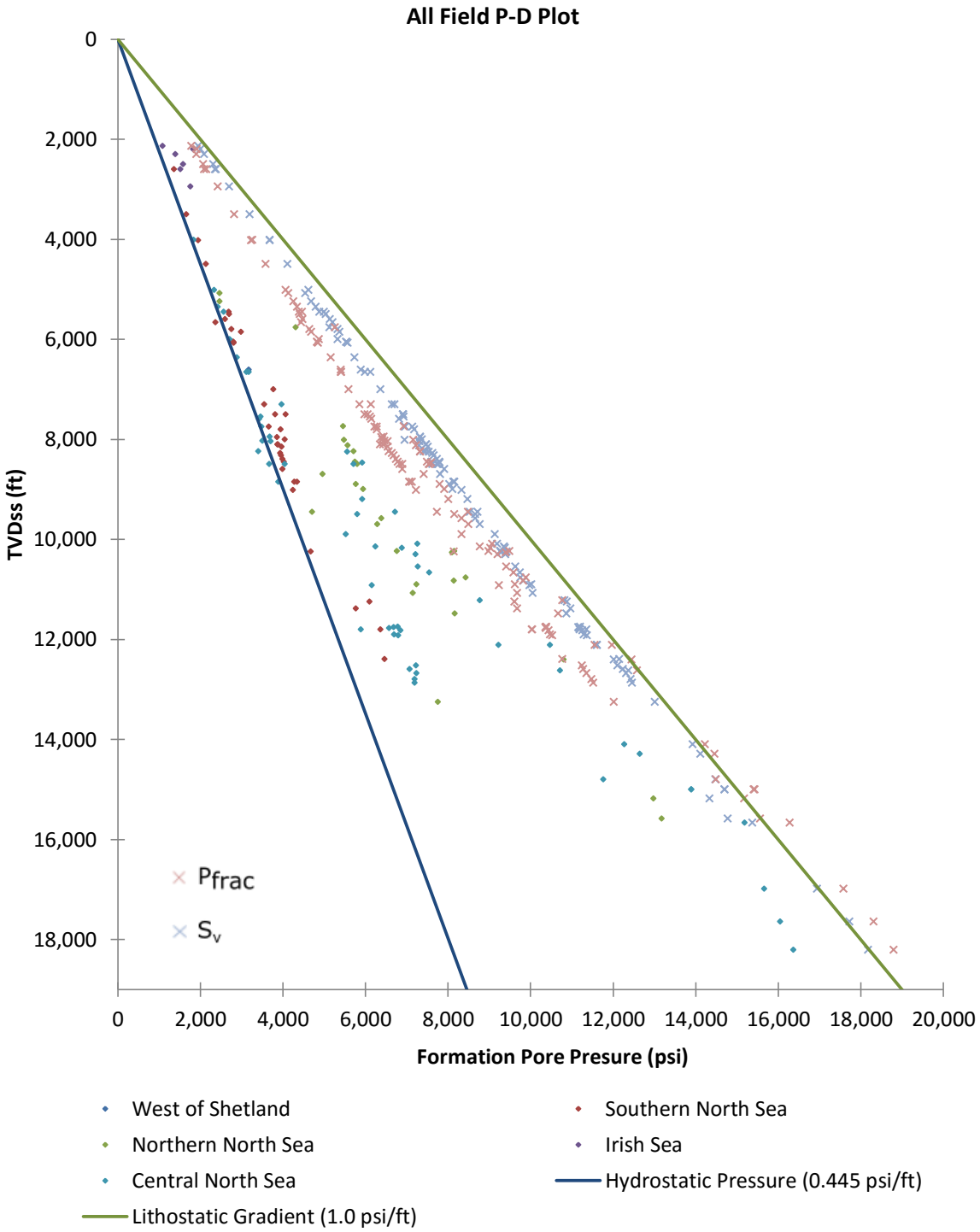

Figure 5.10 - Pressure-depth plot with all data included. Field formation pressures are coloured by region and a standard hydrostatic 0.445 psi ft^{-1} gradient is indicated in blue and a generalist 1.0 psi ft^{-1} lithostatic pressure is shown in green. Of importance are the P_{frac} and σ_v datum points. At depths greater than 14,000 ft, due to high formation pressures and P_p/σ_h coupling the σ_h values increase to a higher value then the σ_v. This causes the curved nature of the P_{frac} trend line. 3rd polynomial lines are used as they are considered to provide the best fit with all the data.

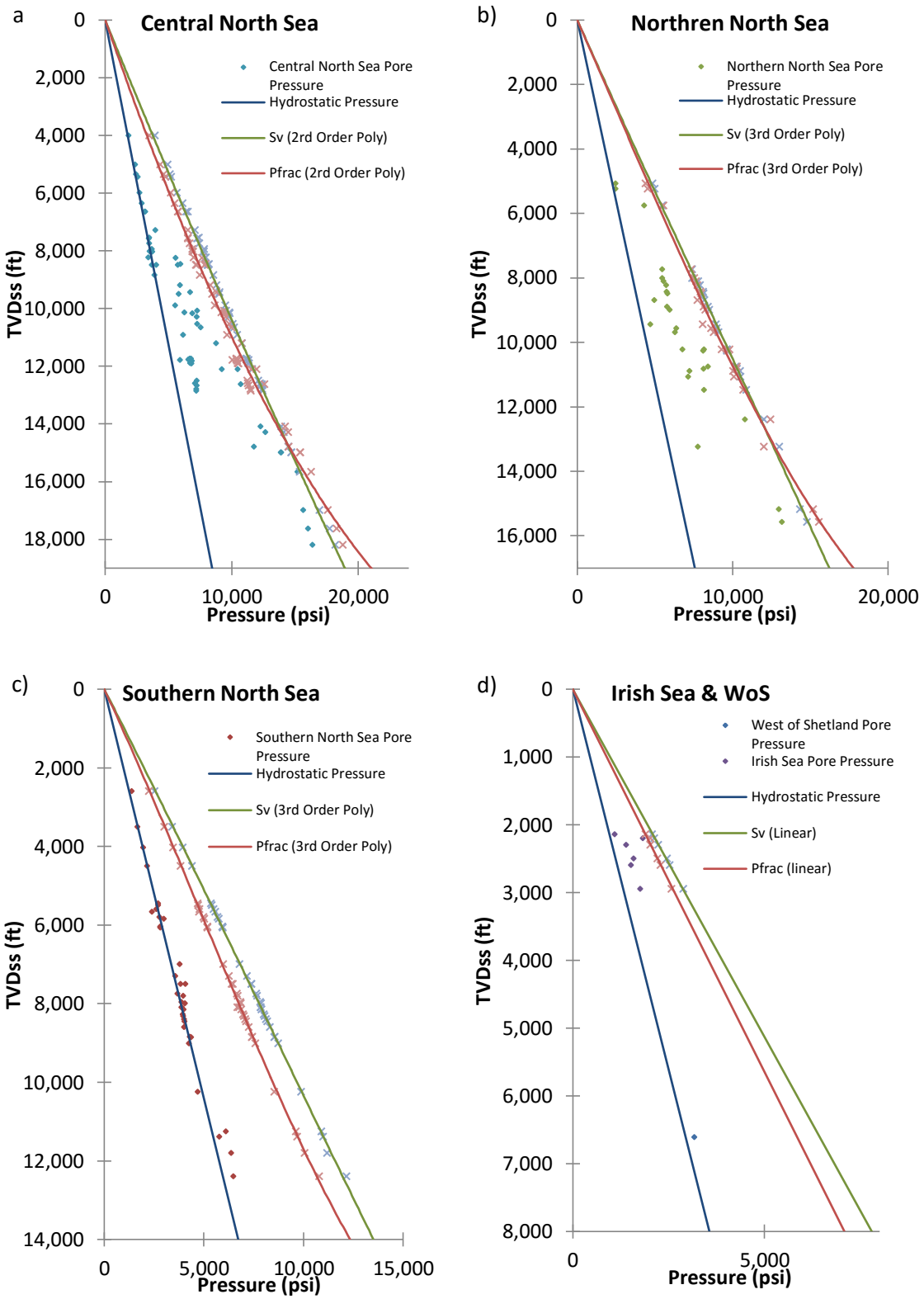

Figure 5.11 - Pressure depth plot similar to that of Figure 5.10 broken down by region. The Northern North Sea and Central North Sea are the only regions within the study to show a stress convergence and transition. Principal stress convergence values of 13,000 ft and 11,500 ft for the Central North Sea and Northern North Sea respectively are noted. 3rd order polynomial trend lines are adopted for the Central and Northern North Sea. These simply indicate a line that best represents the best fit of the data. The Southern North Sea does not indicate a convergence although a slight curve is seen as overpressure does increase slightly within the deeper fields.

Polynomial P_{frac} and S_v best fit lines are utilised for the Northern, Central and Southern North Sea. The Irish Sea and West of Shetlands trend line fits the data better with a simple linear line, due to the smaller data volumes over a narrower depth interval coupled with normally pressured fields. The breakdowns of regional P-D plots are displayed in Figure 5.11. The Southern North Sea, Irish Sea and West of Shetland (WoS) data set all display trend lines and values that do not converge. However, the Central and Northern North Sea cross plots (Figure 5.11a & b) indicate a clear convergence. The minimum stress transition depth from P_{frac} to S_v is noted as approximately 14,500 ft for the Central North Sea (Figure 5.11a) and a shallower depth of 13,000 ft within the Northern North Sea (Figure 5.11b). This corresponds well with 14,000 ft documented by Swarbrick et al. (2010) and is not overly different to 13,100 ft suggested by Holm (1998) for the Central North Sea. The value does, however, differ drastically from Gaarenstroom (1993), Nordgard Bolas et al. (2005) and Winefield et al. (2005) whose values range from 16,000 ft to 16,500 ft.

The Southern North Sea and WoS S_v and P_{frac} gradients do not appear to converge or show a transition in principal stresses (Figure 5.11c & d). The non-linear nature of the P_{frac} gradient is caused by P_p/S_h coupling. Although a slight increase in overpressure, causing a gentle P_{frac} curve is associated within the deeper Southern North Sea fields, the S_v and P_{frac} values remain on the whole a constant gradient.

5.2.2.1.1 Interpretation

A stress convergence and transition of P_{frac} and S_v trend lines occurs within the Central and Northern North Sea. The analysis for calculation of the fracture pressure was undertaken on a well-by-well basis, as used by Swarbrick et al. (2010), the rationale for undertaking regional analysis is to compare stress convergence depths to previous literature. The lesser of the P_{frac} or S_v value is thought to represent σ_3 and as such the pressure at which mechanical leakage of hydrocarbons can occur. This pressure is then used within seal capacity and fault reactivation equations.

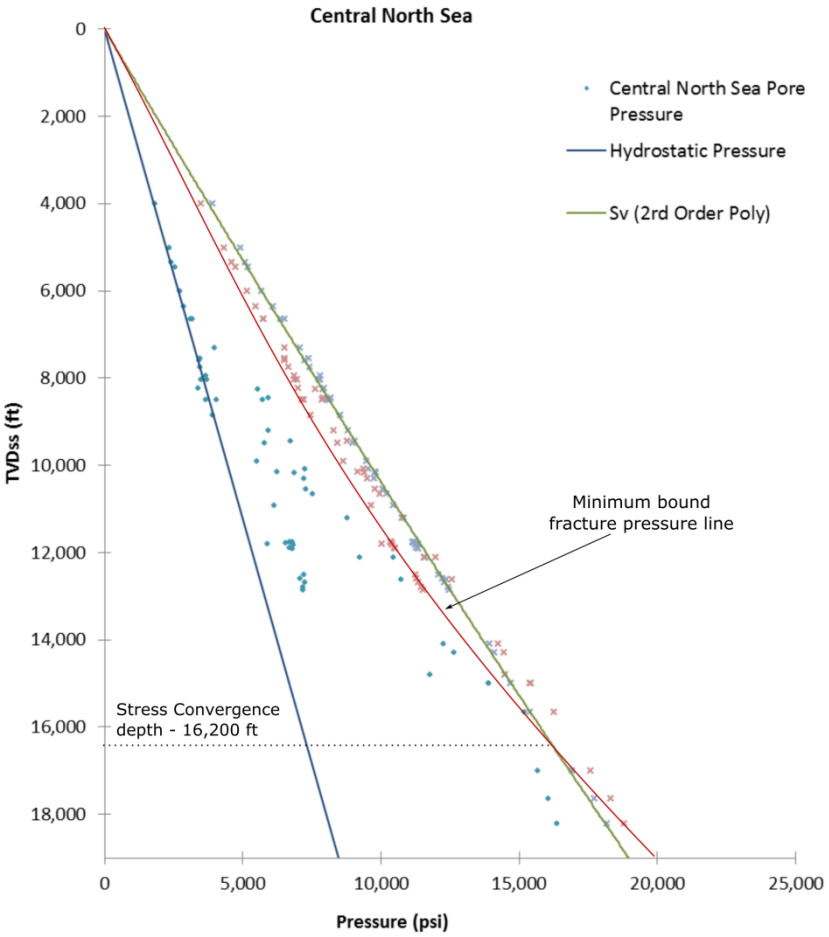

Figure 5.12 - Pressure-depth cross plot of the Central North Sea fields with a minimum bound line indicating a lower convergence value to 16,200 ft – closer to those observed by Winefield et al. (2005) and Gaarenstroom et al. (1993).

After further regional breakdown (Figure 5.11) values of 14,500 ft and 13,000 ft were taken for the Central and Northern North Sea respectively. Convergence values, noted in Chapter 4 range from 13,100 ft (Holm, 1998) to 16,500 ft (Winefield et al. 2005) for the Central North Sea. No analysis has been found regarding a minimum stress convergence/transitions within the Northern North Sea. The differing values of the Central North Sea convergence depths noted by authors results from the differing techniques used to generate the best fit trend line. If a minimum trend line (Gaarenstroom et al. 1993 approach) was applied to Central North Sea data from this study, a value closer to 16,200 ft would result (Figure 5.12). This value corresponds with the higher depths suggested by Gaarenstroom et al. (1993) and Winefield et al. (2005). A difference will also result from the varying methods used to calulate both P_{frac} and S_v. Furthermore, a non-linear S_v gradient is applied within this report to represent

the varying overburden stresses with depth; this is not readily applied to the previous literature. The data presented here parallels, to a larger degree, with the shallower convergence depth as suggested by Holm (1998) and Swarbrick et al. (2010).

5.2.2.2 Fault Reactivation Pressures

The impact of overpressure on fault reactivation is also important to consider (see Section 3.4.3.3). The fault reactivation algorithm (see section 4.5, Eq. 4.5) used is based purely on cohesionless faults that are optimally orientated for slip to occur.

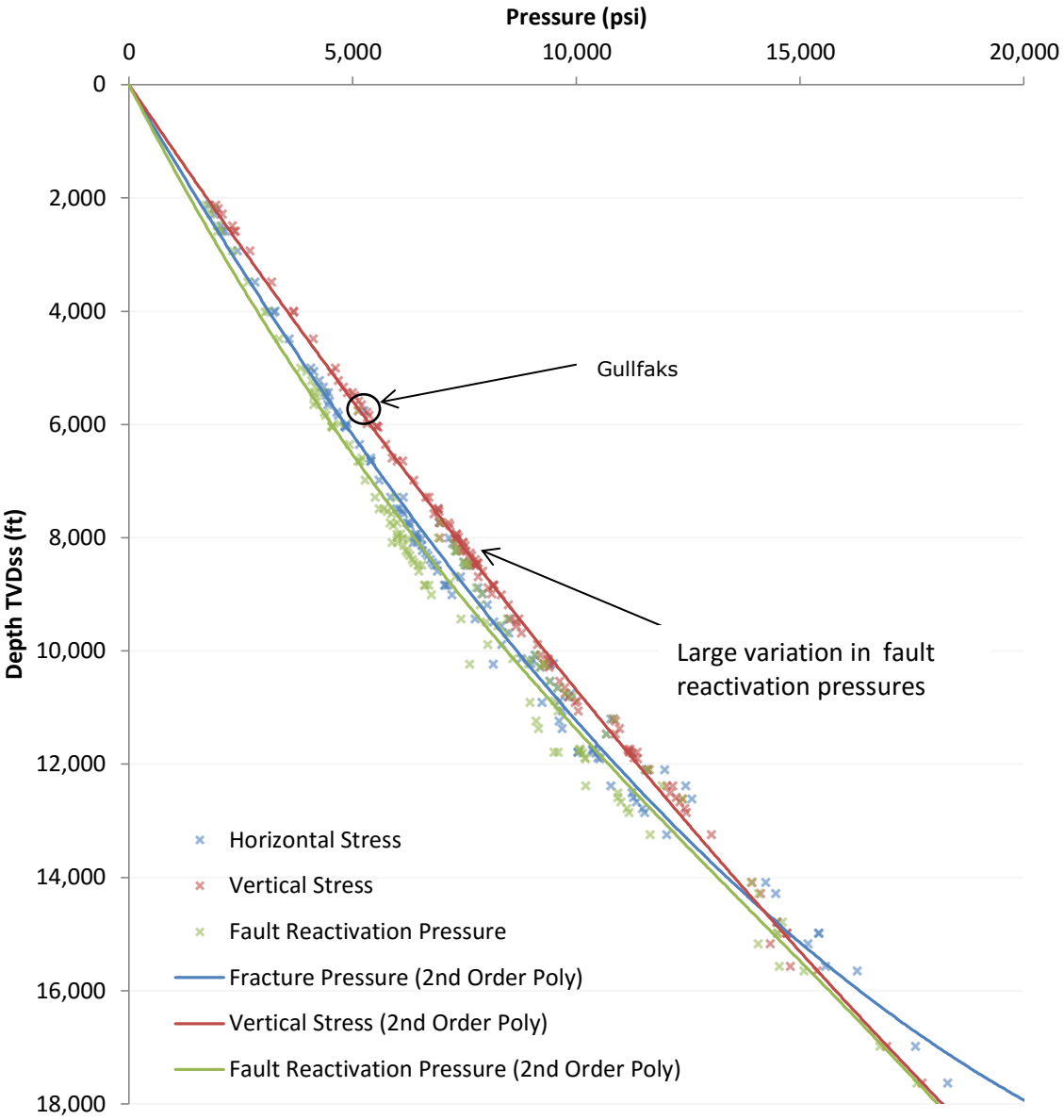

Figure 5.13 – P-D cross plot indicating the lesser value fault reactivation data compared with that of the σ_v and P_{frac}.

Within the scope of this report it is not possible to assess the stress and fault orientations, but, assuming a fault meets both criteria a minimum re-activation pressure can be defined. The values generated from the algorithm will, as such, likely be an underestimation of the pressures.

When comparing fault reactivation pressures (FRP), S_v and P_{frac} all follow a relatively linear gradient to 8,000 ft (Figure 5.13). The exception is an abnormally high FRP from the Gullfaks field. Best fit trend lines start to deviate from a constant gradient to a non-linear gradient as pore-overpressures increase and stress coupling becomes more applicable. Fault reactivation pressures, for the most, lie at lesser pressures than their corresponding S_v and P_{frac} values. As with S_v and P_{frac}, fault reactivation overpressure pressures increase with depth. This is a result of a combination of generally higher formation pressures coupled with greater vertical stress. As S_v becomes σ_3 the FRP start to converge with that of the S_v. This gradual shallowing of the fault reactivation pressure gradient with increasing depth indicates fault reactivation, S_v/P_{frac} almost converging. It is noted that at approximately 8000 ft there is a strong variation in fault reactivation pressure. Ellon, Dunbar and Johnston, for example, all show abnormally high fault reactivation pressures relative to the trend line.

5.2.2.2.1 Interpretation

The Gullfaks field indicates fault reactivation pressures of 5474 psi, which is ~ 1000 psi greater than the trend would suggest. The Gullfaks field is subject to higher pore pressures as a result of the effects of lateral transfer. As the pore pressure is integrated into the fault reactivation algorithm this results in the higher fault reactivation pressure. A similar reason is attributed to the larger range of fault reactivation pressures at from 8000 ft – 1000 ft. This results from fields with pressures comparable to those at greater depths.

The fault reactivation pressure for optimally-orientated faults represents the lowest pressure at which a caprock could undergo mechanical failure, facilitating

vertical migration and loss of hydrocarbons for most fields. This implies that if a caprock has faults that are optimally orientated to the maximum stresses to aid re-shearing, and are also cohesionless, the fault reactivation pressures represent the greatest formation pressure a reservoir may possess. Further overpressure increases, through disequilibrium compaction, influx or cracking of hydrocarbons the existing faults will re-shear, and may result in the loss of hydrocarbons from the reservoir. Faults that are not optimally orientated will possess higher fault reactivation pressures. However, should S_v or P_{frac} indicate a lower value than the fault reactivation pressures these will represent the minimum stress necessary to mechanically fail the caprock.

5.2.2.3 Differential Stress of North West Europe Dataset

Due to difficulties in defining the tensile strength of the rock (T), and contradicting views within the literature of the magnitude of T for each individual field within this study, P_{frac} is taken as equal to that of S_h (see section 3.4.1.1, Eq. 3.4 for importance). Taking P_{frac} as equal to S_h may be incorrect, but it is beyond the scope of this project to attempt to define the impact of T. It should, therefore, be noted that the P_{frac} value could be an overestimation of the true horizontal effective stress (HES) values[18]. It is only in this section (Section 5.2.2.3) regarding effective stresses that P_{frac} is taken to equal S_h and **it is not** used throughout the rest of the study. Figure 5.14 (A) displays the effective stress for the whole dataset. The red lines (modified from a failure envelope published in Converse et al., 2000) represent a generic shale failure envelope for an intact rock. The grey line indicates a general stress trend with depth. The dominant/maximum effective stress for the majority of fields (112 of 129) is in a vertical orientation.

[18] The true P_{frac} value represents the pressure at which a caprock can fail facilitating the leakage of hydrocarbons. S_h does not include the effects of tensile strength.

Important to note from this cross plot are the failure envelopes. All fields plot within the envelopes of failure and lie a considerable margin from shear failure. An extrapolation of the effective stress trend indicates that deeper, more highly

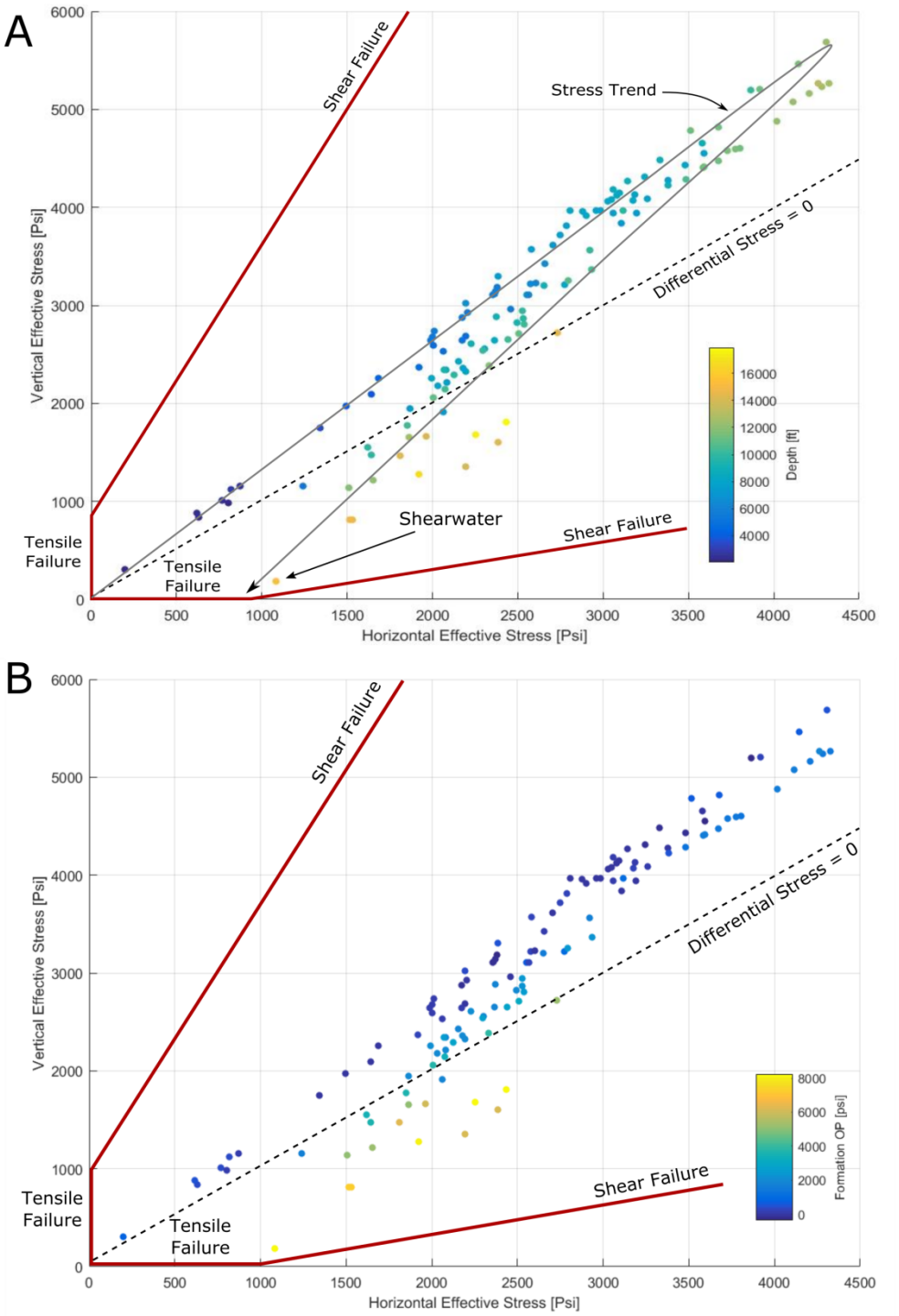

Figure 5.14 - Effective stress cross plot showing VES vs HES coloured by depth (A) and formation OP (B) of each field. A stress trend on A indicates a habit towards vertical effective stress being dominant. However as depth increases a stress trend reversal is observed. Shear failure envelopes from Converse et al. (2000). All fields are far from the shear failure envelope. However, continuing the stress trend indicates that the North Sea, should effective stresses become small enough tensile failure is favoured.

overpressured fields would converge with the tensile failure envelope, not the shear envelope.

Figure 5.14B displays an effective stress cross plot with formations values coloured by formation overpressure. Warmer colours (for example oranges and yellows) indicate higher formation pressures respective to those of the cooler blue colours. As overpressures increase a shift is observed in an orientation parallel to the 0 differential stress line. Fields with high overpressures lying below the isotropic stress line indicating a switch from VES being σ_1 to HES being the larger value.

5.2.2.3.1 Interpretation

The analysis of this NW Europe data set implies that shear related hydrofracturing within the region is unlikely, as differential effective stresses are not sufficiently high (Figure 5.14). The stress transition (as discussed in section 5.2.2.1) is observed when studying deeper, more highly overpressured fields. Extending the stress trend line to greater depths indicates an intersection within the tensile division of the failure envelope. Therefore, using this data as a proxy for the North Sea, it is clear that formation of new shear fractures are very unlikely as effective stress differentials simply are not sufficient enough. However, in deep, severely overpressured reservoirs tensile failure is a possibility. The Shearwater field, indicated on Figure 5.14A, displays the lowest vertical effective stress of just 185 psi and differential stress of 900 psi. Shearwater is discussed further below and in Chapter 6.

5.2.3 Overpressures Limiting Hydrocarbon Column Height

The study hypotheses suggest that only small hydrocarbon column heights are expected in areas with little *preserved* overpressure[19], resulting from a caprock with limiting sealing and trapping capacity. Furthermore, areas of high overpressure are thought to have a role in limiting column height through failing seals resulting from hydrofractures or fault reactivation. Areas of moderate overpressures indicate a presence of an adequate seal capacity and as such hydrocarbon columns may be present in a range of sizes, but importantly substantial columns can be preserved.

Emphasis was focused upon 'field data', therefore, by definition all the data points possess a hydrocarbon column height and, consequently, the excess buoyancy associated with a hydrocarbon presence. In order to eliminate prejudice between fields that possess larger column, and a larger pore pressure, the excess buoyancy was removed by utilising aquifer pressures[20].

At first glance it is apparent that there is little correlation with the proposed hypothesis from Figure 15.15(a & b). Despite this, patterns can be observed. Initially it would seem that as aquifer overpressure increases, hydrocarbon column height decreases. Furthermore, this is coupled with the gradual decrease in the number of hydrocarbon fields at higher overpressures.

When observing normally pressured fields (± 600 psi), those with no or very little overpressure, an abrupt cut off for column height can be seen at ~ 1000 ft. Although 5 normally pressured fields[21] display columns greater than 1000 ft these make up a minimal proportion of all the normally pressured fields and all but one are Irish Sea or Southern North Sea fields (see Figure 5.15b).

[19] The observed overpressure is less than that of what would be expected considering the surrounding pressure regime.
[20] Aquifer pressures are calculated by extrapolation of a water gradient from the HWC to the structural crest/top hydrocarbon column.
[21] Fields lying on/near to the hydrostatic gradient. ± 250 psi takes into account error associated with using a constant 0.445 psi ft^{-1}, standardised hydrocarbon gradients and extrapolation method variances.

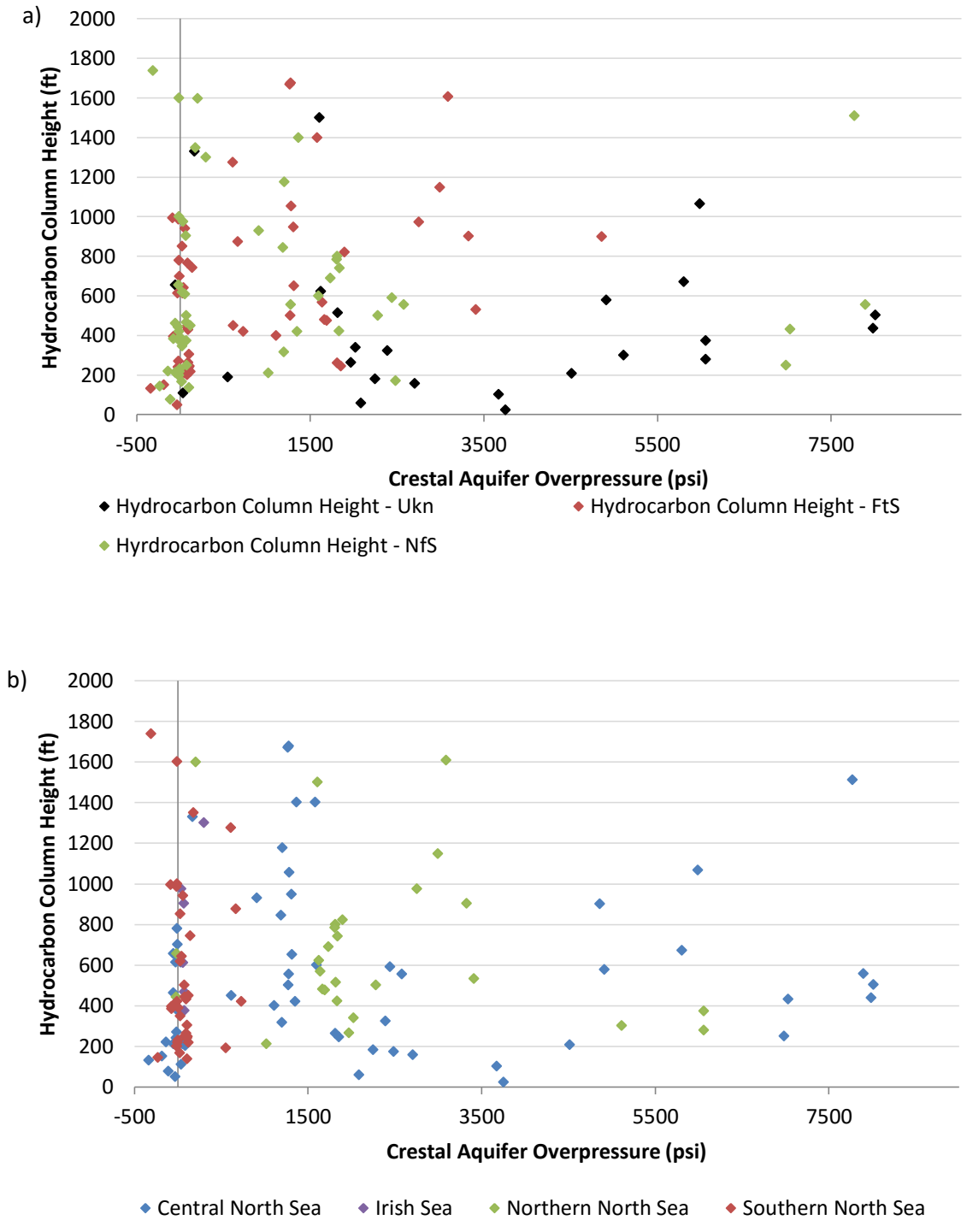

Figure 5.15 - Graph showing hydrocarbon column height against crestal overpressure inclusive of all data sets. The data points are colour coded by closure fill.

Working in measured column height (i.e. feet), although allows a quick overview of the data, different fluid densities, associated with differing hydrocarbon types and compositions, perhaps means that a gas field and oil field cannot be compared. This is a result of their hydrocarbon buoyancy will be very different or vice versa. For example, the SNS Mercury field and NNS Heather field both indicate hydrocarbon buoyancy pressures of 240 psi (± < 1 psi), yet the Mercury field's measured column height is 956 ft less than the Heather field as a result of the differing densities of hydrocarbon phases. Relating the formation/aquifer OP to the hydrocarbon fluid density i.e. using the excess buoyancy pressure, eliminates this prejudice associated with density contrasts.

Figure 5.16 displays a graph using hydrocarbon buoyancy pressures, replacing measured column heights, and thus eliminating the fluid density issue outlined above for the Central and Northern North Sea fields. A decline in hydrocarbon buoyancy with rising aquifer overpressure is still present. However, the abrupt cut off at 1000 ft for column heights associated with normally pressured fields is no longer as distinct.

The trend now indicates more of a continuous distribution of hydrocarbon buoyancies, with an overall gradual decline of sample densities as buoyancy increases. Progressing into moderately overpressured fields (600 – 4000 psi), in general, displays fields with lower hydrocarbon buoyancy pressures. Fields within this category of overpressures lie in a close cluster, broadly with buoyancy values of less than 200 psi, with only 9 fields indicating higher buoyancies. The highest hydrocarbon buoyancy pressure of 460 psi within this interval is the Gullfaks Sor field, 210 psi greater than the Brae South field as the closest similarly overpressured equivalent. The Dunbar field, although not as extreme, also displays slightly uncharacteristically high hydrocarbon buoyancy pressures of 370 psi, although, at a higher overpressure of 2925 psi.

Fields with high overpressure (> 4,001 psi OP) displays the smallest proportion of fields relative to the other 2 categories. All fields, excluding Shearwater, possess hydrocarbon buoyancy pressures less than 225 psi. The field with the highest aquifer overpressure values (8012 psi) within the data set has a hydrocarbon buoyancy of 145 psi. This field, Glenelg, holds a 500 ft gas condensate column.

When considering hydrocarbon column heights and buoyancy pressures to aquifer/formation pressures it is justified to question why fields that are under-filled have this status within the North Sea. Fields that are full-to-spill are limited, not exclusively, but primarily by structure and closure height[22]. Therefore, by eliminating these fields the remainder have hydrocarbon columns limited by another factor, potentially leakage. A plot displaying fields from the North Sea that are under-filled (or have unknown fill) is shown as Figure 5.17. Purely under-filled fields from the North Sea are indicated in Figure 5.18.

[22] The distance height distance from the shallowest point/crest and the lowest closing contour or leak point.

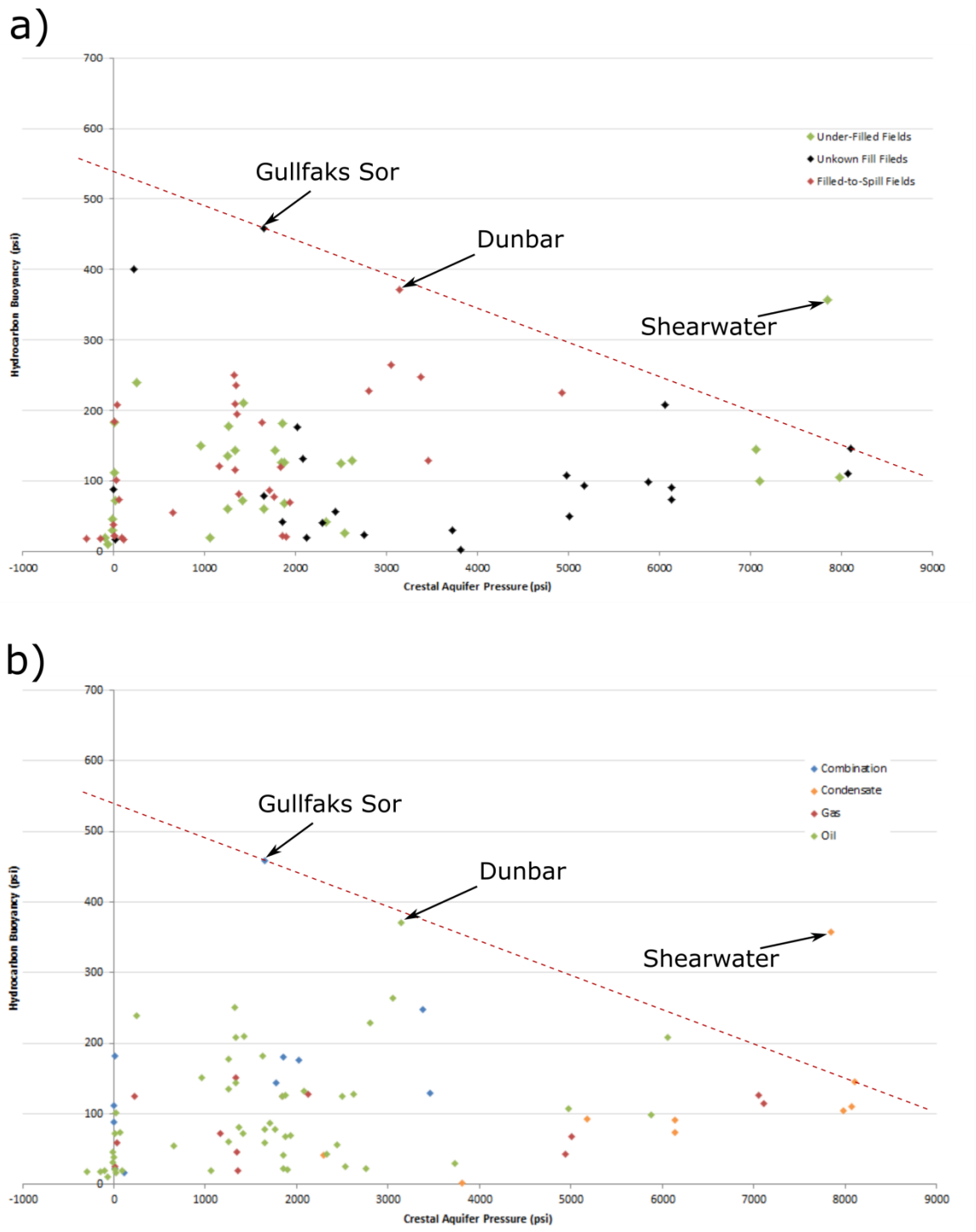

Figure 5.16 – Graph of hydrocarbon buoyancy against crestal aquifer pressure for the Central and North Sea fields. The dashed red line indicate maximum bound with all fields sitting below with the exception of the Shearwater field. Figure a is coloured to closure fill state and b) coloured by fluid type.

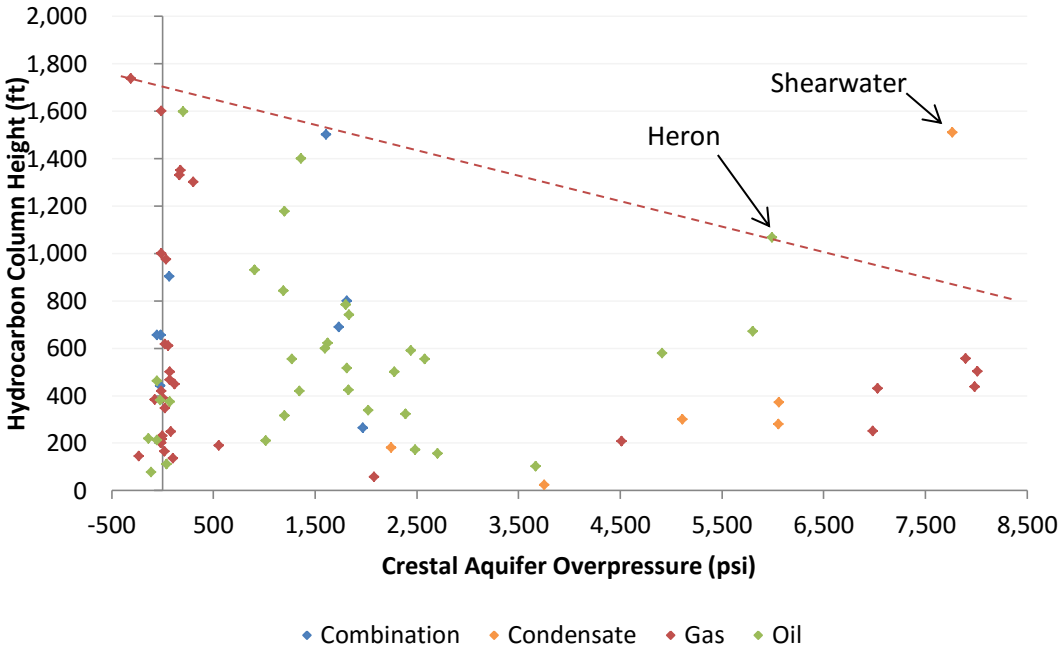

Figure 5.17 - Graph of hydrocarbon column height against crestal aquifer overpressure within under filled and unknown fill North Sea fields. The red dashed line indicates an upper bound line with all but two (Heron and Shearwater) plotting below. Fields are colour coded by fluid type.

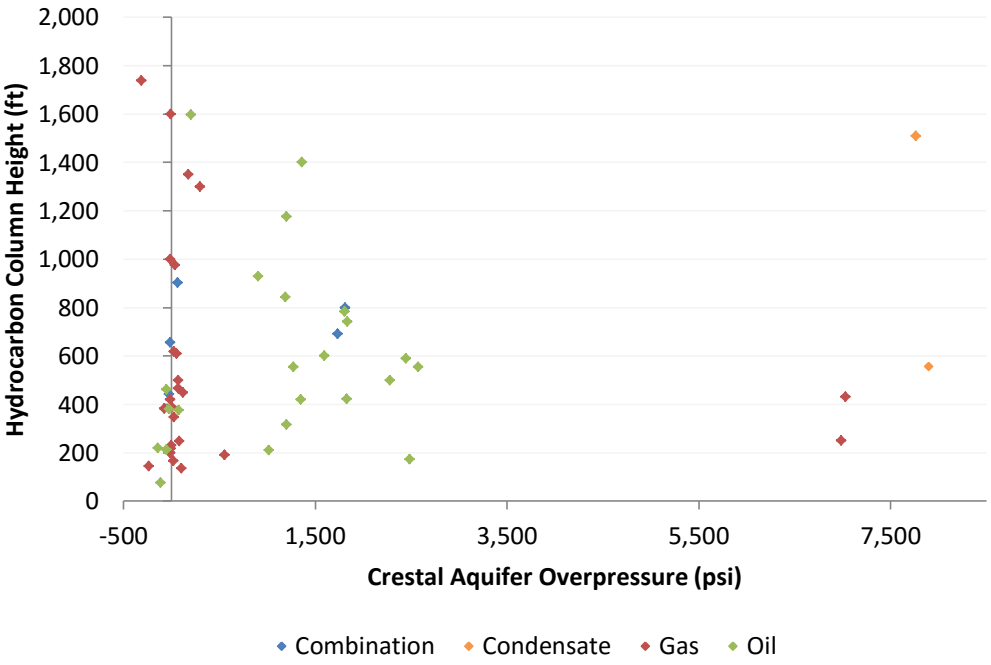

Figure 5.18 - Hydrocarbon column height against crestal aquifer overpressure within all North Sea fields known to be under-filled. Colours indicate hydrocarbon accumulation fluid type.

Variable column heights are still observed within normally pressured formations with little overpressure (Figure 5.17). Moderately overpressured fields (501 – 4000 psi) and highly overpressured fields (> 4001 psi) display a sharp decline in column height with increasing aquifer OP, with a maximum column height value at ~ 800 ft. Similar to the analysis of the whole dataset, a decline in field numbers is observed with increasing aquifer overpressure. There is also little evidence to suggest that different hydrocarbon phases (gas, oil or condensate fields) have any upper limit regarding aquifer overpressure. All condensate fields lie above 2000 psi overpressure with the maximum field (Heron) holding an oil column is 5992 psi, whereas gas fields are present with > 7000 psi overpressure in addition to being normally pressured. The fields with the highest aquifer overpressures are Elgin, Franklin, Glenelg and Shearwater, all of which possess a gas condensate column.

A general negative trend (marked as a dashed red line) has been applied marking a maximum bound trend line throughout the data on Figure 5.17. This line has been applied as a rough upper limit to column heights as a function of aquifer overpressure. Shearwater represents a significant anomaly and is discussed further in Chapter 6. It is also discounted from the upper limit line criteria. The Heron field lies along the envelope, and although displaying a column height larger than would be expected it still follows the rough trend.

By eliminating all unknown-fill fields from Figure 5.17 the remaining under-filled fields are shown in Figure 5.18. The overpressured field data can be suggestively separated into 2 categories; those with aquifer pressures of < 2600 psi and fields over 7000 psi. Shearwater, still an anomalous result, plots high in comparison to the 3 other highly overpressured field (Elgin, Franklin and Erskine) which display smaller column heights relative to those fields in a category of lesser overpressure. Further analysis comparing hydrocarbon buoyancy pressure instead of column height, determines 3 categories (highlighted on Figure 5.19). A large range of buoyancy pressures can be observed within reservoirs of little or no aquifer overpressures. This is the result of long gas columns (primarily in the Southern North Sea fields) producing large buoyancy pressures, being plotted with oil columns from the Central and Northern

North Sea. Fields with aquifer overpressures of 500 and 2600 psi display limited hydrocarbon buoyancy (ca. 200 psi maximum) and, finally, the 3 high overpressure fields (Elgin, Franklin and Erskine) identified previously. The little, to no, aquifer overpressure range is dominated by gas accumulations (70 % gas, with the remainder comprising combination and oil fills). However, compared to that of the moderately overpressured fields a clear reversal is observed with close to 90 % oil accumulations. The highly overpressured assembly is composed entirely of gas or gas condensate fields.

5.2.3.1 Interpretation

When considering Figure 5.15 a 1000 ft column height cut off is observed, however this is less of a dominant feature when measured column height (ft) is replaced with buoyancy overpressure. Figure 5.18 show the divisions of hydrocarbon fluid types, with gas fields dominating the low/little overpressure and high overpressure categories and oil dominating the medium overpressure fields. This is not to say that gas accumulations are more preferential at higher pressures, these results are likely the result of data picking and availability. The fact that gas comprises highly overpressured and deeper fields relative to oil, may result from cracking of oil reservoirs to gas, as shown in Converse et al. (2000), but likely the product of the data

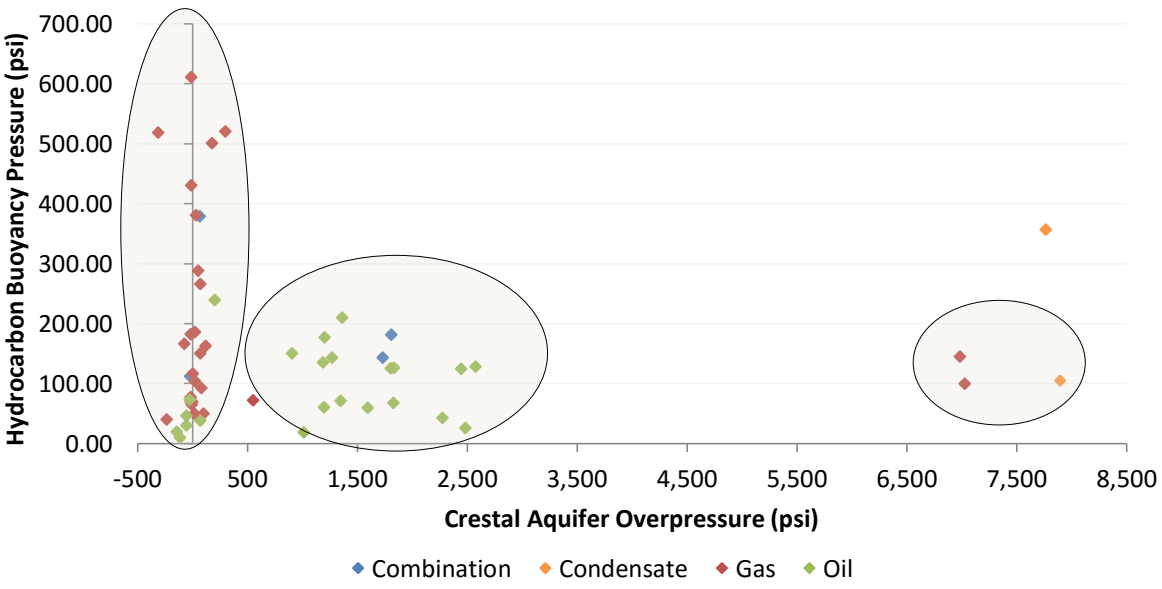

Figure 5.19 - Hydrocarbon buoyancy against aquifer pressure in under-filled fields. 3 categories are observed within differing OP.

selection process.

More of an indication of aquifer overpressure possibly limiting column heights is observable from Figure 5.17. This is shown by the reduction in column heights in fields with increasing aquifer overpressures. A red dashed line on Figure 5.17 designates a general maximum bound line with all but the Shearwater field lying above. This maximum bound line can tentatively assign maximum hydrocarbon column heights at a specific aquifer seal capacity and assuming a gas fill. For example at 1000 psi aquifer overpressures hydrocarbon columns would not be expected greater than ~ 1,650 ft. By contrast, at high overpressures of 8,000 psi, column heights of no more than 600 ft would be expected. The Shearwater field, noted as having an exceptionally high hydrocarbon column height comparable to aquifer overpressure is a clear anomaly. The reason assumed for its dissimilarity to the trend lies with the concept of a protected trap discussed further in Chapter 6.

5.2.4 Seal Capacities Limiting Hydrocarbon Column Height

When simply comparing overpressured fields the fact remains that formation/aquifer overpressure is seen to increase with depth. This means that a prejudice is applied to deep, more highly overpressured fields. Using seal capacity helps eliminate this varying depth factor.

Prior to considering the impact of seal capacity and hydrocarbon column height an assessment on whether this study accounts for the excess hydrocarbon buoyancy pressure, and whether it influences the rock fracture regime, needs to be undertaken. The idea, proposed by Swarbrick et al. (2010), suggested that in a water wet seal, due to the hydrocarbon phase having no contact with the rock matrix, the buoyancy pressure, which is above the aquifer pressure and related to the hydrocarbon column, has no impact on rock failure due to hydraulic fracturing. Swarbrick et al. (2010) show evidence to support this; however it is far from being a universally accepted concept. Despite this, it is imperative to consider this when examining seal capacity. The obvious process to prove, or disprove, this theory is to assess whether any fields possess pore pressures higher than σ_3, but aquifer pressures less than that of σ_3. It is

also important to note that a key component in the analysis by Swarbrick et al. (2010) is the re-evaluation of the effective seal to hydrocarbons from the commonly attributed top reservoir to a higher structural level within the seal, e.g. the BCU and/or Base Chalk in the case of the Central North Sea. When compared with the Swarbrick et al. (2010) approach it is therefore unlikely a pressure pattern of aquifer and formation pressures lying below and above respectively of σ_3 will be present. At top reservoir all of the Swarbrick et al. (2010) data indicate positive aquifer seal capacities.

From Figure 5.20, displaying aquifer & hydrocarbon seal capacities[23] < 2000 psi, it is clear that all fields indicate positive seal capacity values for both aquifer and hydrocarbon fluid pressures. The lowest hydrocarbon and aquifer seal capacity values within the data set are possessed by the Shearwater field – already shown in the previous section to possess an abnormally large hydrocarbon column, irrespective of its very high overpressure. A hydrocarbon seal capacity of 185 psi is calculated, with a 542 psi aquifer seal capacity plots Shearwater very close to σ_3. A large proportion of fields with low aquifer seal capacities are from the Irish Sea, thus result from being shallow fields in comparison to the Central and Northern North Sea. If these are removed just Shearwater and Erskine with aquifer seal capacities less than 1000 psi (see Figure 5.21). What is interesting is the preferential sorting of under-filled fields with low aquifer seal capacities comparable to fields full-to-spill. Under-filled reservoirs comprise 26 % of all fields on the graph with 63 % with unknown fill. Therefore, only 11 % of the fields (just 2 fields) are full-to-spill. 45 % of the Central and Northern North Sea dataset is composed of filled-to–spill fields yet only 6 % of full-to-spill field's (2 % of the overall data set) shows aquifer seal capacities of less than 2000 psi. It is only after 2500 psi ASC full-to-spill fields start to compose a stronger dominance.

[23] σ_3 (determined by the lesser value of P_{frac} or σ_v) minus the noted pore/aquifer pressure.

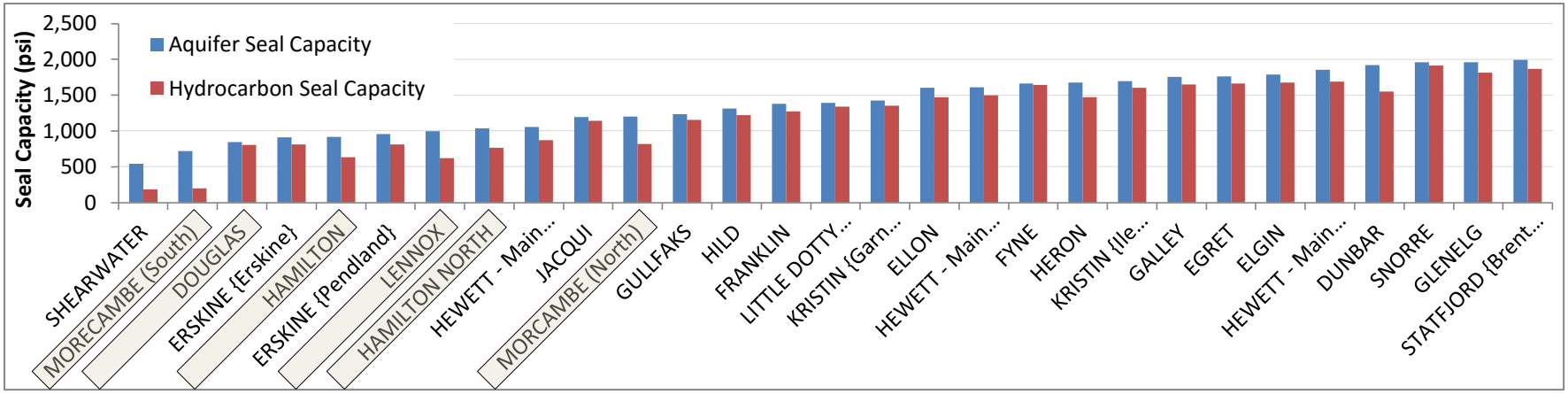

Figure 5.20 - Aquifer and hydrocarbon seal capacities < 2000 psi from all regions. The fields shaded in yellow represent the Irish Sea fields with low seal capacity due to shallow crest depth with respect to the Central and Northern North Sea

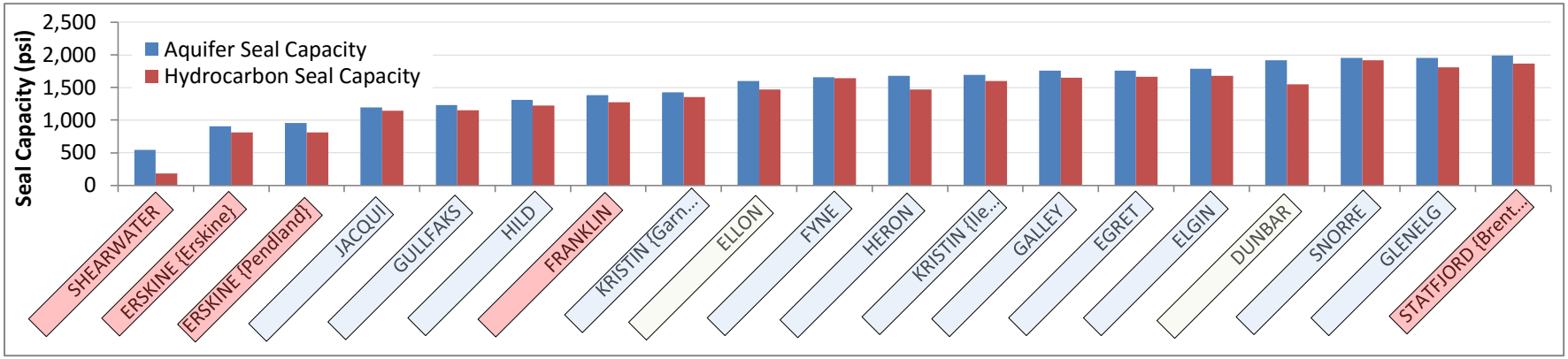

Figure 5.21 - Aquifer and hydrocarbon seal capacities < 2000 psi using solely Central and Northern North Sea data. Field names are shaded by closure fill. Red indicates under-filled fields, blue unknown fill and green full-to-spill.

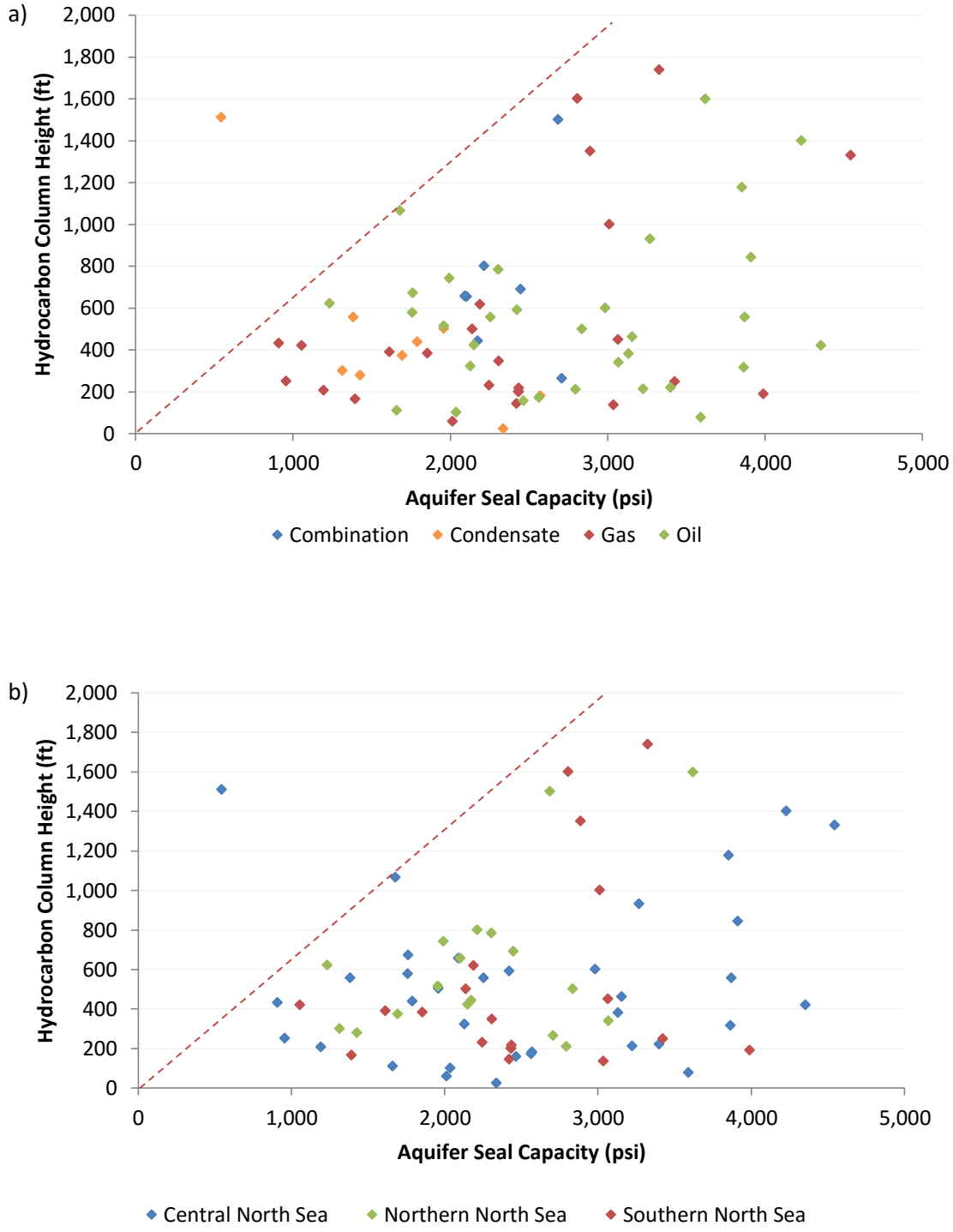

Figure 5.22 - – Hydrocarbon column height against aquifer seal capacity. An upper bound trend line (in red) indicates an upper bound line with the majority of fields lying below this line. The Shearwater field lies above this line. Figure 5.22a points are coloured by hydrocarbon phase and 5.22b coloured by Central North Sea region.

As with previous graphs, the aim of this study is to assess how pressure may influence hydrocarbon column height. As such the following analysis focuses on fields that are under-filled, with a small amount of focus upon the unknown fields also. A general increase in hydrocarbon column height can be observed with increasing seal capacity from Figure 5.22. The low ASC (< 1500 psi) are dominated by gas and condensate bearing fields and a reasonable combination of hydrocarbon phases are present with moderate (1501 – 2500) and high (> 2501) ASC. Shearwater is, again, an exception. The lowest ASC category contains a range of column heights from 220 ft, to the Shearwater field with 1500 ft. The mid-range ASC category, although possesses the highest proportion of fields, only displays column heights up to 800 ft. The Heron field is an exception with an oil column of 1,066 ft. The main separation between low and moderate seal capacities is the addition of oil reservoirs in moderate aquifer seal capacities. Following this, the high ASC category shows a clear range of column heights from < 100 ft to 1700 ft plus. A maximum bound trend has been applied to the data on Figure 5.22(a & b) with all fields but the Shearwater field lying beneath the line. Hydrocarbon column heights against aquifer seal capacities are plotted on Figure 5.22b and coloured by region. No regional separations by seal capacities are witnessed. Figure 5.23 illustrates the same variables as Figure 5.22 but only displaying under-filled fields (unknown-fill fields are no longer displayed) of the Central and Northern North Sea. We see a slight gradient variation associated with the upper bound lines resulting from the removal of some fields. The maximum bound gradient extrapolated from Figure 5.22 indicates a value of 1.5 psi/ft compared with that from Figure 5.23 of 2.08 psi/ft.

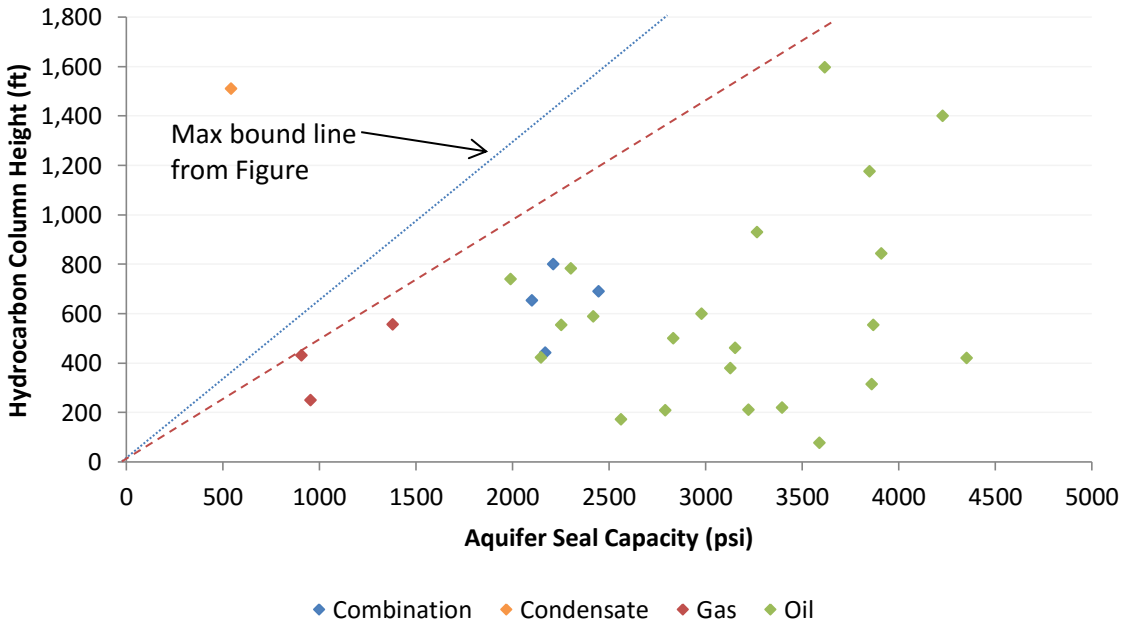

Figure 5.23 - – Hydrocarbon column height against aquifer seal capacity, similar to Figure 5.22, however using under-filled Central and North Sea fields. Colour coded by fluid type. The blue line indicates a maximum bound line from Figure 5.22 and the red line indicative of the new maximum bound from this plot.

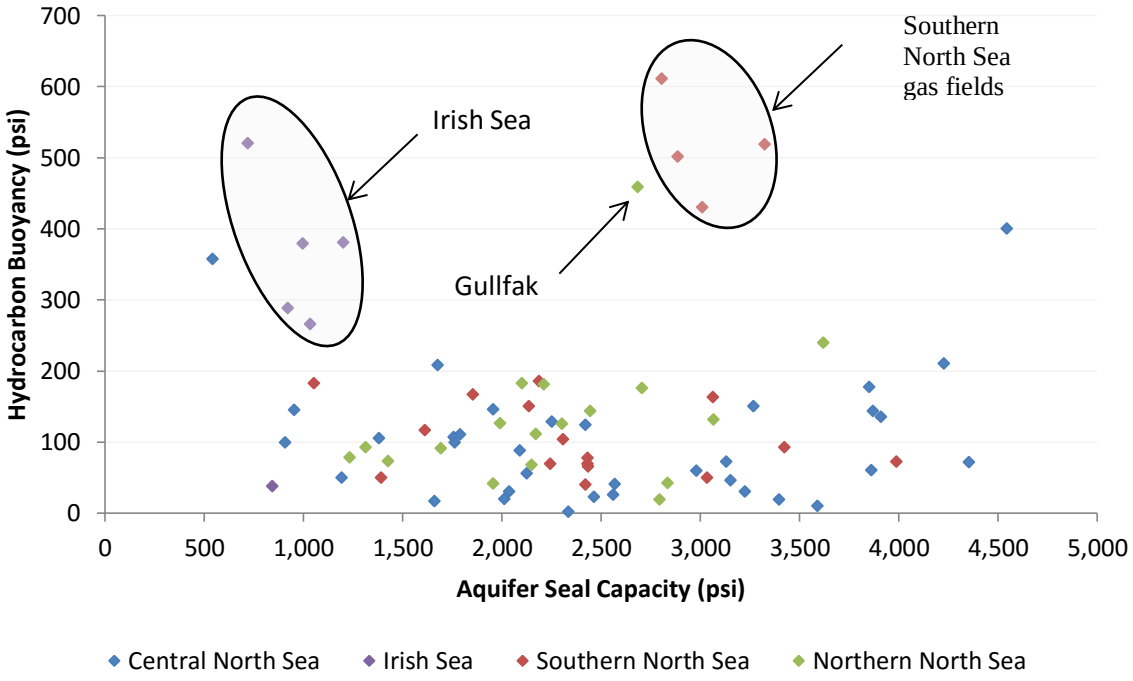

Figure 5.24 - Hydrocarbon buoyancy pressures against aquifer seal capacities of all regions with unknown or full to spill closure fills. 2 groups indicate outlier data; Southern North Sea and Irish Sea.

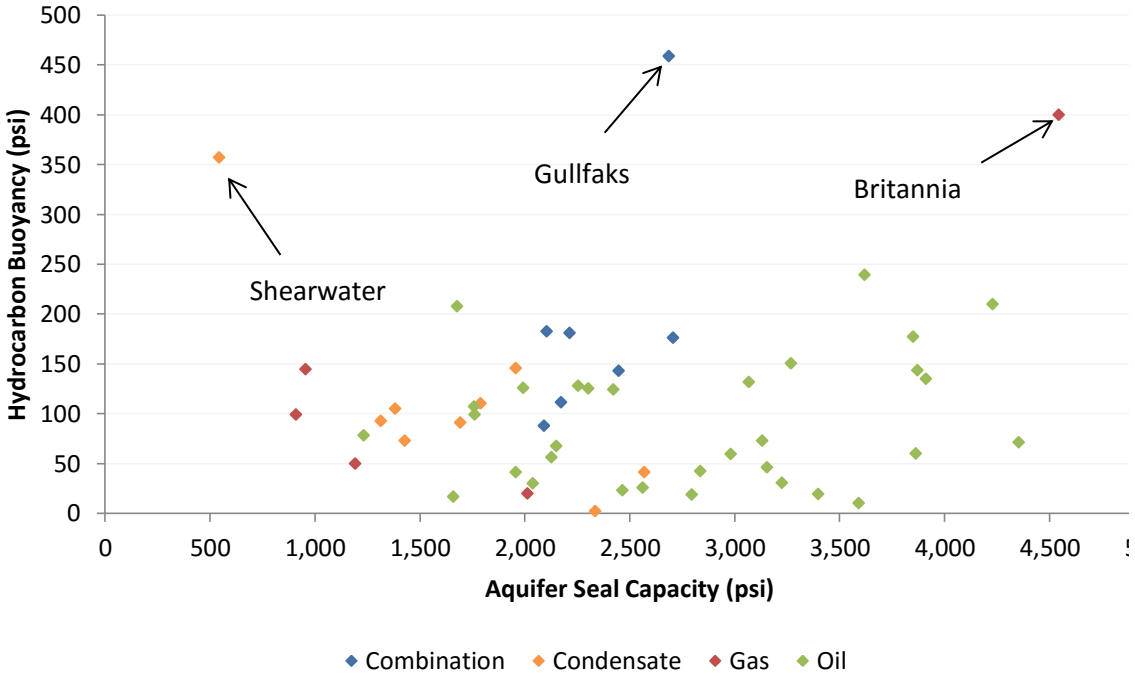

Figure 5.25 – Hydrocarbon buoyancy pressure of the Central and Northern North Sea unknown fill and under-filled fields. Points colour coded by hydrocarbon phase.

Exchanging hydrocarbon column height with hydrocarbon buoyancy removes the positively correlated maximum bound trend lines associated with Figure 5.22 and 5.23. There are 2 groups that exhibit higher buoyancy overpressures than the data set as a whole (Figure 5.24). When examined more closely the Irish Sea fields have large buoyancy pressures at low seal capacities – higher than the remaining data set due to sizable gas columns and low ASC due to shallower depths. The Southern North Sea cluster also indicates high buoyancy pressures compared to that of the remaining data. The Shearwater field (leftmost point on Figure 5.24) again, is anonymous. The Gullfaks field is also indicating higher hydrocarbon buoyancy pressures than the norm, especially within the same Northern North Sea region. Figure 5.25 displays similar data as Figure 5.24, however, located from the Northern and Central North Sea only, colour coded to hydrocarbon phase. The dominant fluid type is oil, not unsuspected due to the removal of the Southern North Sea gas dominated fields. However, gas and condensate fields dominated the low ASC range. Three fields stand prominent, Shearwater, Gullfaks and the Britannia field.

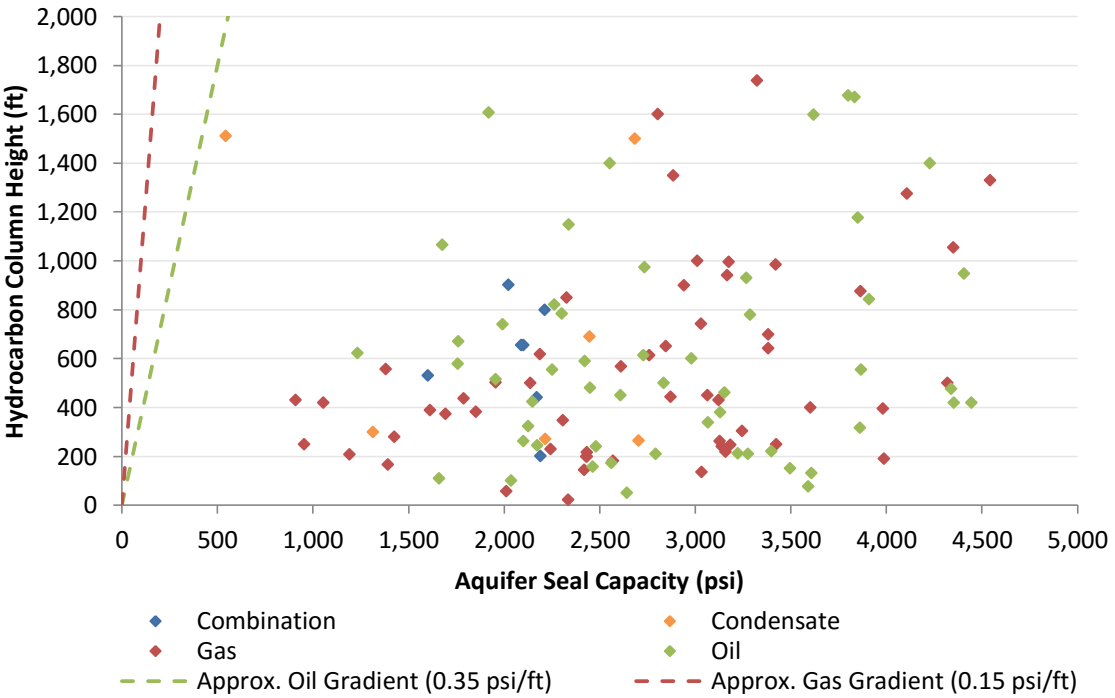

Figure 5.26 - Hydrocarbon column height as a function of aquifer seal capacity. The dashed green line represents a generic 0.35 psi ft^{-1} oil gradient and red a generic 0.15 psi ft^{-1} gas gradient. If column height was solely controlled by aquifer seal capacity, data points should lie close to their representative fluid gradient line. Column heights clearly are all significantly less than their maximum potential with the exception of Shearwater.

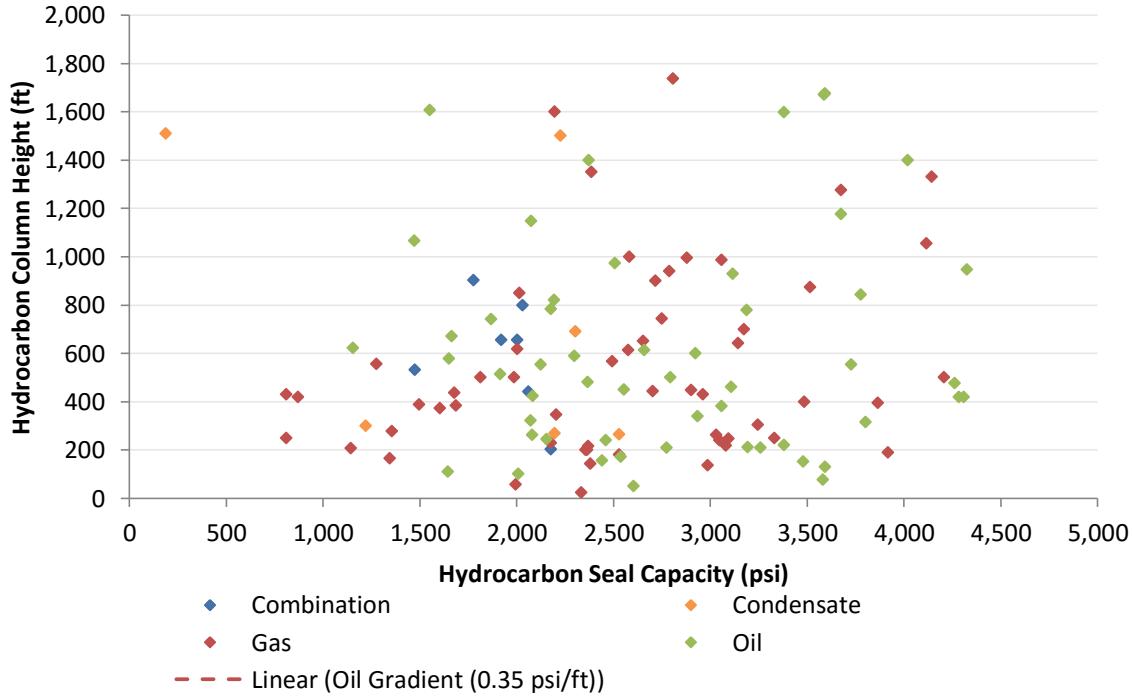

Figure 5.27 - Hydrocarbon column height as a function of hydrocarbon seal capacity. If column height was solely controlled by hydrocarbon seal capacity, data points should lie at 0 hydrocarbon seal capacity. Column heights clearly are all significantly less than their maximum potential with the exception of Shearwater.

Figure 5.26 displays hydrocarbon column height as a function of aquifer seal capacity for the North Sea. The dashed green line represents a generic 0.35 psi ft^{-1} oil gradient and the dashed red a generic 0.15 psi ft^{-1} gas gradient and correspond to the theoretical maximum height that could be sustained for a given seal capacity. These lines are taken as an average for the respective hydrocarbon fluid. All values are colour coded by hydrocarbon fluid type. The graph indicates that all but 1 field lie a reasonable distance from the generic hydrocarbon density lines. The Shearwater field sits on the oil gradient line. Theoretically, if any fields lie along (or close to their corresponding gradient) it can be assumed that overpressure is limiting the column height based on the principal that aquifer pressure is the variable that controls mechanical failure, not formation pressure. Figure 5.27 plots hydrocarbon seal capacity instead of aquifer. There are no gradient lines as if hydrocarbon seal capacity is a limiting variable to column heights then fields will lie on 0 psi. Shearwater is the closest field to 0.

5.2.4.1 Interpretation

Shearwater has the lowest, but still a positive aquifer seal capacity. Although not by much, and likely within margins of error associated with the method, it is never the less, very close to the calculated fracture pressure. The actual difference between hydrocarbon seal capacity and aquifer seal capacity within this dataset indicates a very small value as a result of a trend towards small column/closure height capacities.

Fields displayed on Figure 5.21, showing seal capacities < 2000 psi, are primarily composed of fields that either have unknown or under-filled reservoirs. The fact only 6 % of under-filled fields show seal capacities of less than 2000 psi could imply that although seal capacities are, for the most, positive, the result of lying within a close proximity to the minimum stress could have an impact on preserving hydrocarbon columns. All fields show aquifer seal capacities and hydrocarbon seal capacities greater than 0.

A further maximum bound cut off line is applied within Figure 5.22. This is due to the gradual increase in hydrocarbon column height with increasing aquifer seal capacities. This cut-off, much like one defined 5.2.3, can be used as a limit line

indicating maximum column heights expected at specific aquifer seal capacities within the North Sea. For example, at 500 psi aquifer seal capacity column heights are not expected to reach higher than 300 ft, however, at 2000 psi heights of 950 ft are thought to be a maximum.

Considering buoyancy pressure as an alternative to hydrocarbon column height, as with section 5.2.3 comparing overpressures, removes the observable trend, of increasing hydrocarbon buoyancy with increasing aquifer seal capacity. Using data from the whole dataset, including the Irish Sea, West of Shetland & North Sea fields, and the majority of fields indicate < 200 psi of hydrocarbon buoyancy, the exception being the Irish Sea and Southern North Sea. This is the result of these fields being affected by undercompaction and shallow crestal depths. These should not be considered in the same category as the North Sea fields. The abnormally large hydrocarbon buoyancy within the Southern North Sea results from typical gas densities much lower than other fluids. Therefore, despite these fields possessing routine column heights (400 – 600 ft) the density contrast produces high hydrocarbon buoyancy values.

Figures 5.26 indicate average gradients of hydrocarbons and seal capacities against hydrocarbon column height within the North Sea. The graph will indicate fields that are being limited by pressure to a better degree. What is immediately obvious is that no fields, with the exception of Shearwater lie close to the control gradients of oil or gas. This proximity to the oil and gas gradient lines indicates that the Shearwater field could be limited by pressure and as such does not possess such a great column.

5.2.5 Fault Reactivation Limiting Column Height

It has already been shown that the required pressures to reactivate slip on a fault are less than those necessary to generate new fractures. This is working on the assumption that, not only are the faults optimally orientated and cohesionless, but also that the caprock is not intact and that faults exist initially.

When comparing fault reactivation seal capacities of other fields all but a few indicate lower values than their fracture pressure (σ_3) counterparts. A collection of fields from all regions is shown as Figure 5.28. The Shearwater field displays the lowest (a negative 101 psi) aquifer fault reactivation seal capacity. All other fields indicate a positive value; however, the Erskine field reservoirs also lie close to the fault reactivation pressure. The next set of fields with low fault reactivation pressures (Morecambe, Douglas, Hamilton, and Lennox) are all located within the Irish Sea basin. When removing the Irish Sea data the remaining data all possess seal capacity values close to 1,000 psi or greater with the Hild field indicating seal capacities twice what the Erskine fields retain. A Southern North Sea field (Hewett) indicates the lowest fault reactivation seal capacity for the SNS region, and is comparable to the highly overpressured fields of the Central North Sea.

In order to compare seal capacities to hydrocarbon column height the additional hydrocarbon buoyancy is removed, using aquifer pressure as a variable instead of the formation pressures. The following graphs plot both hydrocarbon column height and hydrocarbon buoyancy against fault reactivation aquifer seal capacities.

Comparable to other graphs an upper bound cut-off can be observed, the Shearwater field is an exception (Figure 5.29a). Other fields that lie close to the cut off on Figure 5.29 are Erskine field, and Hewett field all with fault reactivation seal capacities of 697 and 750 psi respectively. The Erskine field is heavily overpressured and as such reduces the FR aquifer seal capacity. Also of note is the Erskine and Hewett fields are under-filled. The Hewett field has a crest depth close to 13,000 ft shallower than the Erskine and Heron fields. This has an effect on seal capacity for reasons stated previously. The Dunbar field is an outlier on Figure 5.29a. This is due to the Dunbar field possessing an abnormally long hydrocarbon column coupled with a shallow crest depth with respect to comparable North Sea fields. Furthermore, on Figure 5.29b (replacing measured column height in ft with excess hydrocarbon buoyancy) the Barque field sits outside the maximum bound line as a result of a large 1600 ft gas column coupled with a very shallow (6735 ft) crest depth. An upper bound gradient of 1.56 psi/ft is suggested through figure 5.29a.

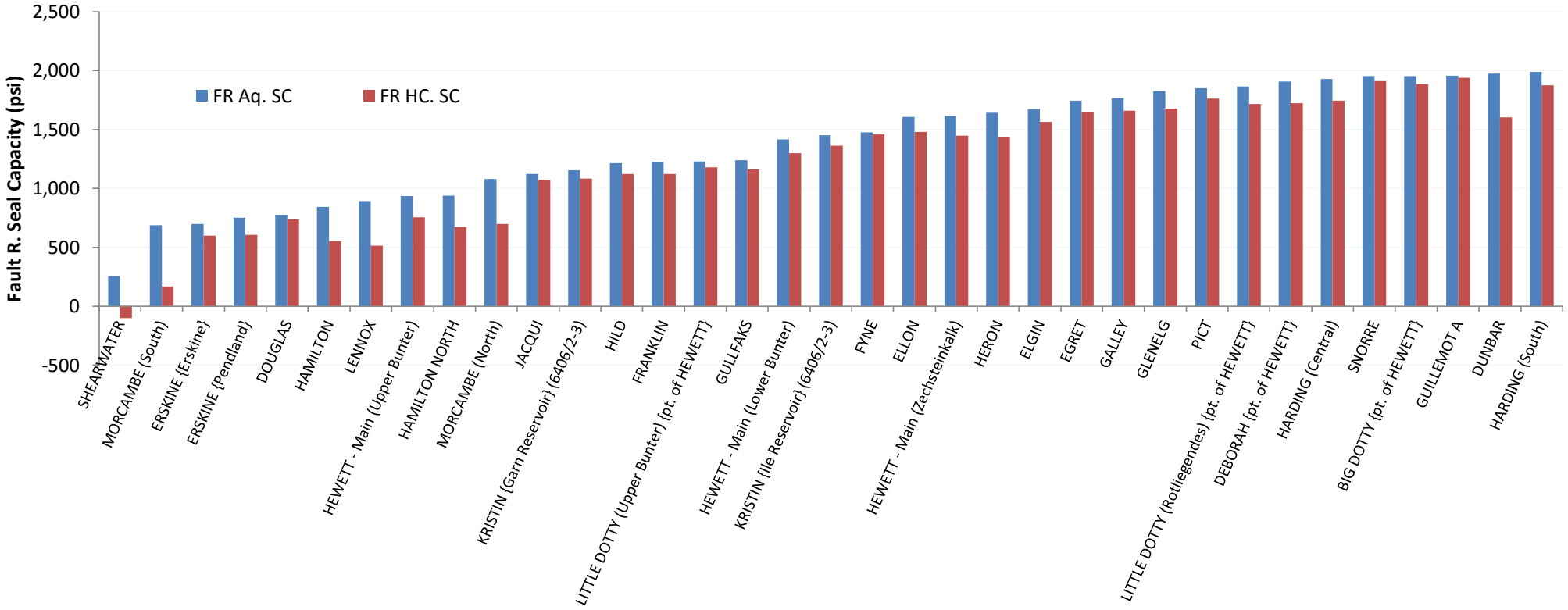

Figure 5.28 - Fault reactivation aquifer and hydrocarbon seal capacity graph < 2000 psi. Shearwater is the only field to indicate a negative value.

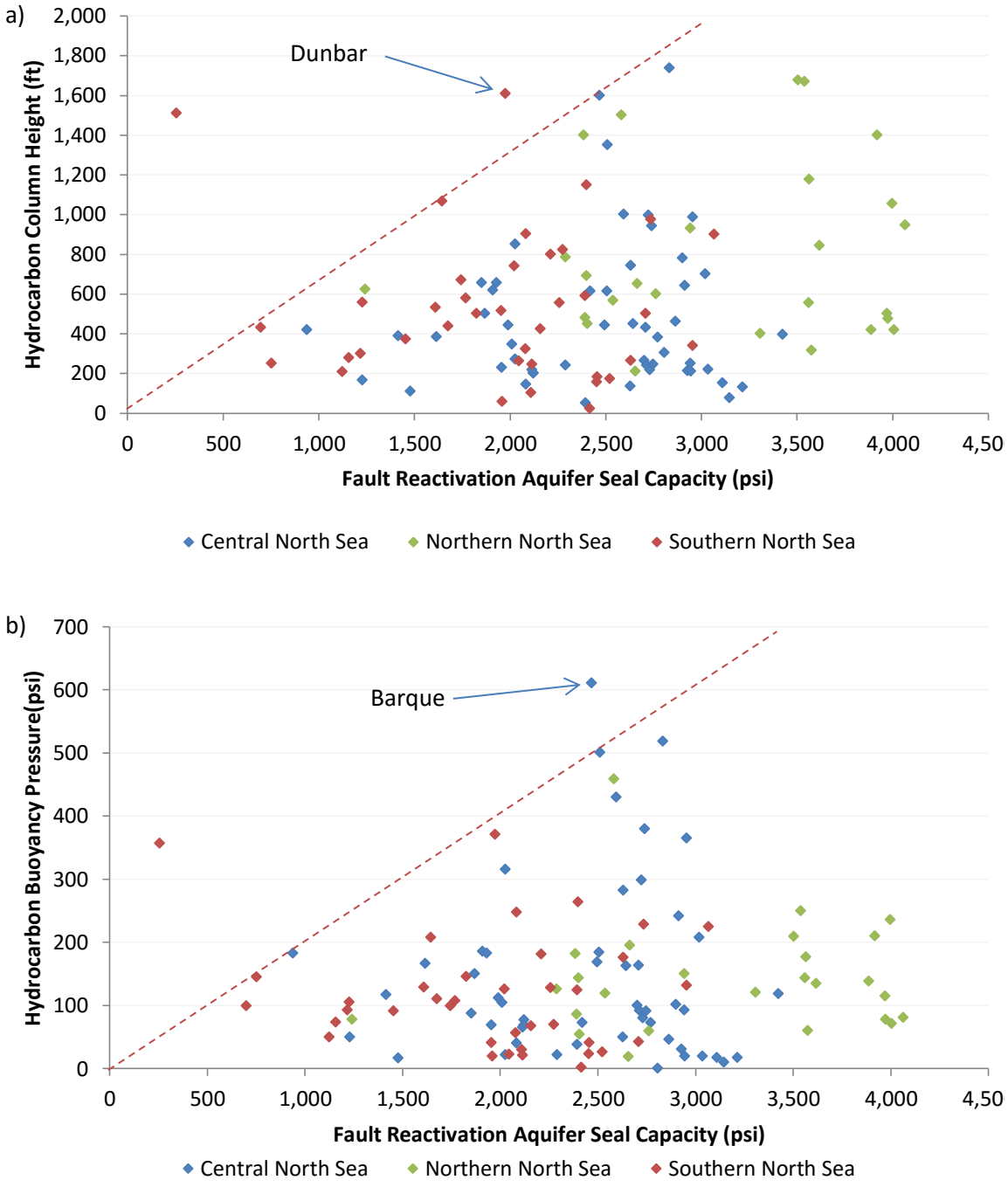

Figure 5.29 - Hydrocarbon column height and hydrocarbon buoyancy pressure against Fault reactivation aquifer seal capacity. Colour coded by region. A upper bound (red dashed line) is observable in both graphs. Below this line sits the majority of fields. Shearwater is a clear exception displaying a large column/hydrocarbon buoyancy at a negative value seal capacity.

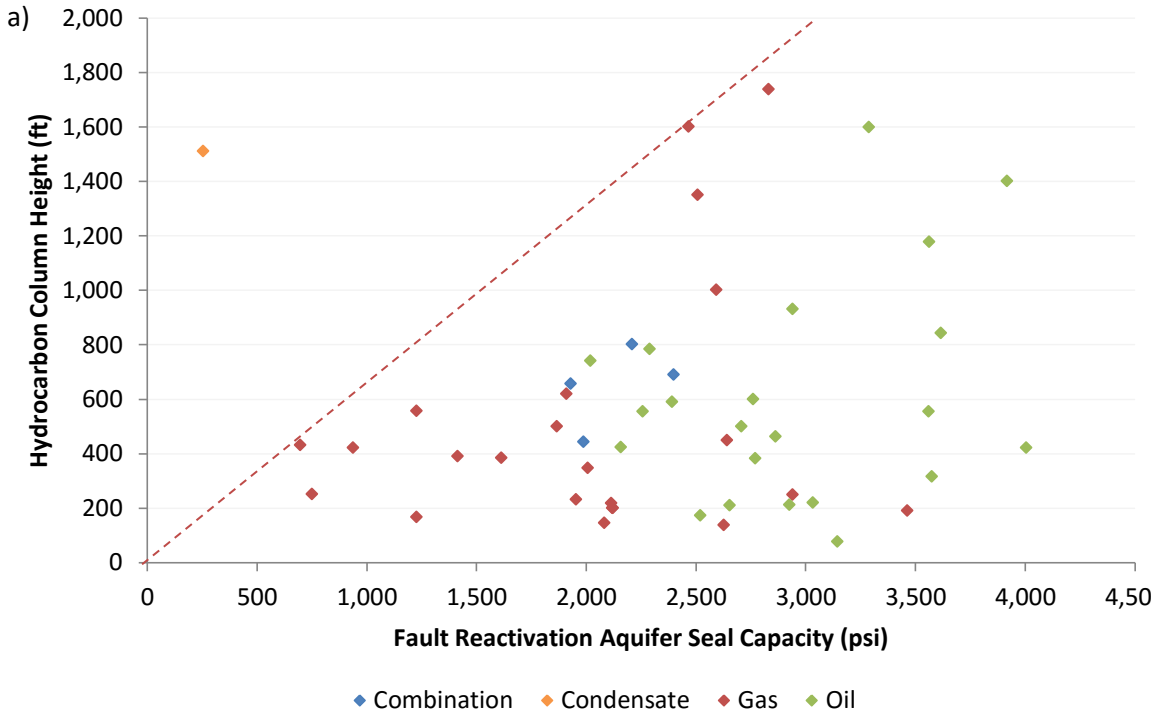

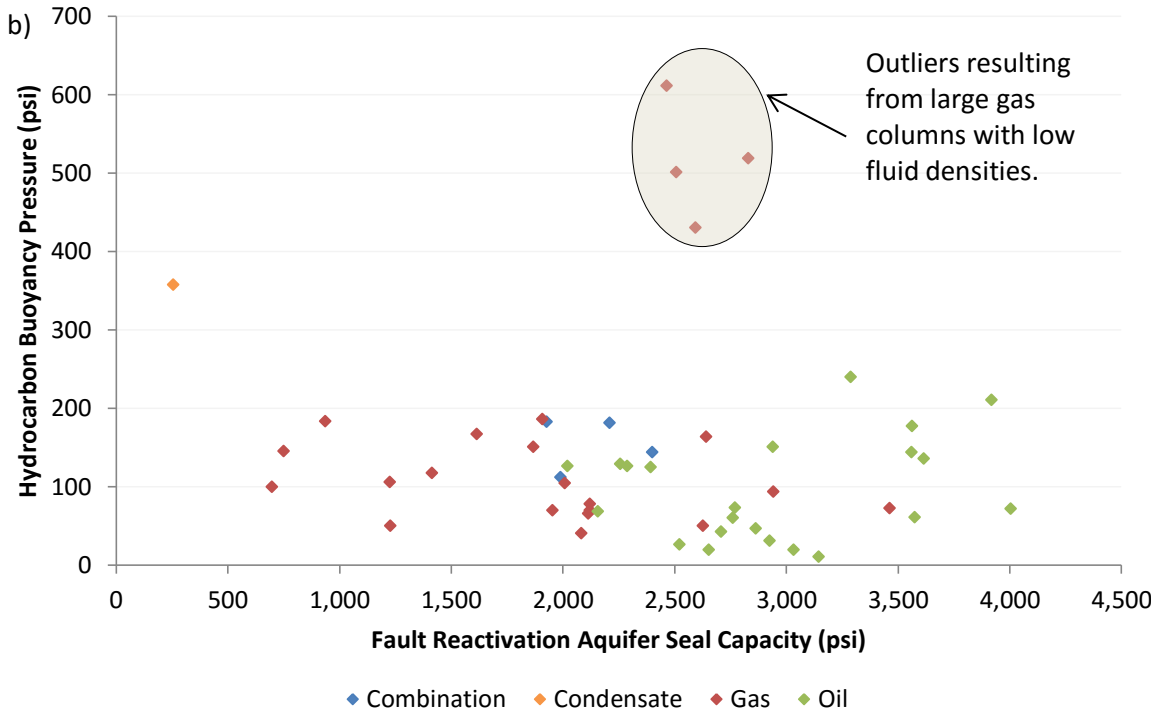

Figure 5.30 - Similar figure to 5.29 however using fields solely from under-filled reservoirs. Colour coded by fluid type, an upper bound line is still applied with column height as a variable. All hydrocarbon buoyancy pressures indicate a limited distribution up to 200 psi with the exception of a few Southern North Sea fields.

Oil accumulations are not present in low FR aquifer seal capacity in the Central and Northern North Sea under-filled fields (Figure 5.30). All accumulations less than this value are solely gas and condensate. Furthermore, when considering hydrocarbon buoyancy pressures, 82 % of all fields that are under-filled have buoyancy pressure less than 200 psi. This value is relatively consistent over the range of FR seal capacities, although the sample density increases with increasing FR seal capacity.

There are 4 fields that hold high hydrocarbon buoyancy pressures comparable to the rest of the data set, marked on Figure 5.30. These fields, Indefatigable, Clipper, Barque and Pickerill (East) all possess large hydrocarbon column heights (1000 - 1700 ft). The accumulation fluid is Southern North Sea gas with a low fluid density. Again, the Shearwater field is also an anomaly.

5.2.5.1 Interpretation

As with other results, due to the Shearwater field's high overpressure, the field displays abnormal results. The Irish Sea fields, shown in Figure 5.28 as having seal capacities comparable to the highly overpressured Central and Northern North Sea fields, is likely a result from uplift related overpressure generation and shallow crest depths leading to the observed small seal capacities. The Southern North Sea fields also indicate small seal capacities relative to the remaining data set. The reason for this, however, is similar to that of the Irish Sea fields. The crest depth of the Hewitt field sits at just 2,600 ft TVDss and thus places a bias due to the narrower envelope between the hydrostatic pressures and principal stresses initially.

Maximum bound lines are applied to Figure 5.29, as with previous figures regarding column height. It can be stated that possible column height is shown to increase with increasing fault reactivation seal capacity. A gradient of 1.56 psi/ft indicates a rough maximum cut off for North Sea data. As such, with fields indicating a fault reactivation aquifer seal capacity of 1000 psi column heights are unlikely present larger than 640 ft. The process of only viewing under-filled fields is to gain a perspective of fields that are limited by a factor separate from trap structure.

The marked assembly on Figure 5.30 indicating high buoyancy pressures relating to the rest of the data can be assumed to result from a combination of large column heights and low fluid densities associated with a gas.

A summary of all the key results and how they inter-relate is found in the following chapter. Furthermore, the anomalous Shearwater field is elaborated upon and a hypothesis of a protected trap is suggested as an explanation.

Chapter 6

Seal Capacity & Hydrocarbon Column Height of North West Europe

Chapter 6 - Discussion & Protected Traps

The following chapter summarises the key results discussed in Chapter 5. Further explanation and hypotheses are suggested to explain anonymous results, like that of Shearwater. It is suggested that a protected trap is the reason to the Shearwater field's abnormality in respect to the remaining dataset. The Lusi Mud Volcano (Porong) is discussed briefly as an example of both the impacts of a protected trap and hydraulic fracturing as a result of poor well practise.

6.1 The Shearwater Field & Protected Traps

Protected traps are important to identify and understand. Within a play fairway associated with a protected trap, a hydrocarbon column can be present in a closure which would otherwise have been expected to fail. It is this phenomenon that is used as a suggested explanation for the anomalous values associated with the Shearwater field.

6.1.1 Definition of a Protected Trap

A protected trap can be defined as a structurally deeper closure which is in hydraulic connectivity with a shallower, neighbouring trap(s). The structure, depicted in Figure 6.1 as B, is shallower, but still hydraulically connected to structure A and, therefore, must have a smaller aquifer seal capacity (see Figure 6.1 P-D plot).

Line 1 represents the aquifer pressure gradient within the pressure cell containing structures A & B. Note how line 1 at the crest of structure B has a positive aquifer seal capacity, as does structure A. When the aquifer pressure within the pressure cell increases (line 1 → 2) the aquifer pressure at the crest of structure B intersects the least principal stress gradient – the aquifer seal capacity equals 0. The 2 contrasting views on the effects of hydrocarbon buoyancy influencing failure is important to consider here.

1. Taking the conventional route, excess buoyancy should be accounted for; any hydrocarbon accumulation within structure B will be expelled through hydraulic fracturing. However, the **protected trap** (structure A) still retains a positive aquifer seal capacity. The consequence of this is that the hydrocarbon accumulation within structure A is protected from top seal hydraulic leakage due to the pressure valve present at the crest of structure B. Structure B is shallower and will, therefore, breach and pressure will remain in equilibrium within the A-B pressure cell. As a result of this, structure A can fill to its spill-point and any increase in pressure will bleed off in structure B, not modifying the column height in structure A. Once structure A is full-to-spill, hydrocarbons will leak out into structure B, increasing buoyancy pressure, hydrofracturing the caprock in B and permitting vertical leakage of hydrocarbons.

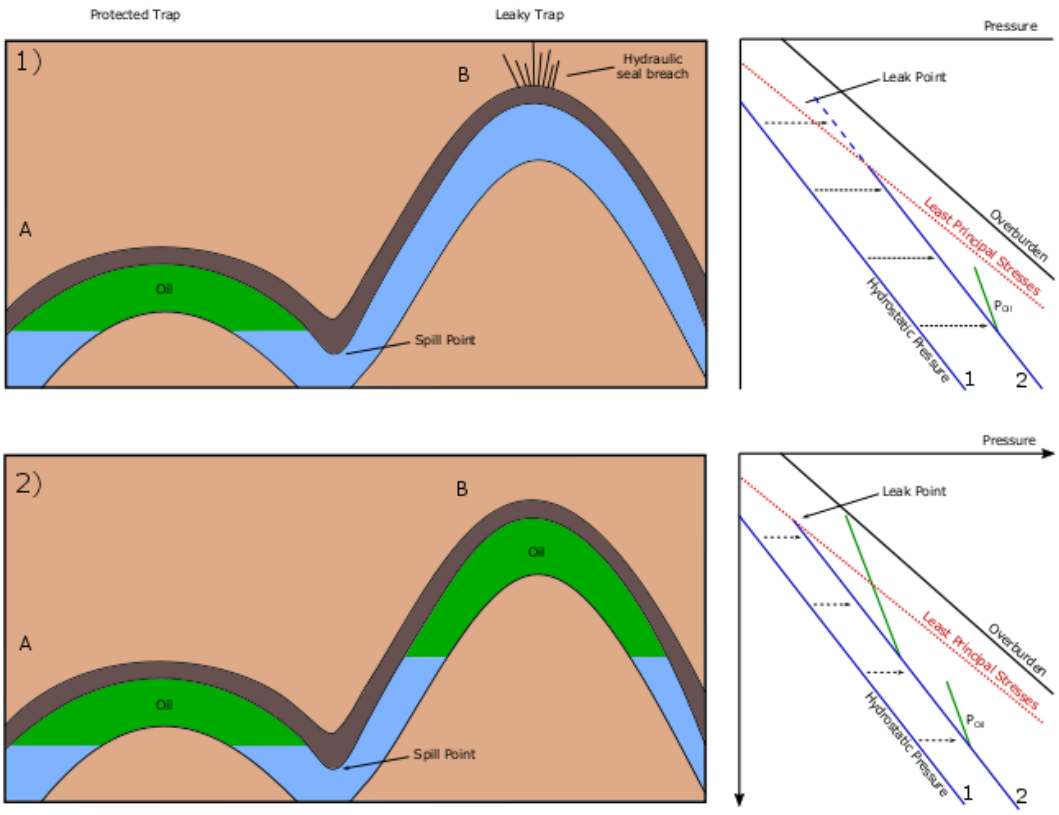

Figure 6.1 – Schematic illustration representing a protected trap (A). Trap (A) has a protected column unable to hydrofracture the formation under current pressure regime, indicated with the P-D plot to the right. A Pressure valve is present at the crest of structure B, therefore any pore pressure increases will hydrofracture trap B, releasing the pressure back to an equilibrium state.

2. The alternative theory, supported by Swarbrick et al. (2010), is that excess hydrocarbon buoyancy associated with hydrocarbon accumulation should not be accounted for when discussing caprock hydrofracturing. Figure 6.1 (2) displays how this could influence the schematic structure illustrated. Structures A and B both contain an oil accumulation. The positive aquifer pressures, although close to value as σ_3, still allow for an oil column to accumulate, despite a negative formation pressure seal capacity. Any further increases in aquifer pressures will hydrofracture the formation bringing the aquifer pressures back into equilibration however the oil column still remains. The application of this in regards to the Shearwater field is discussed further in Section 6.1.3.

6.1.2 Case Study - Genesis/Popeye Fields

The Popeye and Genesis fields are located within the HPHT Green Canyon region in the Gulf of Mexico (see Figure 6.2). The minibasin (with the Popeye field to the north and Genesis field on the southern margin) lies in approximately 2000-2900 ft water depths and has bowl-shape reservoir sands ca. 9000 – 15,000 ft TVDml (Seldon & Flemings 2005) (see Figure 6.3).

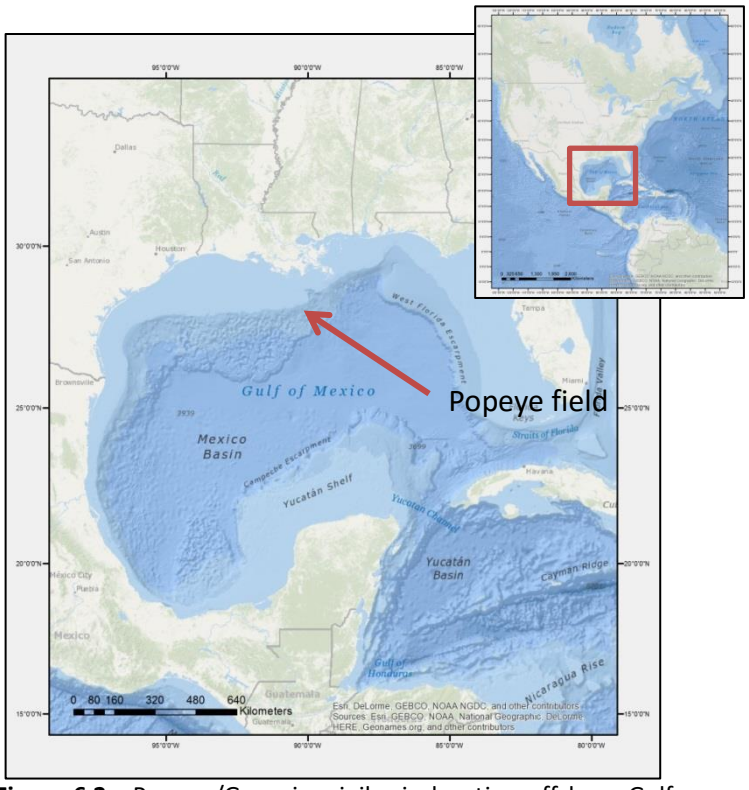

Figure 6.2 - Popeye/Genesis minibasin location offshore Gulf of Mexico. The white circles represent the gas bearing Popeye field and Genesis oil field.

The shallowest points, where the reservoir sands pinch out, are up-dip of both fields and are hypothesised to be hydraulically fracturing the

caprock at the top level of the connected sands; pore pressure is equal to the least principal stress. This ultimately ensures the integrity of the neighbouring, hydraulically connected, Genesis and Popeye hydrocarbon traps. Similar to described above, the reservoir pore pressures within the deeper Genesis and Popeye fields cannot approach their corresponding fracture pressures due to the pressure valve at the crests of the shallower sands. This allows a hydrocarbon column to be maintained within the Popeye and Genesis traps, protected from hydrofracturing. Should the pore pressures increase, through further burial, for example, the columns can still be maintained by the shallower sands pressure valve maintaining a positive seal capacity within the hydrocarbon bearing reservoirs. Figure 6.3(A) shows a schematic of the Popeye/Genesis minibasin and field locations. Figure 6.3(B) represents a P-D plot of the N1 sands. σ_3, the least horizontal stress (S_h) is the fracture gradient determined by Genesis LOT, the white circles on Figure 6.3(B). As shown on the diagram, the protected trap cannot intersect with σ_3 and will always maintain a positive $\sigma_h'_{TRAP}$ (hydrocarbon seal capacity in this reports eyes). The hydrocarbon accumulation is 'protected' from hydraulic failure related leakage.

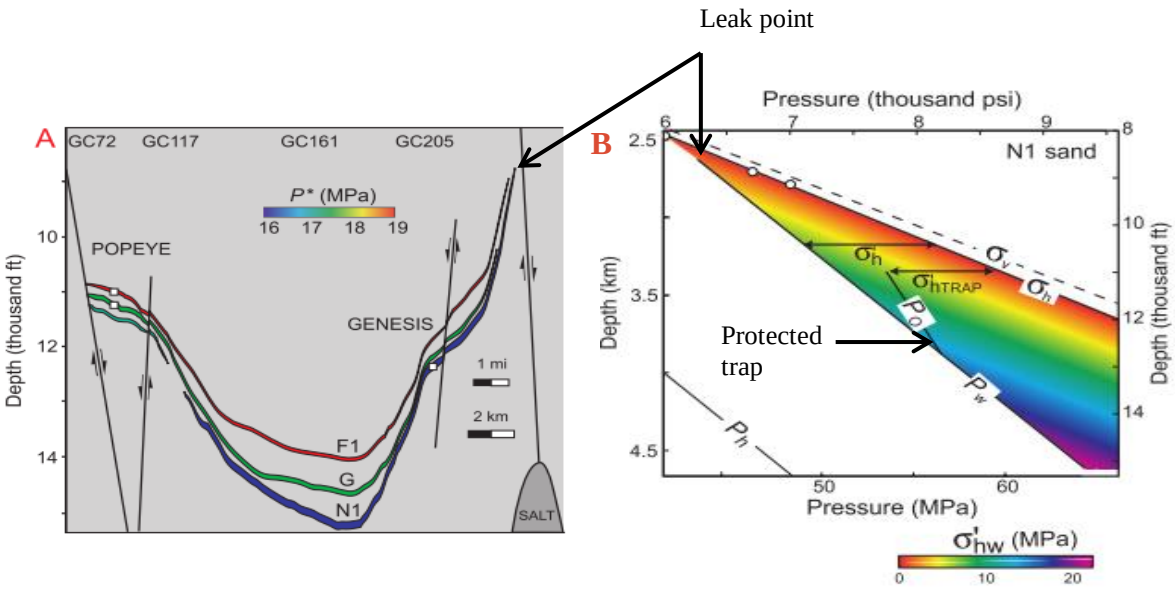

Figure 6.3 - A - Simplified diagram of the Popeye/Genesis minibasin. Fig. B illustrates a Pressure-Depth plot highlighting the structural leak point and protected deeper hydrocarbon bearing trap. $\sigma_h'_{TRAP}$ and σ_h' represent the effective stress. Seldon & Flemings 2005).

6.1.3 Hydrocarbon Column Height Significance of a Protected Trap

In terms of hydrocarbon column height significance, protected traps can have a substantial impact. The breadth of this significance depends on the failure criteria. It has already been discussed in Chapter 3 that there are 2 opposing views to the effect hydrocarbon buoyancy has upon caprock hydraulic failure and leakage. The general consensus is the reservoir pore pressures, i.e. taking excess buoyancy into account, will cause hydraulic fracturing of the seal once they equal that of the minimum principal stress (Gaarenstroom et al. 1993; Converse et al. 2000; Nordgård Bolås et al. 2005, Seldon & Flemming, 2005 etc.). However, a new concept proposed by Swarbrick et al. (2010) states that it is solely aquifer pressure in a water wet seal that causes hydraulic fracturing. Assuming the first hypothesis is true a stratigraphically deeper crest (like that of A in Figure 6.1 or the Popeye field) can possess a column height of unexpected length or simply presence at all.

Furthermore, little is discussed within the literature about protected traps within North West Europe (or the North Sea in particular). The Shearwater Field, however, is discussed briefly within a paper section by Winefield et al. (2005). A similar concept to Figure 6.1, instead of a 2 closure system, a 3 closure system is proposed. Within the Shearwater pressure cell 3 closures all lie along a single aquifer gradient, strong evidence for hydraulic connectivity. These fields are Shearwater, the deepest structure, Juno and Martha (Martha being the shallowest). It is noted that although it is thought a small attic accumulation may be present within the Juno structure, from exploration well 22/29-6s2 (Winefield et al. 2005), Shearwater is the only structure containing economic hydrocarbons (Gilham & Hercus 2005). Martha, was proven to be water wet (22/30a-1), although core has indicated oil and condensate quartz inclusions (Winefield et al. 2005), evidence of the presence of a palaeo hydrocarbon column.

Winefield et al. (2005) uses the principal that when the pore pressure equals that of the fracture pressure or minimum stress, mechanical failure can occur. Figure 6.4 is an adaption of the theory proposed within the paper. The minimum stress line is defined by the crest depths of structures known to be leaking, on the assumption that

the pressures at their structural crests are equal to that of the mechanical failure pressure. As shown, Martha has an aquifer pressure equal to that of the failure pressure and, therefore, does not have any envelope to accommodate hydrocarbons. Juno has a narrow envelope and is thought to possess a marginal hydrocarbon column height, whereas, Shearwater has a large envelope and therefore can accommodate a large column. Winefield et al. (2010) considers Shearwater to be a leaking structure and is still limited by the fracture pressure. The hydrocarbon column height is protected and will remain the same height due to the Martha pressure valve.

Within this report's dataset it is seen that Shearwater indicates an aquifer seal capacity of 542 psi and a hydrocarbon seal capacity of 185 psi. The following image (Figure 6.5) represents a P-D plot of the Shearwater field pressure cell. From the Winefield et al. (2005) paper, the Martha and Juno structures are known to be shallower and contain either no accumulation or a possible little column in Juno's case. There are 3 possible outcomes from this analysis; none are conclusive at this point.

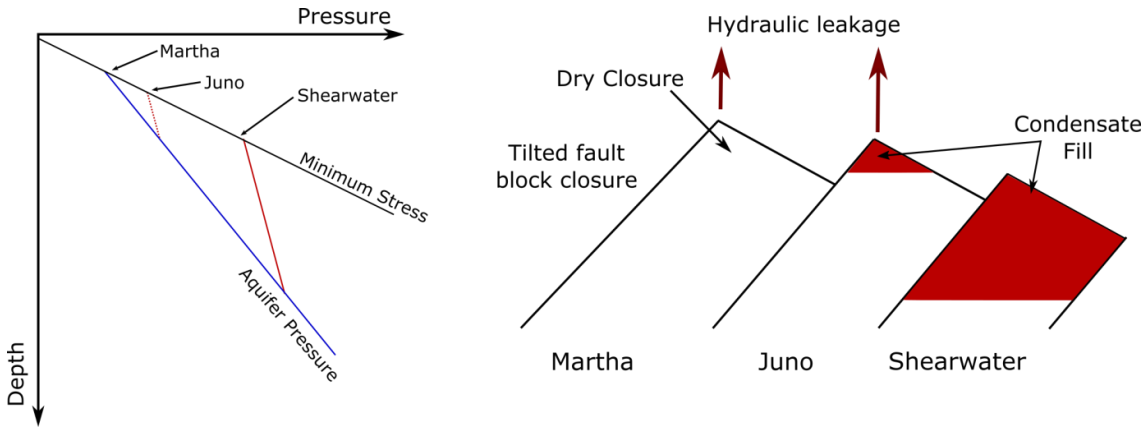

Figure 6.4 – Schematic diagram adapted from Winefield et al. (2005). Concept is based on the traditional view of hydraulic fracturing (i.e. pore pressures are key, not aquifer pressures). The Shearwater trap is the deepest structure and 'protected' by the shallower hydraulically fractured Martha, and potentially the Juno structures.

1. Taking the conventional, pore pressure influences mechanical fracture, approach the Martha and Juno closures are dry simply because they have failed, or Juno possesses an insignificant condensate attic but is limited by the fracture pressure. The Shearwater field's pore pressure only sits 185 psi away

from the fracture pressure, and as such could potentially have failed, hence the limited under-filled column. However, fractures have since closed and due to the protection of the shallower pressure valve, a significant hydrocarbon column remains.

2. Taking the Swarbrick et al. (2010) approach of aquifer pressure being the driving force for hydraulic fracturing. The aquifer pressures within Juno and Martha are both very close to the fracture pressure, an explanation for the lack of charge. However, the aquifer seal capacity is still positive, hence the presence of a hydrocarbon column. The explanation for the under-filled status must lie within the lack of charge. Considering the deeper Elgin, Franklin and Glenelg fields possessing only a small column could imply that charge is lacking within the area. Or hydrofracturing has occurred and the closures are still being charged at present.
3. Both aquifer and hydrocarbon seal capacities are positive for the shearwater field. However, we know that Shearwater had a palaeo oil column that has already leaked through the hydrofracturing process. We can therefore say conclusively that the Shearwater field caprock has pre-existing faults embedded within, already proven drainage conduits. The fact remains that the fault reactivation seal capacities indicate a very close to failure 225 psi aquifer seal capacity and a negative formation seal capacity. It can be suggested that it is not in fact the least principal stress that is limiting the Shearwater field's hydrocarbon column but the reactivation of pre-existing faults. The presence of the Martha pressure valve is still maintaining a considerable hydrocarbon column in the first place.

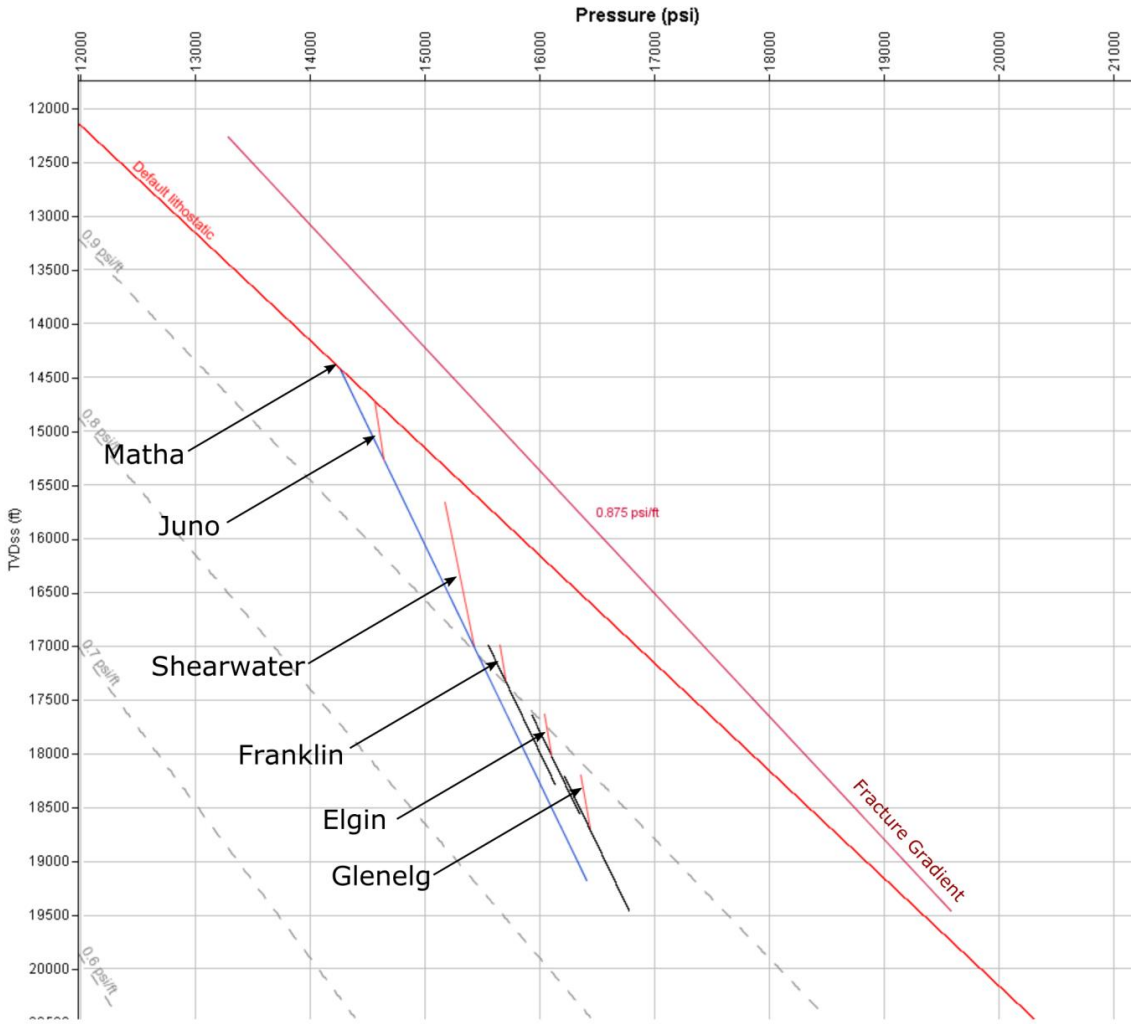

Figure 6.5 – P-D plot of the Shearwater pressure cell. The Matha Structure is located at the crest of the cell and has an aquifer pressure equal to that of the fracture pressure. The remaining deeper structures are protected, to a degree, by the Matha pressure valve, hence the presence of hydrocarbons in each deeper structure.

Whatever the true explanation, it is fair to say that the HPHT pressure regime is clearly having an input in limiting the column height in the Shearwater field and has resulted in two neighbouring dry/uneconomic structures. The Shearwater field is undoubtedly not the only protected trap within the North Sea or data set. Elgin, Franklin and Glenelg are all hydraulically connected to the Shearwater structure and, therefore, can be classed as protected traps themselves. Shearwater stands as being a clear outlier due to very small seal capacities. The Elgin, Franklin and Glenelg fields all lie deeper and, as such, have larger seal capacities. The Shearwater field is an anomaly within the data set and proves 2 things. Firstly, it highlights the pitfalls and general lack of understanding in accurately predicting rock failure pressures and criteria. Secondly, on

a more positive note, the presence of a long 1500 ft hydrocarbon column in a HPHT area designates that there should still be a positive outlook on exploration in very high pressure regions as this field alone proves the economic gains to be made from closures that may be expected to have leaked.

6.2 Case Study - Lusi Mud Volcano

The following case study is relevant to this report for two reasons. Firstly, associated wells and seismic lines give evidence of natural hydraulic fracturing within the Porong 1 well resulting from subsurface overpressures. Secondly, the failure with best practice drilling protocol results in formation of hydraulic fractures resulting from inadequate well safety and misinterpreted LOT and seismic plans.

6.2.1 Introduction to Lusi Mud Volcano

The LUSI mud volcano story can, disputably, be classified as one of the worst environmental disasters resulting from an oil industry mishap. The large volumes of subsurface mud being expelled at the surface has displaced > 30,000 people and is the largest and best known mud volcano globally (Davies et al. 2008). A picture of the catastrophe is pictured in figure 6.7.

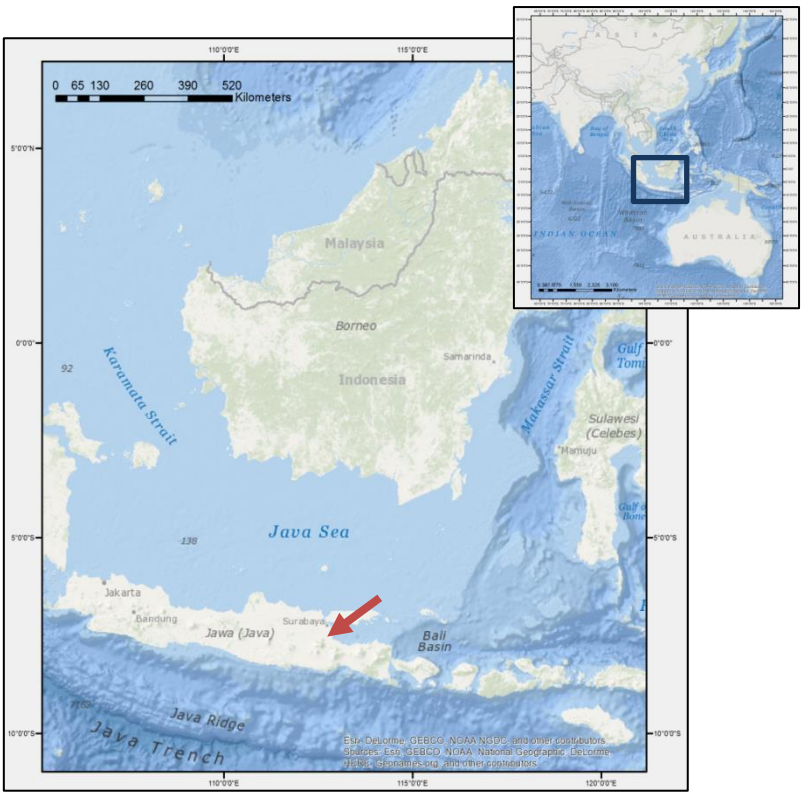

Figure 6.6 - Location map of the Porong mud volcano in Indonesia.

In mid-2006 PT Lapindo Bravas Petroleum Company drilled the Banjar-Panji 1 exploration well, targeting gas in the Kujung Carbonate Formation. The Banjar-Panji 1 BOPs were activated and the well was shut-in when a considerable kick was encountered drilling into the overpressured limestone (Kujung formation). The well was only cased to 3580 ft leaving a 5,720 ft open-hole section. It is hypothesised that overpressured fluids from the limestone formation travelled up the shut-in Banjar-Panji 1 borehole to a permeable formation, accessible due to poor casing decisions and a long stretch of an open-hole section. Resulting hydrofractures propagated to the surface, expelling huge volumes of formation muds approximately 150 m from the borehole site. Should this hypothesis be correct (evidence suggests a degree of earthquake influence), the Lusi Mud Volcano is an example of the impact of natural pressure induced hydraulic fracturing. The leak point within this example is the surface and, therefore, overpressured fluids (with pore pressures greater than that of the fracture pressure) hydraulically fracture a formation causing a natural seal breach.

A) B)

Figure 6.7 – Image indicating the degree of damage resulting from the Lusi Mud volcano mishap. a) Credit – Mark TIngay, University of Alidade b) Credit – National Geographic

The case study was selected as it clearly captures a nice example of hydraulically induced fractures and highlights how bad drilling practices can lead to complications. Furthermore, the BJP-1 structure can be termed a protected trap with a pressure valve at a neighbouring structure drilled by the Porong-1 well.

6.2.2 *Pre-Drill vs Actual Casing Designs and Consequence of BJP-1 Well*

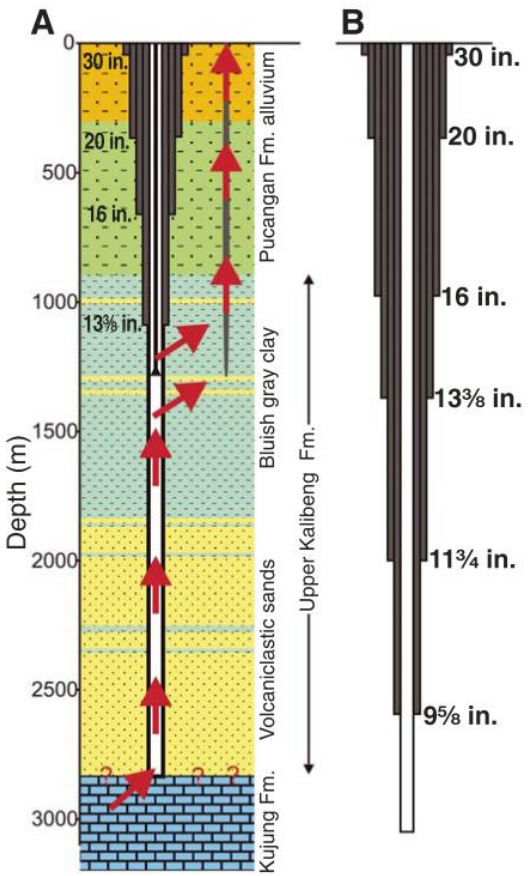

Figure 6.8 – Proposed (B) vs actual (A) casing shoe depths and stratigraphy of the BJP-1 well. (Tingay et al. 2008)

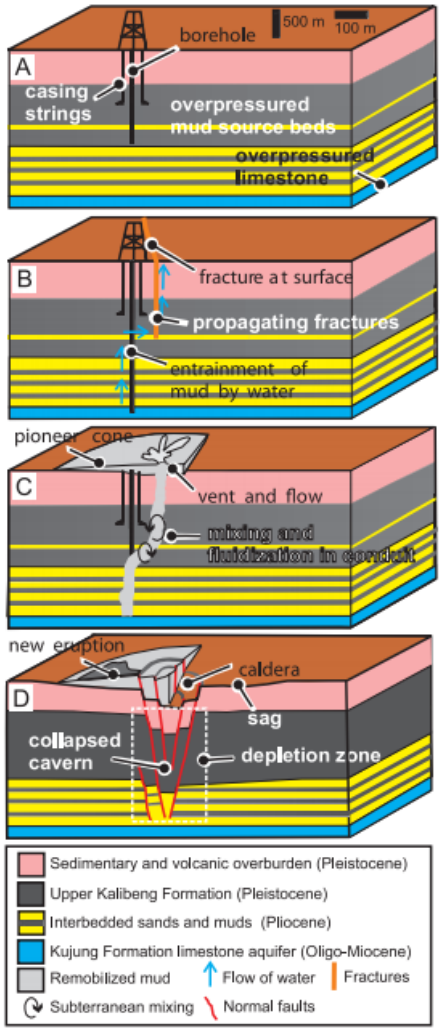

Figure 6.9 - Schematic representation of the Luci mud volcano highlighting the major developmental stages. A - Bajar-Panji 1 well drilled through interbedded sand and overpressured mud formations. B - Drilling kick encountered once overpressured Kujing Carbonates penetrated. Formation fluids hydrofracture overlying formations. Entrainment of mud occurred. C – Subsurface conduit formation undergoing periodic collapse. D – Caldera formation and subsequent caldera sagging and further conduit development. Davies et al. (2007)

Possibly the largest error associated with the Lusi mud volcano disaster is the lack of drilling practices followed. It is commonly known that steel casings are cemented at various intervals throughout a well, not only to increase the stability of the borehole but, primarily, to compensate for higher mud weights used to safely drill into formations with increasing subsurface pressures (Tingay et al. 2008). Casings should be set prior to entering formations with considerably higher overpressures than the overlying strata, thus allowing a higher mud weight to be utilised that could fracture

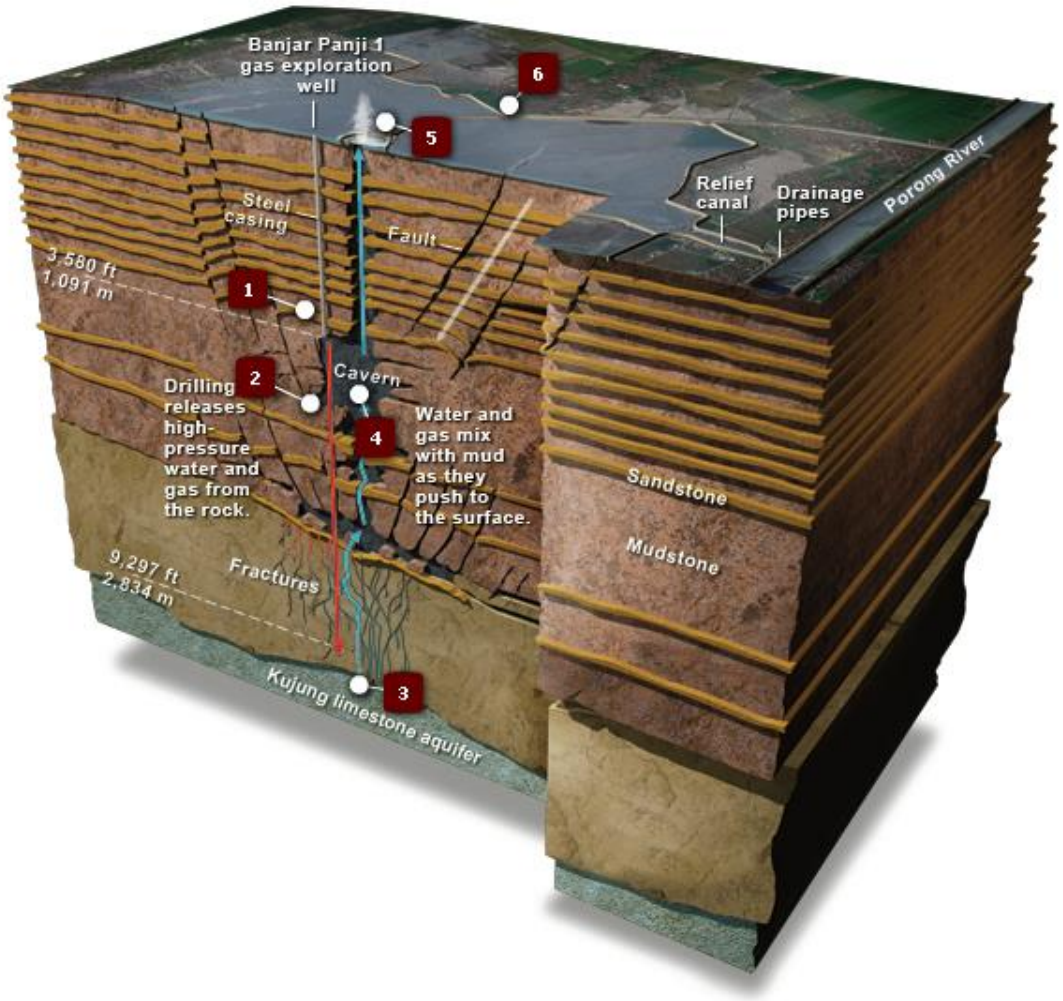

Figure 6.10 – Schematic image indicating a cross-section of the BJP-1 well and subsurface.
1) Depth of casing run 1. 2) Open hole section experiences kicks and losses. 3) Well penetrates Kujung aquifer with high pressure. 4) Formation fluids flow up well, liquefy mud masses. 5) Caldera of mud volcano. 6) Dykes and control measures built in attempt to control mud flow. Credit – National Geographic

the overlying formations and cause serious well losses. The pre-drill report for the BJP-1 well indicated that casing points would be set to allow no more than a 610 m open-hole section. However, minor kicks and unstable well-bores meant that the 16" and 13 3/8" casings were set lower than anticipated. Later, further casing points (1981 m & 2591 m) were proposed with the latter set for 2591 m (just prior to the highly overpressured Kujung Formation). Despite this, the 1981 m casing point was skipped as was the latter when the Kujung formation was not encountered. Drilling continued until complete losses were encountered at 2834 m TVDss and a 1742 m long open hole section had been drilled (Tingay et al. 2008) This is shown as the red borehole line on Figure 6.10 . Once the Kujung formation was penetrated (point 3 of Figure 6.10) over pressured fluids (3200 psi OP) flowed up the wellbore and the BOP activated (shown as a schematic in Figure 6.8). The overpressured fluids from the reef are then thought to have naturally hydrofractured the overlying formations, eventually breaching the surface 190 m from the well pad. A subsurface cavern (point 4 on Figure 6.10) formed via liquefaction of mud, thus facilitating in the caldera collapse structure (point 5, Figure 6.10) at the surface as well as the source for the expelled mud. The developmental stages of the creation of the Porong mud volcano are summarised in Figure 6.9 from Davies et al. (2007).

6.2.3 Precursor - The Porong 1 Well

Prior to the drilling commencement of the disastrous BJP-1 well, a well was drilled named Porong 1. The target was reef accumulations within the overpressured Kujung formation. The well was reported dry and abandoned. Seismic indicate the Porong-1 well was located just adjacent to a mass of near-vertical fractures. Furthermore, situated above the top Kujung limestone horizon a large 4 km diameter and 400 - 450 m deep circular depression is observed after mapping 2D seismic. This depression is hypothesised to have resulted from evacuation of high pressured fluids to the surface at least 250,000 years ago. Mapping of the Kujung formation suggests that the Porong-1 and BJP-1 well are targeting the same formation in lateral hydraulic communication with each other. The top formation marker for the Porong-1 well

however, is located 780 ft shallower (at 8520 ft) than that within the horizon of the BJP-1 well Figure 6.11). The sets of near vertical fractures indicate that the Porong-1 well location is close to the shallowest point within the Kujung formation and the pressures within the limestones were great enough to hydrofracture the rock. As such this suggests the Porong-1 well closure can be defined as a pressure valve for all deeper closures, including that of the BJP-1 well – as such defining them as protected traps. Any increase in pore pressure opens the pressure valve in the Porong-1 closure, hydrofracturing the formation until pressure equilibrium is reached and the valve closes. The deeper connected structures (BJP – 1 crest) are protected from pressures reaching the fracture pressure as a result (See Figure 6.11).

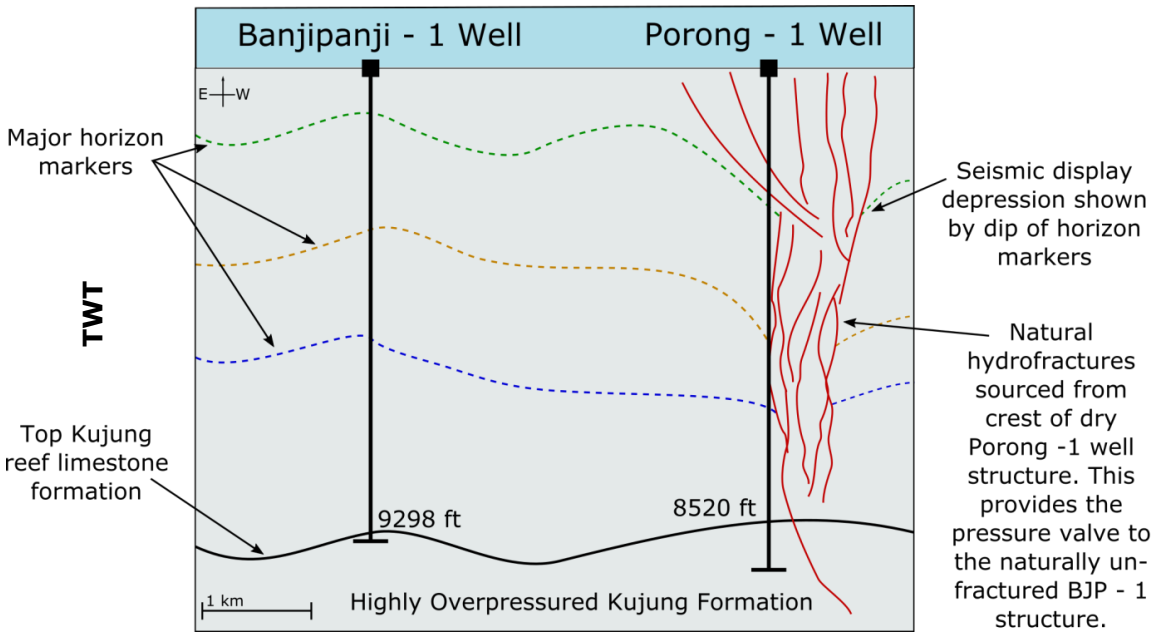

Figure 6.11 – Annotated overlay from seismic highlight important study features. Seismic shot pre-BJP – 1 well disaster. Faults sets observable from crest of Porong – 1 well structure thought to be hydrofractures from the crest Kujung Formation. Note the lack of fractures surrounding the BJP – 1 drill site. This is due to the BJP – 1 well being a protected trap with the pressure valve at the Porong – 1 crest. Credit - Adapted from image displayed at the Geological Society meeting on soft sediment deformation (October 2008)

6.2.4 Project Significance

Both the Porong-1 well and BJP-1 examples here have a great deal of relevance with this study as well as highlighting the importance of following best practice behaviours. The dry Porong-1 well gives a clear indication of a naturally mode-1 fractured formation associated with high pore pressures. The BJP-1 well is indicative a protected trap associated with a pressure valve from the Porong-1 structure. Prior to drilling the BJP-1 well the BJP closure was protected from hydrofracturing as the deeper structure within the BJP-Porong trap complex. This is directly applicable to the Shearwater pressure cell. The Porong – 1 closure has hydraulically fractured the caprock and formation fluids have been lost prior to drilling. The same scenario is observed with the Martha and Juno closures. The Shearwater closer is a protected deeper trap and has not fractured (post-charge) draining formation fluids.

6.2.5 Conclusion

The past section has provided an explanation to the Shearwater field anomaly. It is thought that pressures within the Shearwater field have breached that required to reactivate pre-existing faults. This is limiting the length of the hydrocarbon column. The reason behind the presence of such a large column in the first place, causing the Shearwater field to stand out from the data in the first place is attributed to the presence of a protected trap. Shallower dry/uneconomical closures of Martha and Juno respectively are acting as pressure values to the deeper formations allowing a column to be held within the closure. Following this, two example case studies (the GoM Poppeye/Genesis fields and the Lusi Mud volcano) add further background to the assumptions made with Shearwater. The concept of protected traps are very rarely mentioned within the North Sea literature (the exception being by Winefield et al., 2005 who discusses the implication briefly). It should be noted that as the North Sea becomes more of a mature region, abnormal pressure regimes and unconventionally located accumulations recoverable due to the presence of protected traps should be considered within HPHT formations.

6.3 Discussion of North West Europe Results & Implications

The results published in chapter 5 are all interpreted within their appropriate sub headings. The following section discusses links and concludes the key findings.

The dataset used within this report, although not exclusively, focuses upon fields located within the North Sea, the Northern and Central regions in particular. The Irish Sea fields are thought to possess overpressures resulting from multi-phase uplift post charge and not disequilibrium compaction. As such, these are removed from much of the subsequent data analysis as they are deemed non-comparable to the overpressured formations of the Central and Northern North Sea. Differing overpressure generation mechanisms aside, the shallower crest depths also skew the data due to the closer proximity to the fracture and lithostatic gradients, despite possessing only a small degree of overpressure. A similar process was applied to the Southern North Sea regions. The title and focus of this study is to assess relationships between seal capacity, overpressure and hydrocarbon column height. The Southern North Sea fields all display hydrostatic pressures (or very low degrees of overpressure). As such pressure (and thus seal capacity) is not influencing hydrocarbon column lengths. For this reason a prejudice is present within the data collection process towards fields with very high overpressures, normally and moderately overpressured fields may be underrepresented. This bias is emphasised within Figure 6.12 of under-filled fields. Patterns may present themselves as much as a result of the collection process, than the consequence of the comparable variables, an important principal to consider.

The minimum stress convergence and transition depth value has always been of interest. This relates to the regional depth at which the fracture gradient transitions form values less than that of S_v to greater values than S_v. A convergence depth, resulting from P_p/S_h coupling, is noted throughout the literature (see Section 3.5.7), however, the depth discrepancies between authors are clear (see table 3.1). The results of analysis undertaken within this data set indicate a minimum stress transition of 14,500 ft for the Central North Sea and 13,000 ft for the Northern North Sea. The Central North Sea convergence value is synonymous with the values presented by Swarbrick et al. (2010). Regional analysis of the Northern North Sea minimum stress convergence and transition is, to this report's understanding, not previously documented within the literature. The importance of this value lies with the calculation of seal capacities, both aquifer and hydrocarbon. Within an extensional basin, such as the North Sea, it would be expected that σ_3 will be the P_{frac} and this value represents the maximum pressure a caprock can withstand prior to mechanically failing, releasing hydrocarbons from the closure. This study proposes that post the minimum stress convergence depth S_v (plus any additional tensile rock strength) becomes σ_3 and thus

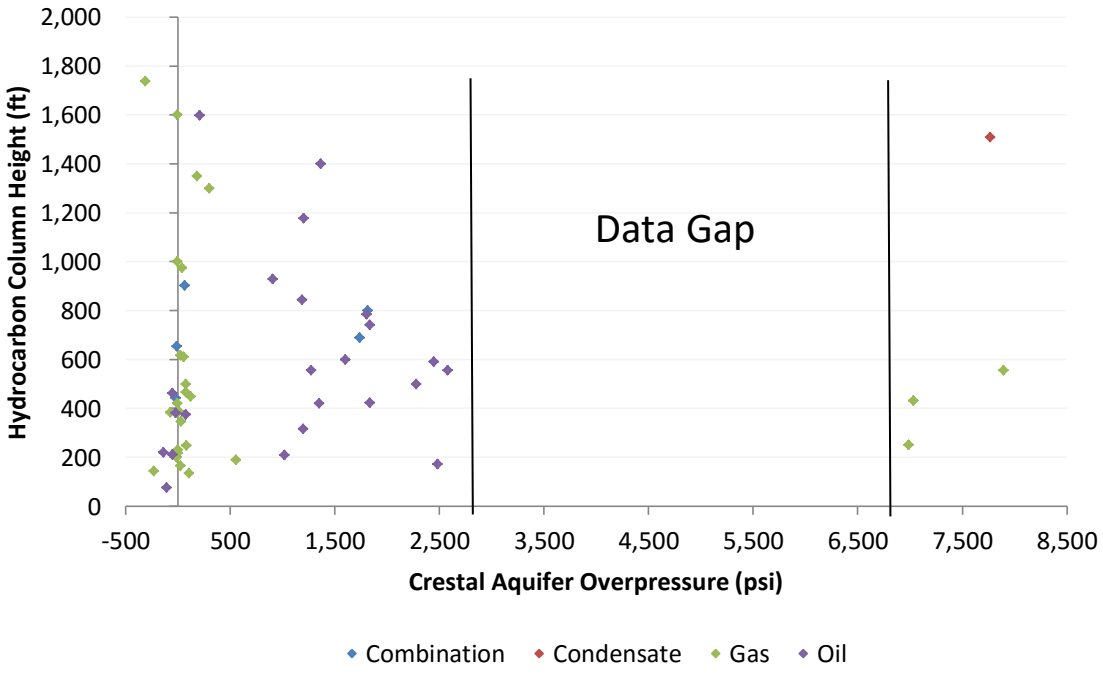

Figure 6.12 – Figure displaying results of only under-filled fields, with column height vs aquifer overpressure. Important to note is the data gap.

the maximum pressure a caprock can tolerate prior to mechanically failing. This transition is further emphasised in Figure 5.14 indicating a transition for fields based above the isotropic stress line to below it. Figure 5.14 also importantly highlights the proximity of fields to their failure envelopes. It is clear that all fields within the dataset lie a considerable distance from both the shear and tensile failure envelopes. The exception to this starts to become apparent with increasing overpressure. The distance between the data point and these envelopes represent the seal capacity and, as shown in Figure 5.21, all fields possess a positive aquifer and formation seal capacity. The Shearwater field is the closest to the failure envelopes and would intersect with the tensile sector. Figure 5.28 indicates that the fault reactivation pressures are less than the P_{frac} or S_v, as such suggesting that re-shearing of existing fractures is the preferred failure mechanism for fields that are not significantly overpressured. This corresponds with Hillis & Nelson (2005) suggesting that tensile failure only really becomes relevant in the highly overpressured Central North Sea fields, fault reactivation is the primary risk elsewhere.

When considering the limitations to hydrocarbon column heights in regards to formation pressure, fields which are known to be full-to–spill should be removed. The hydrocarbon column heights within these fields are limited by structural capacity, not the influences of overpressure. The following summary, therefore, accounts for under-filled and unknown-fill fields only. A process used throughout the data analysis was the application of maximum bound trend lines. These represent the upper limit of the maximum hydrocarbon column heights that can be expected, based on this dataset. A summary of these gradients are indicated in Table 6.1 and in graph formation (Figure 6.13).

Measured Variable (psi)	Aquifer Overpressure	Aquifer Seal Capacity	Aquifer Fault Reactivation Seal Capacity
Maximum Bound Hydrocarbon column Height Gradient (psi/ft)	6.8	2.1	1.56

Table 6.1 – Table showing the maximum bound gradients discerned by all points (with few exceptions) located below the line. This indicates the maximum column height expected based upon the North Sea data.

The use of image 6.13 simply shows that should a pore pressure prediction of a wildcat well within the North Sea indicate an aquifer overpressure of χ by simply tracing to the aquifer overpressure maximum limit line a suggested maximum hydrocarbon column height of γ can be expected. The same process can be applied for those fields with aquifer seal capacities, either using the fault reactivation aquifer seal capacity gradient or the aquifer seal capacity gradient based on whether the prospect is thought to fail under a tensile or shear regime. This is, of course, a very crude application, but is simply an application based on the results from this study. Should a prospect suggest an abnormal column height in regards to seal capacity or overpressure it would be suggested to re-asses pressure and stress regimes and consider, for example, an alternative process like that of a protected trap.

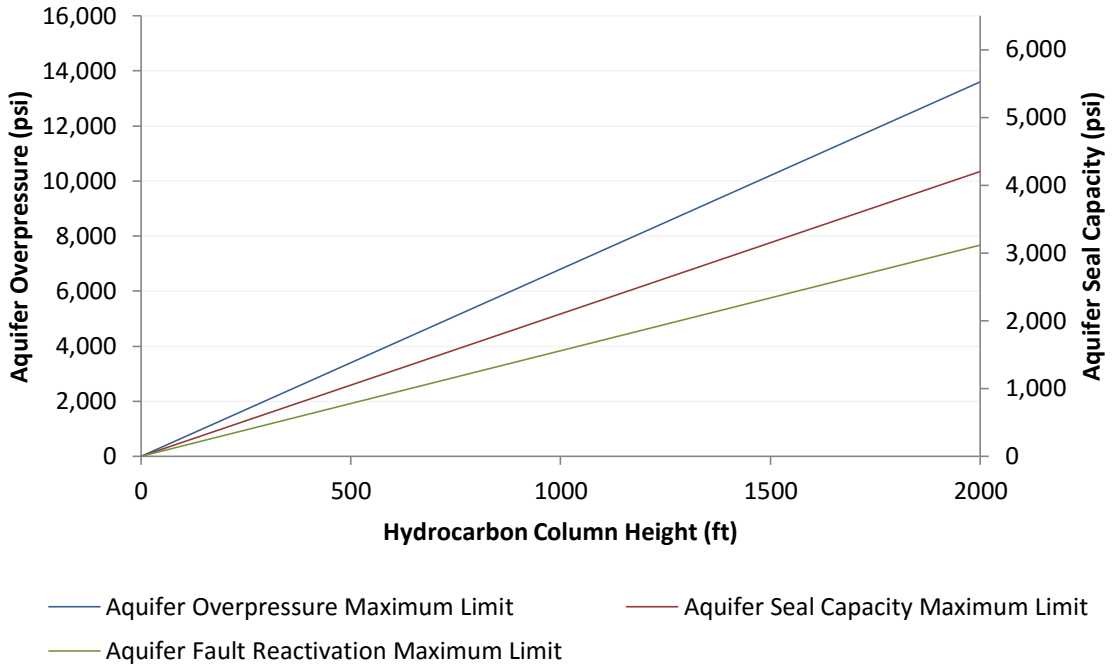

Figure 6.13 – Graph indicating the upper limit lines applied to the data. Aquifer overpressure is displayed on the primary y-axis and seal capacities on the secondary y-axis. Hydrocarbon column height lies along the x. Seal capacities (clearly not comparable to simple overpressure) can be compared and as expected the fault reactivation seal capacity is a lesser gradient than that of aquifer seal capacity.

As discussed within the literature, minimum retention capacities are suggested. The 1000 psi retention capacity is proposed by Gaarenstroom et al. (1993) and since publication others have implied retention/seal capacities of varying value. Although relatable to this analysis it is not directly applicable. Minimum retention/seal capacity analysis is undertaken on a well-by-well basis, importantly, including dry/breached wells within the study. This study's approach focuses purely upon fields, which by definition, possess a hydrocarbon accumulation and as such a hydrocarbon column height. No authors claim that below a certain positive seal capacity the chance of discovery breaches 0. What is claimed is that below a threshold (1000 psi in Gaarenstroom et al, 1993's case) the chances are reduced significantly. It is, therefore, not unsurprising that all the fields within this study possess a positive seal capacity. Furthermore, it does not surprise that the proportion of fields that are highly overpressured are significantly less than those that are low to moderately pressured (figure 6.14). Not only would this result from the fact that highly overpressured formations are a rarer occurrence than hydrostatically/moderately overpressured formations, but also because the risk of caprocks that have mechanically failed leaking

hydrocarbons increases. What can be suggested is that this report possess three hydrocarbon bearing formations with aquifer seal capacities less than 1000 psi in regards to the Central North Sea, Shearwater, Erskine (Erskine reservoir) and Erskine (Pentland reservoir). Little is known about the Erskine fields. Their associated hydrocarbon column heights do not present as being abnormal when compared to that of the remaining data set in Figure 5.22. The Shearwater field does however, and is attributed to the impacts of the protected trap hypothesis (Section 6.1).

Another topic of concern, highlighted in Chapter 4, is the concept that the added buoyancy pressures associated with a hydrocarbon accumulation influence the criteria for a caprock to hydraulically fracture. A concept proposed by Swarbrick et al. (2010). However, also discussed is the level at which the top seal will fail. Time constraints, but primarily the availability of data with this project didn't justify testing aquifer seal capacities at different stratigraphic levels, in particular the base chalk (proposed as the "ultimate seal" horizon by Swarbrick et al., 1993 & Casabianca & Cosgrove, 2012). Within the Swarbrick et al. (1993) database all wells containing hydrocarbons had a positive aquifer seal capacity at top reservoir horizon. This is also comparable to this studies dataset. However, this data set also presents all fields with positive hydrocarbon buoyancy pressures also. It would, therefore, be presumptuous to advocate this hypothesis with a great deal of certainty, but likewise there is no evidence suggesting the contrary. What is noted, however, is that the maximum hydrocarbon buoyancy pressure within this study is the Barque field with 610 psi. This shows that, within the North Sea region, the excess buoyancy pressures are still moderately minimal. Where the impact of aquifer vs formation failure criteria could be relevant is within the Gulf of Mexico mini-basins where column heights have the potential to reach many thousands of feet and the overpressures are already high. Therefore, due to no analysis of seal capacities at varying stratigraphic units, only considering field data and all fields possessing positive hydrocarbon and aquifer seal capacities an evidence based conclusion through this dataset cannot be made.

As stated previously, when considering aquifer and hydrocarbon overpressure both indicate a reduction in column heights associated with increasing aquifer pressures. This is the case when comparing to the whole dataset and to just fields with unknown and under-filled status. Therefore, it is not possible to conclusively accept or reject the study hypothesis, discussed in Section 1.3. It is the opinion of the author of this report that the outright rejection of this hypothesis would be premature as the major limiting factor is the lack of data. There simply is not the volume of openly available, highly overpressured field data obtainable through public sources. What is clear is that as aquifer overpressure increases the volume of fields reduces. Furthermore, this report has highlighted the importance of considering abnormal pressure circumstances like that of protected traps. The trends exposed from this research suggest that the Shearwater field should have a minimal column, if any. Yet a 1500 ft column height prevails, thus emphasising the importance of fully understanding the subsurface pore pressures and importantly the location of where the caprock will fail within a system.

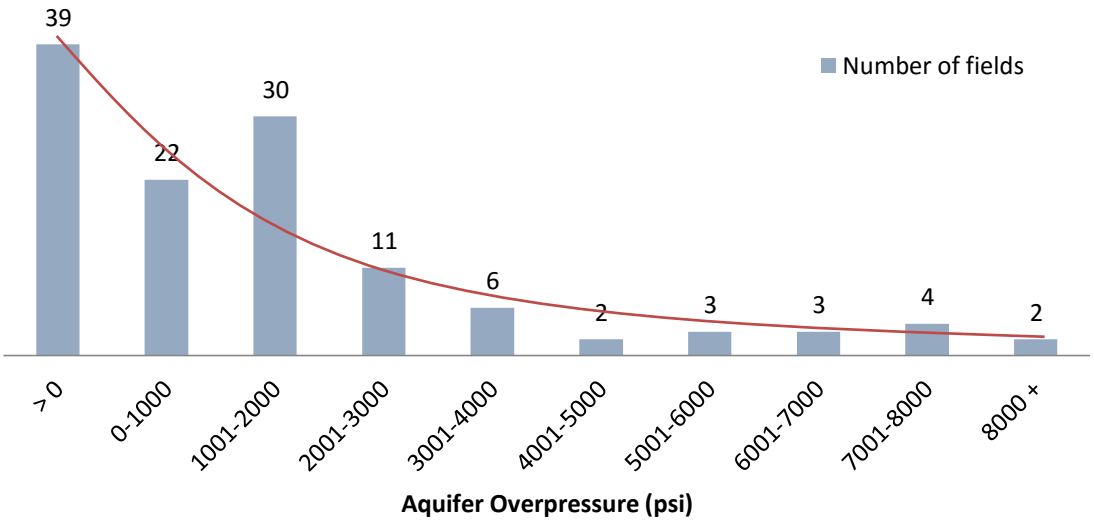

Figure 6.14 – Histogram graph indicating fields within this study by aquifer overpressure range. The numbers clearly decline with increasing aquifer overpressure. The red line is a simple drawn on line highlighting the decline.

Chapter 7

Conclusions

Chapter 7 - Conclusion

The following section concludes the results of this report, both from a literary review point of view and also from a data front. The findings are compared to the key research questions outlined in Chapter 1. Further work suggestions are outlined highlighting areas of additional research that could add validity and understanding to this subject area.

7.1 Conclusions

The following bullet points summarise the key findings from this study:

i. Overpressure is depth dependent and, therefore, what is termed 'significant overpressure' at shallow depth may be comparatively insignificant in deeper formations. The use of seal capacity helps bypass this issue.

ii. Pp/S_h coupling is the expected reason for the P_{frac} being greater than S_v in highly overpressured fields within the North Sea. The point at which the minimum stresses meet is termed "the minimum stress convergence" and switch is termed "the minimum stress transition". At depths below 14,500 ft and 13,000 ft TVDss for the Central and Northern North Sea respectively, the minimum stress switch and S_v is σ_3 and used to determine the seal capacity.

iii. Increasing aquifer overpressure indicates a reduction in the **maximum** column heights within fields in the North Sea.

iv. Decreasing aquifer seal capacity and fault reactivation seal capacity indicates a reduction in **maximum** column heights within fields in the North Sea.

v. All fields within the study have a positive aquifer and hydrocarbon seal capacity as expected considering the presence of an economic hydrocarbon accumulation.

vi. Upper limit gradients based upon maximum column heights expected given a certain aquifer overpressure, aquifer seal capacity and aquifer fault reactivation pressure are suggested for the Central and Northern North Sea.

vii. Shearwater is anomalous relative to the rest of the fields in having a much smaller seal capacity, although having a very long hydrocarbon column

viii. The most likely explanation for Shearwater is that it is a protected trap, whose crest is only a little deeper than the breach point. It is the only field within this dataset likely to be controlled by seal capacity, and most probably limited by fault reactivation.

ix. Cornford (1998) states that the Kimmeridge Clay is a sufficient source to not be a limiting factor in filling a trap. However, this data set shows 48 % of fields with a known fill state[24] are under-filled with only Shearwater indicating a possible control by pressure.

x. The assertion that excess buoyancy pressure does not control hydraulic failure (Swarbrick et al. 2010) is neither accepted nor rejected from this study.

In Chapter 1 three key research questions were posed;

1. **What is already known from previous research regarding the impact of formation overpressure on hydrocarbon column heights, seal capacities and dry hole vs. discovery analysis?**
   - A detailed review of previous work within this field of study is discussed in Section 5.3. All authors use differing techniques to assess a well's propensity to retain hydrocarbons in regards to pressure related seal failure. Since the publication of the Gaarenstroom et al. (1993) paper a quantification of minimum seal/retention capacities is explored. Gaarenstroom et al. (1993) suggested the risk of seal breach in the Central North Sea is significant when seal capacity is < 1000 psi. Swarbrick et al., 2010 suggest 1400 psi, using a dataset from a larger set of fields.
   - Swarbrick et al. 2010 and Casabianca & Cosgrove 2012 suggest that the top reservoir is not in fact the 'ultimate seal' to trap, but somewhere within the seal. Swarbrick et al. (2010) suggest it is the Base Chalk. As such, should

[24] Fields that are known to be under-filled or full-to-spill. Unknown-fill fields are discounted.

retention/seal capacities be measured from this horizon? The time and data limitations within this study unfortunately hindered analysis of this topic, but it is certainly advised as a consideration for future research.

- Maximum overpressure gradients have been discussed by Timko & Fertl (1971) and Leach (1994), however, fracture pressures increases with depth and, although high overpressures indicate a reduction in field densities, it is seal/retention capacity that will be the controlling parameter (Gaarenstroom et al. 1993; Swarbrick et al. 2010).
- Winefield et al. (2005) discusses briefly how the Shearwater field's condensate column may be limited by its fracture pressure but the validity of this assumption may be questioned.

2. **Does seal capacity/overpressure control or limit hydrocarbon column height within the dataset?**
    - A common pattern throughout all analysis undertaken with the data from this study is a reduction in column height with a) increasing aquifer overpressure, b) reducing aquifer seal capacity and c) decreasing fault reactivation seal capacity. As a result, maximum bound gradients have been applied indicating the largest hydrocarbon column height expected within the North Sea (indicated in Table 6.1 and Figure 6.13).
    - A clear exception to the trends described above is the Shearwater field. This field holds a 1500 ft condensate column yet a very small aquifer seal capacity (542 psi). It is suggested that two phenomena are influencing this field. Firstly, the presence of a significant hydrocarbon column despite very low aquifer seal capacities is attributed to the presence of a protected trap and a pressure valve at a shallower (blown) closure named Martha (drilled and found to be dry). Secondly, this field is under-filled and this is accredited to fault reactivation. Palaeo-faults and fractures already causing a palaeo-column to leak from the closure (and empty the trap) have reactivated due to high formation/aquifer pressure (implied from minimal/negative fault reactivation seal capacities).

- All fields (and, therefore, hydrocarbon bearing structures) within this study possessed positive aquifer/hydrocarbon seal capacities.

3. **What are controls on hydrocarbon retention and hydrocarbon column height within the study region?**
   - The main categories and controls on hydrocarbon column height are presented in Section 3.1. From the results of this study the main limitations on hydrocarbon column height are not associated with pore pressure. All fields possess positive hydrocarbon/aquifer seal capacities, and their column heights will be limited by another factor. Within the North Sea we see that a major controlling factor is the structural closure/relief of the trap. Within the North Sea dataset 40 % of the field are known to be full-to-spill, 41 % are thought to be under-filled and 19 % have unknown fill. Out of the 41 % known to be under-filled the Shearwater field was the only field where the data indicate a possible control by pressure (deduced by minimal seal capacities). This field is assumed to be limited by formation/aquifer pressures reactivating pre-existing faults in the caprock.
   - Despite the remaining under-filled fields indicating positive aquifer seal capacities at the field crest, previous literature by Swarbrick et al. (2010) and Casabianca & Cosgrove (2012) suggests that seal capacity calculations within the Central North Sea should be taken at the 'ultimate seal' i.e. somewhere in the seal above Top Reservoir. Extrapolating aquifer/hydrocarbon gradients to this 'ultimate seal' depth may indicate aquifer pressures as more of a limiting factor. For example, an under-filled field may indicate a positive aquifer/hydrocarbon seal capacity at top reservoir, but by extrapolating the corresponding gradient to the base chalk the hydrocarbon/aquifer seal capacity may reduce to zero.
   - Research into previous literature also highlighted the varying controls on hydrocarbon leakage by region. Nordgård Bolås et al. (2005) show how changeable stress regimes will have a different impact on hydrocarbon leakage. The presence of a glacial edge overlying certain prospects within the

Haltenbanken region increases differential stress leading to shear failure.. This regime is shown not to have been present within the North Sea, but highlights the importance of assessing not only regional but local area breakdowns.

- Fields not filled-to-spill is noteworthy, and counter intuitive as the Kimmeridge Clay is thought to be an ample source of hydrocarbon volumes, enough to fill closures (Cornford 1998). It is, of course, possible that variation in stress through geological time since first filling may have been induced hydraulic failure and hydrocarbon leakage, and that the under filled traps we see at present are in the process of being refilled.

Many results from this study are inconclusive but various different methods and concepts have been collaborated and reviewed providing a suitable foothold for further research to be undertaken. The original hypothesis, discussed in Section 1.3, can neither be accepted nor rejected, as put simply; the limitations with time and availability of data are too great. With the suggestions for future work outlined below additional research could be undertaken increasing the validity, and importantly the understanding of this much misunderstood field of petroleum geology.

7.2 Further Work

The main limitations of this study are associated simply with the time constraints and limited availability of data. As such, the following section suggests further work to help follow this study's research and add further validity and conclusions to the results.

1. **Dry hole/non-economical discovery analysis –** This study has solely involved the use of hydrocarbon fields. However, what has become evident is that wells which comprise a palaeo-presence of hydrocarbons (either through fluid inclusion analysis or hydrocarbon pore staining) are of great interest. The history of why these traps no longer contain a column is interesting in itself regarding the story of breach. From an industry point of view it is also

imperative in finding 'secondary accumulations' present purely from breached seal related migration. It is suggested that a full analysis be undertaken in the Shearwater HPHT region where pressures are known to be equal to that of the fracture pressure, hydrofracturing has occurred and subsequent leakage of hydrocarbons are inferred from inclusion and quartz grain staining analysis (Winefield et al. 2005).

2. **Research into failure pressure algorithm method –** The need to examine uncertainty in the estimation of fracture pressures. One of those lines of investigation would be to capture the range of LOTs at all depth and see if it is possible to establish what the controls are. Another would be to compare the Swarbrick et al (2010) fracture gradient algorithm with other published methods to estimate Pfrac and assess the range that way too.

3. **Aquifer v's Hydrocarbon Pressures** – Throughout this report there has been uncertainty into the criteria used to define the seal capacity. The majority of authors (Gaarenstroom et al. 1993; Holm 1998; Converse et al. 2000; Winefield et al. 2005) agree with the statement that 'when formation pressures equal that of the fracture pressure a caprock with hydraulically fracture'. However, as discussed in Section 3.6, there is controversy around this hypothesis. Swarbrick et al. (2010) building on physical constraints established by Bjorkum et al. (1998), suggest that in fact aquifer pressures are the controlling parameter. It is proposed that work could be undertaken in the Gulf of Mexico (GOM) Plio-Miocene mini-basins. The purpose of this captures 2 points. Firstly, the structural relief of the North Sea closures, as stated previously, is not sufficient to reduce seal capacities to low numbers. Within the GOM mini-basins the structural nature of the closures permits thousands of feet worth of potential hydrocarbons, unlike the North Sea where closures are very limited. Secondly, high reservoir pressures are known to encroach upon the fracture pressure (Seldon & Flemings 2005). Ideally, an example where aquifer pressure is less than the fracture pressure, and formation pressure is greater would start to add

further validity to the Swarbrick et al. (2010) approach (see Figure 7.1). Lab simulations could also be undertaken to assess the strength of this hypothesis. Furthermore, the Plio-Miocene mini-basins in the GOM may be a more suitable location to test the relationship between hydrocarbon column height and seal capacity as many more long columns are expected since the structural relief of closures can be immense.

4. **Analysis into the Ultimate Seal** – Again, a recent concept discussed by Swarbrick et al. (2010) and Casabianca & Cosgrove (2012) and highlighted in Section 3.5.5, suggests controversy amongst the 'ultimate seal' depth. Both authors suggest the ultimate seal is somewhat shallower than the base seal/top reservoir marker for the Jurassic/Triassic reservoirs within the Central North Sea and may b e as shallow as Base Chalk. This therefore, means that seal capacity analysis should be taken at shallower markers and not just top reservoir.

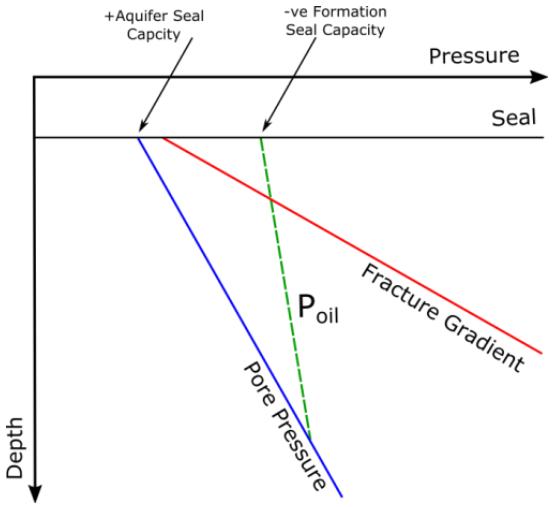

Figure 7.1 - Schematic indicating a HC bearing field possessing a positive aquifer seal capacity and negative hydrocarbon seal capacity. This could be suggested as evidence towards the Swarbrick et al. (2010) approach.

Chapter 8

References

Chapter 8 – References

Alberts, M.A., Underhill, J.R. & Spencer, A.M. (editor), 1991. The effect of Tertiary structuration on Permian gas prospectivity, Cleaver Bank area, southern North Sea, UK. *Special Publication of the European Association of Petroleum Geoscientists*, 1, pp.161–173.

Aplin, A.C. & Larter, S.R., 2005. Fluid Flow, Pore Pressure, Wettability, and Leakage in Mudstone Cap Rocks. *American Association of Petroleum Geologists Special Bulletin American Association of Petroleum Geologists Hedberg Series*, 2(2), pp.1–12.

Bachu, S. & Underschultz, J.R., 1995. Large-scale underpressuring in the Mississippian-Cretaceous succession, southwestern Alberta Basin. *American Association of Petroleum Geologists Bulletin*, 79(7), pp.989–1004.

van den Bark, E. & Thomas, O., 1981. Ekofisk: First of the Giant Oil Fields in Western Europe. *American Association of Petroleum Geologists Bulletin*, 65(11), pp.2341–2363.

Barker, C., 1972. Aquathermal Pressuring-Role of Temperature in Development of Abnormal-Pressure Zones. *AAPG Bulletin*, 56(10), pp.2068–2071.

Barker, C., 1990. Calculated Volume and Pressure Change During Oil Cracking.Pdf. *AAPG bulletin*, 74(8), pp.1254–1261.

Berg, R.R., 1975. Capillary Pressures in Stratigraphic Traps. *AAPG Bulletin*, 59(6), pp.939–956.

Bjørkum, P.A., Walderhaug, O. & Nadeau, P.H., 1998. Physical constraints on hydrocarbon leakage and trapping revisited. *Petroleum Geoscience*, 4(3), pp.237–239.

Bjørlykke, K., 2006. Effects of compaction processes on stresses, faults, and fluid flow in sedimentary basins: examples from the Norwegian margin. *Geological Society, London, Special Publications*.

Boles, J.R. & Franks, S.G., 1979. Clay Diagenesis in Wilcox Sandstones of Southwest Texas--Implications of Smectite-Illite Reaction for Sandstone Cementation. *AAPG Bulletin*, 62(1), pp.55–70.

Bond, K, J., 2001. *Mudstone cap rocks as vertical migration pathways: Case studies from the Norwegian sector of the North Sea*. University of Newcastle upon Tyne.

Boullier, A.M. & Robert, F., 1992. Palaeoseismic events recorded in Archaean gold-quartz vein networks, Val d'Or, Abitibi, Quebec, Canada. *Journal of Structural Geology*, 14(2), pp.161–179.

Bowers, G., 1995. Pore Pressure Estimation From Velocity Data: Accounting for Overpressure Mechanisms Besides Undercompaction (SPE 27488). *SPE Drilling & Completion*, 10(2), pp.89–95.

Bradley, J.S., 1975. Abnormal Formation Pressures. *Aapg Bulletin-American Association of Petroleum Geologists*, 59(6), pp.957–973.

Bradley, J.S. & Powley, D.E., 1994. General Considerations Pressure Compartments in Sedimentary Basins: A Review. *Basin Compartments and Seals*, pp.3–26.

Breckels, I.M. & van Eekelen, H. a. M., 1982. Relationship Between Horizontal Stress and Depth in Sedimentary Basins. *Journal of Petroleum Technology*, 34(September), pp.2191–2199.

Buhrig, C., 1989. Geopressured Jurassic reservoirs in the Viking Graben: modelling and geological significance. *Marine and Petroleum Geology*, 6(1), pp.31–48.

Caillet, G., 1993. The caprock of the Snorre Field, Norway: a possible leakage by hydraulic fracturing. *Marine and Petroleum Geology*, 10(1), pp.42–50.

Capuano, R.M., 1993. Evidence of Fluid-Flow in Microfractures in Geopressured Shales. *Aapg Bulletin-American Association of Petroleum Geologists*, 77(8), pp.1303–1314.

Cartwright, J., Huuse, M. & Aplin, A.C., 2007. Seal bypass systems. *AAPG Bulletin*, 91(8), pp.1141–1166.

Casabianca, D. & Cosgrove, J., 2012. A new method for top seals predictions in high-pressure hydrocarbon plays. *Petroleum Geoscience*, 18(1), pp.43–57.

Chadwick, R.A., Kirby, G.A. & Baily, H.E., 1994. The post-Triassic structural evolution of north-west England and adjacent parts of the East Irish Sea. *Proceedings of the Yorkshire Geological and Polytechnic Society*, 50(1), pp.91–102.

Chapman, R.E., 1980. Mechanical versus thermal cause of abnormally high pore pressures in shales. *American Association of Petroleum Geologists Bulletin*, 64(12), pp.2179–2183.

Chen, W. et al., 1990. Diagenesis through coupled processes: modeling approach, self-organization, and implications for exploration. *Prediction of Reservoir Quality through Chemical Modeling*, pp.103–130.

Clayton, C.J. & Hay, S.J., 1994. Gas migration mechanisms from accumulation to surface. *Bulletin of the Geological Society of Denmark*, 41(1), pp.12–23.

Converse, D.R. et al., 2000. Controls on Overpressure in Rapidly Subsiding Basins and Implications for Failure of Top Seal. *Petroleum systems of South Atlantic margins,: AAPG Memoirs 73*, pp.133–150.

Cornford, C., 1994. Mandal-Ekofisk(!) Petroleum System in the Central Graben of the North Sea: Chapter 33: Part VI. Case Studies--Eastern Hemisphere. , 77, pp.537–571.

Cornford, C., 1998. Source Rocks and Hydrocarbons of the North Sea. In *Petroleum Geology of the North Sea*. pp. 376–462.

Cox, S.F., 1995. Faulting Processes at High Fluid Pressures - an Example of Fault Valve Behavior from the Wattle Gully Fault, Victoria, Australia. *Journal of Geophysical Research-Solid Earth*, 100(B7), pp.12841–12859.

Daines, S.R., 1982. Prediction of Fracture Pressures for Wildcat Wells. *Journal of Petroleum Technology*, 34(04), pp.863–872.

Darby, D. & Funnell, R.H., 2001. Overpressure associated with a convergent plate margin: East Coast Basin, New Zealand. *Petroleum Geoscience*, 7(3), pp.291–299.

Darby, D., Haszeldine, R.S. & Couples, G.D., 1996. Pressure cells and pressure seals in the UK Central Graben. *Marine and Petroleum Geology*, 13(8), pp.865–878.

Davies, R.J. et al., 2007. Birth of a mud volcano: East Java, 29 May 2006. *GSA Today*, 17(2), pp.4–9.

Davies, R.J. et al., 2006. Giant clastic intrusions primed by silica diagenesis. *Geology*, 34(11), pp.917–920.

Davies, R.J. et al., 2008. The East Java mud volcano (2006 to present): An earthquake or drilling trigger? *Earth and Planetary Science Letters*, 272(3-4), pp.627–638.

Deming, D., 1994. Factors necessary to define a pressure seal. *AAPG Bulletin*, 78(6), pp.1005–1010.

Deming, D., Cranganu, C. & Lee, Y., 2002. Self-sealing in sedimentary basins. *Journal of Geophysical Research*, 107(B12), p.2329.

Dewhurst, D.N. & Jones, R.M., 2002. Geomechanical, microstructural, and petrophysical evolution in experimentally reactivated cataclasites: Applications to fault seal prediction. *AAPG Bulletin*, 86(8), pp.1383–1405.

Dickey, P.A., 1976. Abnormal Formation Pressure: DISCUSSION. *AAPG Bulletin*, 60(7), pp.1124–1128.

Dickinson, G., 1953. Geological Aspects of Abnormal Reservoir Pressures in Gulf Coast Louisiana. *AAPG Bulletin*, 37(2), pp.410–432.

Drinkwater, N.J., Pickering, K.T. & Siedlecka, A., 1996. Deep-water fault-controlled sedimentation, Arctic Norway and Russia: Response to Late Proterozoic rifting and the opening of the Iapetus Ocean. *Journal of the Geological Society of London*, 153, pp.427–436.

Eaton, B., 1969. Fracture Gradient Prediction and Its Application in Oilfield Operations. *Journal of Petroleum Technology*, 21(10).

England, W. a. et al., 1987. The movement and entrapment of petroleum fluids in the subsurface. *Journal of the Geological Society*, 144(2), pp.327–347.

Erratt, D. et al., 2005. Exploration history of the high-pressure, high-temperature plays: UK Central North Sea. *Petroleum Geology: North-West Europe and Global Perspectives - Proceedings of the 6th Petroleum Geology Conference*, pp.253–267.

Erratt, D. et al., 2010. North Sea hydrocarbon systems: some aspects of our evolving insights into a classic hydrocarbon province. *Petroleum Geology Conference Series*, 7, pp.37–56.

Erratt, D., Thomas, G.M. & Wall, G.R.T., 1999. The evolution of the Central North Sea Rift. , pp.63–82.

Evans, D. et al., 2003. *Millennium Atlas: Petroleum Geology of the Central & Northern North Sea*, London: The Geological Society of London.

Evans, D., 2003. The Millennium Atlas: Petroleum geology of the central and northern North Sea. *The Geological Society of London.*

Fisher, A.T., Zwart, G. & Ocean Drilling Program Leg 156 Scientific Party, 1996. Relation between permeability and effective stress along a plate-boundary fault, Barbados accretionary complex. *Geology*, 24(4), pp.307–310.

Gaarenstroom, L. et al., 1993. Overpressures in the Central North Sea: implications for trap integrity and drilling safety. *Petroleum Geology of Northwest Europe: Proceedings of the 4th Conference on Petroleum Geology of NW. Europe, at the Barbican Centre, London*, 2(1990), pp.1305–1313.

Gilham, R. & Hercus, C., 2005. *Shearwater (UK Block 22/30b): managing changing uncertainties through field life*, Geological Society of London.

Glennie, K.W., 1998. *Petroleum geology of the North Sea: basic concepts and recent advances / edited by K.W. Glennie* 4th ed., Oxford: Blackwell Science Ltd.

Gluyas, J.G. & Hichens, H.M., 2003. *United Kingdom oil and gas fields. Commemorative millennium volume* J. G. Gluyas & H. M. Hitchens, eds., Geological Society of London.

Goff, J.C., 1983. Hydrocarbon generation and migration from Jurassic source rocks in the E Shetland Basin and Viking Graben of the northern North Sea. *Journal of the Geological Society*, 140(3), pp.445–474.

Gudmundsson, A., 2011. *Rock Fracture in Geological Processes* First., New York: Cambridge University Press.

Habicht, J.K.A., 1979. *Paleoclimate, paleomagnetism, and continental drift*, Tulsa, Oklahoma: The American Association of Petroleum Geologists.

Hansom, J. & Lee, M.-K., 2005. Effects of hydrocarbon generation, basal heat flow and sediment compaction on overpressure development: a numerical study. *Petroleum Geoscience*, 11(4), pp.353–360.

Harris, A.L. et al., 1994. The Dalradian Supergroup in Scotland, Shetland and Ireland. In *A revised corrolation of Precambrian rocks in the British Isles. Geological Society, London Special Reports*. London: Geological Society of London, p. 21.

Helgeson, D.E., 1999. Structural development and trap formation in the Central North Sea HP/HY play. *Petroleum Geology of Northwest Europe: Proceedings of the 5th Conference on the Petroleum Geology of Northwest Europe*, 2, pp.1029–1036.

Henning, A. et al., 2002. Pore-Pressure Estimation in an Active Thrust Region and Its Impact on Exploration and Drilling. *Pressure regimes in sedimentary basins and their prediction: AAPG Memoir 76*, pp.89–105.

Hermanrud, C. et al., 2014. Petroleum column-height controls in the western Hammerfest Basin, Barents Sea. *Petroleum Geoscience*, 20(3), pp.227–240.

Hermanrud, C. & Nordgård Bolås, H.M., 2002. Leakage from overpressured hydrocarbon reservoirs at Haltenbanken and in the northern North Sea. *Norwegian Petroleum Society Special Publications*, 11, pp.221–231.

Hillis, R.R., 2001. Coupled changes in pore pressure and stress in oil fields and sedimentary basins. *Petroleum Geoscience*, 7(4), pp.419–425.

Hillis, R.R., 2003. Pore pressure/stress coupling and its implications for rock failure. *Geological Society, London, Special Publications*, 216(1), pp.359–368.

Hillis, R.R. & Nelson, E.J., 2005. In situ stresses in the North Sea and theirapplications: petroleum geomechanics from exploration to development. *Petroleum Geology: North-West Europe and Global Perspectives - Proceedings of the 6th Petroleum Geology Conference*, pp.551–566.

Hodgson, N. a., Farnsworth, J. & Fraser, a. J., 1992. Salt-related tectonics, sedimentation and hydrocarbon plays in the Central Graben, North Sea, UKCS. *Geological Society, London, Special Publications*, 67(1), pp.31–63.

Holm, G.M., 1998. Distribution and origin of overpressure in the Central Graben of the North Sea. *Abnormal pressures in hydrocarbon environments*, 70, pp.123–144.

Hunt, J.M., 1990. Generation and migration of petroleum from abnormally pressured fluid compartments. *American Association of Petroleum Geologists Bulletin*, 74(1), pp.1–12.

Ingram, G.M. & Urai, J.L., 1999. Top-seal leakage through faults and fractures: the role of mudrock properties. *Geological Society, London, Special Publications*, 158(1), pp.125–135.

Ingram, G.M., Urai, J.L. & Naylor, M.A., 1997. Sealing processes and top seal assessment. *Norwegian Petroleum Society Special Publications*, 7(C), pp.165–174.

Iverson, W.P., Martinsen, R.S. & Surdam, R.C., 1994. Pressure Seal Permeability and Two-Phase Flow. In P. J. Ortoleva, ed. *Basin Compartments and Seals*. AAPGMemoir 61, pp. 313–319.

Jaeger, J., Cook, N.G. & Zimmerman, R., 2007. *Fundamentals of Rock Mechanics, 4th Edition*,

Jennings, J.B., 1987. Capillary Pressure Techniques: Application To Exploration and Development Geology. *American Association of Petroleum Geologists Bulletin*, 71(10), pp.1196–1209.

Jones, G. et al., 1999. Tectonostratigraphic development of the southern part of UKCS Quadrant 15 (eastern Witch Ground Graben): implications for the Mesozoic-Tertiary evolution of the Central North Sea Basin. *Petroleum Geology of Northwest Europe: Proceedings of the 5th Conference on the Petroleum Geology of Northwest Europe*, 1, pp.133–152.

Jowett, E.C., Cathles, L.M. & Davis, B.W., 1993. Predicting depths of gypsum dehydration in evaporitic sedimentary basins. *American Association of Petroleum Geologists Bulletin*, 77(3), pp.402–413.

Kerrich, R., 1986. Fluid infiltration into fault zones: Chemical, isotopic, and mechanical effects. *Pure and Applied Geophysics*, 124(1-2), pp.225–268.

King Hubbert, M. & Rubey, W.W., 1959. Role of fluid pressure in mechanics of overthrust faulting: I. Mechanics of fluid-filled porous solids and its application to overthrust faulting. *Bulletin of the Geological Society of America*, 70(2), pp.115–166.

Lahann, R., 2002. Impact of Smectite Diagenesis on Compaction Modeling and Compaction Equilibrium. *AAPG Memoir 76: Pressure Regimes in Sedimentary Basins and Their Prediction*, (2), pp.61–72.

Lahann, R.W. & Swarbrick, R.E., 2011. Overpressure generation by load transfer following shale framework weakening due to smectite diagenesis. *Geofluids*, 11(4), pp.362–375.

Law, B.E. & Dickinson, W.W., 1985. Conceptual Model for Origin of Abnormally Pressured Gas Accumulations in Low-Permeability Reservoirs. *American Association of Petroleum Geologists Bulletin*, 69(8), pp.1295–1304.

Leach, W., 1994. Distribution of hydrocarbons in abnormal pressure in south Louisiana, USA. *Developments in Petroleum Science*.

Lee, Y. & Deming, D., 2002. Overpressures in the Anadarko basin, southwestern Oklahoma: Static or dynamic? *American Association of Petroleum Geologists Bulletin*, 86(1), pp.145–160.

Leith, T.L. & Fallick, a E., 1997. Organic Geochemistry of Cap-Rock Hydrocarbons, Snorre Field, Norwegian North Sea. *Seals, Traps, and the Petroleum System*, (67), pp.115–134.

Leonard, R.C., 1993. *Distribution of sub-surface pressure in Norwegian Central Graben and applications for exploration*, Geological Society of London.

Luo, X. & Vasseur, G., 1997. Sealing efficiency of shales. *Terra Nova*, 9(2), pp.71–74.

Mallon, A.. & Swarbrick, R.., 2002. A compaction trend for non-reservoir North Sea Chalk. *Marine and Petroleum Geology*, 19(5), pp.527–539.

Mathias, S.A. et al., 2009. Screening and selection of sites for CO2 sequestration based on pressure buildup. *International Journal of Greenhouse Gas Control*, 3(5), pp.577–585.

Matthews, W.R. & Kelly, J., 1967. How to predict formation pressure and fracture gradient. *The Oil and Gas Journal*, 65(8), pp.92–106.

Momper, J.A., 1978. *Oil Migration limitations suggested by geological and geochemical considerations*,

Morgans-Bell, H.S. et al., 2001. Integrated stratigraphy of the Kimmeridge Clay Formation (Upper Jurassic) based on exposures and boreholes in south Dorset, UK. *Geological Magazine*, 138(05), pp.511–539.

Morris, A.P. et al., 2012. Production-induced fault compartmentalization at Elk Hills field, California. *AAPG Bulletin*, 96(6), pp.1001–1015.

Mouchet, J.-P. & Mitchell, A., 1989. *Abnormal Pressures While Drilling: Origins, Prediction, Detection, Evaluation*,

Muggeridge, A. et al., 2005. The rate of pressure dissipation from abnormally pressured compartments. *AAPG Bulletin*, 89(1), pp.61–80.

Neuzil, C.E., 1995. Abnormal pressures as hydrodynamic phenomena. *American Journal of Science*, 295, pp.742–786.

Neuzil, C.E., 2000. Osmotic generation of "anomalous" fluid pressures in geological environments. *Nature*, 403(6766), pp.182–4.

Nordgard Bolas, H.M. et al., 2003. Hydrocarbon leakage processes and trap retention capacities offshore Norway. *Petroleum Geoscience*, 9(4), pp.321–332.

Nordgård Bolås, H.M. & Hermanrud, C., 2003. Hydrocarbon leakage processes and trap retention capacities offshore Norway. *Petroleum Geoscience*, 9(4), pp.321–332.

Nordgård Bolås, H.M., Hermanrud, C. & Teige, G.M.G., 2005. The Influence of Stress Regimes on Hydrocarbon Leakage. *AAPG Special Volumes*, AAPG Hedbe, pp.109–123.

O'Connor, S. a. & Swarbrick, R.E., 2008. Pressure regression, fluid drainage and a hydrodynamically controlled fluid contact in the North Sea, Lower Cretaceous, Britannia Sandstone Formation. *Petroleum Geoscience*, 14, pp.115–126.

Ortoleva, P.J., 1994. Basin compartmentation: definitions and Mechanisms. *Journal of Petrology*, 25, pp.39–51.

Osborne, M.J. & Swarbrick, R.E., 1999. Diagenesis in North Sea HPHT clastic reservoirs-consequences for porosity and overpressure prediction. *Marine and Petroleum Geology*, 16(4), pp.337–353.

Osborne, M.J. & Swarbrick, R.E., 1997. Mechanisms for generating overpressure in sedimentary basins: a reevaluation. *American Association of Petroleum Geologists Bulletin*, 81(6), pp.1023–1041.

Osborne, M.J. & Swarbrick, R.E., 1998. Mechanisms for generating overpressure in sedimentary basins: a reevaluation: reply. *American Association of Petroleum Geologists Bulletin*, 82(12), pp.2270–2271.

Parnell, J., 1982. Genesis of the graphite deposit at Seathwaite in Borrowdale, Cumbria. *Geological Magazine*, 119(5), pp.511–512.

Pegrum, R.M. & Spencer, a. M., 1990. Hydrocarbon plays in the northern North Sea. *Geological Society, London, Special Publications*, 50(1), pp.441–470.

Peters, K.E. et al., 1989. Origin of Beatrice oil by co-sourcing from Devonian and Middle Jurassic source rocks, Inner Moray Firth, United Kingdom. *American Association of Petroleum Geologists Bulletin*, 73(4), pp.454–471.

Powley, D., 1990. Pressures and hydrogeology in petroleum basins. *Earth-Science Reviews*, 29(1-4), pp.215–226.

Price, N.J. & Cosgrove, J.W., 1990. *Analysis of geological structures*, Cambridge University Press.

Rattey, R.P. & Hayward, A.B., 1993. Sequence stratigraphy of a failed rift system: the Middle Jurassic to Early Cretaceous basin evolution of the Central and Northern North Sea. *Petroleum Geology of Northwest Europe: Proceedings of the 4th Conference on Petroleum Geology of NW. Europe, at the Barbican Centre, London*, 1, pp.215–249.

Robert, F. & Brown, A.C., 1986. Archean gold-bearing quartz veins at the Sigma Mine, Abitibi greenstone belt, Quebec; Part I, Geologic relations and formation of the vein system. *Economic Geology*, 81(3), pp.578–592.

Roberts, A.M. et al., 1993. Mesozoic Extension in the North-Sea - Constraints From Flexural Backstripping, Forward Modeling and Fault Populations. *Petroleum Geology of Northwest Europe: Proceedings of the 4th Conference*, pp.1123–1136.

Roberts, S.J. & Nunn, J. a., 1995. Episodic fluid expulsion from geopressured sediments. *Marine and Petroleum Geology*, 12(2), pp.195–204.

Schowalter, T., 1979. Mechanics of Secondary Hydrocarbon Migration and Entrapment. *AAPG Bulletin*, 63(0149), pp.723–760.

Secor, D.T., 1965. Role of fluid pressure in jointing. *American Journal of Science*, 263(8), pp.633–646.

Seldon, B. & Flemings, P.B., 2005. Reservoir pressure and seafloor venting: Predicting trap integrity in a Gulf of Mexico deepwater turbidite minibasin. *AAPG Bulletin*, 89(2), pp.193–209.

Sibson, R.H., 1994. Crustal stress, faulting and fluid flow. *Geological Society, London, Special Publications*, 78(1), pp.69–84.

Smith, R.I., Hodgson, N. & Fulton, M., 1993. Salt control on Triassic reservoir distribution, UKCS Central North Sea. *Petroleum Geology of Northwest Europe: Proceedings of the 4th Conference*, 4, pp.547–557.

Soper, N.J. & Anderton, R., 1984. Did the Dalradian slides originate as extensional faults? *Nature*, 307, pp.357–360.

Spencer, C.W., 1987. Hydrocarbon Generation as a Mechanism for Overpressuring in Rocky Mountain Region. *AAPG Bulletin*, 71(4), pp.368–388.

Stainforth, J.G., 1984. Gippsland hydrocarbons - a perspective from the basin edge. *Australian Petroleum Exploration Association Journal*, 24, pp.91–100.

Streit, J.E., 1997. Low frictional strength of upper crustal faults: A model. *Journal of Geophysical Research-Solid Earth*, 102(B11), pp.24619–24626.

Streit, J.E. & Cox, S.F., 2001. Fluid pressures at hypocenters of moderate to large earthquakes. *Journal of Geophysical Research-Solid Earth*, 106(B2), pp.2235–2243.

Streit, J.E. & Hillis, R.R., 2004. Estimating fault stability and sustainable fluid pressures for underground storage of CO2 in porous rock. *Energy*, 29(9-10), pp.1445–1456.

Streit, J.E., Siggins, A.F. & Evans, B.J., 2005. Predicting and Monitoring Geomechanical Effects of CO2 Injection. *Carbon Dioxide Capture for Storage in Deep Geologic Formations*, 2, p.752.

Svare, E., 1995. *Relations between Rock Stresses and Pore Pressure on the Norwegian Margin, 62-67 north - a study based on leak-off tests and formation pressure*. Norwegian Technical University, Trondheim.

Swarbrick, R.E. et al., 2000. Integrated study of the Judy Field (Block 30/7a) - an overpressured Central North Sea oil/gas field. *Marine and Petroleum Geology*, 17(9), pp.993–1010.

Swarbrick, R.E. et al., 2010. Role of the Chalk in development of deep overpressure in the Central North Sea. *Petroleum Geology Conference series*, 7, pp.493–507.

Swarbrick, R.E. & Osborne, M.J., 1998. Mechanisms that generate abnormal pressures: an overview. *Abnormal Pressures in Hydrocarbon Environments: AAPG Memoir 70*, pp.13–34.

Swarbrick, R.E., Osborne, M.J. & Yardley, G.S., 2002. Comparison of Overpressure Magnitude Resulting from the Main Generating Mechanisms. *AAPG Memoirs*, 76, pp.1–12.

Swarbrick, R.E., Seldon, B. & Mallon, A.J., 2005. Modelling the Central North Sea pressure history. In *Petroleum Geology Conference Series*. pp. 1237–1245.

Teige, G.M.G. et al., 2002. Evaluation of caprock integrity in the western (high-pressured) haltenbanken area - a case history based on analyses of seismic signatures in overburden rocks. *Norwegian Petroleum Society Special Publications*, 11(C), pp.233–242.

Terzaghi, K., 1943. *Theoretical soil mechanics*, Hoboken, NJ, USA: John Wiley & Sons, Inc.

Thomsen, E., Lindgreen, H. & Wrang, P., 1983. Investigation on the source rock potential of Denmark. In *Geologie en Mijnbouw*. pp. 221–239.

Timko, D.J. & Fertl, W.H., 1971. Relationship Between Hydrocarbon Accumulation and Geopressure and Its Economic Significance. *Journal of Petroleum Technology*, 23(8), pp.923–933.

Tingay, M. et al., 2008. Triggering of the Lusi mud eruption: Earthquake versus drilling initiation. *Geology*, 36(8), pp.639–642.

Tingay, M.R.P. et al., 2009. Origin of overpressure and pore-pressure prediction in the Baram province, Brunei. *AAPG Bulletin*, 93(1), pp.51–74.

Tissot, B.P., Pelet, R. & Ungerer, P.H., 1987. Thermal History of Sedimentary Basins , Maturation Indices , and Kinetics of Oil and Gas Generation ^ Oil field Gas field. *AAPG Bulletin*, 12(12), pp.1445–1466.

Underhill, J.R. & Partington, M. a, 1993. Jurassic thermal doming and deflation in the North Sea: implications of the sequence stratigraphic evidence. *Petroleum Geology of Northwest Europe: Proceedings of the 4th Conference on Petroleum Geology of NW. Europe, at the Barbican Centre, London*, 1, pp.337–345.

Ungerer, P., Behar, E. & Discamps, D., 1983. Tentative calculation of the overall volume expansion of organic matter during hydrocarbon genesis from geochemistry data. Implications for primary. *Advances in organic geochemistry*, 10, pp.129–135.

Vella, M. et al., 1992. The Nuts and Bolts of Well Testing. *Oil Field Review*, pp.14–27.

Ward, C.D., Coghill, K. & Broussard, M.D., 1994. The Application of Petrophysical Data to Improve Pore and Fracture Pressure Determination in North Sea Central Graben HPHT Wells. *SPE Annual Technical Conference and Exhibition*.

Watts, N.L., 1987. Theoretical aspects of cap-rock and fault seals for single- and two-phase hydrocarbon columns. *Marine and Petroleum Geology*, 4(4), pp.274–307.

White, A.J., Traugott, M.O. & Swarbrick, R.E., 2002. The use of leak-off tests as means of predicting minimum in-situ stress. *Petroleum Geoscience*, 8(2), pp.189–193.

White, N. & Lovell, B., 1997. Measuring the pulse of a plume with the sedimentary record. *Nature*, 4192(1995), pp.1995–1998.

White, R.S., 1988. A hot-spot model for early Tertiary volcanism in the N Atlantic. *Geological Society, London, Special Publications*, 39(1), pp.3–13.

Winefield, P., Gilham, R. & Elsinger, R.L., 2005. Plumbing the depths of the Central Graben: towards an integrated pressure, fluid and charge model for the Central North Sea HPHT play. *Petroleum Geology: North-West Europe and Global Perspectives - Proceedings of the 6th Petroleum Geology Conference*, pp.1301–1316.

Xiaorong Luo & Vasseur, G., 1992. Contributions of compaction and aquathermal pressuring to geopressure and the influence of environmental conditions. *American Association of Petroleum Geologists Bulletin*, 76(10), pp.1550–1559.

Yielding, G., Lykakis, N. & Underhill, J.R., 2011. The role of stratigraphic juxtaposition for seal integrity in proven CO2 fault-bound traps of the Southern North Sea. *Petroleum Geoscience*, 17(2), pp.193–203.

Ziegler, P.A. & Den Haag, 1977. *Geology and hydrocarbon provinces of the North Sea*,

Zoback, M.D., 2010. *Reservoir Geomechanics*, New York: Cambridge University Press.